Table F-1 Automatic, continuous monitoring sites considered in the assessment

Organisation	Project	Site name	Location	Site type	Easting	Northing	Period covered
OEH	N/A	Chullora	Southern Sydney TAFE - Worth Street	Urban background	319248	6247889	2004-2014
		Earlwood	Beaman Park	Urban background	327568	6245394	2004-2014
		Lindfield	Bradfield Road	Urban background	328711	6260391	2004-2014
		Liverpool	Rose Street	Urban background	306440	6243322	2004-2014
		Prospect	William Lawson Park	Urban background	306745	6258646	2004-2014
		Randwick	Randwick Barracks	Urban background	337511	6243844	2004-2014
		Rozelle	Rozelle Hospital	Urban background	330033	6251201	2004-2014
RMS	M5 East tunnel	M5E: CBMS	Gipps Street, Bardwell Valley	Urban background[(a)]	327706	6243494	2008-2013
		M5E: T1	Thompson Street, Turrella	Urban background[(a)]	328821	6244176	2008-2013
		M5E: U1	Jackson Place, Undercliffe	Urban background[(a)]	328254	6244455	2008-2013
		M5E: X1	Wavell Parade, Earlwood	Urban background[(a)]	328091	6244425	2008-2013
		M5E: F1	Flat Rock Rd, Kingsgrove (M5 East Freeway)	Peak (roadside)[(b)]	325204	6243336	2008-2013
		M5E: M1	M5 East tunnel portal	Peak (roadside)[(b)]	329258	6243280	2008-2013
	NorthConnex	NC-01	Headen Sports Park	Urban background	322016	6266783	Dec 2013 to Jan 2015
		NC-02	Rainbow Farm Reserve	Urban background	318890	6262905	Dec 2013 to Jan 2015
		NC-03	James Park	Urban background	325161	6269429	Dec 2013 to Jan 2015
		NC-04	Observatory Park	Peak (roadside)	320644	6264948	Dec 2013 to Jan 2015
		NC-05	Brickpit Park	Peak (roadside)	318896	6262651	Dec 2013 to Jan 2015
	Lane Cove Tunnel	Aristocrat	Longueville Road / Epping Road	Peak (roadside)	330662	6257119	Oct 2008 to Nov 2009
WDA	WestConnex M4 East	M4E: 01	Wattle Street, Haberfield	Peak (roadside)	327558	6250221	Aug 2014 to Apr 2015
		M4E: 02	Edward Street, Concord	Peak (near-road)[(c)]	323765	6251147	Sep 2014 to Apr 2015
		M4E: 03	Bill Boyce Reserve, Homebush	Peak (near-road)[(c)]	322467	6251603	Sep 2014 to Apr 2015
		M4E: 04	Concord Oval, Concord	Peak (roadside)	325022	6250748	Nov 2014 to Apr 2015
		M4E: 05	St Lukes Park, Concord	Urban background	325190	6251155	Nov 2014 to Apr 2015

(a) These sites were established to characterise air quality in the vicinity of the M5 East tunnel ventilation outlets, but are effectively at urban background locations.

(b) These sites were established to characterise air quality in the vicinity of the M5 East tunnel portals.

(c) Due to practical constraints at this location, the monitoring site is some distance from the closest major road (M4 motorway). Nevertheless, the monitoring station should adequately characterise exposure to air pollution at nearby properties.

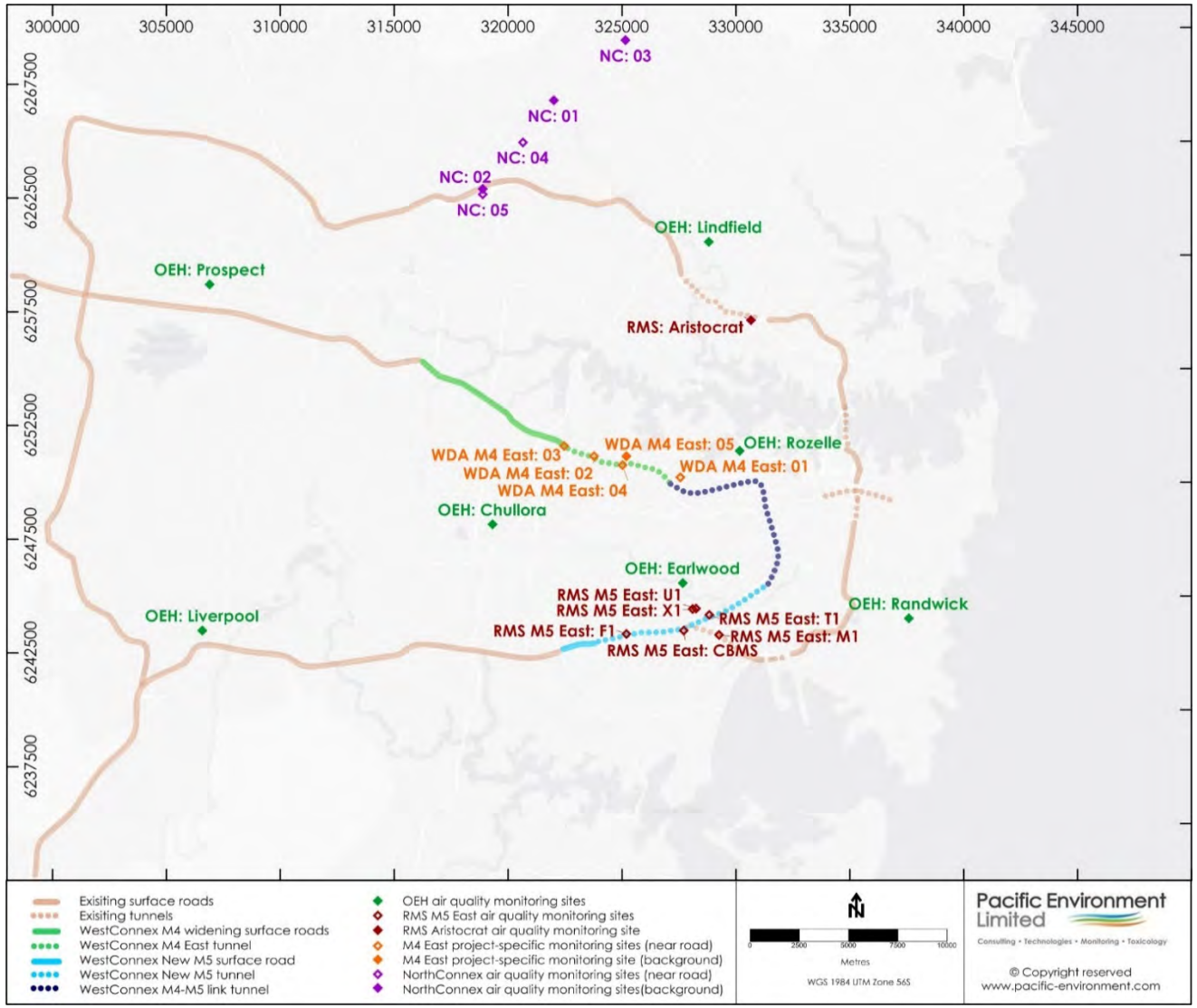

Figure F-1 Locations of air quality monitoring sites in relation to WestConnex

F.3 Measured parameters and methods

The parameters measured at each site are given in Table F-2. The coverage of pollutants was variable. CO was measured at most sites, and NO, NO_2 and NO_X were measured at all sites. Ozone was measured at the OEH, WDA and RMS NorthConnex sites, but not at the RMS M5E and Aristocrat sites. PM_{10} was measured at all sites but one[1], but $PM_{2.5}$ was measured at fewer sites, and there was only a longer-term record of $PM_{2.5}$ at three OEH sites. There were no multi-year data for hydrocarbons.

Table F-2 Parameters by monitoring station (roadside sites are shown by shading)

Monitoring station		Pollutants					Meteorological parameters			
		CO	NO, NO_2, NO_X	O_3	PM_{10}	$PM_{2.5}$	WS, WD[(a)]	Temp.	Humidity	Solar radiation
OEH	Chullora	✓	✓	✓	✓	✓	✓	✓	✓	✓
	Earlwood	-	✓	✓	✓	✓	✓	✓	✓	-
	Lindfield	-	✓	✓	✓	-	✓	✓	✓	-
	Liverpool	✓	✓	✓	✓	✓	✓	✓	✓	✓
	Prospect	✓	✓	✓	✓	-	✓	✓	✓	✓
	Randwick	-	✓	✓	✓	-	✓	✓	✓	-
	Rozelle	✓	✓	✓	✓	-	✓	✓	✓	✓
RMS	M5E: CBMS	✓	✓	-	✓	-	✓	✓	✓	✓
	M5E: T1	✓	✓	-	✓	-	✓	✓	✓	✓
	M5E: U1	✓	✓	-	✓	-	✓	✓	✓	✓
	M5E: X1	✓	✓	-	✓	-	✓	✓	✓	✓
	M5E: F1	✓	✓	-	✓	-	✓	✓	✓	✓
	M5E: M1	✓	✓	-	✓	-	✓	✓	✓	✓
	NC-01	✓	✓	✓	✓	✓	✓	✓	✓	✓
	NC-02	✓	✓	✓	✓	✓	✓	✓	✓	✓
	NC-03	✓	✓	✓	✓	✓	✓	✓	✓	✓
	NC-04	✓	✓	✓	✓	✓	✓	✓	✓	✓
	NC-05	✓	✓	✓	✓	✓	✓	✓	✓	✓
	Aristocrat	✓	✓	-	-	-	✓	✓	✓	✓
WDA	M4E: 01	✓	✓	✓	✓	✓	✓	✓	✓	✓
	M4E: 02	✓	✓	✓	✓	✓	✓	✓	✓	✓
	M4E: 03	✓	✓	✓	✓	✓	✓	✓	✓	✓
	M4E: 04	✓	✓	✓	✓	✓	✓	✓	✓	✓
	M4E: 05	✓	✓	✓	✓	✓	✓	✓	✓	✓

(a) WS = wind speed; WD = wind direction

[1] PM_{10} was actually monitored at the Aristocrat site, but the record was relatively short and incomplete.

The pollutant measurements at each site were conducted in accordance with the relevant Australian Standards[2]. The methods used were, in general terms:

- CO - Gas filter correlation infrared (GFC-IR).
- $NO/NO_2/NO_X$ - chemiluminescence detection (CLD).
- O_3 - Non-dispersive ultra-violet (NDUV) spectroscopy.
- $PM_{10}/PM_{2.5}$ - Tapered-element oscillating microbalance (TEOM) and/or beta-attenuation monitor (BAM).

In the case of PM it is well documented that the values obtained are sensitive to the measurement method used. The data used in this analysis were collected using different instruments, and this clearly introduces some uncertainty in the results. For example, for $PM_{2.5}$ TEOM monitors were used for all OEH sites up to early 2012. A combination of TEOM and BAMs were used during 2012 when a decision was made to replace the continuous TEOM $PM_{2.5}$ monitors with the USEPA equivalent-method BAM. However, for traceability all data were used as received.

F.4 Data processing and analysis

The monitoring data were used in the form provided, with the following exceptions:

- For gases, any volumetric concentrations (*e.g.* ppm or ppb) were converted to mass units (*e.g.* mg/m^3 or $\mu g/m^3$). For consistency, an ambient pressure of 1 atmosphere and a temperature of 0^oC were assumed throughout for the conversions. In the Approved Methods, for some pollutants a conversion temperature of 25^oC is used, which gives slightly lower mass concentrations. The use of 0^oC is therefore slightly conservative.
- For PM_{10} and $PM_{2.5}$, the data on days with bush fires and/or dust storms were removed, as the inclusion of the high concentrations on some of these days would have resulted in an inaccurate picture of underlying trends. The affected days were identified by OEH.

All data were handled using a consistent time base of one-hour. The data were then further averaged, where appropriate, according to the time periods in the Approved Methods. Values were only deemed to be valid where there was a sufficient amount of data; a period was taken to have sufficient data where the data capture rate was greater than 75 per cent[3].

F.5 Long-term trends at background sites

In this part of the analysis the long-term trends in air pollution at background monitoring sites in Sydney were investigated. Only the OEH and Roads and Maritime monitoring sites with a multi-year record were considered, and the following aspects were examined:

- Trends in annual mean concentration.
- Trends in monthly mean concentration, to identify any seasonal patterns.
- Trends in other relevant short-term criteria specified in the Approved Methods.
- Exceedances of the air quality criteria in the Approved Methods.

[2] Full details of the methods and procedures used at the WDA monitoring sites are presented in monthly monitoring reports for the M4 East network, and these are available on request from WDA.

[3] Clause 18 (5) of the AAQ NEPM specifies that the annual report for a pollutant must include the percentage of data available in the reporting period. An average concentration can be valid only if it is based on at least 75 per cent of the expected samples in the averaging period. The 75 per cent data availability criterion is specified as an absolute minimum requirement for data completeness (PRC, 2001).

F.5.1 Carbon monoxide

F.5.1.1 Annual mean concentration

In NSW there is no air quality criterion for the annual mean CO concentration, but the trends and patterns are still of interest. The annual mean CO concentrations at the OEH and RMS monitoring sites are shown in Figure F-2, and the corresponding statistics are provided in Table F-3. The Mann–Kendall nonparametric test was used to determine the statistical significance of trends at the 95 per cent confidence level.

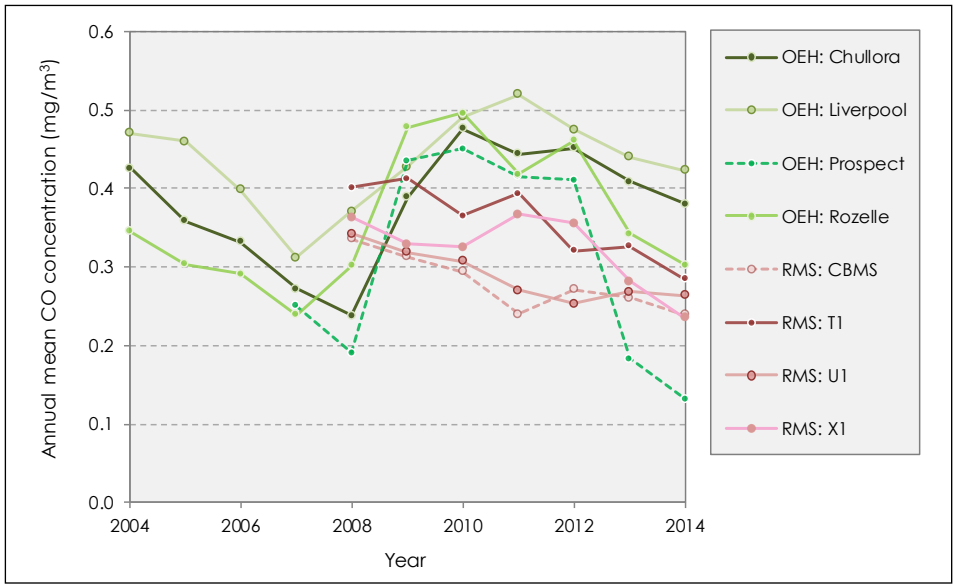

Figure F-2 Trend in annual mean CO concentration

Table F-3 Annual mean CO concentration at OEH and RMS background sites

Year	Annual mean concentration (mg/m^3)[(a)]										
	OEH Chullora	OEH Earlwood	OEH Lindfield	OEH Liverpool	OEH Prospect	OEH Randwick	OEH Rozelle	RMS CBMS	RMS T1	RMS U1	RMS X1
2004	0.43	-	-	0.47	-	-	0.34	-	-	-	-
2005	0.36	-	-	0.46	-	-	0.30	-	-	-	-
2006	0.33	-	-	0.40	-	-	0.29	-	-	-	-
2007	0.27	-	-	0.31	0.25	-	0.24	-	-	-	-
2008	0.24	-	-	0.37	0.19	-	0.30	0.34	0.40	0.34	0.36
2009	0.39	-	-	0.43	0.44	-	0.48	0.31	0.41	0.32	0.33
2010	0.48	-	-	0.49	0.45	-	0.50	0.29	0.37	0.31	0.33
2011	0.44	-	-	0.52	0.42	-	0.42	0.24	0.39	0.27	0.37
2012	0.45	-	-	0.48	0.41	-	0.46	0.27	0.32	0.25	0.36
2013	0.41	-	-	0.44	0.18	-	0.34	0.26	0.33	0.27	0.28
2014	0.38	-	-	0.42	0.13	-	0.30	0.24	0.28	0.26	0.24
Long-term mean	**0.38**	-	-	**0.44**	**0.31**	-	**0.36**	**0.28**	**0.36**	**0.29**	**0.32**
Significance[(c)]	◄►	-	-	◄►	◄►	-	◄►	◄►	◄►	◄►	◄►

(a) Only years with >75 per cent complete data shown
(b) Average of year from October 2008 to September 2009.
(c) ▼ = significantly decreasing, ▲ = significantly increasing, ◄► = no trend

At the OEH sites the annual mean concentration decreased between 2004 and the start of 2008, but then began to increase again during 2008, and continued to do so until around 2010. CO concentrations then decreased again between 2010 and 2014. There was a net overall decrease of

around 10 per cent between 2004 and 2014. A different pattern was apparent in the data from the RMS sites, where there was a more systematic downward trend in concentrations between 2008 and 2013. However, the Mann-Kendall test showed that there was no significant trend in annual mean CO concentration at any of the sites.

The long-term mean concentrations at the RMS sites were within the range of values observed at the OEH sites (around 0.3-0.4 mg/m^3). Whilst CO was not measured at Earlwood, the concentration profiles at the other OEH monitoring stations closest to WestConnex – Chullora and Rozelle were similar, and the long-term average concentrations were almost the same (0.38 and 0.36 mg/m^3 respectively).

By comparison, the long-term mean CO concentrations at the RMS roadside sites (F1 and M1) were 0.54 and 0.45 mg/m^3 respectively.

F.5.1.2 Monthly mean concentration

Monthly mean concentrations provide additional data on seasonal patterns in air pollution. An example of the seasonal variation in CO concentrations at a monitoring site – in this case OEH's Chullora site - is given in Figure F-3. The Figure was produced using the 'smooth trend' function in the Openair[4] software, and the shading around the trend line gives the 95 per cent confidence intervals.

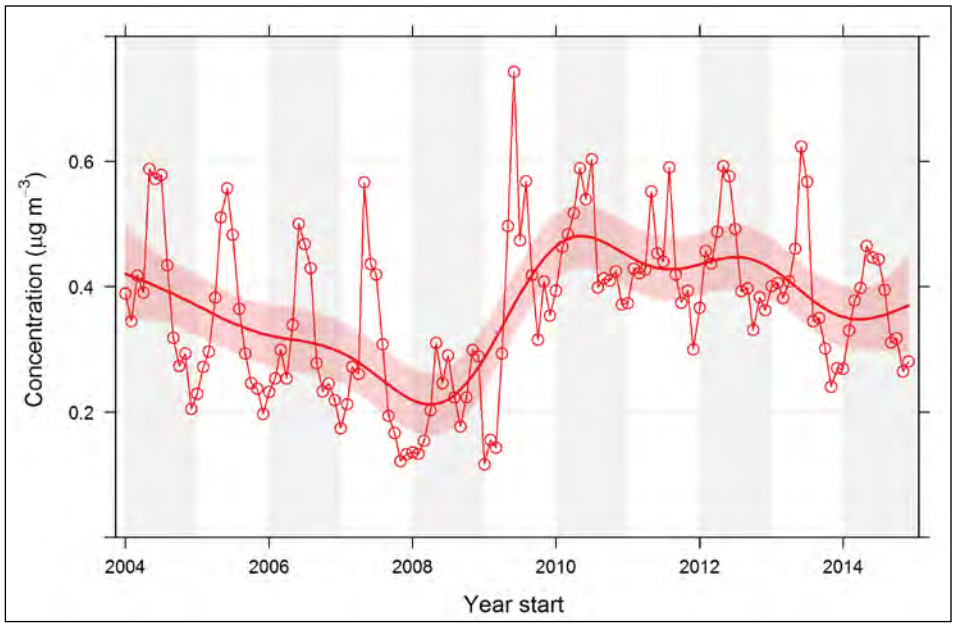

Figure F-3 Monthly mean CO concentration at OEH Chullora monitoring site

There is a strong seasonal influence on CO concentrations, with the values being much higher in winter than in summer. This is commonly observed for CO, and is due to a combination of winter-time factors such as an increase in combustion for heating purposes, elevated 'cold start' emissions from road vehicles, and more frequent and persistent temperature inversions in the atmosphere reducing the effectiveness of dispersion. It was desirable to ensure that such seasonal effects were represented in the assumed background concentrations for the M4 East project.

F.5.1.3 Maximum one-hour mean concentration

The trends in the maximum one-hour mean CO concentration by year are shown in Figure F-4 and Table F-4. All maximum values were well below the air quality criterion of 30 mg/m^3. The patterns at all background sites were broadly similar, with a general downward trend. The trend was statistically significant at two of the OEH sites.

[4] http://www.openair-project.org/Default.aspx

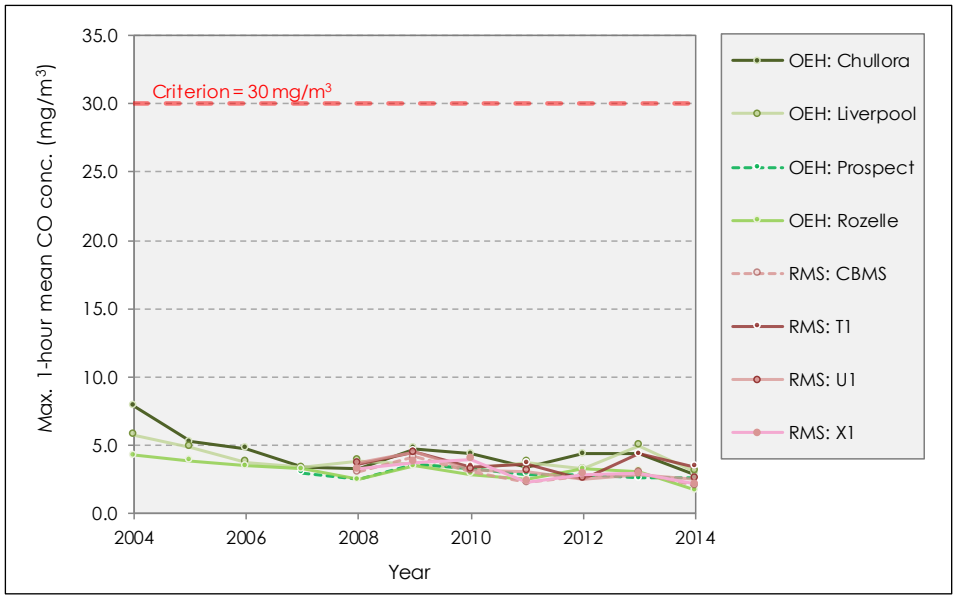

Figure F-4 **Trend in maximum one-hour mean CO concentration**

Table F-4 **Maximum one-hour mean CO concentration at OEH and RMS background sites**

Year	Annual mean concentration (mg/m^3)[(a)]										
	OEH Chullora	OEH Earlwood	OEH Lindfield	OEH Liverpool	OEH Prospect	OEH Randwick	OEH Rozelle	RMS CBMS	RMS T1	RMS U1	RMS X1
2004	7.87	-	-	5.75	-	-	4.25	-	-	-	-
2005	5.25	-	-	4.87	-	-	3.87	-	-	-	-
2006	4.75	-	-	3.75	-	-	3.50	-	-	-	-
2007	3.37	-	-	3.37	3.00	-	3.25	-	-	-	-
2008	3.25	-	-	3.87	2.50	-	2.50	3.03	3.66	3.69	3.30
2009	4.75	-	-	3.62	3.62	-	3.50	4.18	4.55	4.47	3.77
2010	4.37	-	-	3.25	3.25	-	2.87	3.10	3.43	3.24	3.98
2011	3.37	-	-	3.75	2.87	-	2.50	2.29	3.65	3.09	2.33
2012	4.37	-	-	3.25	2.87	-	3.25	2.73	2.57	2.58	2.87
2013	4.37	-	-	5.00	2.62	-	3.12	3.00	4.36	2.89	2.95
2014	2.87	-	-	3.12	2.62	-	1.75	2.06	3.45	2.56	2.15
Long-term mean	**4.42**	-	-	**3.96**	**2.92**	-	**3.12**	**2.91**	**3.67**	**3.22**	**3.05**
Significance[(c)]	▼	-	-	◄►	◄►	-	▼	◄►	◄►	◄►	◄►

(a) Only years with >75 per cent complete data shown
(b) Average of year from October 2008 to September 2009.
(c) ▼ = significantly decreasing, ▲ = significantly increasing, ◄► = no trend

F.5.1.4 Maximum rolling 8-hour mean concentration

The trends in the maximum rolling 8-hour mean CO concentration by year are shown in Figure F-5 and Table F-5. All maximum values were well below the air quality criterion of 10 mg/m^3; the long-term averages were between around 2 and 3 mg/m^3. By comparison, the long-term mean values at the RMS roadside sites (F1 and M1) were 3.5 and 2.5 mg/m^3 respectively. The patterns at all background sites were broadly similar; there was a general downward trend, but it was not statistically significant at any site. Whilst there was some spatial variation in CO, it was not systematic, and the between-site variation was small compared with the criterion.

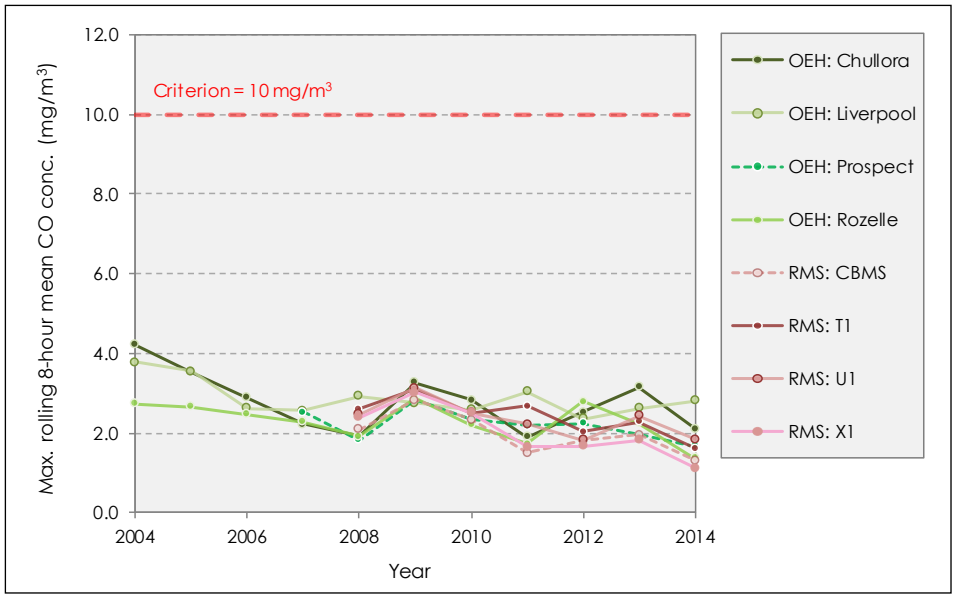

Figure F-5 **Trend in maximum rolling 8-hour mean CO concentration**

Table F-5 **Maximum rolling 8-hour mean CO concentration at OEH and RMS background sites**

Year	Annual mean concentration (mg/m^3)[a]										
	OEH Chullora	OEH Earlwood	OEH Lindfield	OEH Liverpool	OEH Prospect	OEH Randwick	OEH Rozelle	RMS CBMS	RMS T1	RMS U1	RMS X1
2004	4.22	-	-	3.78	-	-	2.73	-	-	-	-
2005	3.53	-	-	3.54	-	-	2.66	-	-	-	-
2006	2.89	-	-	2.62	-	-	2.46	-	-	-	-
2007	2.22	-	-	2.57	2.52	-	2.28	-	-	-	-
2008	1.93	-	-	2.93	1.82	-	1.91	2.08	2.60	2.46	2.38
2009	3.27	-	-	2.75	2.83	-	2.87	2.84	3.10	3.14	3.01
2010	2.82	-	-	2.59	2.35	-	2.21	2.33	2.51	2.50	2.51
2011	1.89	-	-	3.03	2.18	-	1.73	1.51	2.67	2.23	1.66
2012	2.53	-	-	2.36	2.25	-	2.79	1.81	2.02	1.83	1.68
2013	3.14	-	-	2.62	1.96	-	2.23	1.97	2.27	2.43	1.82
2014	2.11	-	-	2.80	1.68	-	1.37	1.31	1.61	1.84	1.13
Long-term mean	**2.78**	-	-	**2.87**	**2.20**	-	**2.30**	**1.98**	**2.40**	**2.35**	**2.03**
Significance[c]	◄►	-	-	◄►	◄►	-	◄►	◄►	◄►	◄►	◄►

(d) Only years with >75 per cent complete data shown
(e) Average of year from October 2008 to September 2009.
(f) ▼ = significantly decreasing, ▲ = significantly increasing, ◄► = no trend

F.5.1.5 Exceedances of air quality criteria

Between 2004 and 2014, there were no exceedances of the rolling 8-hour mean criterion for CO of 10 mg/m^3, or the one-hour criterion of 30 mg/m^3, at any of the background sites included in the analysis.

F.6 Nitrogen oxides

F.6.1.1 Annual mean concentration

The annual mean NO_X concentrations at the monitoring sites are shown in Figure F-6, and the corresponding statistics are provided in Table F-6. There are no air quality criteria for NO_X in NSW, but it is important to understand NO_X in order to characterise NO_2 (see Appendix G).

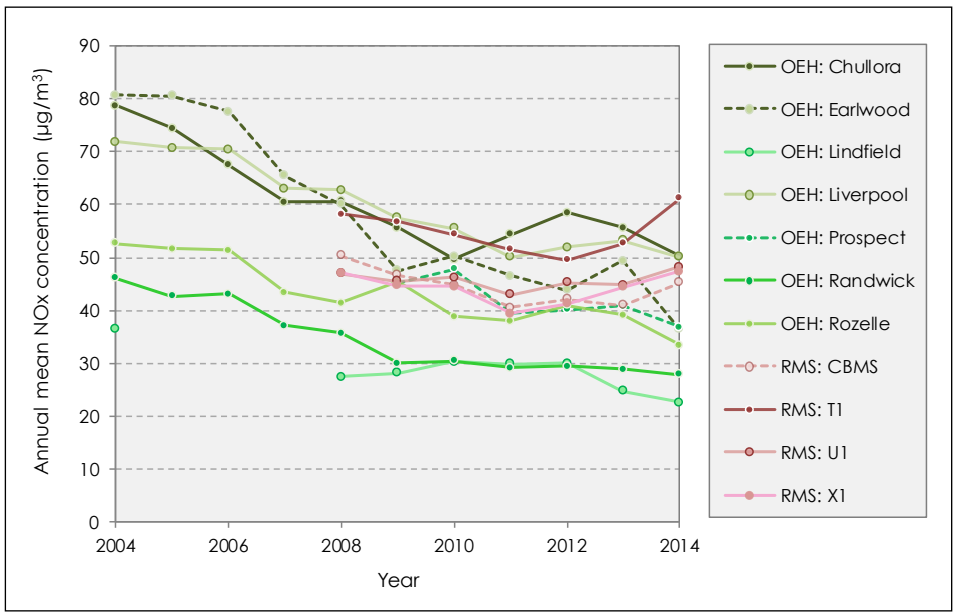

Figure F-6 Trend in annual mean NO_X concentration

Table F-6 Annual mean NO_X concentration at OEH and RMS background sites

Year	Annual mean concentration (µg/m^3)[(a)]										
	OEH Chullora	OEH Earlwood	OEH Lindfield	OEH Liverpool	OEH Prospect	OEH Randwick	OEH Rozelle	RMS CBMS	RMS T1	RMS U1	RMS X1
2004	78.7	80.6	36.6	71.8	-	46.0	52.7	-	-	-	-
2005	74.4	80.5	-	70.7	-	42.7	51.7	-	-	-	-
2006	67.5	77.5	-	70.5	-	43.2	51.3	-	-	-	-
2007	60.4	65.5	-	63.0	-	37.2	43.4	-	-	-	-
2008	60.7	60.0	27.5	62.7	-	35.8	41.5	50.3	58.2	47.0	47.1
2009	55.7	47.5	28.2	57.5	45.1	30.1	45.4	46.7	56.7	45.5	44.6
2010	49.7	50.2	30.4	55.4	47.7	30.4	38.9	44.8	54.3	46.2	44.6
2011	54.3	46.5	29.9	50.0	39.5	29.2	38.0	40.5	51.5	42.9	39.4
2012	58.5	43.8	30.0	52.0	40.1	29.4	40.9	42.2	49.6	45.3	41.3
2013	55.6	49.4	24.8	53.3	40.8	28.9	39.1	41.0	52.7	44.8	44.4
2014	50.2	36.5	22.6	50.1	36.9	27.9	33.5	45.2	61.1	48.2	47.3
Long-term mean	**60.5**	**58.0**	**28.7**	**59.7**	**41.7**	**34.6**	**43.3**	**44.4**	**54.9**	**45.7**	**44.1**
Significance[(c)]	▼	▼	◄►	▼	◄►	▼	▼	◄►	◄►	◄►	◄►

(a) Only years with >75 per cent complete data shown
(b) Average of year from October 2008 to September 2009.
(c) ▼ = significantly decreasing, ▲ = significantly increasing, ◄► = no trend

There was a general tendency for annual mean NO_X concentrations to decrease between 2004 and 2014. At the OEH sites concentrations typically decreased by around 35 per cent overall between 2004 and 2014, although there was a 55 per cent reduction at the Earlwood site. For those OEH sites with a complete record between 2004 and 2014 the Mann-Kendall test showed that the downward trend in concentrations was statistically significant. At the RMS sites, on the other hand, there was no significant trend in concentrations. There is also a suggestion of a levelling-off of concentrations in recent years, although there are different patterns at the various sites.

There were some quite systematic spatial variations in the annual mean NO_X concentration. For example, at the OEH Chullora, Earlwood and Liverpool sites the long-term mean concentration was around 60 µg/m^3, compared with around 42-43 µg/m^3 at Prospect and Rozelle, 35 µg/m^3 at Randwick and 29 µg/m^3 at Lindfield. Concentrations at the RMS T1 site were comparable with those at the OEH sites having relatively high values, with concentrations at the RMS sites CBMS, U1 and X1 being slightly lower. This spatial variation was taken into account in the derivation of background NO_X concentrations for the M4 East project.

Although not shown here, the long-term mean NO_X concentrations at the RMS roadside sites (F1 and M1) were substantially higher than those at the background sites, and very similar at 106 and 107 µg/m^3 respectively. This illustrates the ongoing contribution of NO_X emissions from road transport.

F.6.1.2 Monthly mean concentration

Figure F-7 provides an example of the monthly mean NO_X concentrations, in this case showing the significant downward trend at the Earlwood site. The reduction in concentrations with time can clearly be seen. As with CO there is a strong seasonal influence on NO_X concentrations, with the values being much higher in winter than in summer. This is again likely to be due to an increase in emissions from combustion sources and more frequent temperature inversions in winter. Another contributing factor may be the reaction of NO_2 with the hydroxyl radical (OH) acting as a sink for NO_X. Concentrations of OH are highest in the summer. As before, it was desirable to ensure that such seasonal variations were represented in the assumed background concentrations for the M4 east project.

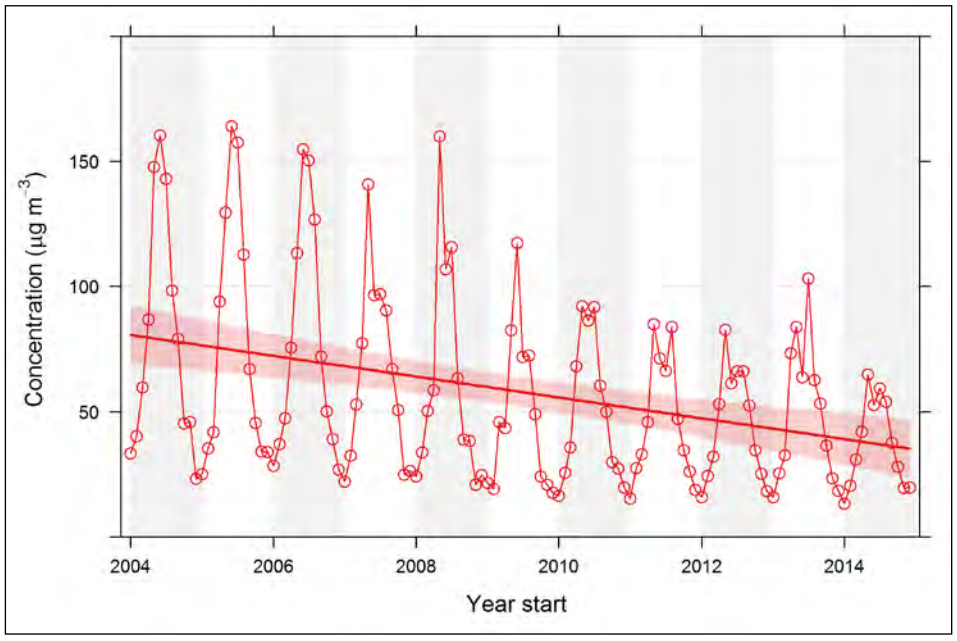

Figure F-7 Monthly mean NOx concentration at OEH Earlwood monitoring site

F.6.1.3 Maximum one-hour mean concentration

The long-term trends in the maximum one-hour mean NO_X concentration are shown in Figure F-8. Again, there are no air quality criteria for NO_X, and these are largely of interest in relation to the one-hour criterion for NO_2. As with the annual mean concentration, there has been a general downward trend in peak concentrations.

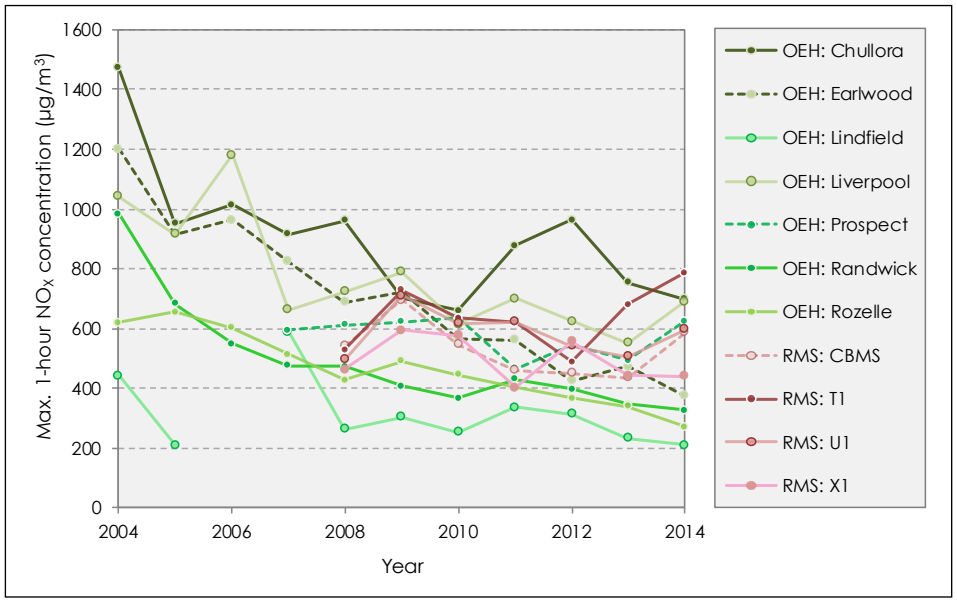

Figure F-8 Trend in maximum one-hour mean NO_X concentration

For comparison, the maximum one-hour mean NO_X concentrations at the RMS roadside sites (F1 and M1) in 2014 were 750 and 650 µg/m^3 respectively. These values are close to the upper end of the range of values for the background sites, but actually lower than the value for RMS site T1. It may be the case that under certain meteorological conditions the background sites are affected by NO_X emissions from busy roads well away from the sites.

F.6.2 Nitrogen dioxide

F.6.2.1 Annual mean concentration

The long-term trends in annual mean NO_2 concentrations are shown in Figure F-9, and the corresponding statistics are provided in Table F-7. The concentrations at all sites were well below the NSW air quality assessment criterion of 62 µg/m^3.

The NO_2 concentrations at the OEH sites exhibited a systematic downward trend - with a reduction of between around 20 per cent and 40 per cent depending on the site - and one that was statistically significant at four of the sites. However, in recent years the concentrations at some sites appear to have stabilised. At the RMS background sites there was no significant downward trend.

As with NO_X, there was some spatial variation in NO_2 concentrations, but the pattern across the monitoring sites was not quite the same. Nevertheless, concentrations were again generally highest at the Chullora site and lowest at Lindfield and Randwick.

The long-term average NO_2 concentrations at the RMS roadside sites (F1 and M1) were 34 and 37 µg/m^3 respectively, and therefore around 10-15 µg/m^3 higher than those at the background sites. Even so, the NO_2 concentrations at roadside were also well below the assessment criterion.

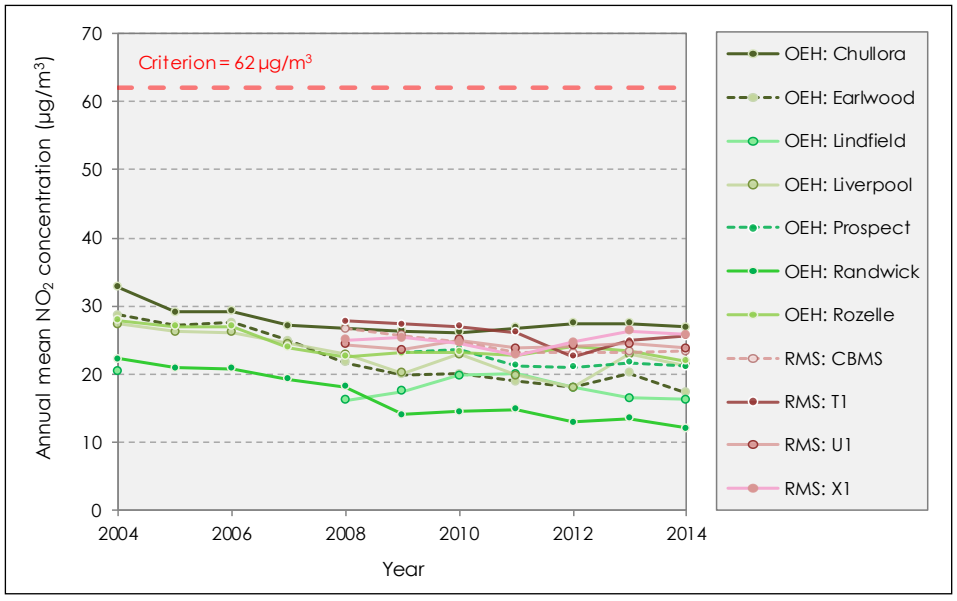

Figure F-9 **Trend in annual mean NO_2 concentration**

Table F-7 **Annual mean NO_2 concentration at OEH and RMS background sites**

Year	Annual mean concentration (µg/m^3)[(a)]										
	OEH Chullora	OEH Earlwood	OEH Lindfield	OEH Liverpool	OEH Prospect	OEH Randwick	OEH Rozelle	RMS CBMS	RMS T1	RMS U1	RMS X1
2004	32.8	28.7	20.4	27.4	-	22.2	27.9	-	-	-	-
2005	29.1	27.1	-	26.2	-	20.9	27.0	-	-	-	-
2006	29.2	27.6	-	26.1	-	20.8	27.0	-	-	-	-
2007	27.1	24.9	-	24.5	-	19.2	23.9	-	-	-	-
2008	26.7	21.7	16.1	22.9	-	18.1	22.6	26.7	27.7	24.3	25.0
2009	26.3	19.9	17.4	20.1	23.1	14.1	23.1	25.7	27.4	23.5	25.4
2010	26.2	20.1	19.8	22.9	23.7	14.6	23.2	24.8	27.1	25.1	24.5
2011	26.8	18.9	20.0	19.9	21.3	14.8	22.9	23.1	26.1	23.8	22.8
2012	27.4	18.1	18.0	18.1	21.1	13.0	24.0	23.1	22.5	24.2	24.7
2013	27.5	20.2	16.5	22.9	21.7	13.5	23.4	23.2	25.0	24.5	26.3
2014	26.9	17.3	16.3	21.3	21.1	12.1	21.9	23.4	25.5	23.8	25.8
Long-term mean	**27.8**	**22.2**	**18.1**	**22.9**	**22.0**	**16.7**	**24.3**	**24.3**	**25.9**	**24.2**	**24.9**
Significance[(c)]	◄►	▼	◄►	▼	◄►	▼	▼	◄►	◄►	◄►	◄►

(a) Only years with >75 per cent complete data shown
(b) Average of year from October 2008 to September 2009.
(c) ▼ = significantly decreasing, ▲ = significantly increasing, ◄► = no trend

F.6.2.2 Monthly mean concentration

The seasonal variation in NO_X was mirrored by that for NO_2. This is illustrated in the data for Earlwood in Figure F-10. This Figure also shows more clearly that NO_2 concentrations at this site have stabilised in recent years.

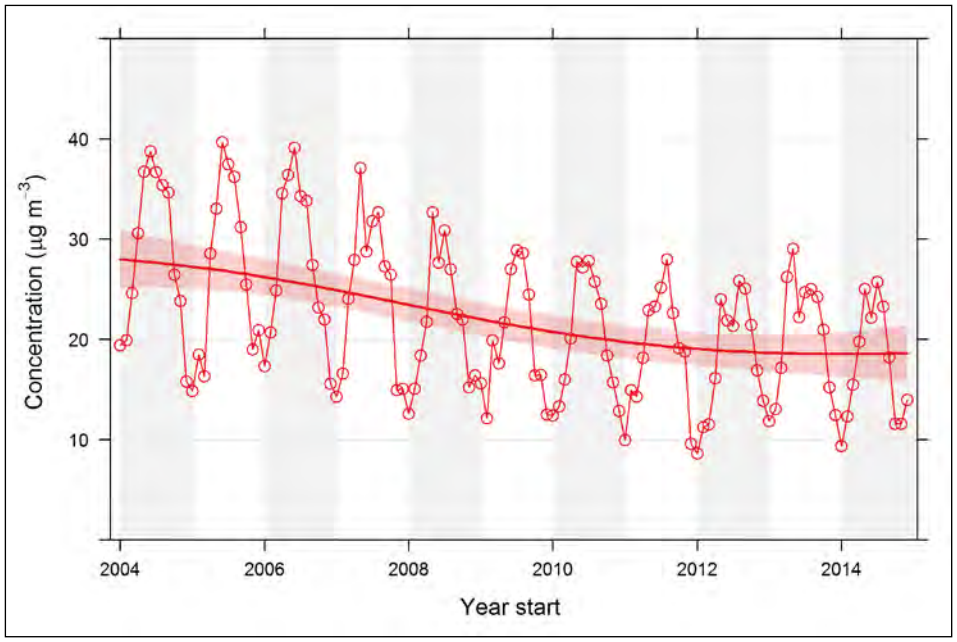

Figure F-10 Monthly mean NO_2 concentration at OEH Earlwood monitoring site

F.6.2.3 Maximum one-hour mean concentration

The trends in the maximum one-hour mean NO_2 concentration by year are given in Figure F-11. The within-site variation for this metric is similar to the between site variation, but when viewed overall the values have been quite stable with time (varying around 100 µg/m^3), and are all below the NSW air quality assessment criterion of 246 µg/m^3. The maximum one-hour mean NO_2 concentrations at the RMS roadside sites (F1 and M1) in 2014 were 115 and 122 µg/m^3 respectively. As with NO_X, these values are on a par with the higher values for the background sites.

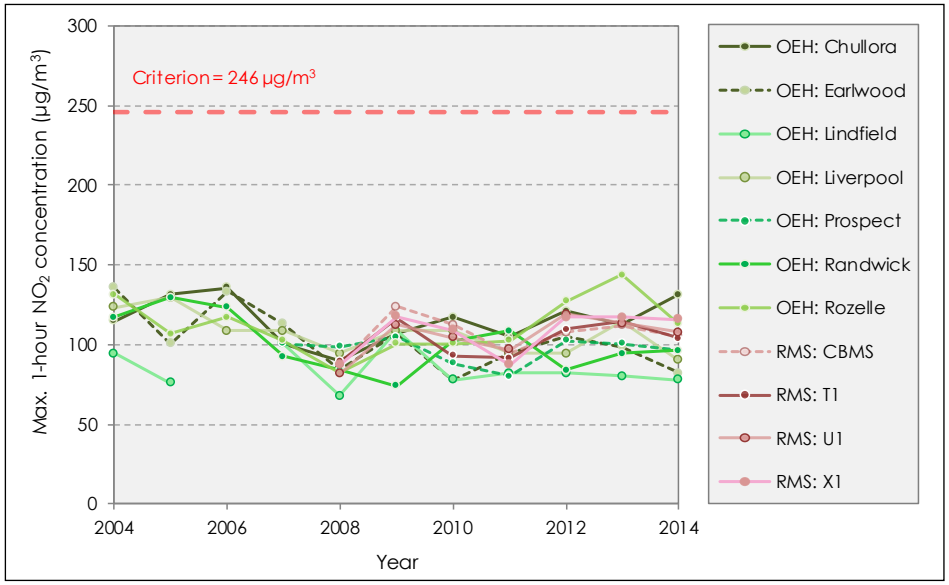

Figure F-11 Trend in maximum one-hour mean NO_2 concentration

F.6.2.4 Exceedances of air quality criteria

There were no exceedances of the annual mean criterion for NO_2 of 62 µg/m^3 (Table F-7). In fact, annual mean concentrations were well below the criterion at all sites and in all years. There were also no exceedances of the one-hour mean criterion for NO_2 (246 µg/m^3).

F.6.3 Ozone

F.6.3.1 Annual mean concentration

Annual mean ozone concentrations at the OEH sites - presented in Figure F-12 and Table F-8 - were relatively stable between 2004 and 2014, being typically around 30-35 µg/m^3. The main exception was the Randwick site, where the typical annual mean concentration was substantially higher, at closer to 40 µg/m^3. This is likely to be due to the coastal nature of Randwick, with easterly winds having low concentrations of ozone-scavenging species, notably NO_X (see Figure F-6).

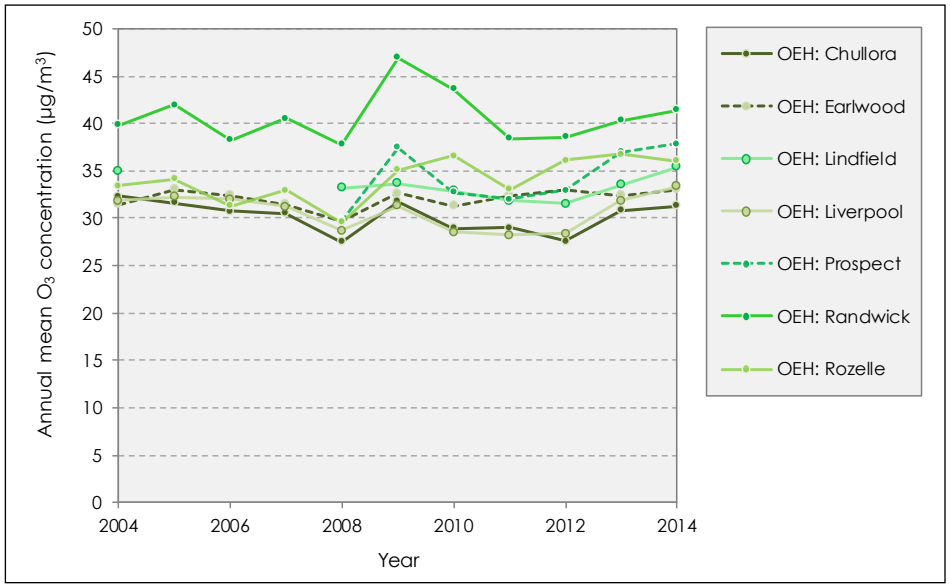

Figure F-12 Trend in annual mean O_3 concentration

Table F-8 Annual mean O_3 concentration at OEH background sites

Year	Annual mean concentration (µg/m^3) [(a)]						
	Chullora	Earlwood	Lindfield	Liverpool	Prospect	Randwick	Rozelle
2004	32.3	31.5	35.0	31.8	-	39.8	33.5
2005	31.6	33.0	-	32.2	-	42.0	34.2
2006	30.7	32.4	-	32.0	-	38.3	31.3
2007	30.5	31.4	-	31.2	-	40.5	32.9
2008	27.5	29.7	33.2	28.7	29.8	37.8	29.6
2009	31.8	32.7	33.7	31.3	37.5	46.9	35.1
2010	28.9	31.3	32.9	28.6	32.8	43.6	36.6
2011	29.0	32.4	31.9	28.2	32.0	38.4	33.0
2012	27.5	33.0	31.5	28.4	33.0	38.6	36.1
2013	30.8	32.4	33.5	31.8	37.0	40.3	36.8
2014	31.3	33.0	35.4	33.4	37.9	41.4	36.0
Long-term mean	**30.2**	**32.1**	**33.4**	**30.7**	**34.3**	**40.7**	**34.1**
Significance[(b)]	◄►	◄►	◄►	◄►	▲	◄►	▲

(a) Only years with >75 per cent complete data shown

(b) ▼ = significantly decreasing, ▲ = significantly increasing, ◄► = no trend

F.6.3.2 Monthly mean concentration

As with NO_X and NO_2, ozone concentrations vary according to the season. They are highest in the late spring and early summer – when photochemical activity is high - and lowest in the autumn and winter. An example profile - for the Earlwood site – shown in Figure F-13.

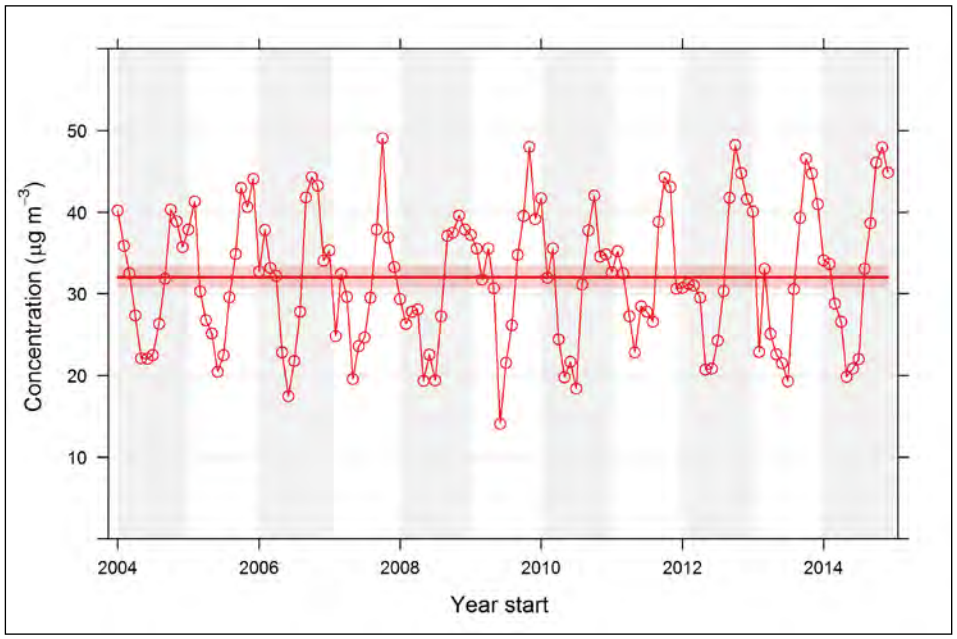

Figure F-13 Monthly mean O_3 concentration at OEH Earlwood monitoring site

F.6.3.3 Exceedances of air quality criteria

Table F-9 and Table F-10 show that there were exceedances of the rolling 4-hour mean and 1-hour mean standards for ozone at several monitoring sites.

Table F-9 Exceedances of rolling 4-hour mean O_3 standard

Year	Number of exceedances of rolling 4-hour standard per year (171 µg/m^3)						
	Chullora	Earlwood	Lindfield	Liverpool	Prospect	Randwick	Rozelle
2004	**7**	**1**	**5**	**11**	-	**2**	**2**
2005	**1**	0	-	**6**	-	0	0
2006	**10**	**4**	-	**17**	-	0	**2**
2007	0	0	-	**7**	-	**2**	0
2008	0	0	0	**1**	**2**	0	0
2009	**6**	**7**	**3**	**10**	**18**	0	0
2010	0	0	0	**1**	**7**	0	0
2011	**4**	**3**	**1**	**5**	**13**	0	0
2012	0	0	0	0	0	0	0
2013	**3**	**3**	0	**6**	**6**	0	0
2014	0	0	0	**3**	**5**	0	0

Table F-10 Exceedances of 1-hour O_3 standard

Year	Number of exceedances of 1-hour standard per year (214 µg/m^3)						
	Chullora	Earlwood	Lindfield	Liverpool	Prospect	Randwick	Rozelle
2004	**2**	0	**1**	**5**	-	**2**	0
2005	0	0	-	**3**	-	0	0
2006	**3**	**2**	-	**11**	-	0	0
2007	0	0	-	**3**	-	0	0
2008	0	0	0	0	**1**	0	0
2009	**3**	**3**	**1**	**3**	**4**	0	0
2010	0	0	0	0	**3**	0	0
2011	**1**	0	0	**1**	**5**	0	0
2012	0	0	0	0	0	0	0
2013	**1**	**1**	0	**5**	**2**	0	0
2014	0	0	0	**1**	**2**	0	0

F.6.4 PM_{10}

F.6.4.1 Annual mean concentration

Annual mean PM_{10} concentrations at the OEH and RMS sites are given in Figure F-14 and Table F-11. Concentrations at the OEH sites showed a net decrease between 2004 and 2014, by as much as 20 per cent in the case of the Chullora site. Only the Chullora and Earlwood sites had a statistically significant downward trend in concentrations.

In recent years the annual mean PM_{10} concentration at the OEH sites has been between 17 µg/m^3 and 20 µg/m^3, except at Lindfield where the concentration is substantially lower (around 14 µg/m^3). The concentration at the RMS sites in recent years appears to have stabilised at around 15 µg/m^3. These values can be compared with air quality criterion of 30 µg/m^3.

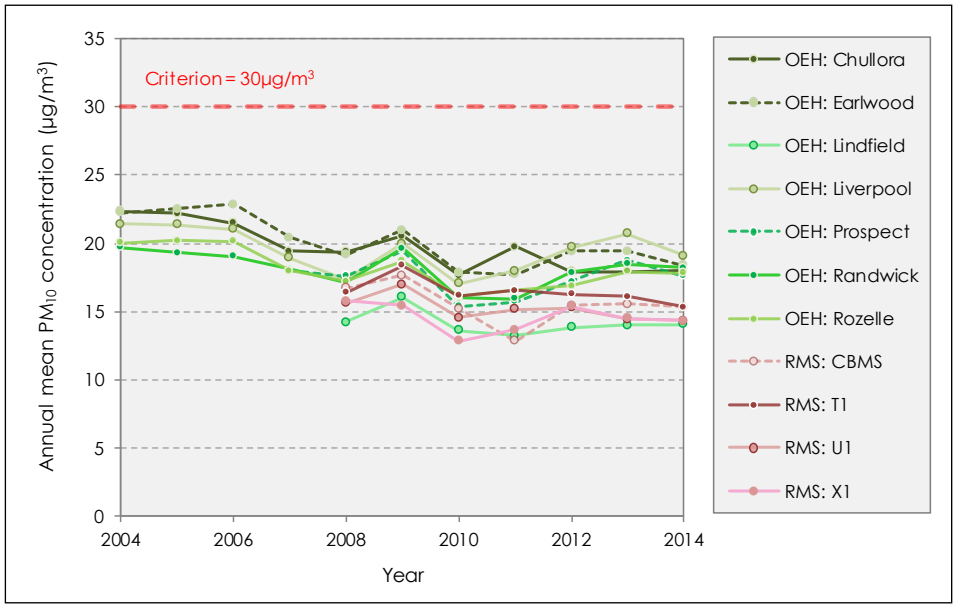

Figure F-14 Trend in annual mean PM_{10} concentration

Table F-11 Annual mean PM_{10} concentration at OEH and RMS background sites

Year	Annual mean concentration (µg/m^3)[(a)]										
	OEH Chullora	OEH Earlwood	OEH Lindfield	OEH Liverpool	OEH Prospect	OEH Randwick	OEH Rozelle	RMS CBMS	RMS T1	RMS U1	RMS X1
2004	22.3	22.2	-	21.4	-	19.7	20.0	-	-	-	-
2005	22.2	22.5	-	21.3	-	19.3	20.2	-	-	-	-
2006	21.5	22.9	-	21.0	-	19.0	20.2	-	-	-	-
2007	19.4	20.4	-	18.9	18.0	18.1	18.0	-	-	-	-
2008	19.4	19.1	14.2	17.4	17.6	17.2	17.2	16.7	16.4	15.6	15.8
2009	20.5	20.9	16.1	20.0	19.5	19.6	18.7	17.7	18.3	17.0	15.5
2010	17.7	17.9	13.6	17.0	15.4	16.0	16.1	15.2	16.2	14.6	12.8
2011	19.8	17.7	13.2	18.0	15.7	15.9	16.6	12.8	16.6	15.2	13.7
2012	17.9	19.4	13.8	19.7	17.2	17.9	16.9	15.5	16.2	15.3	15.4
2013	17.9	19.4	14.0	20.7	18.8	18.5	17.9	15.7	16.1	14.4	14.5
2014	18.1	18.3	14.1	19.1	17.6	18.2	17.8	15.3	15.3	14.4	14.4
Long-term mean	**19.7**	**20.1**	**14.1**	**19.5**	**17.5**	**18.1**	**18.1**	**15.7**	**16.7**	**15.2**	**14.6**
Significance[(b)]	▼	▼	◄►	◄►	◄►	◄►	◄►	◄►	◄►	◄►	◄►

(a) Only years with >75 per cent complete data shown

(b) ▼ = significantly decreasing, ▲ = significantly increasing, ◄► = no trend

F.6.4.2 Monthly mean concentration

The monthly mean concentrations at the Chullora site are shown in Figure F-15**.** For PM_{10} there is a weaker seasonal effect than for the gaseous pollutants, with concentrations tending to be higher in summer and lower in winter. The Figure also shows more clearly how mean concentrations are tending to stabilise at around 20 µg/m^3.

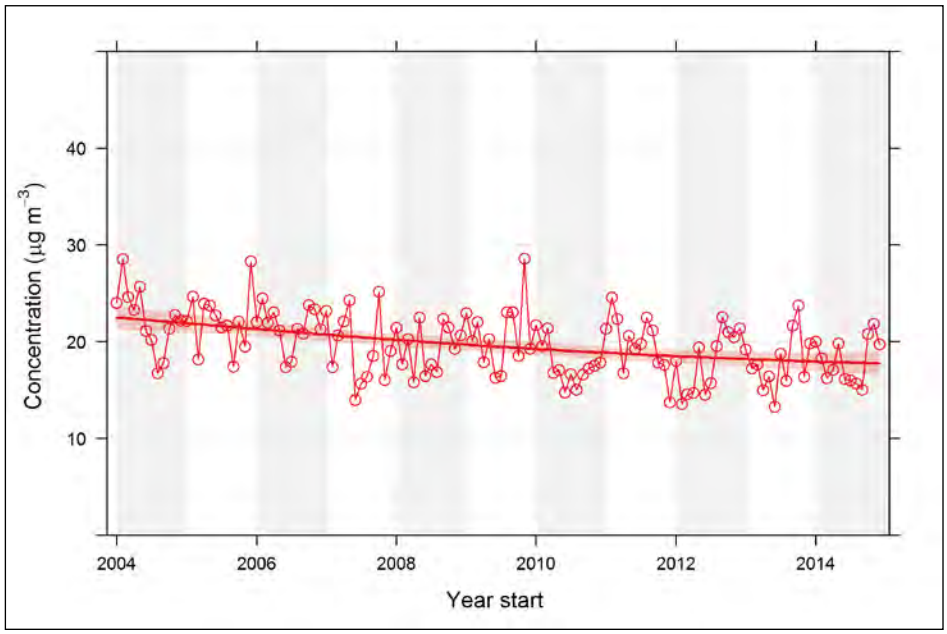

Figure F-15 Monthly mean PM_{10} concentration at OEH Chullora monitoring site

F.6.4.3 24-hour mean concentration

The maximum 24-hour mean PM_{10} concentrations are shown in Figure F-16. These appear to exhibit a slight downward trend overall, but there is a large amount of variation from year to year at most

sites. In 2014 the concentrations at the various sites were clustered around 40 µg/m^3, but the historical patterns suggest that this would be unlikely to continue into the future.

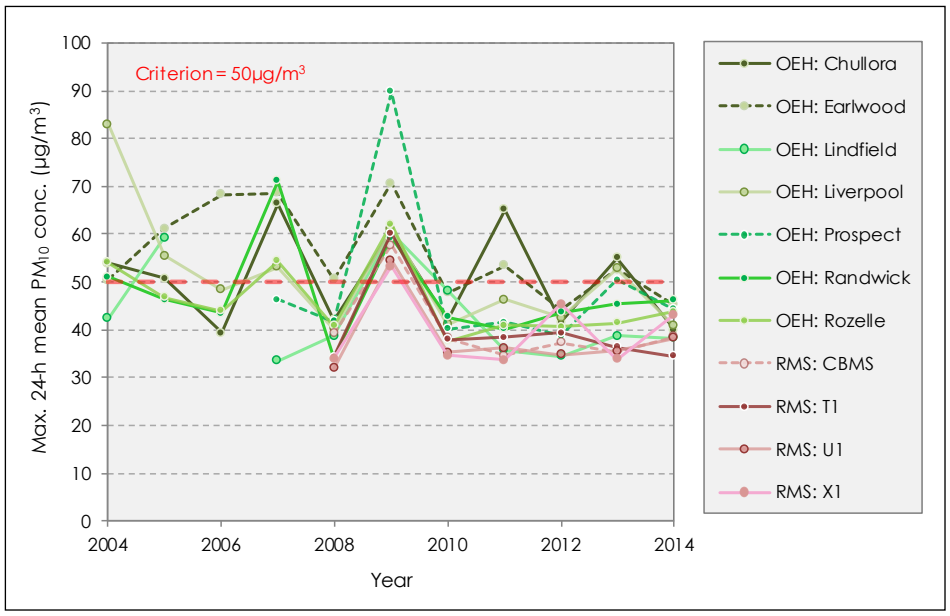

Figure F-16 Trend in maximum 24-hour mean PM_{10} concentration

F.6.4.4 Exceedances of air quality criteria

There were no exceedances of the annual mean criterion for PM_{10} of 30 µg/m^3, but Table F-12 shows that there were exceedances of the 24-hour criterion of 50 µg/m^3, notably in the warm, dry year of 2009 (days with bush fires and dust storms were excluded from this analysis).

Table F-12 Exceedances of 24-hour PM_{10} standard

Year	Number of exceedances of 24-hour standard per year (50 µg/m^3)						
	Chullora	Earlwood	Lindfield	Liverpool	Prospect	Randwick	Rozelle
2004	**3**	**1**	0	1	-	**1**	**1**
2005	**1**	**2**	**1**	**2**	-	0	0
2006	0	**5**	-	0	-	0	0
2007	**2**	**3**	0	**1**	0	**1**	**1**
2008	0	**1**	0	0	0	0	0
2009	**2**	**4**	**1**	**3**	**3**	**2**	**2**
2010	0	0	0	0	0	0	0
2011	**8**	**1**	0	0	0	0	0
2012	0	0	0	0	0	0	0
2013	**1**	**2**	0	**1**	**1**	0	0
2014	0	0	0	0	0	0	0

F.6.5 $PM_{2.5}$

F.6.5.1 Annual mean concentration

An extensive time series of $PM_{2.5}$ measurements was only available for three monitoring sites in the wider study area (Figure F-17 and Table F-13). Concentrations at the two OEH sites close to WestConnex – Chullora and Earlwood - showed a broadly similar pattern, with a systematic reduction

between 2004 and 2012 being followed by a substantial increase between 2012 and 2014. Here, it is important to recognise the following:

- As noted earlier, during 2012 OEH made a decision to replace its continuous TEOM $PM_{2.5}$ monitors with USEPA-equivalent BAMs. This is the main reason for the increase in the measured concentrations between 2012 and 2014. It is well documented that there are considerable uncertainties in the measurement of $PM_{2.5}$ (AQEG, 2012).
- The increases meant that background $PM_{2.5}$ concentrations in the study area during 2014 were already very close to or above the advisory reporting standard in the AAQ NEPM of 8 $\mu g/m^3$.

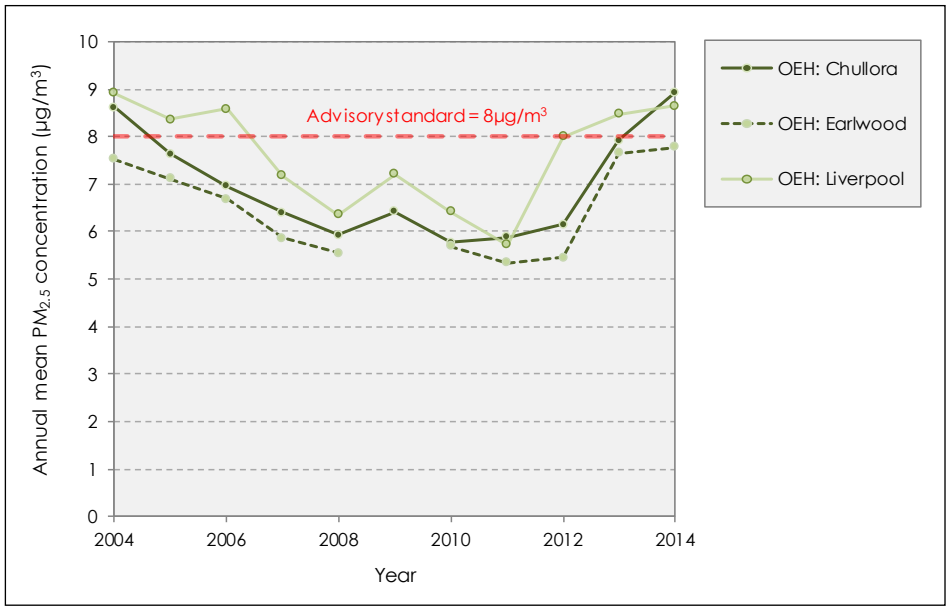

Figure F-17 Long-term trends in annual mean $PM_{2.5}$ concentration

Table F-13 Annual mean $PM_{2.5}$ concentration at OEH background sites

Year	Annual mean concentration ($\mu g/m^3$) [(a)]						
	Chullora	Earlwood	Lindfield	Liverpool	Prospect	Randwick	Rozelle
20-04	8.6	7.5	-	8.9	-	-	-
2005	7.6	7.1	-	8.4	-	-	-
2006	7.0	6.7	-	8.6	-	-	-
2007	6.4	5.9	-	7.2	-	-	-
2008	5.9	5.5	-	6.4	-	-	-
2009	6.4	-	-	7.2	-	-	-
2010	5.8	5.7	-	6.4	-	-	-
2011	5.9	5.3	-	5.7	-	-	-
2012	6.1	5.5	-	8.0	-	-	-
2013	7.9	7.7	-	8.5	-	-	-
2014	8.9	7.8	-	8.7	-	-	-
Long-term mean	**7.0**	**6.5**	**-**	**7.6**	**-**	**-**	**-**
Significance[(b)]	◄►	◄►	-	◄►	-	-	-

(a) Only years with >75 per cent complete data shown

(b) ▼ = significantly decreasing, ▲ = significantly increasing, ◄► = no trend

F.6.5.2 Monthly mean concentration

The monthly mean $PM_{2.5}$ concentrations at the Chullora site are shown in **Figure G17.** There are some differences between seasons, but they are not systematic.

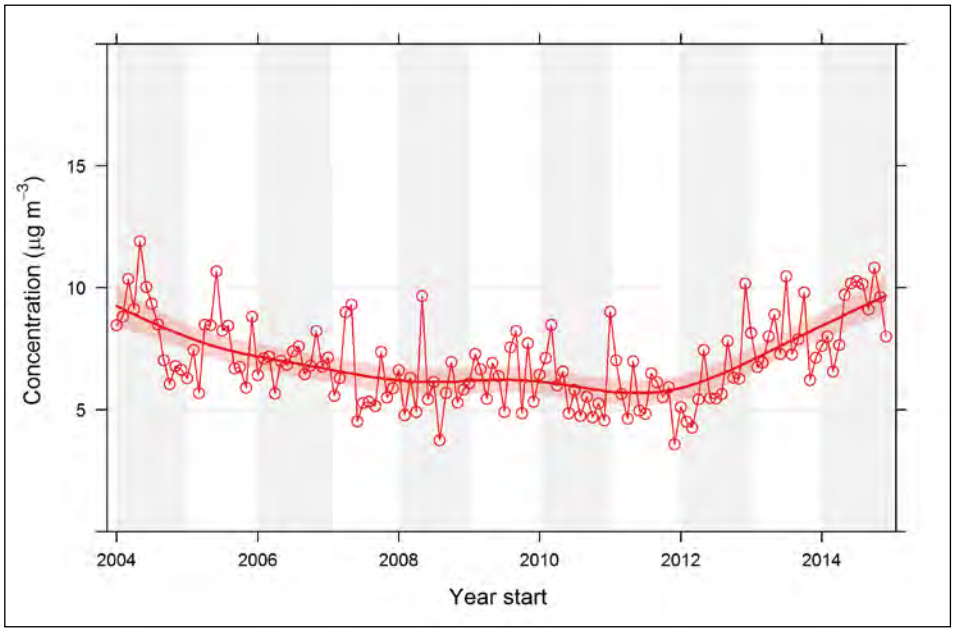

Figure F-18 Monthly mean $PM_{2.5}$ concentration at OEH Chullora monitoring site

F.6.5.3 24-hour mean concentration

The maximum 24-hour mean $PM_{2.5}$ concentrations at the three long-term $PM_{2.5}$ monitoring sites are shown in Figure F-19. There has been no systematic trend in the maximum value, although there appears to have been a general increase between 2006 and 2014. As with the annual mean $PM_{2.5}$ concentrations, the maximum one-hour concentrations are very close to or above the advisory reporting standard in the AAQ NEPM of 25 µg/m^3.

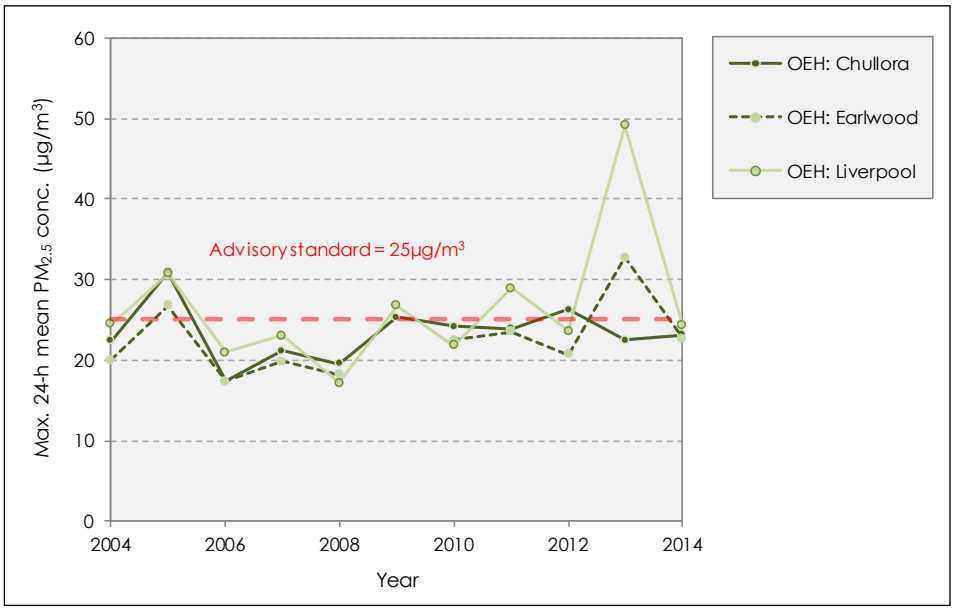

Figure F-19 Trend in maximum 24-hour mean $PM_{2.5}$ concentration

F.6.5.4 Exceedances of air quality criteria

As noted earlier, there there have been some exceedances of the NEPM advisory reporting standard for annual mean $PM_{2.5}$ of 8 µg/m^3, and these seem to be more likely in the future given the change in monitoring method. Table F-14 summarises the exceedances of the 24-hour criterion of 25 µg/m^3.

Table F-14 Exceedances of advisory 24-hour $PM_{2.5}$ standard

Year	Number of exceedances of advisory 24-hour standard per year (25 µg/m^3)						
	Chullora	Earlwood	Lindfield	Liverpool	Prospect	Randwick	Rozelle
2004	0	0	-	0	-	-	-
2005	**3**	**2**	-	**2**	-	-	-
2006	0	0	-	0	-	-	-
2007	0	0	-	0	-	-	-
2008	0	0	-	0	-	-	-
2009	**1**	0	-	**1**	-	-	-
2010	0	0	-	0	-	-	-
2011	0	0	-	**1**	-	-	-
2012	**1**	0	-	0	-	-	-
2013	0	**2**	-	**4**	-	-	-
2014	0	0	-	0	0	-	-

F.6.6 Air toxics

Fewer data were available to characterise the concentrations of air toxics in Sydney. The main sources of data were the following:

- An Ambient Air Quality Research Project that was conducted between 1996 and 2001 (NSW EPA, 2002). The project investigated concentrations of 81 air toxics, including dioxins, VOCs, PAHs and heavy metals. More than 1,400 samples were collected at 25 sites. Three air toxics – benzene, 1,3-butadiene and benzo(α)pyrene – were identified as requiring ongoing assessment to ensure they remain at acceptable levels in the future.
- An additional round of data collection between October 2008 and October 2009. The five NEPM air toxics and additional VOCs were monitored at two sites in Sydney:
    - Turrella: formaldehyde, acetaldehyde, 19 PAHs including benzo(a)pyrene, and 41 VOCs including benzene, toluene and xylenes.
    - Rozelle: formaldehyde, acetaldehyde, 41 VOCs including benzene, toluene and xylenes.

  This study collected 24-hour concentrations of formaldehyde, acetaldehyde, and 34 organic compounds every sixth day, and 19 PAHs at one location on the same days. Sixty-one samples were collected at each location during the sampling period.

The findings of the studies were summarised by NSW DECCW (2010), and some results for selected pollutants are given in Table F-15. In the 1996-2001 monitoring campaign the concentrations of most compounds were very low. Some 23 compounds were not, or rarely, detected. Annual average concentrations of benzene were below the Air Toxics NEPM investigation level (0.003 ppm or 3 ppb) at all sites. The maximum annual concentrations of toluene and xylenes were less than 5 per cent of the investigation levels, and maximum 24-hour concentrations were less than 2 per cent and 4 per cent of the investigation levels respectively. The 2008-09 monitoring campaign also found low concentrations of all compounds, with many observations below detection limits. Concentrations of the five pollutants in the Air Toxics NEPM were low compared to the respective investigation levels.

The concentrations of the pollutants in Table F-15 generally halved between the two campaigns. Improved engine technology and a greater proportion of the vehicle fleet being fitted with catalysts reduced emissions from road vehicles. Benzene concentrations showed a larger decrease as a result

of a reduction in the maximum allowed benzene concentration in automotive fuels (NSW DECCW, 2010).

Table F-15 Average concentrations of selected organic pollutants

Pollutant	Concentration (ppb)				
	1996-2001			2008-2009	
	Sydney CBD	Rozelle	St Marys	Turrella	Rozelle
Benzene	2.3	1.1	0.4	0.4	0.3
Toluene	4.2	2.2	0.8	1.8	0.9
Xylene (m + p)	2.2	1.0	0.4	0.7	0.5
Xylene (o)	0.8	0.4	0.1	0.3	0.2
1,3-butadiene	0.4	0.2	0.1	<0.1	<0.1

Source: (NSW DECCW, 2010)

In the 2008-2009 campaign the highest benzo(a)pyrene concentration was 0.4 ng/m^3, and the average for the year was 0.12 ng/m^3. Concentrations of formaldehyde were low: the highest concentration was only 11 per cent of the investigation level (NSW DECCW, 2010).

The results clearly showed levels of air toxics were below the monitoring investigation levels, and well below levels observed in overseas cities. There were no occasions on which any of the air toxics monitored exceeded the monitoring investigation levels at any location. The results for benzo(a)pyrene, with levels of approximately 65 per cent of the NEPM monitoring investigation level, were the most significant (NEPC, 2011b).

F.7 Bivariate polar plots

F.7.1 Overview

Polar plots for each of the OEH monitoring sites were created using the *Openair* software. Whilst these plots were not used directly in the determination of the background concentrations for the M4 East project, they did assist in the understanding of differences between pollutant concentrations at the different sites.

Some examples of polar plots are shown in Figure F-20. These indicate how concentrations vary by wind speed and wind direction, with statistical smoothing techniques giving a continuous surface. The monitoring station is located at the centre of each plot. The axes show the directions from which the wind is coming, and the distance from the origin indicates the wind speed; the further from the centre that concentrations appear, the higher the wind speeds when they were measured. Calm conditions appear close to the centre. The examples are for a secondary pollutant – ozone – which tends to be distributed quite evenly in space, and hence there are few strong features in the plot. The Figure does show, however, that ozone formation is greatest in the summer months.

The polar plot is a useful diagnostic tool for understanding potential sources of air pollutants at a given site. For many situations an increasing wind speed generally results in lower concentrations due to increased dilution through advection and increased turbulence. Ground-level, non-buoyant sources - such as road traffic – therefore tend to have highest concentrations under low wind speed conditions, but various processes can lead to other concentration-wind speed dependencies. For example, buoyant plumes from tall outlets can be brought down to ground level, resulting in high concentrations under high wind speed conditions. Wind-blown dust (*e.g.* from exposed areas of soil) also increases with increasing wind speed, and particle suspension can be important close to coastal areas where higher wind speeds generate more sea spray (Carslaw, 2015).

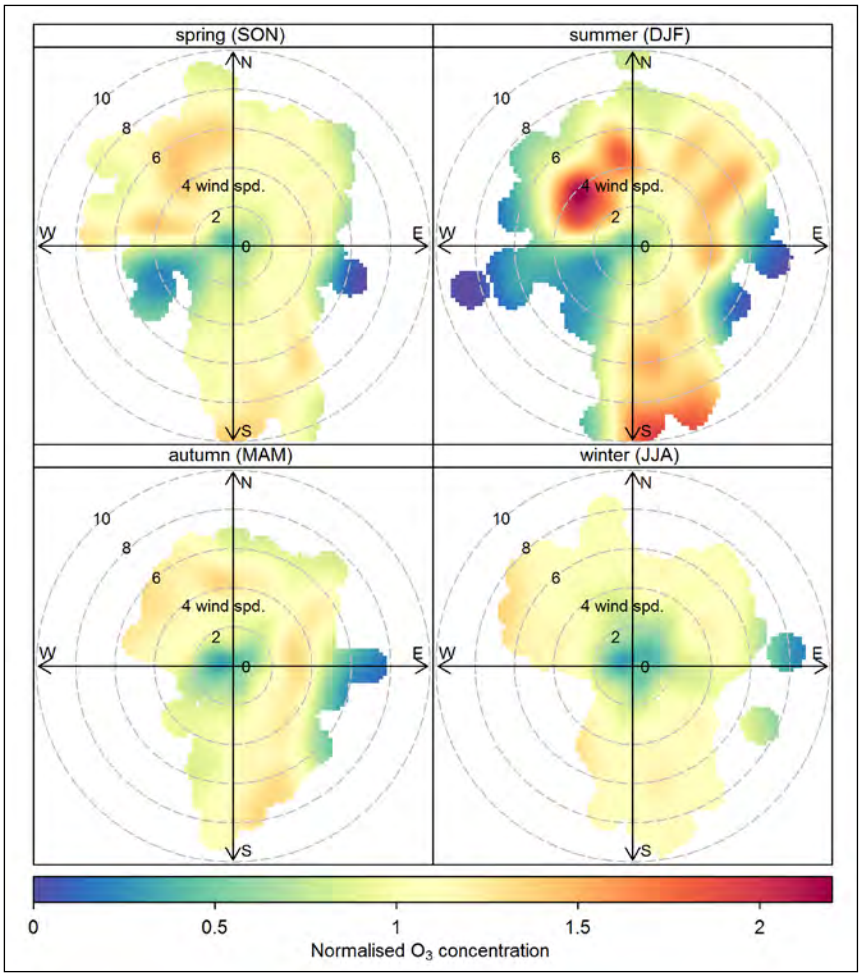

Figure F-20 Polar plots of normalised ozone concentration by season at Rozelle

Some typical features of polar plots include the following:

- A maximum concentration, or a 'smeared' peak, at low wind speed, which is indicative of a local, ground-level source such as road traffic. As the wind speed increases concentrations due to a road source will tend to decrease due to the increased dilution of the plume.
- Highly resolved features at high wind speeds, but possibly low concentrations, which indicate more distant sources.
- Relationships between pollutants which provide information on the emission characteristics of different sources. For example, a site with high 'smeared' NO_X concentrations at low wind speeds, is likely to be a nearby road.

The Openair polar plots for the OEH sites have been interpreted below. Each plot is based upon all the available data for the period 2004-2014, and the concentrations have been normalised to permit easier comparison. The interpretation is qualitative, and to some degree speculative.

F.7.2 Chullora

The polar plots for the Chullora site are shown in Figure F-21. The plots for CO, NO_X and NO_2 show strong similarities, with the highest concentrations occurring for low wind speeds and a tendency for elevated concentrations along a broad north-south wind direction axis. There also appears to be a source of these pollutants to the east. The similarities between these plots indicate a common combustion source - probably the local road network.

The plots for O_3 and NO_X show the well-established inverse relationship between these pollutants. This is also apparent in the data from the other OEH monitoring sites, and is not commented upon further.

The patterns for CO and NO_X do not show up strongly in the PM_{10} and $PM_{2.5}$ plots. This is likely to be due to contributions from several other sources of PM. PM_{10} concentrations appear to be influenced by a source to the west of the monitoring site under high wind speeds. This may be wind-blown dust from open land to the west of the site. $PM_{2.5}$, on the other hand, is more evenly distributed (probably reflecting the secondary PM contribution), although there is a strong source to the south-east under high wind conditions.

There were no strong seasonal influences in the polar plots for the Chullora site.

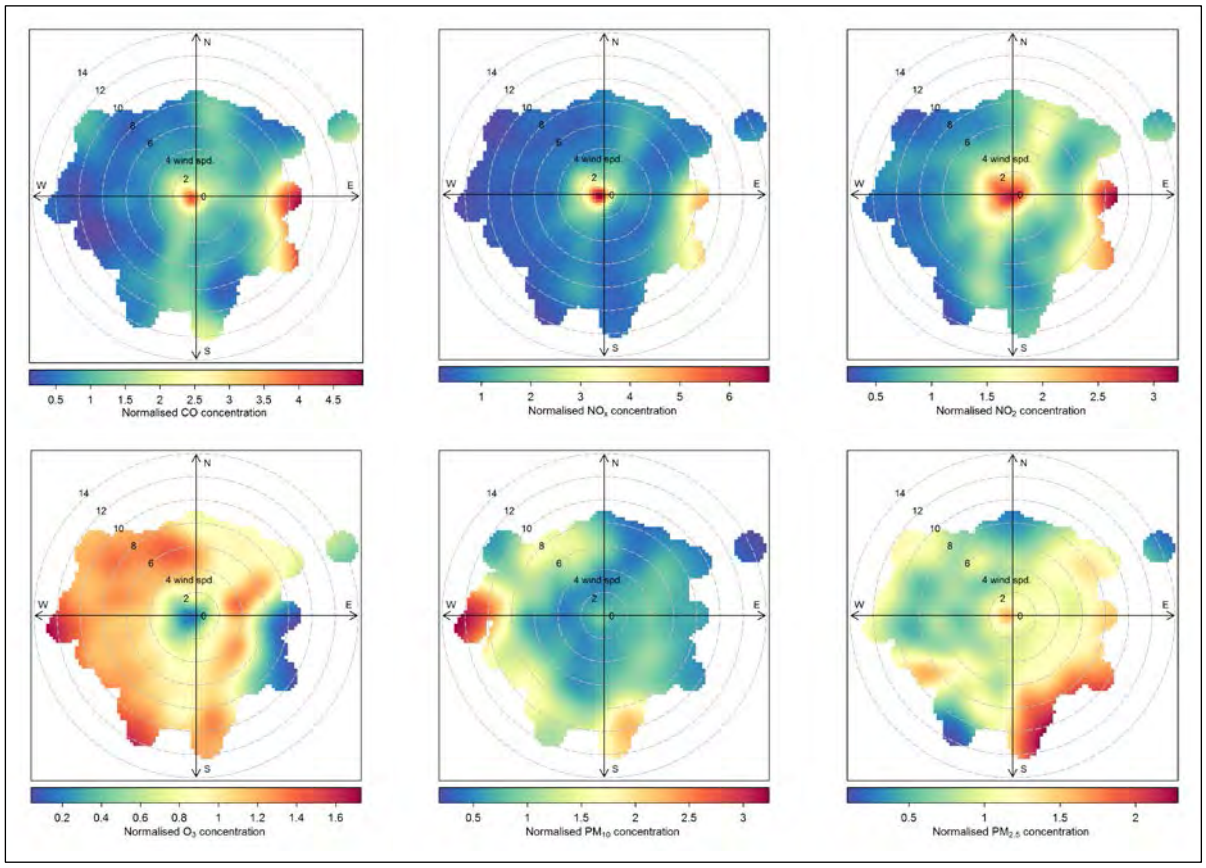

Figure F-21 Polar plots – Chullora, normalised

F.7.3 Earlwood

The polar plots for the Earlwood site are shown in Figure F-22. These plots have relatively simple patterns. NO_X and NO_2 concentrations are highest when the winds are strong and from an easterly direction. The seasonal data showed that this influence was especially strong during winter, hinting strongly that this is an effect of combustion for heating purposes.

PM_{10} concentrations are highest when the winds are strong and from a westerly direction (especially in winter and spring). $PM_{2.5}$ concentrations, while more evenly distributed than PM_{10}, are high when the winds are strong from a southerly direction (especially in summer). The reasons for these patterns were not clear, but different sources and effects are evidently influencing PM_{10} and $PM_{2.5}$.

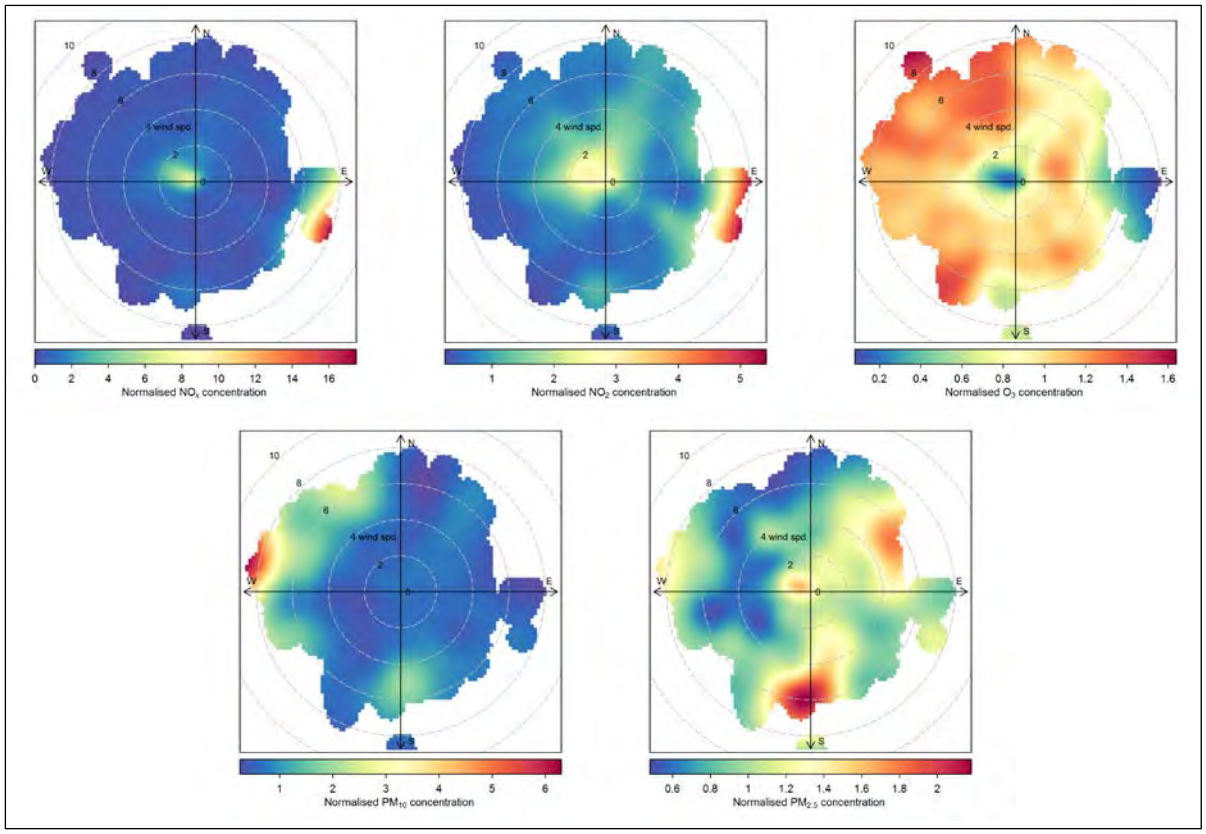

Figure F-22 Polar plots – Earlwood, normalised

F.7.4 Lindfield

In Figure F-23, The smeared NO_X and NO_2 concentrations at the plot origin indicate the presence of a local ground-level source, as well as a broad source further afield to the north. This probably reflects the population distribution around the monitoring sire. There is also an influence further way and to the west, which may be the M2 Motorway and Lane Cove Road.

PM_{10} concentrations are high when there is a strong westerly wind. This may be due to wind-blown dust from the open land immediately to the west of the monitoring site.

There are no strong seasonal effects at the Lindfield site, apart from higher concentrations from the west under high wind speed conditions in spring, and higher concentrations from the south under high wind speed conditions in the summer. It is not clear what is responsible for these effects.

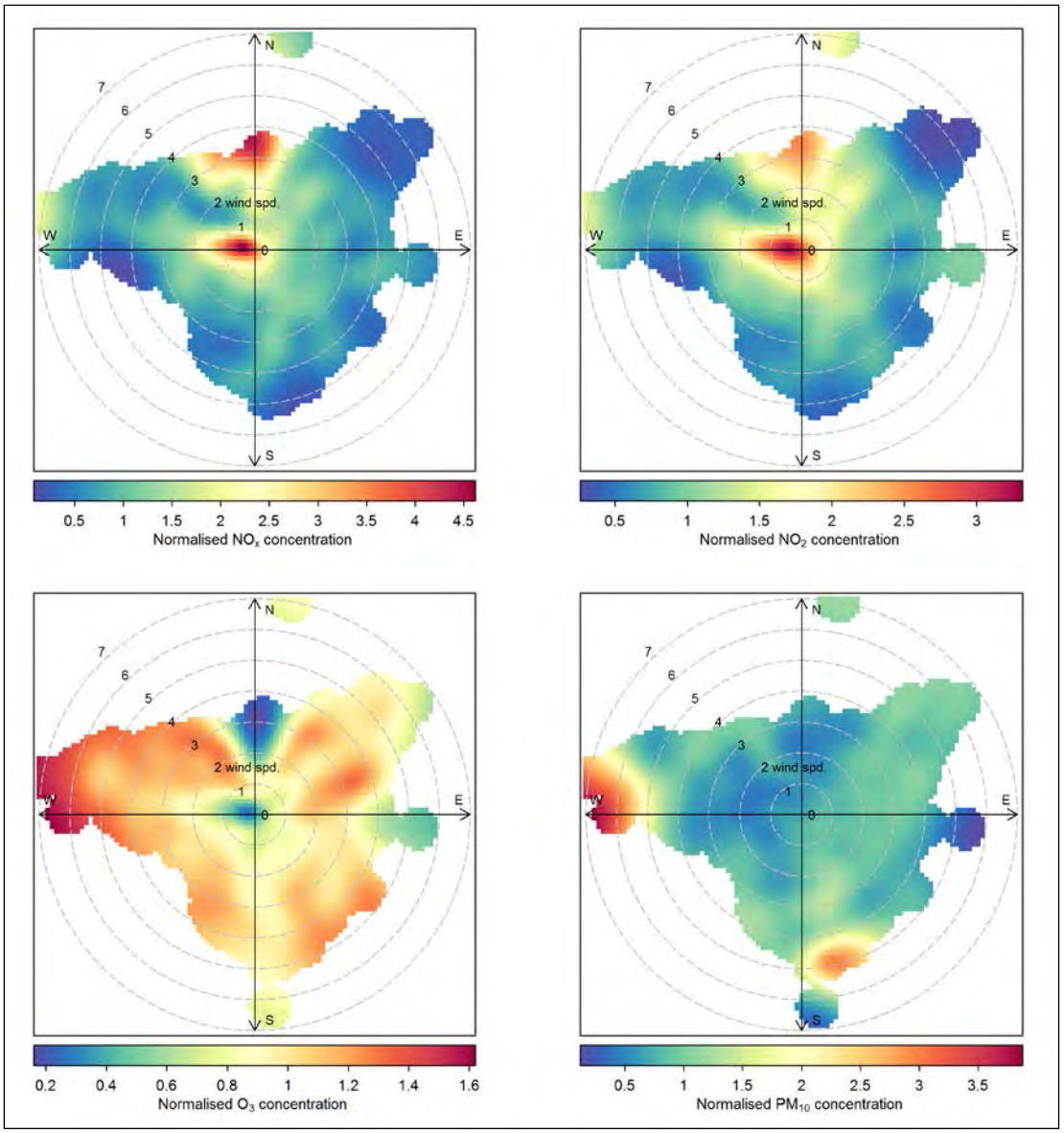

Figure F-23 Polar plots – Lindfield, normalised

F.7.5 Liverpool

At the Liverpool monitoring site the concentrations of CO, NO_X, NO_2 and $PM_{2.5}$ for low wind speeds are not particularly high (Figure F-24). There is, however, a distinct influence form a north-westerly direction, indicating a common combustion source. This may involve a contribution from Hoxton Park Road. However the effect is most prominent in winter, and this is more indicative of combustion for heating purposes, probably from the commercial centre of Liverpool. The M5 Motorway, around 500 m south of the monitoring site, does not appear to have a significant influence on the measured concentrations.

PM_{10} concentrations are influenced by a source to the north-north-west of the monitoring site, but only under strong wind conditions and during the winter months. Again, this coincides with open land to the north-west of the site, and could be a result of wind-blown dust.

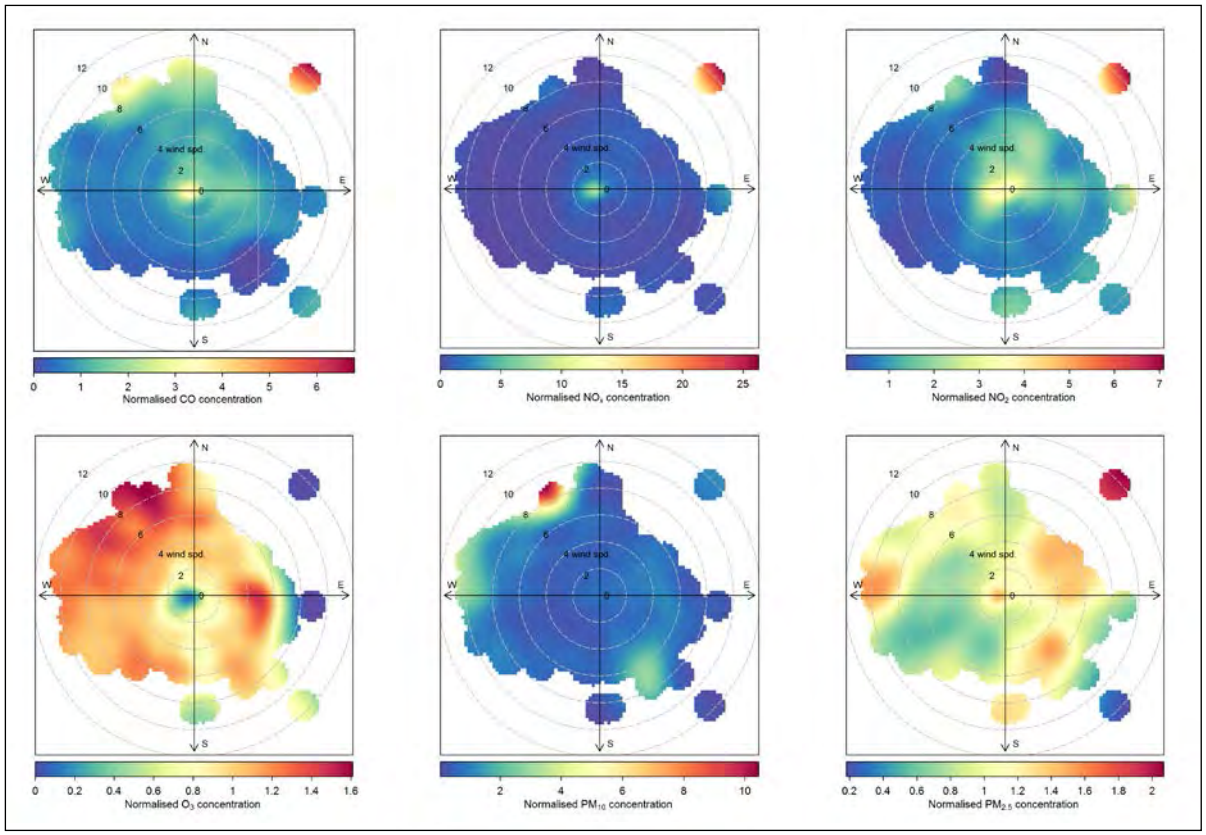

Figure F-24 Polar plots – Liverpool, normalised

F.7.6 Prospect

Concentrations of CO, NO_X and NO_2 at the Prospect site (Figure F-25) are highest when wind speeds are low, and the high concentration are almost centred on the monitoring station. There are, however, sources of NO_X to the east and south-east under high wind speeds. This may be associated with the transport of NO_X from major roads in the area, although these are some distance away (Prospect Highway, 500 m to the east; Great Western Highway, 800 m to the south; M4 Motorway, 1.2 km to the south). There is no strong seasonal influence on NO_X at the site, suggesting that it is not related to combustion for heating purposes.

PM_{10} seems to be strongly influenced – under high winds - by sources which are spread out quite widely to the west of the monitoring site. As at the other sites, this may be due to wind-blown dust from the open land, gravel and sand areas adjacent to the site.

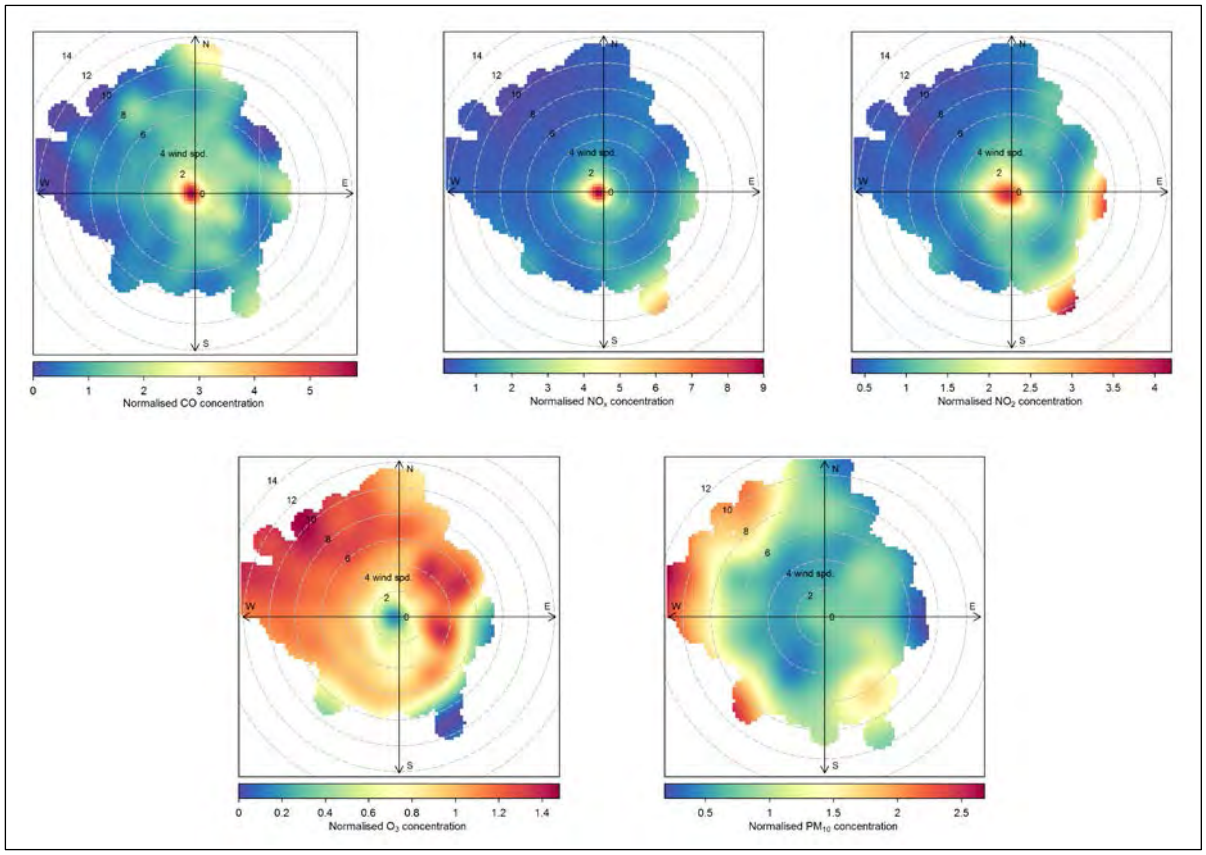

Figure F-25 Polar plots – Prospect, normalised

F.7.7 Randwick

At the Randwick site, NO_X and NO_2 concentrations are highest when the wind speed is low and the wind is coming from the west, with dispersion under stronger winds. There is no seasonal effect in the polar plot for NO_X. This indicates the presence of a road near to the monitoring site, which could be Anzac Parade and/or Avoca Street. Sydney Airport, around 5 km to the west of the monitoring site, may also be affecting NO_X concentrations in this area.

The PM_{10} plot for Randwick shows that the highest concentrations occur when the wind speed is high and is blowing from three distinct directions. Given that these directions coincide with open land and land under development, this seems to be a confirmation that high PM_{10} concentrations are associated with wind-blown dust from local sources.

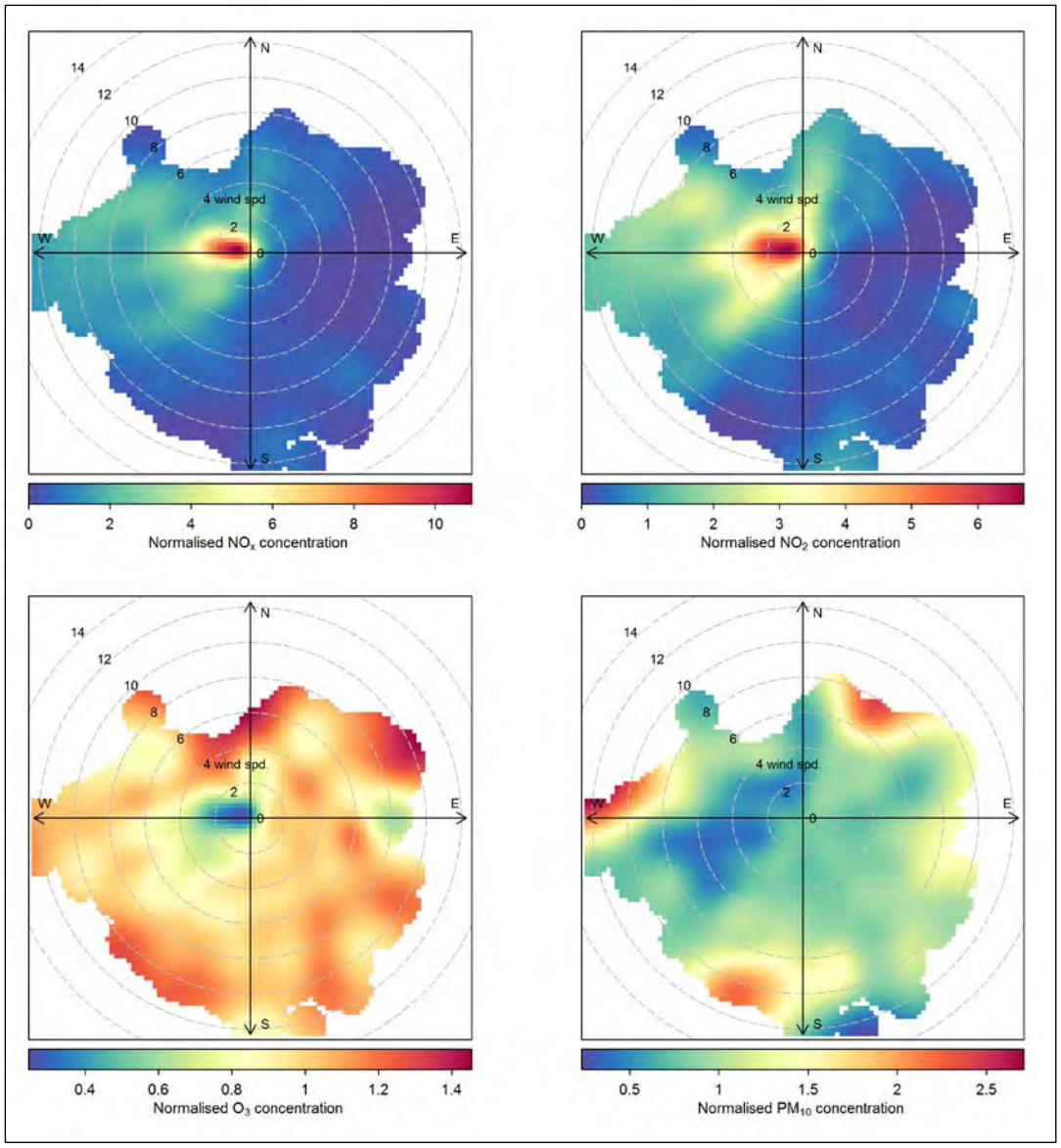

Figure F-26 Polar plots – Randwick, normalised

F.7.8 Rozelle

The polar plot for CO at the Rozelle site indicates that there are multiple combustion sources affecting the site. These are likely to be associated with the University of Sydney campus immediately to the south-west, and roads within 500 m (Victoria Road to the north-east, and Darling Street to the south-west).

The highest NO_X/NO_2 concentrations occur when winds are along an east-west axis, which suggests contributions from the University campus and residential areas. The peak associated with easterly winds may also be linked to Victoria Road.

The highest PM_{10} concentrations at the monitoring site are associated with strong southerly winds, especially in summer. As at the other OEH monitoring sites, this seems to be due to wind-blown dust from open land to the south of the Rozelle site.

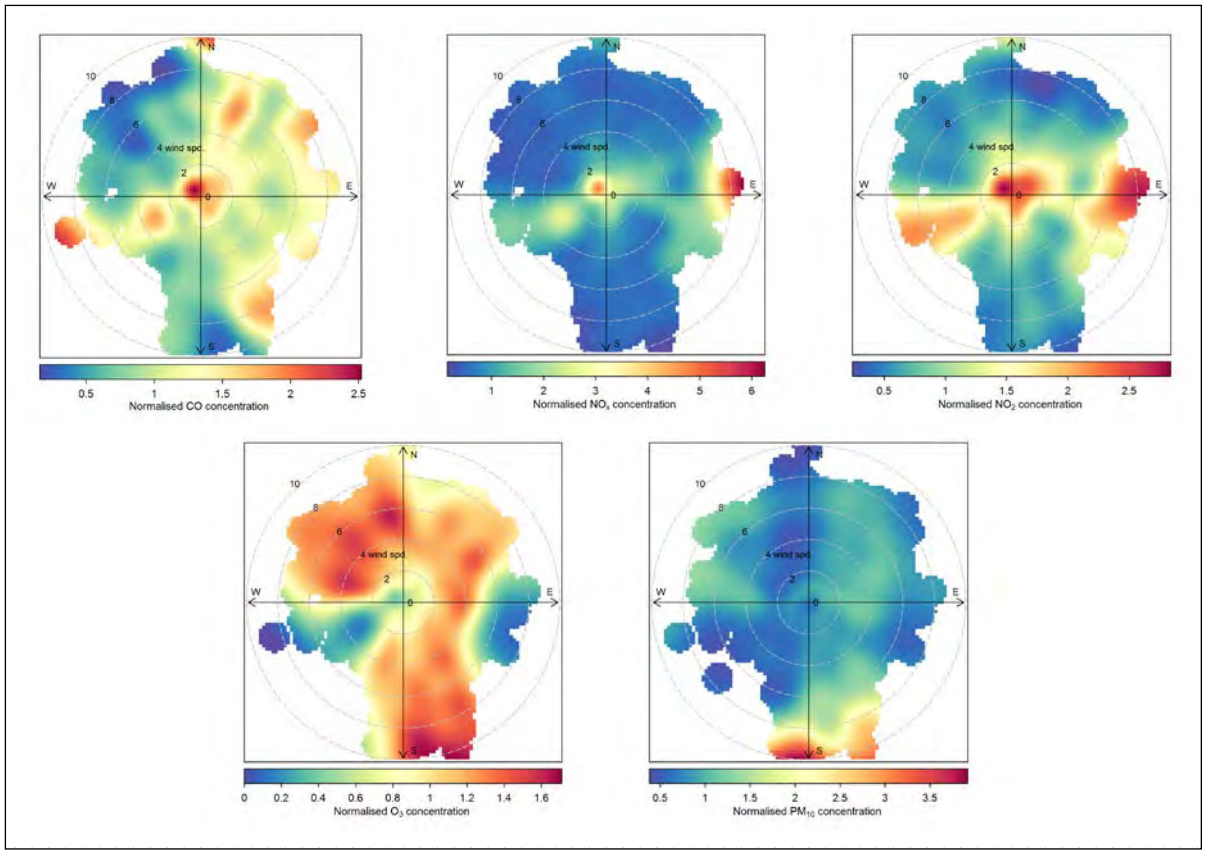

Figure F-27 Polar plots – Rozelle, normalised

F.8 Results for project-specific background monitoring site

The measurements from the project-specific background monitoring site at St Lukes Park were compared with those from the OEH monitoring stations, the aim being to assess the general representativeness of the data from the OEH sites for the M4 East study area. The measurements were compared on a month-by-month basis for the period between August 2014 and April 2015[5], and the following statistics were calculated for each pollutant:

- The monthly mean concentration.
- The maximum concentration in a month (for a relevant metric).
- The 98th percentile of concentrations in a month (again, for a relevant metric). The 98th percentile was considered as it is more stable than the maximum.

Hourly mean concentrations from the OEH monitoring sites were acquired for the period to the end of 2014, and therefore some of the statistics for these sites in 2015 could not be calculated. However, some mean and maximum values were obtained for the months in 2015 from the OEH web site. This explains the gaps in the time series.

The comparsions are shown in Figure F-28 to Figure F-30. Each graph includes the mean value for the OEH urban background monitoring stations (grey line) and the range of values for the OEH stations (grey shading). The values at the project background site at St Lukes Park shown by the blue line.

[5] The site remains operational.

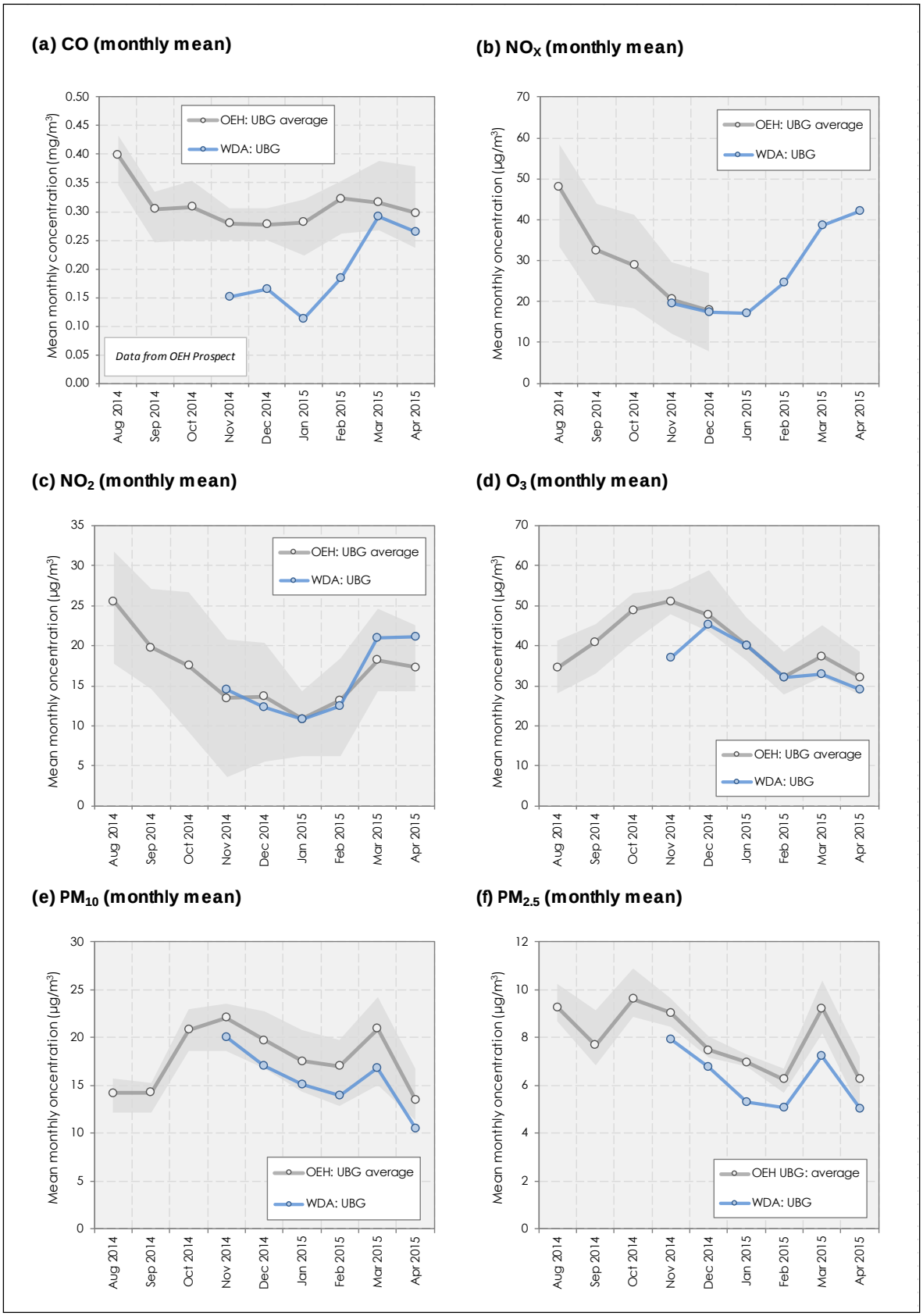

Figure F-28 **Mean concentrations at WDA M4 East monitoring sites (grey shading shows range of values at OEH sites)**

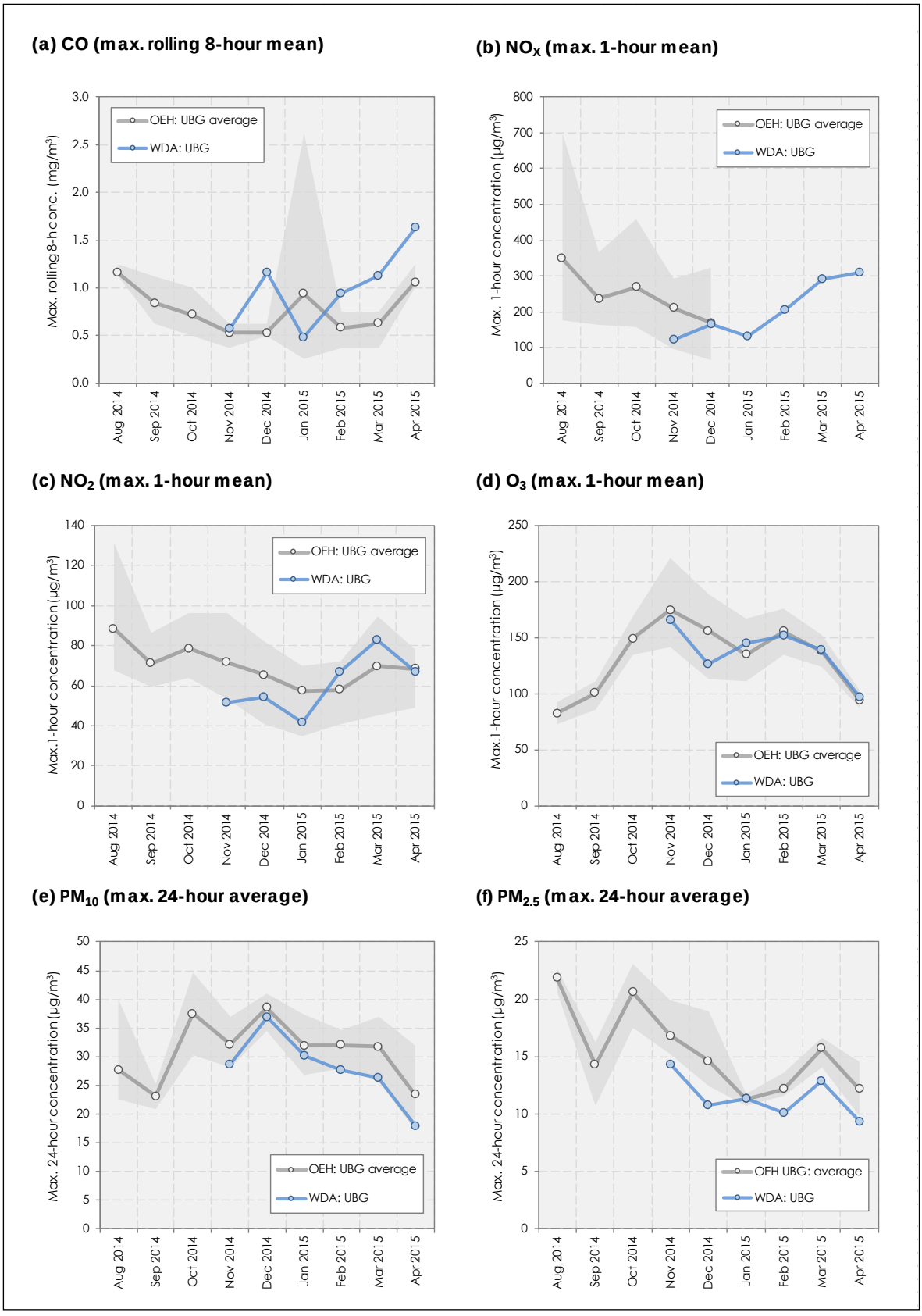

Figure F-29 **Maximum concentrations at WDA M4 East monitoring sites (grey shading shows range of values at OEH sites)**

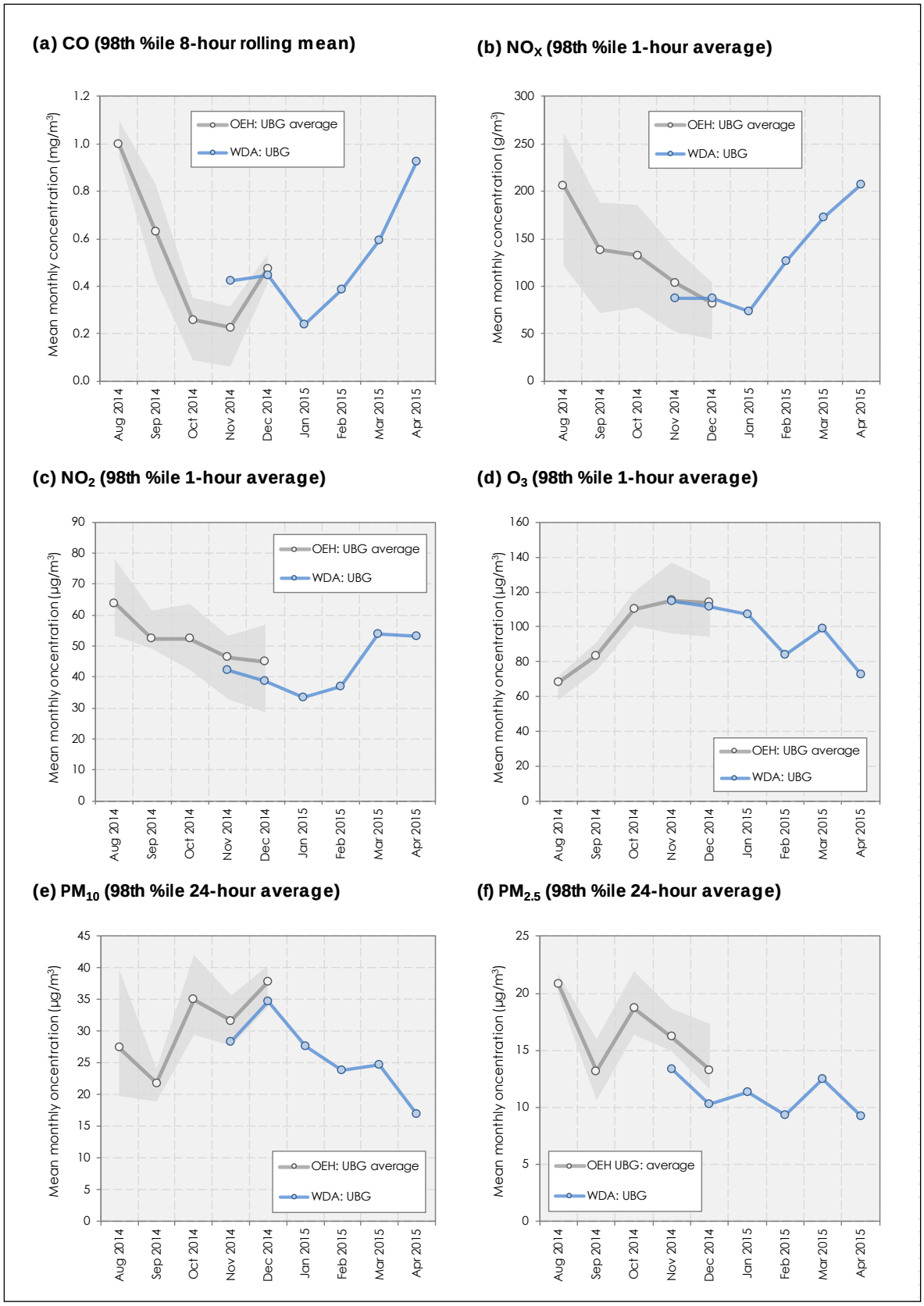

Figure F-30 **98th percentile concentrations at WDA M4 East monitoring sites (grey shading shows range of values at OEH sites)**

The monthly mean values at the OEH sites generally showed a good agreement with the mean values at the project background site. The main exception was CO, for which concentrations at the OEH sites were higher than those at the project site, although there was a good agreement in March and April of 2015. NO_x and NO_2 concentrations at the OEH sites were very similar to those at the project background site. For ozone the results were mixed, but the most recent results agreed very well. Monthly mean PM_{10} and $PM_{2.5}$ concentrations at the OEH sites were slightly higher than those at the project site. These conclusions were similar if either all OEH sites were included, or only those sites near to WestConnex (Chullora, Earlwood, Rozelle) were used.

The was also, generally speaking, a good agreement between the maximum and 98th percentile values at the OEH sites (on average) and those at the project site.

It was concluded from this comparison that the OEH monitoring sites were broadly representative of background locations in the M4 East study area, and that it was appropriate to use the dats from the OEH sites to define background air quality for the assessment (see Section G9). The concentrations at the OEH sites were generally equivalent to, or slightly higher than, those at the project monitoring site. For some pollutants this would introduce a small safety margin in the modelling.

F.9 Assumed Background concentrations

F.9.1 General approaches in M4 East assessment

Various approaches have been used in previous air quality assessments to define long-term (annual mean) and short-term (*e.g.* 1-hour, 24-hour) background concentrations. The selection of a suitable method is strongly dependent on the quantity and quality of available data. The general approaches used in the M4 East assessment are introduced below. The specific approaches for the various pollutants and metrics are then described in the subsequent Sections.

F.9.1.1 Annual mean concentrations

In the case of annual mean concentrations (such as those for PM_{10} and $PM_{2.5}$) it is relatively straightforward to define background values. For smaller projects it has often been sufficient to use a single background value, and to assume that this is representative of the whole study area. However, for a project such as WestConnex, which covers a large geographical area and features different types of land use, it was considered important to allow for spatial variation in annual mean concentrations where possible. Maps of background annual mean concentrations of some pollutants were therefore developed for the WestConnex study area. When developing these maps the data from any non-background sites were excluded.

F.9.1.2 Short-term concentrations

It is more difficult to accurately predict short-term concentration peaks, as these vary considerably in magnitude, in time of occurrence, and in location. In some previous assessments a single value has also been used for short-term concentrations, such as the maximum measured 24-hour mean PM_{10} concentration. This is the 'Level 1' method in the NSW Approved Methods. However, such an approach is highly conservative, and results in unrealistically high cumulative concentrations; it is very unlikely that the maximum background values will coincide in space and time with the maximum predicted values. The approach was therefore not used for the M4 East project.

The approach used for the M4 East assessment was broadly consistent with the 'Level 2' method in the Approved methods. This requires that existing background concentrations of a pollutant in the vicinity of a proposal should be included in the assessment as follows (NSW DEC, 2005):

- At least one year's worth of continuous ambient pollutant measurements should be obtained for a suitable background site. The background data should be contemporaneous with the meteorological data used in the dispersion modelling.
- At each receptor, each individual dispersion model prediction is added to the corresponding measured background concentration (*e.g.* the first hourly average dispersion model prediction is added to the first hourly average background concentration) to obtain total hourly predictions.
- At each receptor, the maximum concentration for the relevant averaging period is determined.

The unstated assumption is that one of the paired project-background concentration combinations will result in a realistic estimate of the maximum concentration that could be expected.

For the M4 East project this approach was applied to the short-term concentration metrics for CO (rolling 8-hour mean), NO_X (1-hour mean), PM_{10} (24-hour mean) and $PM_{2.5}$ (24-hour mean). NO_X was used in place of NO_2 for the reasons given in Appendix H. It would not have been practical to define both the spatial and temporal variation in short-term background concentrations in detail. As the temporal variation is generally more pronounced than the spatial variation, this was considered to be more important. For each short-term air quality metric a synthetic time series of background concentrations was therefore determined.

F.9.2 Carbon monoxide: one-hour mean

The average and maximum CO concentrations at the Chullora monitoring sites were towards the upper end of the range of values observed across all sites, and the values at the Rozelle site were closer to the middle of the range. These two sites were therefore considered to be broadly typical of the WestConnex study area, allowing for a small margin of safety.

Given that there was a slight downward trend in the maximum one-hour mean CO values, the concentrations in 2014 were considered to be appropriate for use in the WestConnex assessment, with the liklihood that the 2014 values would be slightly conservative in future years. Because of the seasonal variation in CO concentrations, a background profile of the rolling one-hour mean CO concentration during 2014 was determined. To maintain a margin of safety a synthetic profile was constructed, with each value for a time period being the maximum of those at the Chullora and Rozelle sites. This profile is shown in Figure F-31.

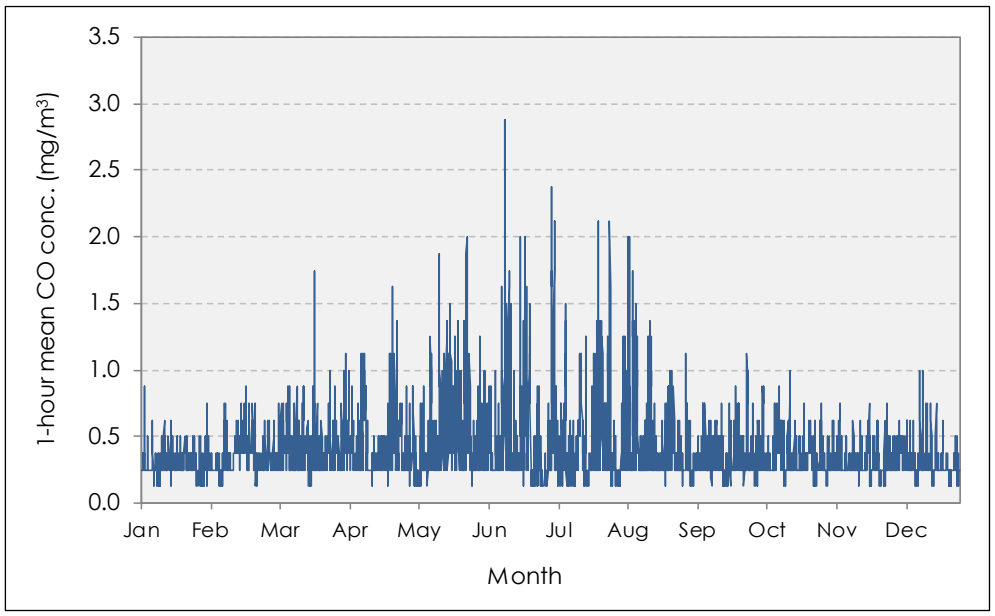

Figure F-31 Synthetic background concentration profile for one-hour mean CO

F.9.3 Carbon monoxide: rolling 8-hour mean

The rationale for the rolling 8-hour mean CO concentration was similar to that for the one-hour mean. A synthetic profile was constructed for 2014, with each value for a time period being the maximum of those at the Chullora and Rozelle sites. This profile is shown in Figure F-32.

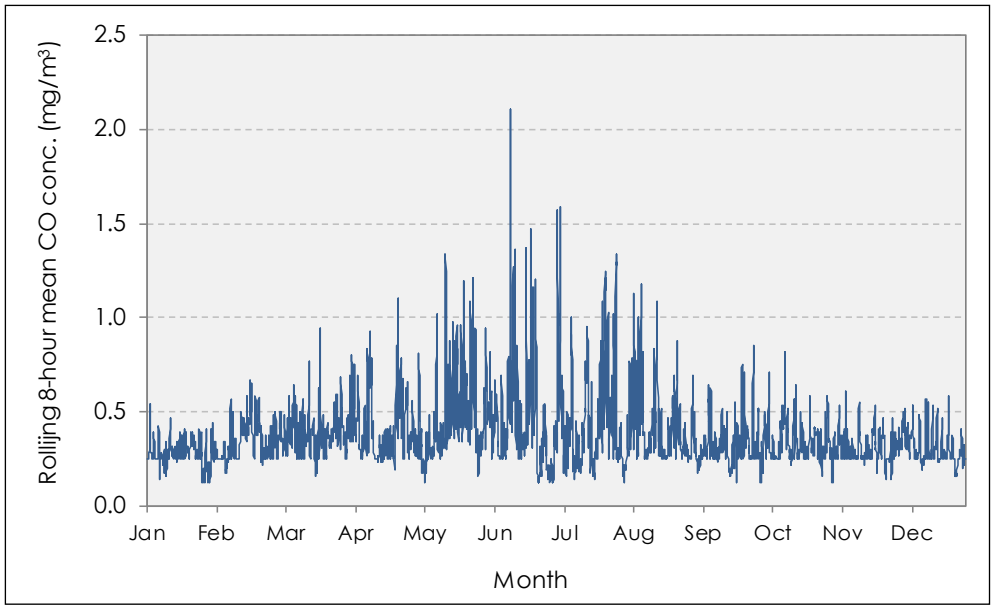

Figure F-32 Synthetic background concentration profile for rolling 8-hour mean CO

F.9.4 NO_X: annual mean

Annual mean concentrations of NO_X at the OEH sites have shown a downward trend in recent years, wheras those at the RMS sites decreased between 2008 and 2011 but have increased in recent years (Figure F-6). On balance, it was considered that the concentrations in 2014 would represent typical (but probably slightly conservative) background concentration going forward into the future. It was also noted earlier that there was quite a systematic spatial pattern in NO_X concentrations.

To allow for this spatial variation, the data from the OEH and RMS background monitoring sites were used to determine a background map for annual mean NO_X across Sydney in 2014, as shown in Figure F-33.

The background map was created in the Golden Software Surfer package using a geostatistical Kriging method, whereby gridded values are interpolated based on the statistical relationship of the surrounding measured values. The RMS site T1 was excluded from the dataset as NO_X concentrations at this location have exhibited a marked upward trend in recent years. The background map shows that there is a general NO_X concentration gradient from the south-west of Sydney to the north-west.

The NO_x map for the full WestConnex modelling (GRAL) domain is shown in more detail in Figure F-34. To determine background NO_X concentrations for discrete receptor locations within the modelling domain that did not coincide with grid nodes, the 'grid residual' function in Surfer was used. This function calculates the difference between the grid value and a specified data value at any X-Y location. By setting the data value for a given X-Y point to zero, it can be used to return the concentration for the point.

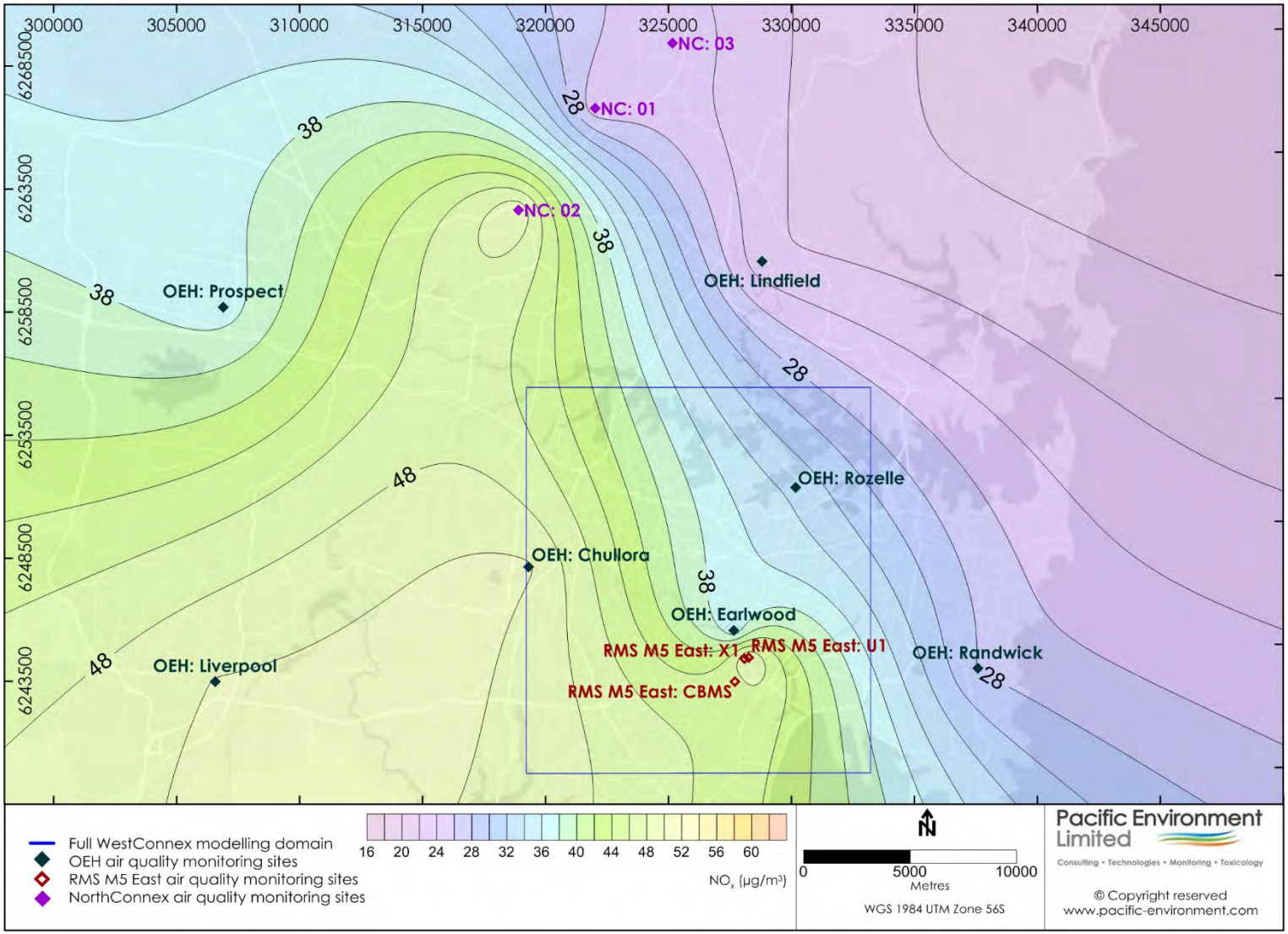

Figure F-33 Background map for annual mean NO_X concentration across Sydney in 2014

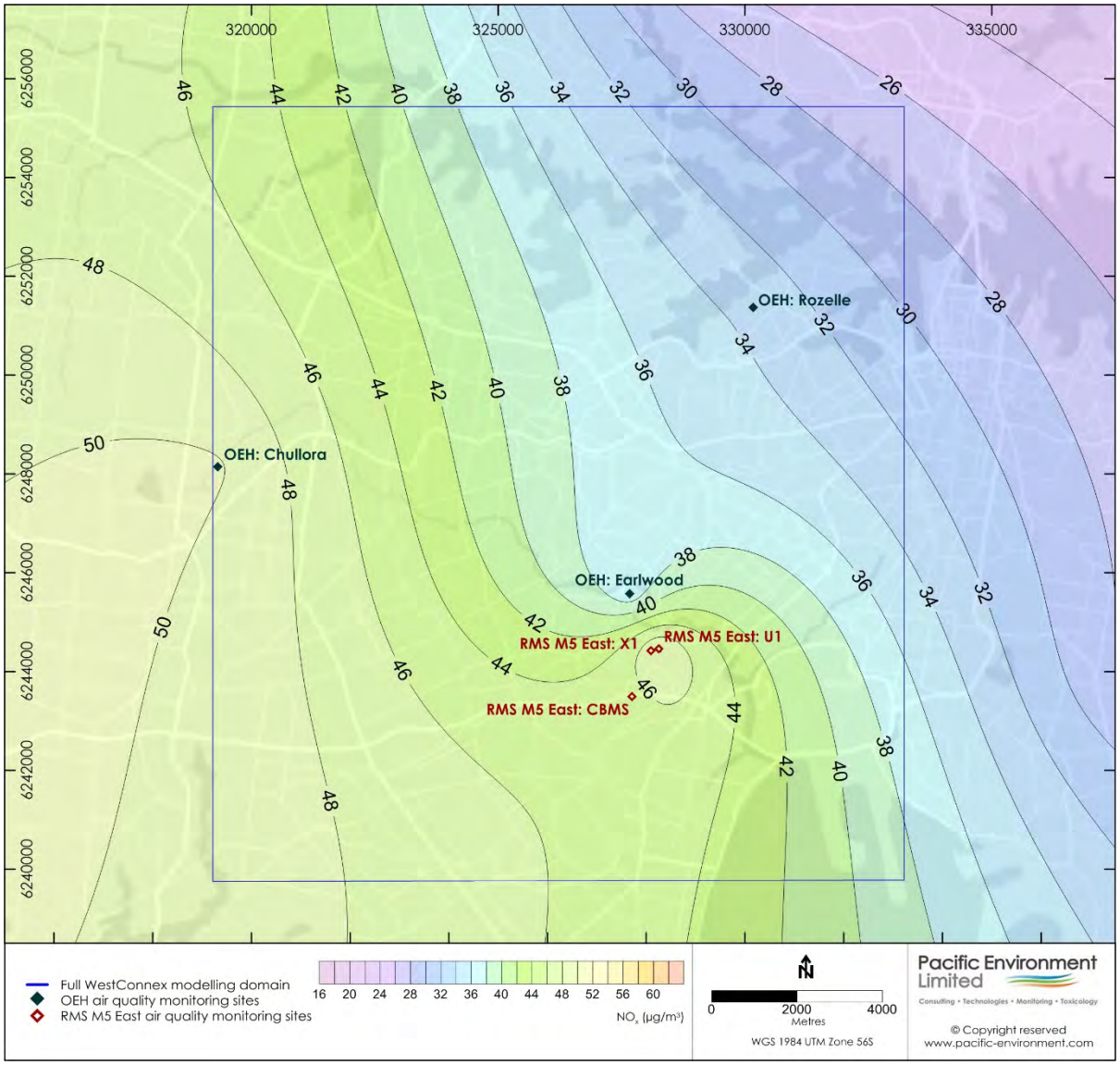

Figure F-34 **Background map for annual mean NO_X concentration in 2014 (detail for WestConnex GRAL modelling domain)**

F.9.5 NO_X: one-hour mean

The approach for one-hour mean NO_X was similar to that used for CO, with a synthetic concentration profile for 2014 being determined to allow for seasonal and spatial variation. Figure F-35 shows examples of one-hour concentration profiles at the OEH Chullora, Earlwood and Rozelle sites during May of 2014. Peak concentrations regularly occurred simultaneously at the three sites, but the concentrations tended to be highest at Chullora and lowest and Rozelle.

Whilst the backgound map for NO_X suggests that the Earlwood site is probably the most representative of the M4 East project, in order to introduce margin of safety the maximum concentration across the three sites in each time step was used to define the background concentration profile for the WestConnex study area in future years. Some filling of gaps was required. Most of the gaps were for single one-hour periods during the night (associated with instrument calibration), and these were filled by linear interpolation. Larger gaps were filled using average values for the month and the hour in the original dataset. Weekdays and weekends were also treated separately. The final concentration profile is shown in Figure F-36.

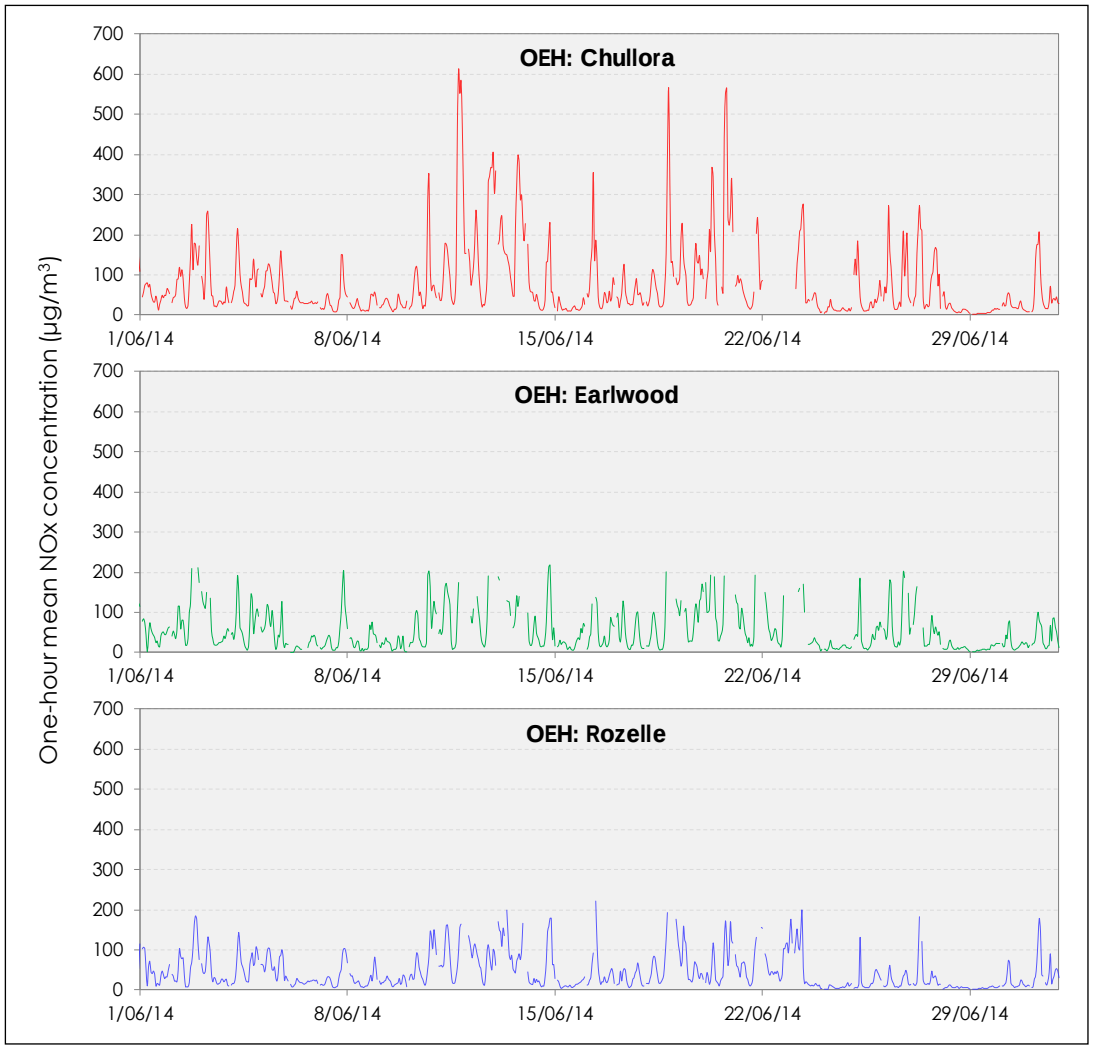

Figure F-35 **One-hour mean NO_X concentration at Chullora, Earlwood and Rozelle (example for May 2014)**

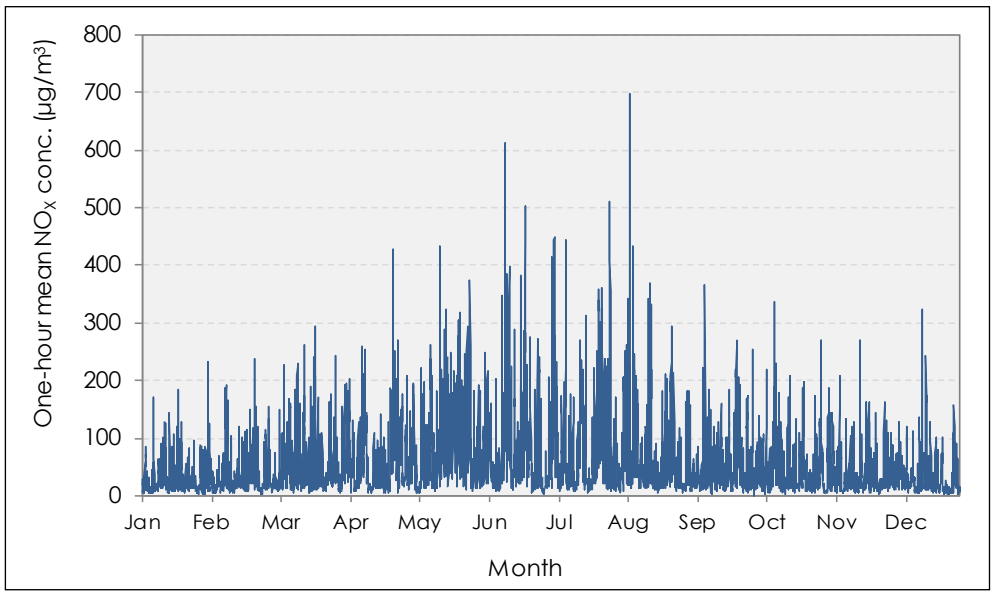

Figure F-36 **Synthetic background concentration profile for one-hour mean NO_X**

F.9.6 NO_2 and O_3

Synthetic background concentration profiles were developed for one-hour mean NO_2 and O_3 concentrations. These were only used to test the empirical NO_X-to-NO_2 conversion methods that were developed for the assessment (Appendix G), and not for the assessment itself. The approach used for NO_X was also applied to NO_2. Figure F-37 shows examples of one-hour concentration profiles at the OEH Chullora, Earlwood and Rozelle sites during May of 2014. The synthetic concentration profile is shown in Figure F-38.

Figure F-39 shows examples of one-hour O_3 concentration profiles at the OEH Chullora, Earlwood and Rozelle sites during May of 2014. The synthetic concentration profile is shown in Figure F-40.

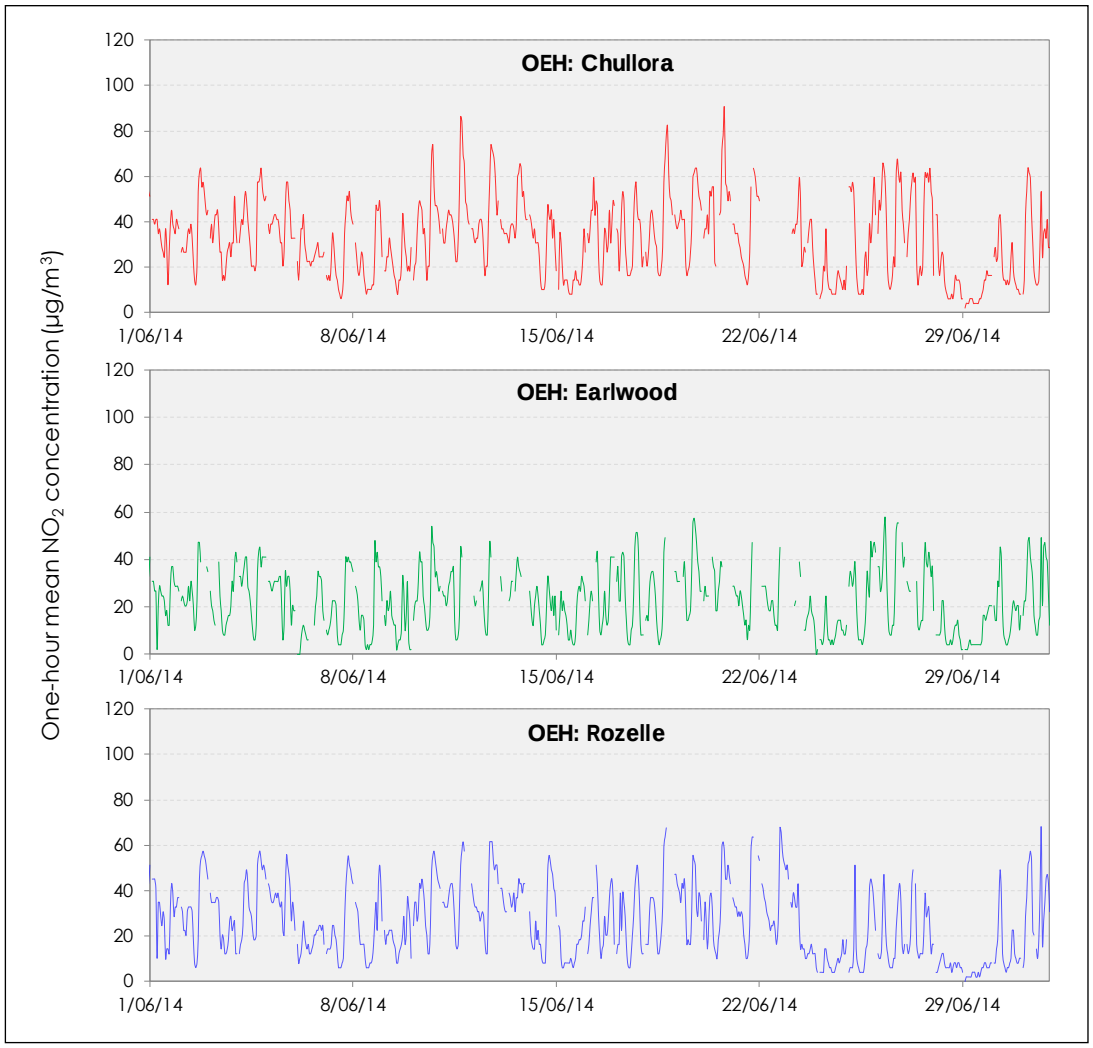

Figure F-37 **One-hour mean NO_2 concentration at Chullora, Earlwood and Rozelle (example for May 2014)**

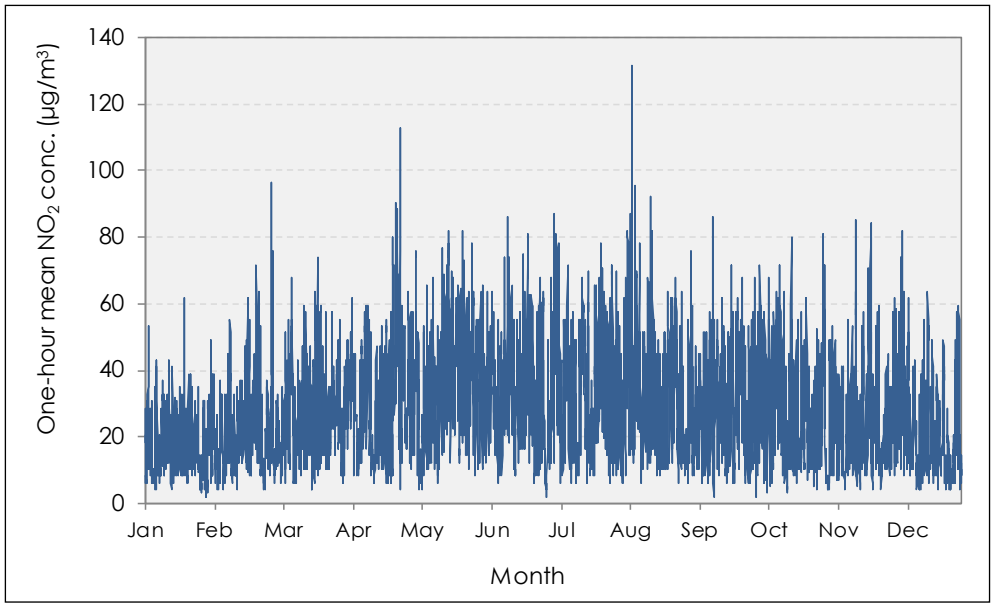

Figure F-38 **Synthetic background concentration profile for one-hour mean NO_2**

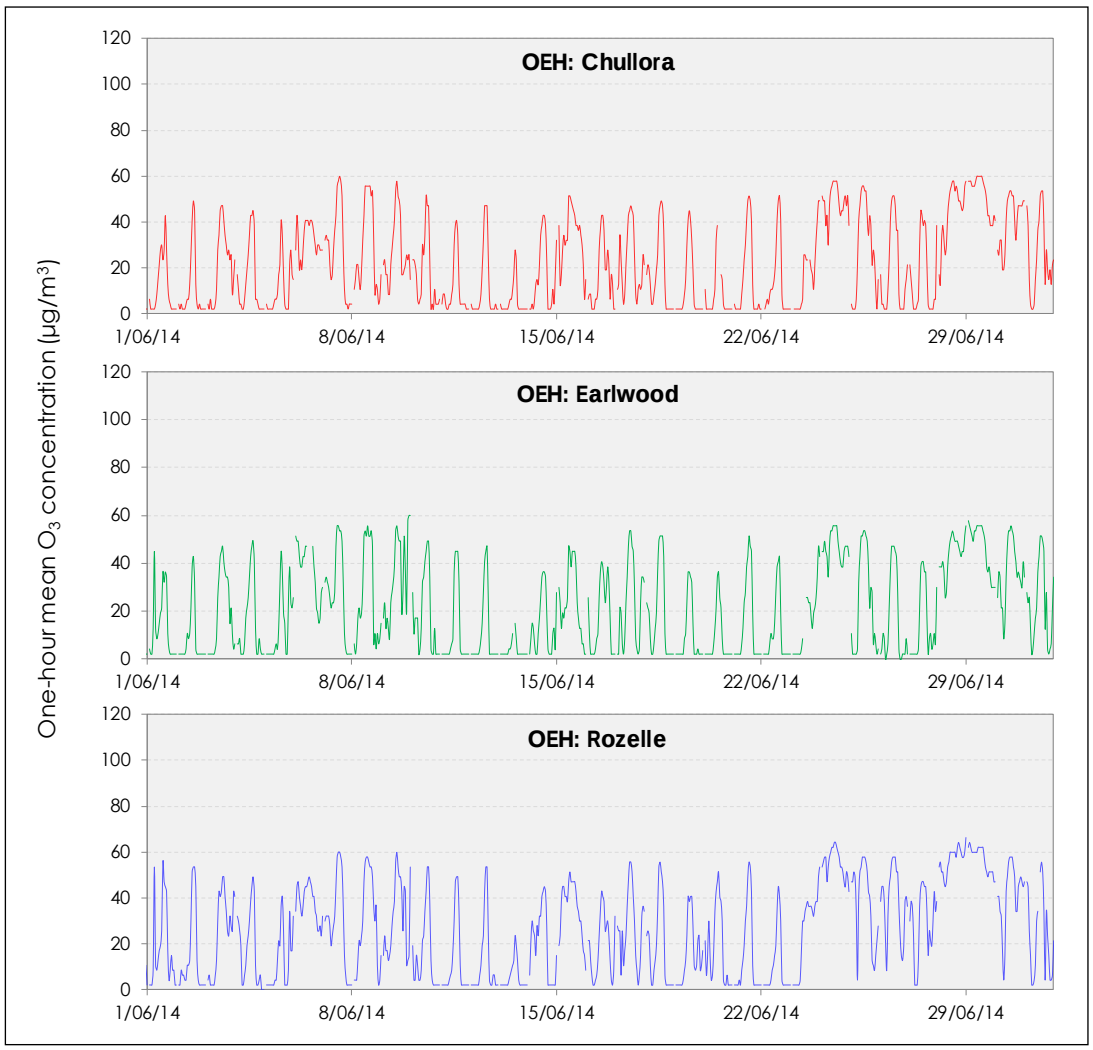

Figure F-39 **One-hour mean O_3 concentration at Chullora, Earlwood and Rozelle (example for May 2014)**

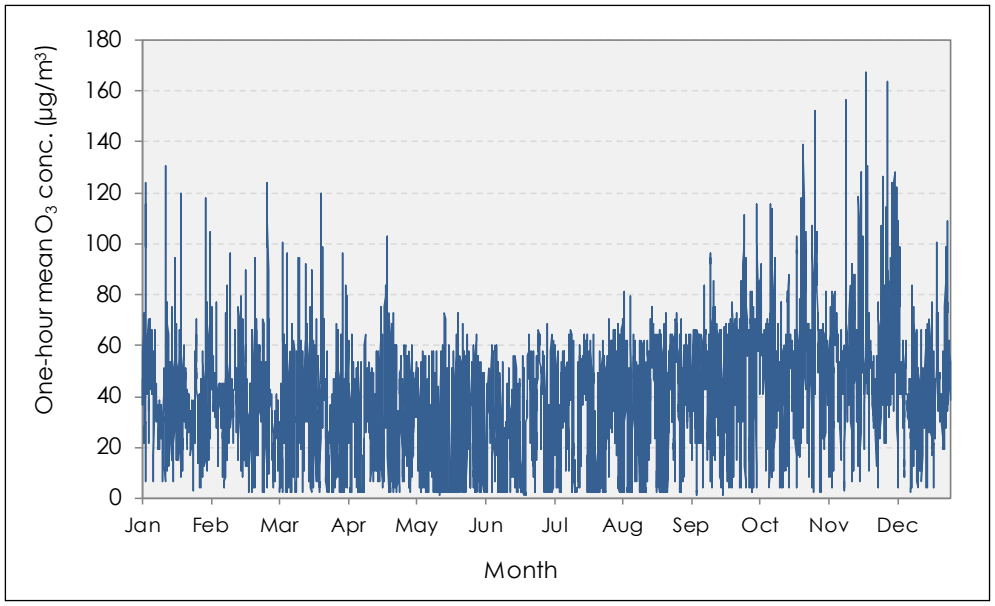

Figure F-40 Synthetic background concentration profile for one-hour mean O_3

F.9.7 PM_{10}: annual mean

The approach for annual mean PM_{10} was the same as that used for annual mean NO_X. The background PM_{10} map for Sydney in 2014 is shown in Figure F-41, and the map for the WestConnex GRAL domain is provided in Figure F-42.

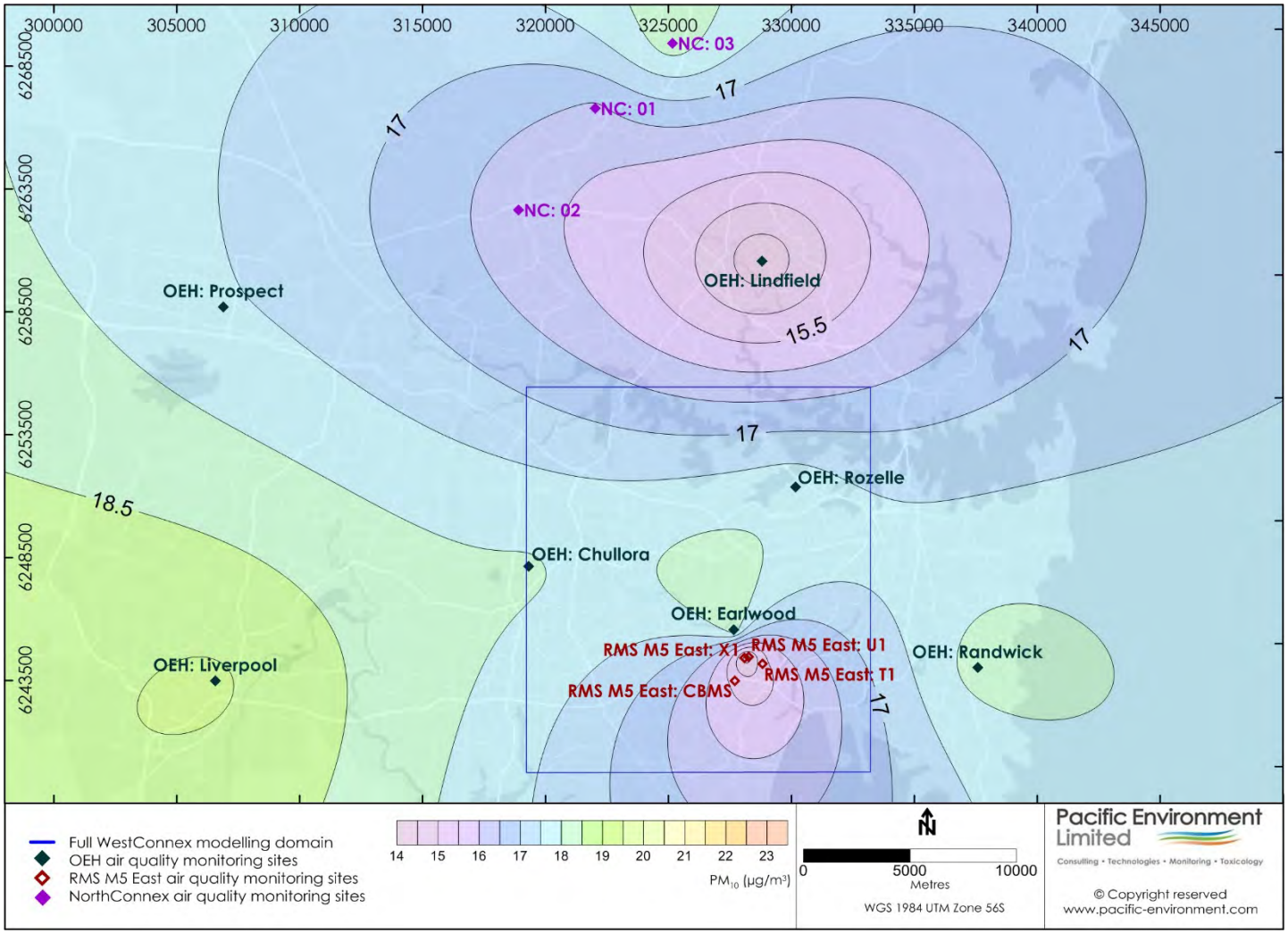

Figure F-41 Background map for annual mean PM_{10} concentration across Sydney in 2014

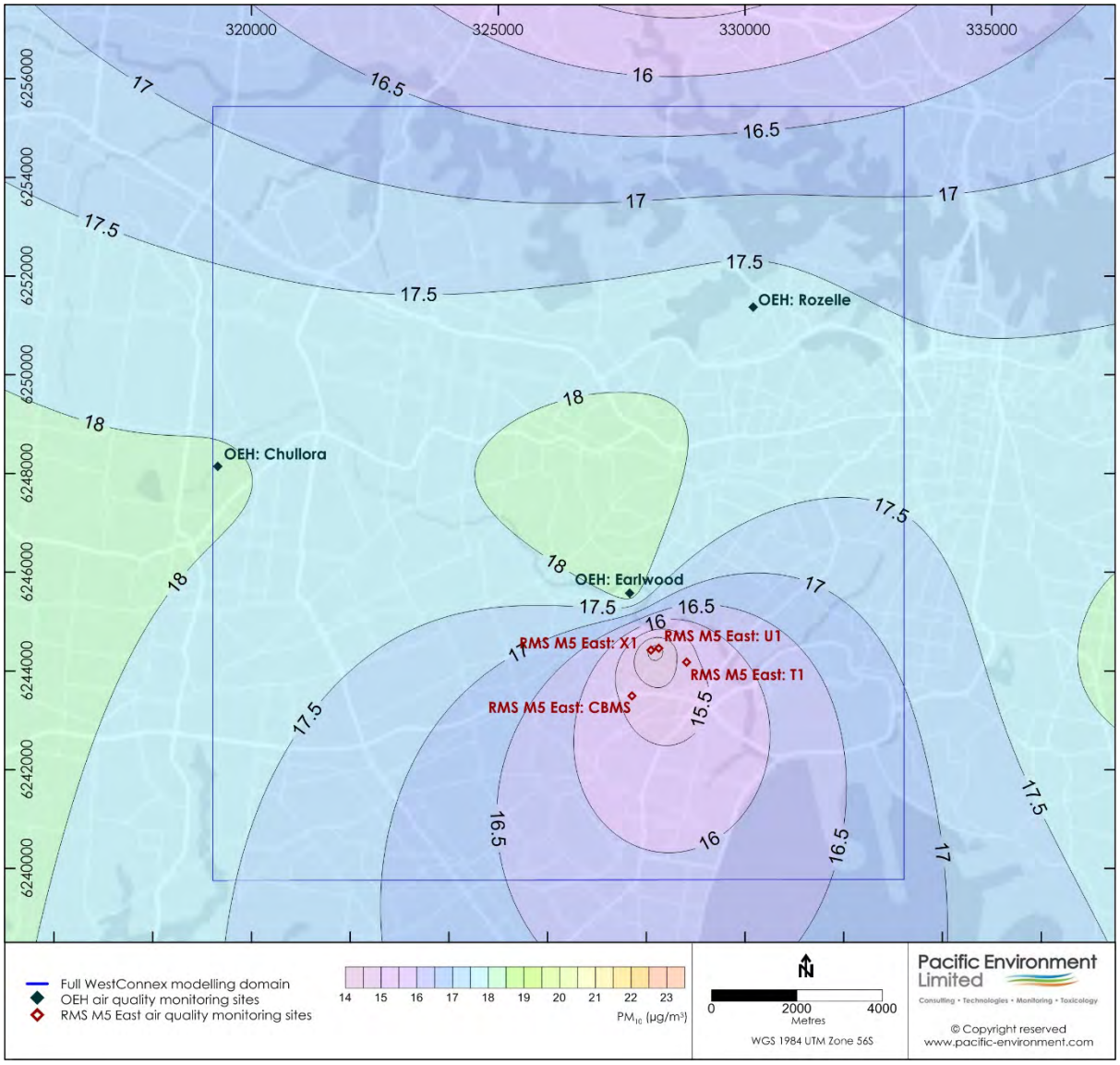

Figure F-42 Background map for annual mean PM_{10} concentration in 2014 (detail for WestConnex GRAL modelling domain)

F.9.8 PM_{10}: 24-hour mean

Figure F-43 shows the concentration profiles for 24-hour mean PM_{10} during 2014 at the OEH Chullora, Earlwood and Rozelle sites. The similarities between the peaks and troughs in the profiles at the three sites show that the OEH sites are characterising the same (*i.e.* regional) patterns in PM_{10}, although the absolute values vary slightly.

A synthetic 24-hour mean PM_{10} concentration profile for 2014 was also determined. As with NO_X, this was based on the maximum concentration across the three sites during each 24-hour time step. The final concentration profile is shown in Figure F-44.

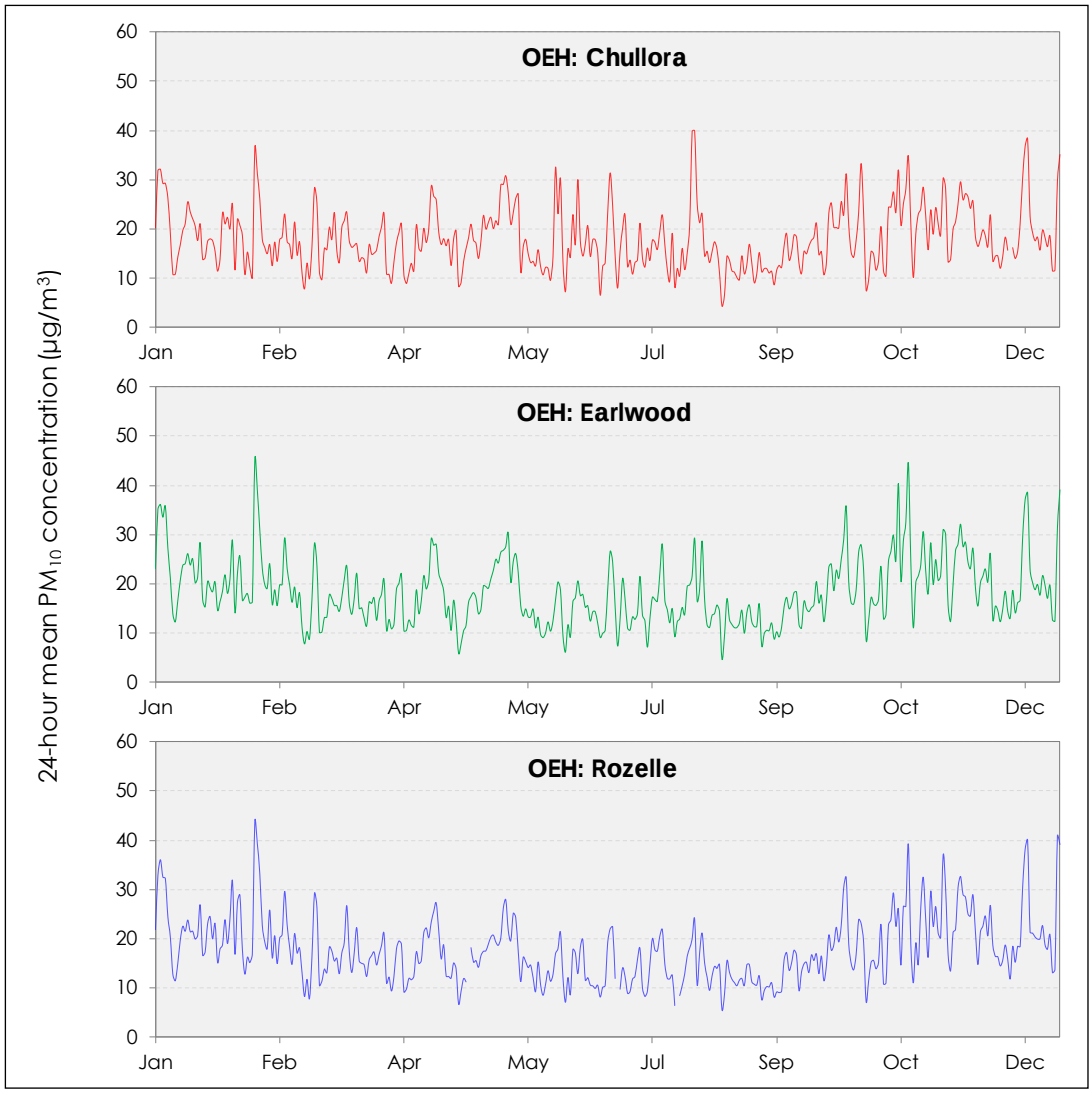

Figure F-43 **24-hour mean PM_{10} concentration at Chullora, Earlwood and Rozelle during 2014**

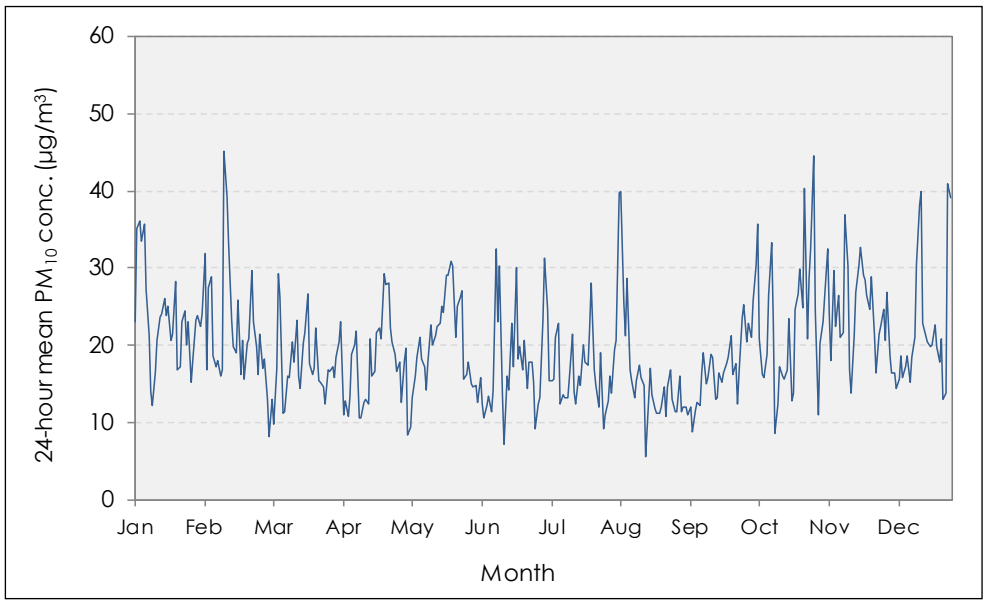

Figure F-44 **Synthetic background concentration profile for 24-hour mean PM_{10}**

F.9.9 $PM_{2.5}$: annual mean

The observations in Section F.6.5.1 render any assessment of the impacts of the M4 East project against the annual mean standard somewhat meaningless. For the purpose of the assessment a nominal $PM_{2.5}$ concentration of 8 µg/m^3 has been assumed, and any incremental changes due to the project have been assessed in relation to this concentration.

F.9.10 $PM_{2.5}$: 24-hour mean

The approach for $PM_{2.5}$ also involved the development of a synthetic concentration profile for 2014, although in this case it was just based on the data for Chullora and Earlwood sites. The concerntrations from the two sites are shown in Figure F-45, and the synthetic profile in Figure F-46.

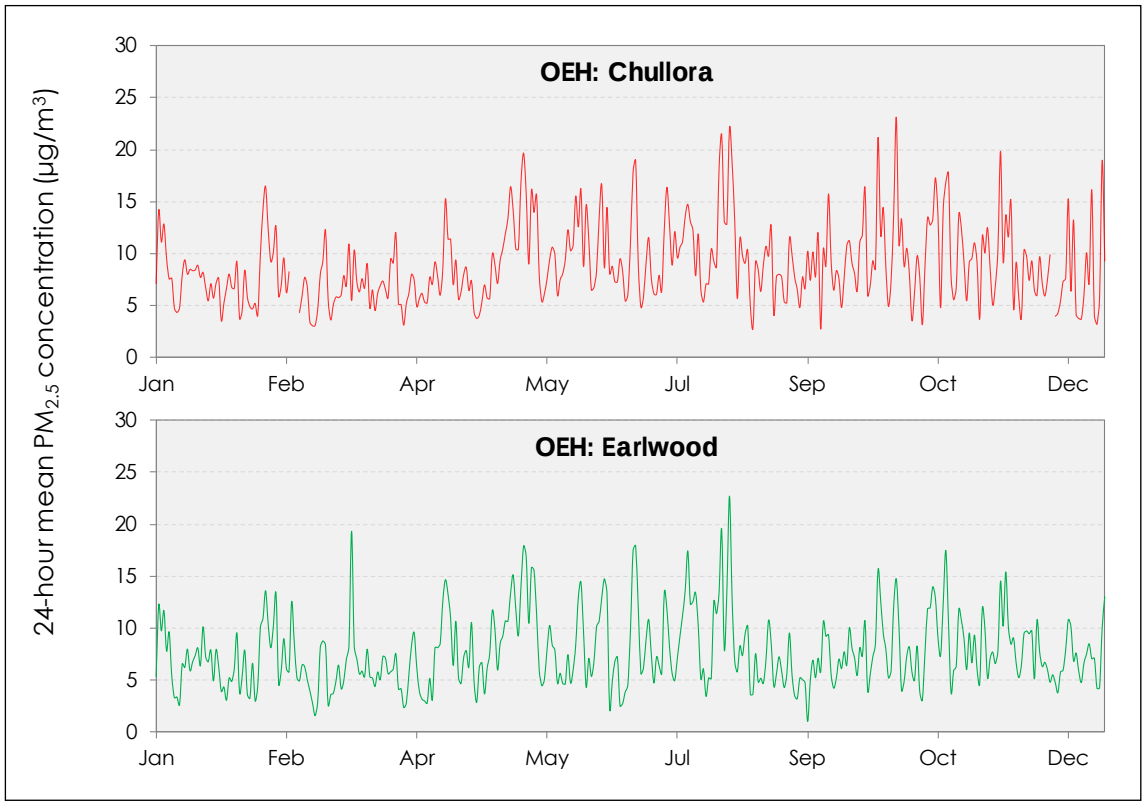

Figure F-45 24-hour mean $PM_{2.5}$ concentration at Chullora and Earlwood during 2014

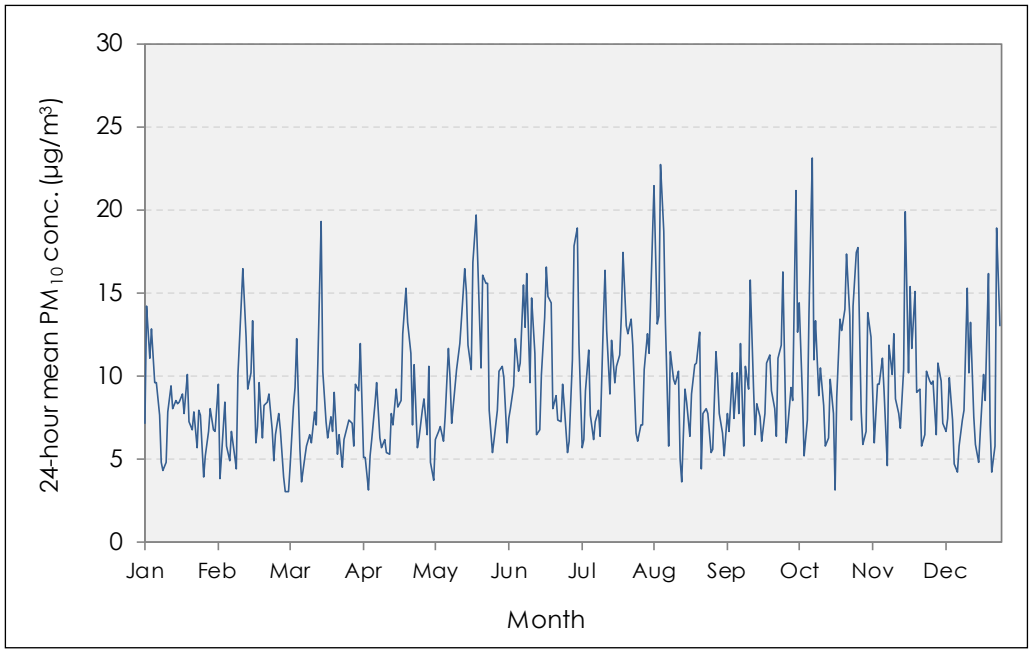

Figure F-46 Synthetic background concentration profile for 24-hour mean $PM_{2.5}$

F.9.11 Summary

The characteristics of the assumed background concentrations, and the forms of the concentrations, are provided in Table F-16. In relation to annual mean concentrations, the synthetic profiles, which are designed for the evaluation of short-term criteria, are slightly more conservative than the data used in the maps.

Table F-16 Characteristics of assumed background concentrations

Pollutant/ metric	Averaging period	Form	Units	Statistical descriptors			
				Mean	Min	Max	98th %ile
CO	1 hour	Synthetic profile	mg/m^3	0.39	0.12	2.87	1.12
	8 hours (rolling)	Synthetic profile	mg/m^3	0.39	0.12	2.11	0.96
NO_X	Annual	Map	$\mu g/m^3$	Spatially varying	-	-	-
	1 hour	Synthetic profile	$\mu g/m^3$	57.3	1.0	697.8	236.0
PM_{10}	Annual	Map	$\mu g/m^3$	Spatially varying	-	-	-
	24 hours	Synthetic profile	$\mu g/m^3$	19.8	5.6	45.2	39.3
$PM_{2.5}$	Annual	Single value	$\mu g/m^3$	8.0	-	-	-
	24 hours	Synthetic profile	$\mu g/m^3$	9.4	3.1	23.1	18.9

(blank page)

Appendix G - NO_X-to-NO_2 conversion

G.1 Introduction

Some atmospheric pollutants have slow chemical reaction rates, and for air quality modelling on an urban scale they can essentially be treated as inert (Denby, 2011). This is not the case for NO_2 since it is rapidly formed through the atmospheric reaction of NO with O_3, and is destroyed by sunlight during the day (see Appendix B). This is one reason why air pollution models are generally configured to predict NO_x concentrations, with the spread of NO_X being simulated as though it were a non-reactive gas (NZMfE, 2008). However, as air quality criteria address NO_2 rather than NO_X it is necessary to estimate NO_2 concentrations from the modelled NO_X concentrations. Many different approaches to this conversion have been developed over the years, and this Appendix describes the approach used for the M4 East assessment.

The estimation of NO_2 concentrations near roads is not straightforward. It requires an understanding of the complexity of NO_2 formation and destruction, and here there are a number of challenges. These include:

- How to account for the amount of primary NO_2 emitted in vehicle exhaust. This is dependent on the composition of the traffic, and is changing as the vehicle fleet evolves.
- How to account for the amount of conversion of NO to NO_2 in the atmosphere following release from the source, as this is dependent on the local atmospheric conditions, including the amount of ozone available.
- How to determine cumulative NO_2 concentrations, or in other words how to combine the road traffic contribution and the background (non-road) contribution.
- How to provide a realistic estimate of the change (whether this be an increment or decrement) in the NO_2 concentration that results from a road project.

The challenges are also greater for the one-hour air quality criterion than for the annual mean criterion. For example, the maximum predicted NO_X concentration will not occur during the same hour of the year at all locations in the model domain.

In order to ensure that an appropriate and pragmatic method was selected for the M4 East assessment, a review of the literature and data was undertaken. This Appendix presents the findings of the review and contains the following:

- A brief summary of the available guidance relating to the estimation of NO_2 concentrations.
- A review of the methods that are commonly used for estimating NO_2 concentrations. These either involve the use of empirical data or the modelling of atmospheric chemistry. In practice empirical approaches tend to be applied, as local knowledge on the inputs required for modelling chemistry is often incomplete.
- An analysis of the NO_X and NO_2 data from ambient air quality monitoring stations in Sydney, including the monitoring stations that were established specifically for the M4 East project. This analysis was used to estimate NO_X-to-NO_2 conversion methods for the specific purpose of the M4 East assessment, and more widely for complex road projects in Sydney.

G.2 Guidance on NO_2 estimation

G.2.1 New South Wales

Guidance on the conversion of modelled NO_X to NO_2 is provided in the Approved Methods for the Modelling and Assessment of Air Pollutants in New South Wales (NSW DEC, 2005). Three methods are described for calculating the oxidation of NO to NO_2, from Method 1, the most simple, to Method 3, the most complex.

G.2.2 North America

The USEPA's Guideline on Air Quality Models (GAQM) provides recommendations on the use of air quality models to determine compliance with National Ambient Air Quality Standards (NAAQS). The Guideline is published as Appendix W of 40 CFR Part 51. In this case, three 'Tiers' of assessment are provided, with Tier1 being the simplest and Tier 3 the most complex. Additional guidance on the assessment of one-hour NO_2 concentrations has recently been provided in the following:

- Applicability of Appendix W Modeling Guidance for the 1-hour NO_2 National Ambient Air Quality Standard, June 28, 2010[1].
- Additional Clarification Regarding Application of Appendix W Modeling Guidance for the 1-hour NO_2 National Ambient Air Quality Standard, March 1, 2011[2].

Other recent guidelines include:

- Modeling Compliance of the Federal 1-Hour NO_2 NAAQS (CAPCOA, 2011).
- Air Quality Model Guideline (Alberta Government, 2013).
- Guidelines for Air Quality Dispersion Modelling in British Columbia (BCMoE, 2008).

G.2.3 New Zealand

The following documents provide guidance on the estimation of NO_2 for air quality assessments in New Zealand:

- Good Practice Guide for Atmospheric Dispersion Modelling (NZMfE, 2004).
- Good Practice Guide for Assessing Discharges to Air from Industry (NZMfE, 2008), which updates the 2004 document.

G.2.4 United Kingdom

Guidance documents from the UK include:

- Review of background air-quality data and methods to combine these with process contributions (Environment Agency, 2006).
- Review of methods for NO to NO_2 conversion in plumes at short ranges (Environment Agency, 2007). This report focusses on the regulation of large industrial point sources.
- Local Air Quality Management Technical Guidance LAQM.TG(09) (Defra, 2009). This document is designed to support UK local authorities in carrying out their duties with respect to air quality management. A number of tools have been developed to support the guidance, including background maps of air pollutants, with year adjustment factors and a calculator that can be used to derive NO_2 from NO_X which is predicted when modelling emissions from roads.

G.3 Estimation methods

G.3.1 General approaches

In some assessments the road traffic and background concentrations to NO_2 at any given receptor have simply been added together to give the cumulative concentration, *i.e.*:

Equation G1

$$[NO_2]_{total} = [NO_2]_{road} + [NO_2]_{background}$$

where:

[1] http://www.epa.gov/scram001/guidance/clarification/ClarificationMemo_AppendixW_Hourly-NO2-NAAQS_FINAL_06-28-2010.pdf
[2] http://www.epa.gov/region7/air/nsr/nsrmemos/appwno2_2.pdf

$[NO_2]_{total}$ is the total estimated NO_2 concentration at the receptor

$[NO_2]_{road}$ is the modelled NO_2 concentration at the receptor due to a road (or roads) in the modelling domain

$[NO_2]_{background}$ is the existing background NO_2 concentration at the receptor due to emissions from all sources other than roads

As the background is often assumed to be fixed, in this formulation the NO_2 increment or decrement associated with a project is simply the change in the value of $[NO_2]_{road}$ for model runs with and without the project. This has to be determined in some way from the road NO_X increment. However, there is a flaw in this approach. Whilst the road and background contributions to NO_X are additive, this is not the case for NO_2. The potential for oxidising NO to NO_2 is dependent on the amount of ozone that is available, which in turn is dependent on the NO concentration. The higher the existing background NO concentration, the less ozone that is available and the smaller the possibility of oxidising the NO from road vehicles to NO_2.

For any given model prediction/scenario it is therefore more appropriate to determine the total NO_2 concentration from the total NO_X concentration. This can be expressed as follows:

Equation G2

$$[NO_X]_{total} = [NO_X]_{road} + [NO_X]_{background}$$

Equation G3

$$[NO_2]_{total} = f([NO_X]_{total})$$

Where $f([NO_X]_{total})$ is the method used to convert total NO_X to total NO_2.

The NO_2 increment or decrement associated with the project is then calculated as follows:

Equation G4

$$[NO_2]_{project} = [NO_2]_{total\ (with\ project)} - [NO_2]_{total\ (without\ project)}$$

G.3.2 Specific methods

Several methods are available for characterising the transformation of NO to NO_2. These include:

- Total conversion method:
    - Assuming that all NO_X from the emission source being modelled is present as NO_2 (*i.e.* there is always total conversion of NO to NO_2. This is 'Method 1' in the NSW Approved Methods and the USEPA's 'Tier 1' approach).
- NO_2/NO_X ratio methods, including:
    - Assuming a constant NO_2/NO_X ratio. This is the USEPA's 'Tier 2' approach, which is referred to as the 'ambient ratio method' (ARM).
    - Assuming a variable NO_2/NO_X ratio to all for influences such as the season and distance from source.

  NO_X to NO_2 conversion methods that use ambient ratios are usually based on empirical data. Empirical relationships fall within the 'Method 3' in the NSW EPA Approved Methods.
- Reactant-limited methods, whereby the instantaneous conversion of NO is constrained only by the amount of oxidant(s) available. Such methods include:
    - The 'ozone limiting method (OLM)', in which NO to NO_2 conversion is limited by the amount of ozone available (known as 'ozone titration'). This is 'Method 2' in the NSW Approved Methods, and is a USEPA Tier 3 approach.

- The plume volume molar ratio method (PVMRM), which is also based on ozone titration. This is a USEPA 'Tier 3' approach. It is not mentioned in the NSW Approved Methods.

- Reactive plume methods. These use complex or simplified atmospheric photochemical reaction schemes which derive NO_2 concentrations from first principles. Such approaches have been incorporated into some of the latest generation of air pollution models.

The different methods presented in the literature are summarised in the following Sections.

G.3.3 Total conversion of NO to NO_2

G.3.3.1 Description

The most basic – and most conservative – method for estimating the NO_2 concentration at a receptor is based on the assumption that all emitted NO is oxidised to NO_2, or in other words all modelled NO_X from roads is present as NO_2:

Equation G5

$$[NO_2]_{road} = [NO_X]_{road}$$

Equation G6

$$[NO_2]_{total} = [NO_2]_{road} + [NO_2]_{background}$$

This approach is often used as a screening step; if compliance with air quality standards is obtained using this approach, then it can be assumed that there will be negligible risk of exceedances in reality and more detailed calculations for NO_2 are not required. If, on the other hand, the estimated NO_2 concentrations are close to or higher than the air quality standards then more detailed, less conservative methods should be applied.

G.3.3.2 Application in NSW Approved Methods

For annual mean concentrations the modelled NO_x concentration is converted to NO_2 (assuming 100% conversion of NO), and the result is then simply added to the background NO_2 concentration.

For one-hour means, the cumulative concentration can be determined in one of two ways:

- Level 1 (maximum): The maximum modelled one-hour mean NO_2 concentration is added to the maximum background one-hour mean NO_2 concentration.
- Level 2 (contemporaneous): Using contemporaneous assessment of model predictions and ambient concentrations. The cumulative NO_2 concentration is determined by adding the modelled one-hour mean NO_2 concentration with the contemporaneous background one-hour mean NO_2 concentration.

G.3.3.3 Limitations and performance

This method represents a worst-case situation. It does not allow for the availability of ozone or NO_2 destruction through photolysis, and will overestimate NO_2 concentrations. The overestimation will be largest at high NO_X concentrations where NO_2 formation is ozone-limited. This is explored further in Section G5. The total conversion method is therefore of limited use where an accurate estimate of NO_2 is required.

G.3.4 NO_2/NO_X ratio methods

G.3.4.1 Description

Constant ratio

In the USEPA's ARM, the predicted NO_X concentration for a receptor is multiplied by an empirically derived NO_2/NO_X ratio to determine the NO_2 concentration at the receptor. The NO_2/NO_X ratio is based upon average NO_2 and NO_X concentrations in ambient air at a representative site. For

example, in the USEPA 'Tier 2' approach the modelled annual mean NO_X concentrations is multiplied by a default NO_2/NO_X ratio of 0.75. For one-hour concentrations a NO_2/NO_X ratio of 0.80 is used.

Variable ratio

ARM2

A new empirical method, known as ARM2, has recently been developed by the American Petroleum Institute in response to the frequent observation that hourly NO_2 concentrations estimated using the existing USEPA three-tier approach are much higher than observed concentrations. ARM2 is based on an empirical fit to the 98th percentiles of the binned one-hour NO_2/NO_X and NO_X values collected from different monitoring stations between 2001 and 2010 (RTP, 2013; Podrez, 2015). The USEPA has approved the use of ARM2 for regulatory one-hour NO_2 assessments under certain circumstances.

Janssen method

The NSW Approved Methods refer to the approach of Janssen et al. (1988). This involves the use of an empirical equation for estimating the oxidation rate of NO in power plant plumes. The equation is dependent on distance downwind from the source and the parameters A and α, and has the following form:

Equation G7

$$[NO_2]/[NO_X] = A (1 - \exp(-\alpha x))$$

where:

x = the distance from the source

A and **α** are classified according to the O_3 concentration, wind speed and season (Janssen et al. (1988) provide values for **A** and **α**).

Given that this method requires the distance from the source to be quantified, the method is not suitable for complex road networks.

Defra method

An empirical approach to calculating NO_2 from NO_X concentrations at roadside sites was developed by Defra in the UK in 2002, then updated in 2007[3]. In 2009 Defra published a revised approach for predicting NO_2 from NO_X concentrations at roadside sites, which takes account of the difference between fresh emissions of NO_x, the background NO_x, the concentration of O_3, and the different proportions of primary NO_2 emissions in different years. The approach has been incorporated into a simple spreadsheet which is available from the Defra web site.

G.3.4.2 Limitations and performance

The ARM2 method has some advantages over other USEPA Tier 3 methods. For example, it does not require ambient ozone data. The performance of the ARM2 method is comparable to that of the OLM and the PVMRM. However, all three methods over-predict NO_2/NO_X ratios (RTP, 2013).

According to NZMfE (2004) the Janssen approach is based upon the rate of diffusion of O_3 into the emission plume rather than the rates of reaction. It is therefore probably only applicable to the particular power station studied, and is of questionable application to other sources. Although the Approved Methods describe the application of the Janssen method to determine annual mean and one-hour mean concentrations, its lack of applicability to road networks means that it has not been explored in detail in this Appendix. There is little information on how the NO_2/NO_X ratio changes with distance from the road; monitoring data are usually only available for roadside and/or background locations.

[3] http://laqm1.defra.gov.uk/review/tools/monitoring/calculator.php

Given that it has been developed to represent vehicle fleets and near road atmospheres in the UK, it is unlikely that the Defra calculator is suitable for use in Sydney, although this ought to be investigated further. However, this was beyond the scope of the M4 East assessment.

G.3.5 Reactant-limited methods

G.3.5.1 Description

Ozone limiting method

The USEPA's ozone limiting method (OLM) is one of several reactant-limited approaches. It uses a simple approach to the reaction chemistry of NO and O_3 in order to estimate NO_2 concentrations. It is assumed that all the available O_3 in the atmosphere will react with the NO from the source until either all the O_3 is consumed or all the NO is used up (Cole and Summerhays, 1979; Tikvart, 1996). A slightly different approach to the OLM has been developed for use in New Zealand (NZMfE, 2008).

Plume volume molar ratio method

The plume volume molar ratio method (PVMRM) extends the basic chemistry of the OLM. The PVMRM determines the conversion rate for NO_x to NO_2 based on a calculation of the number of NO_x moles emitted into the plume, and the number of O_3 moles contained within the volume of the plume between the source and receptor. The ratio between the two molar quantities is multiplied by the NO_X concentration to calculate the NO_2 concentration.

Both the OLM and PVMRM require two key model inputs, namely NO_2/NO_X emissions ratio at source and background ozone concentrations.

G.3.5.2 Implementation in NSW Approved Methods

The USEPA version of the OLM (adapted here for road projects) is represented by the equation (NSW DEC, 2005):

Equation G8

$$[NO_2]_{total} = \{0.1 \times [NO_X]_{road}\} + MIN\ \{(0.9) \times [NO_X]_{road} \text{ or } (46/48) \times [O_3]_{background}\} + [NO_2]_{background}$$

where:

$[NO_2]_{total}$ = predicted concentration of NO_2 in µg/m^3

$[NO_X]_{road}$ = dispersion model prediction of NO_X from roads in µg/m^3

MIN = minimum of the two quantities within the braces

$[O_3]_{background}$ = background ambient O_3 concentration in µg/m^3

(46/48) = molecular weight of NO_2 divided by the molecular weight of O_3 in µg/m^3

$[NO_2]_{background}$ = background ambient NO_2 concentration in µg/m^3

The method involves an initial comparison of the estimated maximum NO_X concentration and the ambient O_3 concentration to determine the limiting factor to NO_2 formation:

- If the O_3 concentration is greater than the maximum NO_X concentration, then total NO_X to NO_2 conversion is assumed.
- If the maximum NO_X concentration is greater than the ozone concentration, the formation of NO_2 is limited by the ambient ozone concentration.

The OLM – in the above form – is based on the assumption that 10% of the initial NO_x emissions are NO_2. The emitted NO reacts with ambient ozone to form additional NO_2. If the ozone concentration is greater than 90% of the predicted NO_x concentration, all the NO_X is assumed to be converted to NO_2. Otherwise, NO_2 concentrations are calculated on the assumption of total conversion of the ozone. The predicted NO_2 concentration is then added to the background NO_2 concentration.

The following approaches are presented in the Approved methods for the 'maximum' and 'contemporaneous' calculations:

- Level 1 (maximum): The maximum one-hour and annual average background concentrations of NO_2 and O_3 ($[NO_2]_{background}$, $[O_3]_{background}$) are used in Equation G8.
- Level 2 (contemporaneous): Continuous one-hour average background concentrations of NO_2 and O_3 are obtained for the same period as the dispersion modelling predictions (usually one year). The value of $[NO_2]_{total}$ is then calculated for every hour of the dispersion model simulation by substituting the hourly values of $[NO_X]_{road}$, $[NO_2]_{background}$ and $[O_3]_{background}$ into Equation G8.

As before, the Level 1 approach is used as a screening step. The OLM is usually applied using the Level 2 approach, and this has the advantage of yielding various statistics for NO_2, including:

- The annual mean concentration (based on the one-hour predictions for a year).
- The maximum concentration.
- Percentile concentration values.
- The frequency with which the one-hour NO_2 criterion is exceeded.

In the NSW submission to the EIS for the NorthConnex project in Sydney, it is stated that that an average value for the NO_2/NO_X ratio of 16%[4] would be more appropriate than 10%. The OLM equation should therefore be adjusted as follows (AECOM, 2014b):

Equation G9

$$[NO_2]_{total} = \{0.16 \times [NO_X]_{road}\} + MIN\ \{(0.84) \times [NO_X]_{road}\ or\ (46/48) \times [O_3]_{background}\} + [NO_2]_{background}$$

The effect of the adjustment is to increase the amount of NO_2 emitted directly, potentially increasing the NO_2 concentrations that are predicted under low ambient O_3 concentrations.

G.3.5.3 Limitations and performance

Several limitations of the OLM have been noted:

- The approach is known to be conservative:
    - The method assumes that the atmospheric conversion of NO to NO_2 occurs instantaneously. In reality, the reaction requires time. This assumption therefore leads to an overestimate of NO_2 concentrations close to the source (NZMfE, 2004).
    - The method assumes that all ozone is available to the emission source being evaluated. The OLM will be too conservative when, for example, a new source is to be located in close proximity to existing sources. The new source will be competing with the existing sources for the available ozone, and the rate of conversion of NO to NO_2 will not be as great as if the new source was in an isolated location (NZMfE, 2004).
    - Ozone is assumed to be uniformly and continuously mixed across the cross section of the plume. The OLM does not account for the molar ratio of NO to ozone in the plume (reactions occur in proportion to the moles of each gas rather than in proportion to the concentrations assumed by the OLM), nor does it account for the gradual entrainment and mixing of ambient ozone in the plume.
    - Situations in which the OLM has been demonstrated to substantially overestimate NO_2 concentrations include during daylight hours when the photochemical equilibrium reverses the oxidation of NO by O_3, and during stable, night-time conditions when both NO_2 and O_3 are removed by reaction with vegetation and other surfaces (NZMfE, 2004).

[4] This is the upper bound of the estimated ratio used for the in-tunnel modelling in Appendix L for primary NO_2. The in-tunnel modelling considers the ratio variations for different traffic speeds and different tunnel grades.

- The OLM model requires a record of one-hour average background concentrations over a year. Apart from the expense of obtaining such information at a single location, there are significant problems in locating the monitoring site relative to existing emission sources and a proposed new emission source because of the perceived difficulty of accounting for scavenging of O_3 by NO (NZMfE, 2004).
- The USEPA states that the OLM should only be used on a 'plume-by-plume' basis. This is a severe limitation in relation to road projects.

Some of these limitations also apply to the PVMRM. Because of the different methods used, there are cases where PVMRM will perform better than OLM, and vice versa. The PVMRM better simulates the NO to NO_2 conversion chemistry during plume expansion, and works well for isolated elevated point sources. However, OLM may be the better choice for low level releases and area sources. For low level releases the modelled plume may extend below ground level, but the PVMRM will still use the full volume of the plume to estimate the NO_x-to-NO_2 conversion. This may lead to overly conservative NO_2 concentrations.

G.3.6 Reactive plume models

Various photochemical reaction schemes are applied in regional-scale and urban-scale air pollution models. One of the most commonly used is the Generic Reaction Scheme (Azzi *et al.*, 1992). More detailed photochemical models and schemes have been developed in recent years, including the EMEP scheme (Simpson *et al*., 2003), the Carbon Bond-IV mechanism (Gery *et al*., 1989), and the CB05 photochemical mechanism (Yarwood *et al*., 2005).

However, the use of such models is uncommon for regulatory local air quality assessments. A major drawback of these methods is that the near-source chemical reactions may not be well described. Many of the atmospheric chemistry schemes developed for regional and global models include reactions on timescales that are much longer than the residence times of pollutants in urban areas, and as such introduce an additional complexity and computational time that is unnecessary (Denby, 2011). As noted by the Environment Agency (2007), care is required to select a chemical mechanism, and advanced photochemical modelling requires a comprehensive set of emissions data for a wide range of compounds (notably hydrocarbons), as well as the appropriate meteorological data. These are major constraints on any regulatory work.

G.4 Development of empirical conversion methods for Sydney

G.4.1 Overview

Various air quality guidance documents recommend the use of local monitoring data to estimate NO_2 concentrations, where such data are available. Empirical methods for converting NO_X to NO_2 were therefore developed specifically for the M4 East assessment.

The analysis involved the fitting of functions to the monitoring data. Functions have been fitted to data of this type for many years, notably in the form of the 'Derwent-Middleton' equation (Derwent and Middleton, 1996), and this continues to be the case (e.g. Podrez, 2015).

The methods were based upon the analysis of substantial amounts of air quality monitoring data from locations in Sydney, and are also applicable more widely to other complex road projects in the airshed. One reason for this analysis was to quantify and address the conservatism in some of the other methods in use, whereby exceedances of NO_2 air quality standards can be predicted for a given NO_X concentration, even where the monitoring data show that this situation is not the reality.

NO_X and NO_2 have been measured for several years at a range of locations across Sydney, as described in Appendix F. Based on the analysis of the data, separate approaches were developed for annual mean and one-hour mean NO_2 concentrations. These approaches were as follows:

- For annual mean NO_2 concentrations:
    - A best estimate approach, which gave the most likely annual mean NO_2 concentration for a given annual mean NO_X concentration. This method was used in the air quality assessment.

- A reasonable worst case estimate which gave the maximum possible annual mean NO_2 concentration for a given annual mean NO_X concentration. This method was developed for sensitivity testing.

- For the maximum one-hour mean NO_2 concentrations the situation was more complicated. Ideally, for every receptor the average NO_2 concentration in each hour of the year should be determined using a contemporaneous approach which combines the hourly background and road NO_X contributions, and then converts the total NO_X to total NO_2. However, this approach is impractical where many receptors are being investigated, and indeed the number of receptors for which a full time series of predictions can be obtained is often limited in the dispersion model (as is the case with GRAL), or is computationally very intensive. Two approaches for calculating maximum one-hour NO_2 concentrations were therefore used:

  - A 'detailed' contemporaneous approach that was only applied to the community receptors (e.g. schools, hospitals, day care centres). This also involved the use of a conservative upper bound function which gave the maximum likely one-hour mean NO_2 concentration for a given one-hour mean NO_X concentration. Given the wide range of possible NO_2 concentrations for a given NO_X concentration, this approach was used to conservatively estimate the maximum one-hour mean NO_2 concentrations.
  - A 'simple' statistical (non-contemporaneous) approach which was applied to determine the maximum one-hour NO_X concentrations for the much larger number of residential, workplace and recreational' (RWR) receptors. The conversion of NO_X to NO_2 was then based on the functions used in the detailed approach.

  The two methods for estimating the maximum one-hour mean NO_2 concentration were also compared for the sensitive receptors.

G.4.2 Methods used in the project assessment

G.4.2.1 Annual mean concentrations

Figure G-1 shows the relationship between the annual mean concentrations of NO_X and NO_2 at the monitoring stations in Sydney across all years. As the values shown are measurements, they equate to $\mathbf{[NO_X]_{total}}$ and $\mathbf{[NO_2]_{total}}$. In the low-NO_X range of the graph there is an excess of ozone and therefore NO_2 formation is limited by the availability of NO. In the high-NO_X range there is an excess of NO, and therefore NO_2 formation is limited by the availability of ozone.

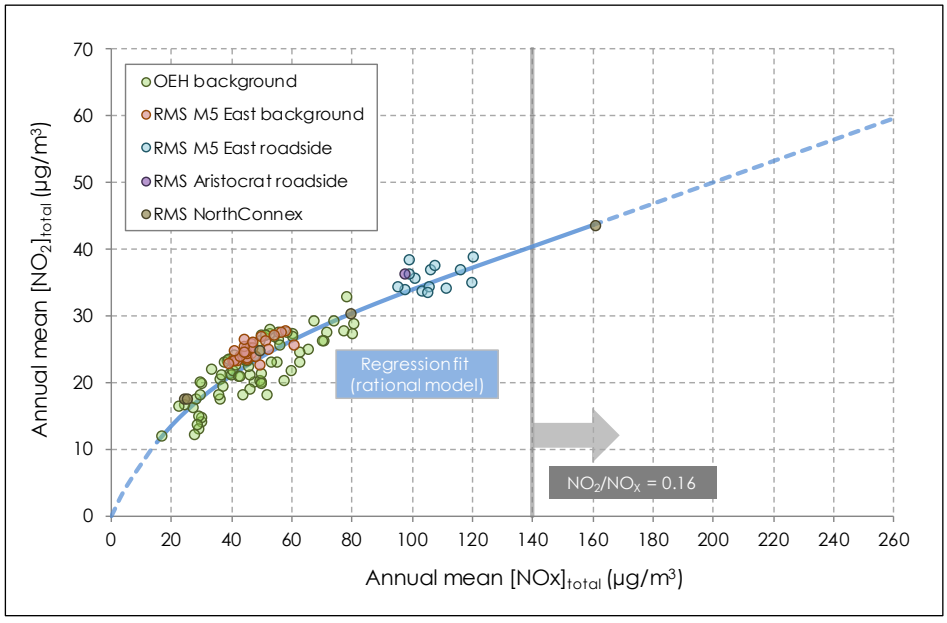

Figure G-1 Annual mean NO_X and NO_2 concentrations at monitoring sites in Sydney

The solid blue in Figure G-1 represents a regression model fit to the data (*i.e.* the best estimate situation) which will give the likely NO_2 concentration for a given NO_X concentration. The function giving the best fit – the rational model – was selected from a large number of alternatives using curve-fitting software. This function, which was used in the M4 East assessment, is described by the following equations:

For $\mathbf{[NO_X]_{total}}$ values less than or equal to 140 µg/m^3:

Equation G10

$$\mathbf{[NO_2]_{total}} = \frac{\mathbf{a + b[NOx]_{total}}}{\mathbf{1 + c[NOx]_{total} + d([NOx]_{total})^2}}$$

Where:

a = -7.6313 x 10^{-4}

b = 9.9470 x 10^{-1}

c = 2.3750 x 10^{-2}

d = -4.5287 x 10^{-5}

For $\mathbf{[NO_X]_{total}}$ greater than 140 µg/m^3 it has been assumed that the available ozone has been consumed and so NO_2 is linearly proportional to NO_X with a NO_2/NO_X ratio of 0.16, representing the current f-NO_2 value for vehicle exhaust quoted by NSW EPA in its response to the EIS for the NorthConnex project (AECOM, 2014b):

Equation G11

$$\mathbf{[NO_2]_{total} = 40.513 + (0.16 \times ([NO_X]_{total} - 140))}$$

The work presented by Boulter and Bennett (2015) suggests that an annual average value for f-NO_2 of 0.16 is an overestimate for the 2014 vehicle fleet, but is likely to be more representative for future years.

The dashed blue line represents the extrapolation of the function to values below and above the range of measurements. Given the absence of high annual mean NO_X concentrations, the extrapolation to concentrations above the measurement range is rather uncertain, but on the basis of the primary NO_2 assumption it is likely to be rather conservative.

Given that the total NO_X concentration was used to determine the total NO_2 concentration, in order to determine the change in NO_2 associated with the project the background NO_2 concentration was subtracted. That is:

Equation G13

$$\mathbf{[NO_2]_{project} = [NO_2]_{total} - [NO_2]_{background}}$$

Where both $\mathbf{[NO_2]_{total}}$ and $\mathbf{[NO_2]_{background}}$ were determined using Equations G10 and G11.

For a given project contribution to NO_X at a receptor, the higher the background NO_X the lower the project NO_2 increment will tend to be, as less ozone will generally be available for converting the NO from the project to NO_2.

The use of the function could theoretically lead to exceedances of the annual mean criterion for NO_2 in NSW of 62 µg/m^3. However, a very high annual mean NO_X concentration - more than 260 µg/m^3 - would be required. This is much higher than the measurements in Sydney have yielded to date.

G.4.2.2 One-hour mean concentrations

Detailed contemporaneous approach

One-hour mean NO_X and NO_2 concentrations are much more variable than annual mean concentrations. Patterns in the hourly data can be most easily visualised by plotting the one-hour mean NO_2/NO_X ratio against the one-hour mean NO_X concentration, as shown for the various monitoring sites – including the M4 East sites - in Figure G-2 to Figure G-7.

In each dataset it is clear that for low NO_x concentrations there is a wide range of possible NO_2/NO_x ratios, whereas for higher NO_X concentrations the range is much more constrained. A distinct outer envelope can be fitted to the data which includes all (or very nearly all) the measurement points, and this envelope has a strong inverse relationship with the NO_X concentration. In the envelope the NO_2/NOx ratio is highest (1.0) at low NO_X concentrations, representing complete, or near-complete, conversion of NO to NO_2. At the high end of the NO_X concentration range the ratio is much lower and levels out at a value of around 0.1. The highest NO_X concentrations occur mostly during the winter months when temperature inversions prevent the effective dispersion of pollution.

Although the range and variability of the data varied by site type, the general patterns in the data were quite consistent. It was therefore considered appropriate to combine the datasets. In particular, the outer envelope of the NO_X:NO_2 ratio was very consistent, and so it was also considered appropriate to define one (conservative) approach to reflect this envelope.

The derivation of a conversion method from these data for the M4 East assessment was adapted from that recommended by BCMoE (2008)[5]. This method involved the following steps:

- The range of NO_X concentrations for which the NO_2/NO_X ratio is equal to 1.0 is estimated.
- The NO_X concentration for which NO_2/NO_X is equal to 0.1 is estimated.
- An exponential equation of the following form is fitted to the upper envelope of the scatter:

  $$\mathbf{NO_2/NO_X = a \times [NOx]^b}$$

  where **a** and **b** are selected through an iterative process to produce a curve that fits the upper bound of the envelope of the scatter.

  The equation is defined so that the NO_2/ NO_x ratio never exceeds unity or falls below 0.1.

- The equation is checked to ensure that NO_2 does not decrease with an increase in NO_X.

The data from all Sydney monitoring sites between 2004 and 2014 (and in the case of the M4 east sites, April 2015) – a total of more than 900,000 data points – are shown in Figure G-8, and the steps described above have been applied. Around 16% of the data points were for roadside monitoring sites.

[5] BCMoE (2008) recommends that the ozone limiting method should only be applied if adequate monitoring data are not available to establish representative NO/NO_2 ratios.

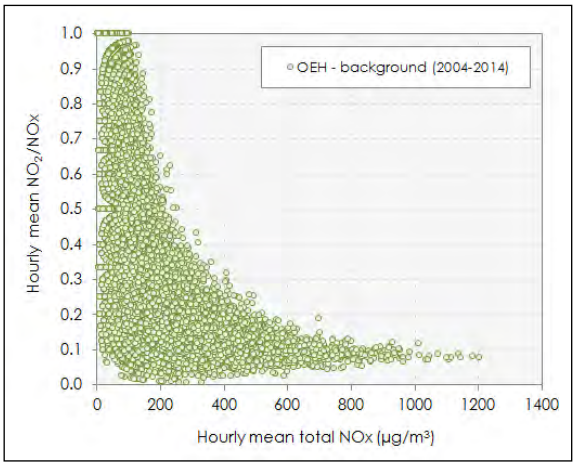

Figure G-2 Hourly mean NO_2/NO_X and NO_X at OEH background sites

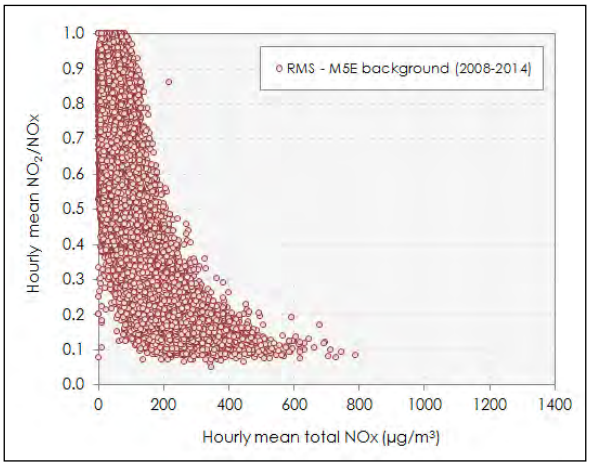

Figure G-3 Hourly mean NO_2/NO_X and NO_X at RMS M5 East background sites

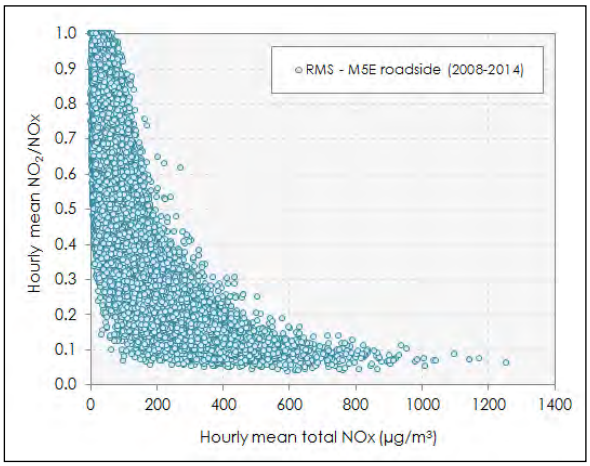

Figure G-4 Hourly mean NO_2/NO_X and NO_X at RMS M5 East roadside sites

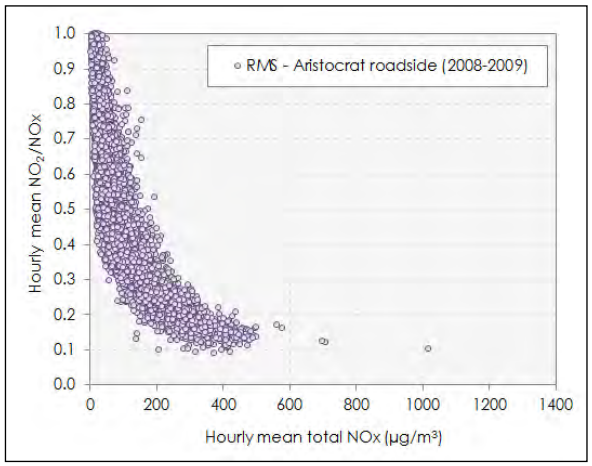

Figure G-5 Hourly mean NO_2/NO_X and NO_X at RMS Aristocrat (roadside) site

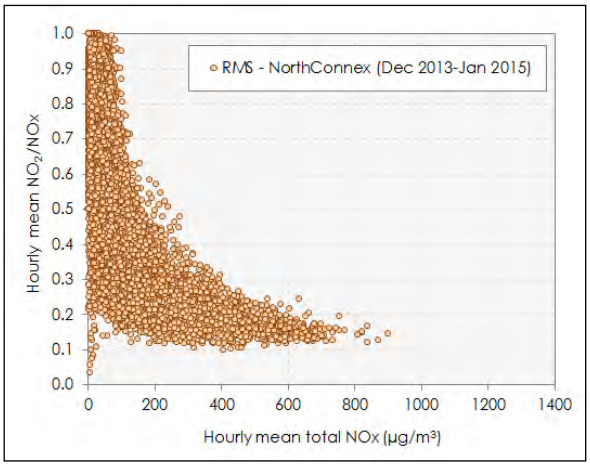

Figure G-6 Hourly mean NO_2/NO_X and NO_X at RMS NorthConnex sites

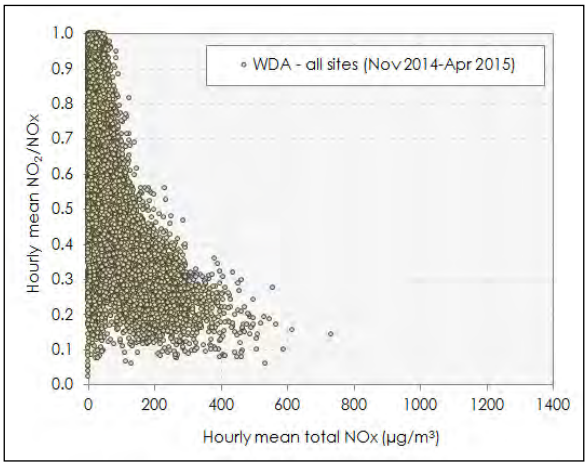

Figure G-7 Hourly mean NO_2/NO_X and NO_X at WDA M4 East sites

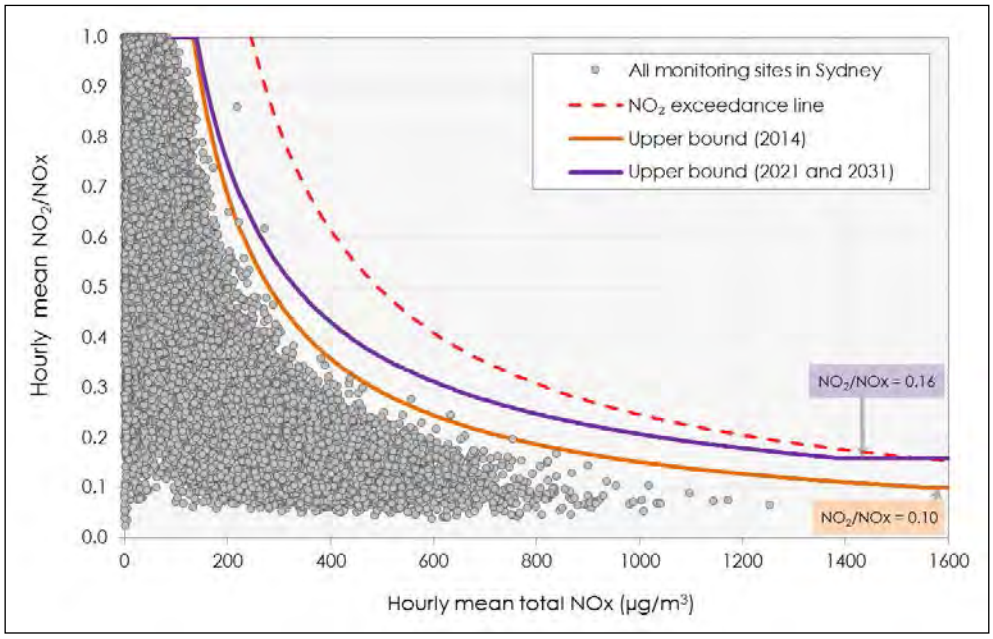

Figure G-8 Hourly mean NO_X and NO_2/NO_X ratio for monitoring sites at various locations in Sydney

The solid orange line in Figure G-8 represents the outer envelope of all data points, and approximates to a conservative upper bound estimate for 2014, or in other words the maximum NO_2/NO_X ratio for a given NO_X concentration in 2014. This is described by the following equations:

For $[NO_X]_{total}$ values less than or equal to 130 µg/m^3:

Equation G14

$$\frac{[NO_2]_{total}}{[NOx]_{total}} = 1.0$$

For $[NO_X]_{total}$ values greater than 130 µg/m^3 and less than or equal to 1,555 µg/m^3:

Equation G15

$$\frac{[NO_2]_{total}}{[NOx]_{total}} = a \times [NOx]_{total}^{\ b}$$

where:

a = 100
b = -0.94

For $[NO_X]_{total}$ values greater than 1,555 µg/m^3 a cut-off for the NO_2/NO_X ratio of 0.10 has been assumed. That is:

Equation G16

$$\frac{[NO_2]_{total}}{[NOx]_{total}} = 0.1$$

The dashed red line in Figure G-8 shows the NO_2/NO_X ratio that would be required for an exceedance of the NO_2 criterion of 246 µg/m^3 at each NO_X concentration. It is clear from Figure G-8 that an exceedance of the one-hour criterion for NO_2 cannot be predicted using the upper bound curve for 2014 across a wide range of NO_X concentrations.

However, as noted earlier, for future years it is possible that the upper bound estimate for 2014 will not be appropriate, given that primary NO_2 emissions could increase. An exploratory analysis by Pacific Environment indicated that, on average for highway traffic in Sydney, *f*-NO_2 could increase to 0.16 by 2031 (Boulter and Bennett, 2015). Whilst the increase in *f*-NO_2 would be combined with lower overall NO_x emissions, in could be expected that for high ambient NO_X concentrations the ambient NO_2/NO_X ratio could exceed 0.1. Here, it has been assumed that a minimum value for the NO_2/NO_X ratio of 0.16 would be appropriate for the 2021 and 2031 scenarios, and a corresponding function (the purple line) is shown in Figure G-8.

This function, which is essentially arbitrary, is described by the following equations:

For $\mathbf{[NO_X]_{total}}$ values less than or equal to 140 µg/m^3, Equation G14 applies.

For $\mathbf{[NO_X]_{total}}$ values greater than 140 µg/m^3 and less than or equal to 1,375 µg/m^3, Equation 15 applies with the following coefficients:

a = 52

b = -0.80

For $\mathbf{[NO_X]_{total}}$ values greater than 1,375 µg/m^3 a cut-off for the NO_2/NO_X ratio of 0.16 has been assumed. That is:

Equation G17

$$\frac{[NO_2]_{total}}{[NOx]_{total}} = 0.16$$

This conservative upper bound estimate for 2021 and 2031 is shown as a purple line in Figure G-8.

Even this assumption would only result in an exceedance of the NO_2 criterion at very high NO_X concentrations (above around 1,500 µg/m^3). If a more conservative estimate for the minimum ambient NO_2/NO_X ratio of 0.20 were to be assumed, the total NO_X concentration required for NO_2 exceedance in Figure G-8 would be around 1,200 µg/m^3.

Given that the background concentrations developed for the M4 East assessment were also slightly conservative (see Appendix G), this will be a conservative estimate of NO_2 using this approach.

Simple statistical approach

The simple approach involved the following steps for a given receptor:

Step 1: The maximum one-hour mean NO_x value predicted by GRAL was added to the 98th percentile NO_x value for the background (in the synthetic profile for 2014 this was 236 µg/m^3). This step will tend to result in an overestimation of the maximum total NO_X concentration, as the probability of the two values coinciding in time is low. The 98th percentile was used in preference to the maximum as it is much less variable.

Step 2: The maximum total NO_X concentration from Step 1 was converted to a maximum total NO_2 concentration using the relevant function for the year from Figure G-8. The validity if this approach was examined through comparison with the contemporaneous approach (see Section G.5.2.2).

G.4.2.3 Limitations and performance

The limitations of empirical methods for NO_X-to-NO_2 conversion include the following:

- They do not make any allowance for future changes, such as a potential increase in primary NO_2 emissions or changes in ozone concentrations. Here, this has been addressed through the use

of a more conservative function for converting NO_X to NO_2 than the ambient measurements to date would suggest.

- In general the methods do not differentiate between receptor locations at different distances from emission sources.
- They are only useful for the general locations where they were developed. The methods will not provide the correct dynamic response to changes in emissions, boundary conditions or meteorology unless these influences are implicitly included in their formulation (Denby, 2011).

However, despite, or as a result of, their empirical nature such models can give quite satisfactory results, especially for annual mean concentrations as there is a clear dependence of NO_2 on NO_X concentrations (Denby, 2011).

G.5 Comparison of methods

In a further analysis, the functions for calculating NO_2 from NO_X based on the monitoring data from Sydney were compared with some alternative approaches. The results of these comparisons for both annual mean and one-hour mean NO_2 concentration are given below.

G.5.1 Annual mean NO_2 concentrations

The following methods for calculating annual mean NO_2 concentrations were compared:

- The best estimate approach based on the Sydney monitoring data (see Section G.4.2.1).
- The complete conversion method (see Section G.3.3).
- The USEPA constant ambient ratio method (ARM), with a NO_2/NO_X ratio of 0.75 (see Section G.3.4.1).
- The ozone limiting method (OLM), with an *f*-NO_2 value of 0.16 (see Section G.3.5.1).

In order to compare the different methods for annual mean NO_2 it was necessary to assume background concentrations of NO_X, NO_2 and, in the case of the OLM, O_3. The synthetic profiles for the WestConnex modelling domain (and associated annual mean concentrations) described in Appendix F were used for this purpose.

In the case of the OLM, the conversion method was applied to the contemporaneous hourly background data and project increment data for one year. An example dataset from a road project was used to provide the NO_X project increments. This project had an hourly time series for more than 500 receptor points. However, many of the receptors had similar concentrations and therefore a much smaller sample was extracted. The sample included a wide range of NO_X concentrations. The results of the comparison are shown in Figure G-9.

The total conversion method gave the highest NO_2 concentrations, and for the conditions defined here it resulted in an exceedance of the NO_2 criterion of 62 µg/m^3 when the total NO_X concentration was around 90 µg/m^3. The ARM and the OLM gave quite similar results, and also resulted in exceedances of the NO_2 criterion when the total NO_X concentration was around 100-120 µg/m^3. All three of these methods gave much higher NO_2 concentrations than the envelope and regression functions based on the Sydney monitoring data.

It is also worth repeating that work in the United States has shown that the performance of the ARM2, PVMRM, and OLM methods is very similar (RTP, 2013).

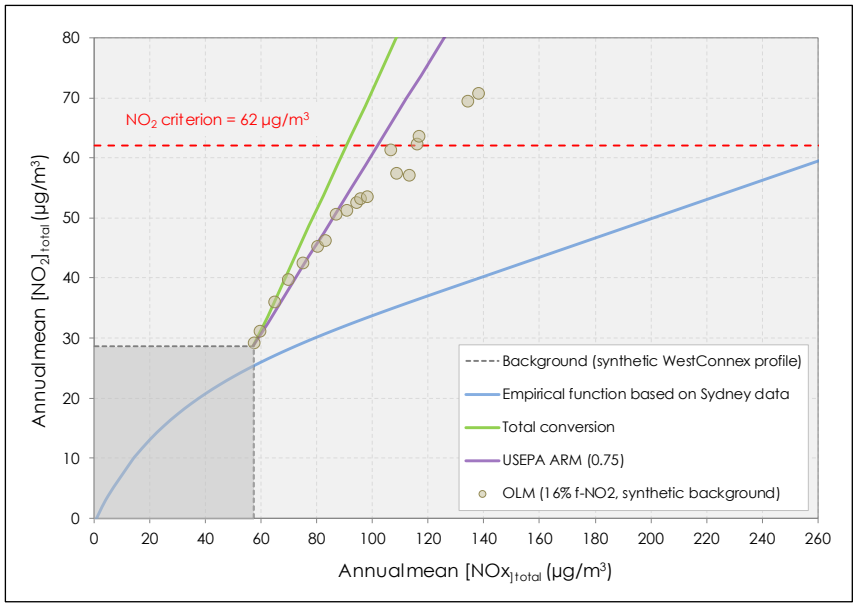

Figure G-9 Comparison of methods for calculating annual mean NO_2 concentration

Although the concentrations in the synthetic background profiles were quite conservative, the results show that that the annual mean NO_2 concentrations predicted using the total conversion, ARM and OLM methods are unrealistically high, and would tend to result in an improbable number of exceedance of the NO_2 criterion. These methods were therefore considered to be unsuitable for the M4 East assessment.

G.5.2 One-hour mean NO_2 concentrations

G.5.2.1 Detailed contemporaneous method

In the case of one-hour mean NO_2 concentrations, only the OLM was compared with the empirical contemporaneous method. Again, the synthetic background profiles for the WestConnex modelling domain were used, and an *f*-NO_2 value of 0.16 was assumed.

For the road contribution to NO_x, the same dataset as that mentioned above for annual mean concentrations was used. The hourly results for ten receptors from the dataset, with representative NO_X concentrations across the range, are shown in Figure G-10. It can be seen that the OLM predicted NO_2/NO_X ratios for many one-hour periods that were higher than those predicted by the conservative upper bound function. The OLM gave a small number of exceedances of the NO_2 criterion of 246 µg/m^3. This work shows that the OLM will yield overly conservative maximum NO_2 concentrations for road projects in Sydney.

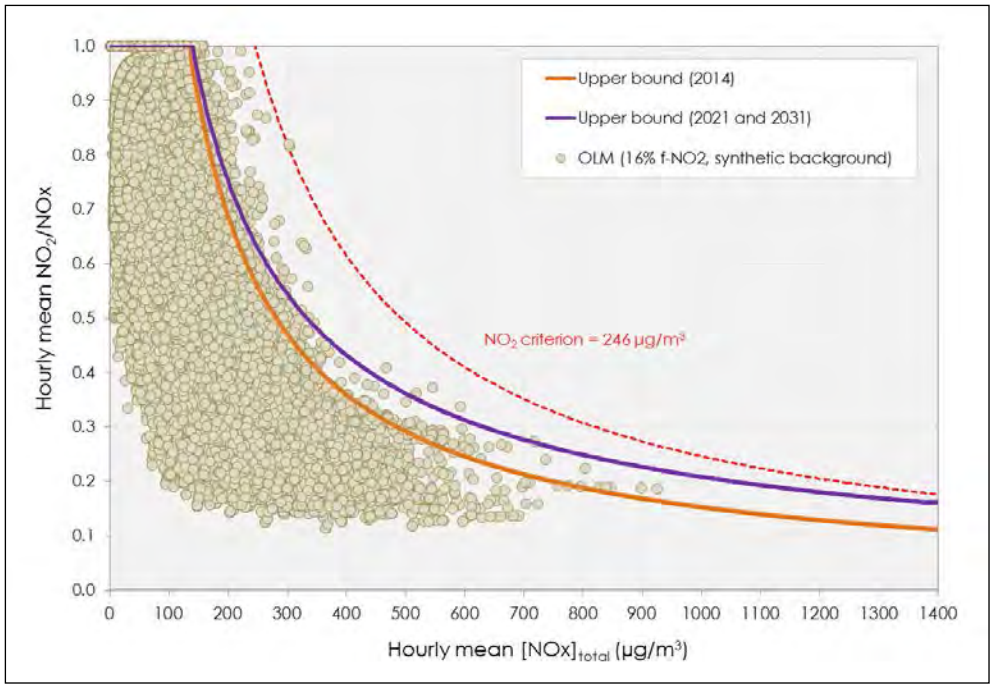

Figure G-10 Comparison of OLM and empirical methods for calculating one-hour mean NO_2 concentration

G.5.2.2 Simple statistical method

Some limited testing of the performance of the simple statistical method was also possible based on a comparison with the more detailed contemporaneous method for the community receptors. The results of this comparison are provided in Chapter 8. In general the simple method performed in a similar manner to the detailed method, giving slightly lower maximum NO_2 values.

Appendix H - Meteorological data analysis and model evaluation

H.1 Meteorological data analysis

Table H-1 provides a summary of the annual data recovery, average wind speed and percentage of calms (wind speeds < 0.5 m/s) for each of the meteorological stations between the years 2009 and 2014. The table shows a generally high percentage of data recovery at each site. It is noted that the Approved Methods require a meteorological dataset to be at least 90 per cent complete to be deemed acceptable for a Level 2 impact assessment. Therefore, any dataset in a year with less than 90 per cent data recovery was disregarded for modelling purposes but was included in the data analysis.

Table H-1 Summary of data recovery, average wind speed and percentage calms

Site and parameter	2009	2010	2011	2012	2013	2014
OEH Chullora						
Data recovery (%)	100	100	100	100	97	100
Average wind speed (m/s)	2.3	2.2	2.1	1.9	1.9	1.8
Annual calms (%)	7.6	7.0	7.4	10.4	11.5	11.6
OEH Earlwood						
Data recovery (%)	100	100	97	100	99	100
Average wind speed (m/s)	1.6	1.6	1.4	1.4	1.4	1.3
Annual calms (%)	18.1	16.8	17.5	22.0	23.1	22.0
OEH Rozelle						
Data recovery (%)	69	94	100	100	98	99
Average wind speed (m/s)	1.8	1.8	1.8	1.7	1.8	1.7
Annual calms (%)	21.7	23.1	21.3	24.9	23.1	22.1
BoM Canterbury Racecourse AWS						
Data recovery (%)	61	88	91	89	89	90
Average wind speed (m/s)	3.3	3.2	3.3	3.3	3.3	3.3
Annual calms (%)	9.4	8.4	8.0	8.7	8.8	8.6
BoM Fort Denison AWS						
Data recovery (%)	97	96	100	100	98	100
Average wind speed (m/s)	4.3	4.4	4.4	4.4	4.4	4.3
Annual calms (%)	1.6	0.8	0.5	0.2	0.4	0.3
BoM Sydney Airport AMO						
Data recovery (%)	67	66	100	100	100	100
Average wind speed (m/s)	5.7	5.7	5.7	5.6	5.7	5.5
Annual calms (%)	0.3	0.2	0.2	0.3	0.1	0.1
BoM Sydney Olympic Park AWS						
Data recovery (%)	55	N/A	N/A	N/A	N/A	N/A
Average wind speed (m/s)	2.0	N/A	N/A	N/A	N/A	N/A
Annual calms (%)	14.7	N/A	N/A	N/A	N/A	N/A
BoM Sydney Olympic Park AWS (Archery Centre)						
Data recovery (%)	N/A	N/A	31	90	89	90
Average wind speed (m/s)	N/A	N/A	2.9	2.7	2.7	2.6
Annual calms (%)	N/A	N/A	8.8	11.1	11.4	10.2

There was a high level of consistency in the annual average wind speed and annual percentage of calms across the years within each meteorological station database. Wind speed conditions (and therefore calms) have remained relatively consistent. The annual average wind speeds at the BoM Fort Denison and BoM Sydney Airport AMO sites were higher than those at the other sites. This can be explained by the generally exposed nature of these sites and their proximity to bodies of water.

Annual and seasonal wind roses for all six years and for all sites were created to analyse the general wind patterns across the WestConnex study area. The wind roses showed very similar patterns for all six years at each individual site. Figure H-1 to Figure H-14 show the annual and seasonal wind roses for the OEH and BoM meteorological stations listed in Table H-1. It is noted that no wind roses are shown for the BoM Sydney Olympic Park AWS station as this site was decommissioned in 2009. The BoM Sydney Olympic Park Archery Centre site was commissioned in 2011. The wind roses show similarities in the dominant wind patterns; winds were predominantly from the north-west and south-east directions. The seasonal patterns were also very similar between sites. The BoM Fort Denison site is located in the harbour and is therefore the wind flow may be strongly influenced by local conditions.

It is noted that the OEH Rozelle and Chullora are located in proximity to the M4 East project area. Figure H-1 and Figure H-2 present the annual and seasonal wind roses for the OEH Chullora site for 2009 to 2014. The wind roses for 2009 to 2011 show mostly similar wind patterns with a fair distribution of winds from all angles annual but with some west south-westerly dominance. The wind roses for 2012 to 2014 however, show a significant change in wind pattern both annually and by season with very dominant northeast/southwest winds not seen in earlier years. The winter wind roses in particular show a shift in the dominant winds from mostly westerlies in 2009 to 2011 to south-westerlies in 2012 to 2014.

Figure H-5 and Figure H-6 present the annual and seasonal wind roses for the OEH Rozelle site for 2009 to 2014. The wind roses for 2009, 2010 and 2014 show similar wind patterns with dominant winds from the northwest, northeast and south to varying degrees in all seasons. The wind roses for 2011, 2012 and 2013 however, show an anti-clockwise shift in this pattern changing the domain winds to the west-northwest, north-northeast and south-southeast. It is not clear what has caused this shift in wind patterns at the OEH Chullora and Rozelle meteorological stations. However, it is noted that according to the OEH website (http://www.environment.nsw.gov.au/AQMS/sitesyd.htm), both of these sites do not currently comply with Australian Standard AS/NZS 3580.1.1:2007[1], as the clear sky angle is < 120˚ due to trees within 20 metres of both monitoring sites. For these reasons, these stations were not chosen for use in the GRAMM model.

Based on the analysis of the available meteorological data within the study area, data from the BoM Canterbury Racecourse AWS meteorological station were chosen as the input to GRAMM for modelling. The site was also located closest to the centre of the GRAMM domain for WestConnex, and was considered to be representative of the general wind patterns in the domain. As 2014 was the most recent year of available meteorological data, it was the preferred year for modelling. The analysis showed that the 2014 data were representative of conditions in previous years. Moreover, the selection of the 2014 meteorological data was consistent with the use of ambient air quality data to define background concentrations for the assessment.

Additional analysis of the data from the BoM Canterbury Racecourse AWS was undertaken and Figure H-7 and Figure H-8 present the annual and seasonal wind roses for this site for 2009-2011 and 2012-2014, respectively. Figure H-15 also shows annual and diurnal plots of wind speed and temperature from the Canterbury Racecourse site for 2014. The annual plots show a typical distribution of wind speed and temperature over the course of a year. The diurnal plots of wind speed and temperature also show typical patterns, with higher wind speeds and temperatures during the day, decreasing at night and in the early morning.

Having determined the representativeness of the 2014 data sets over the previous six years, the next step was to evaluate the performance of the meteorological model (GRAMM) using these data. The various methodologies used to carry out this analysis are described in Section H.2.

[1] AS/NZS 3580.1.1:2007 - Methods for sampling and analysis of ambient air - Guide to siting air monitoring equipment

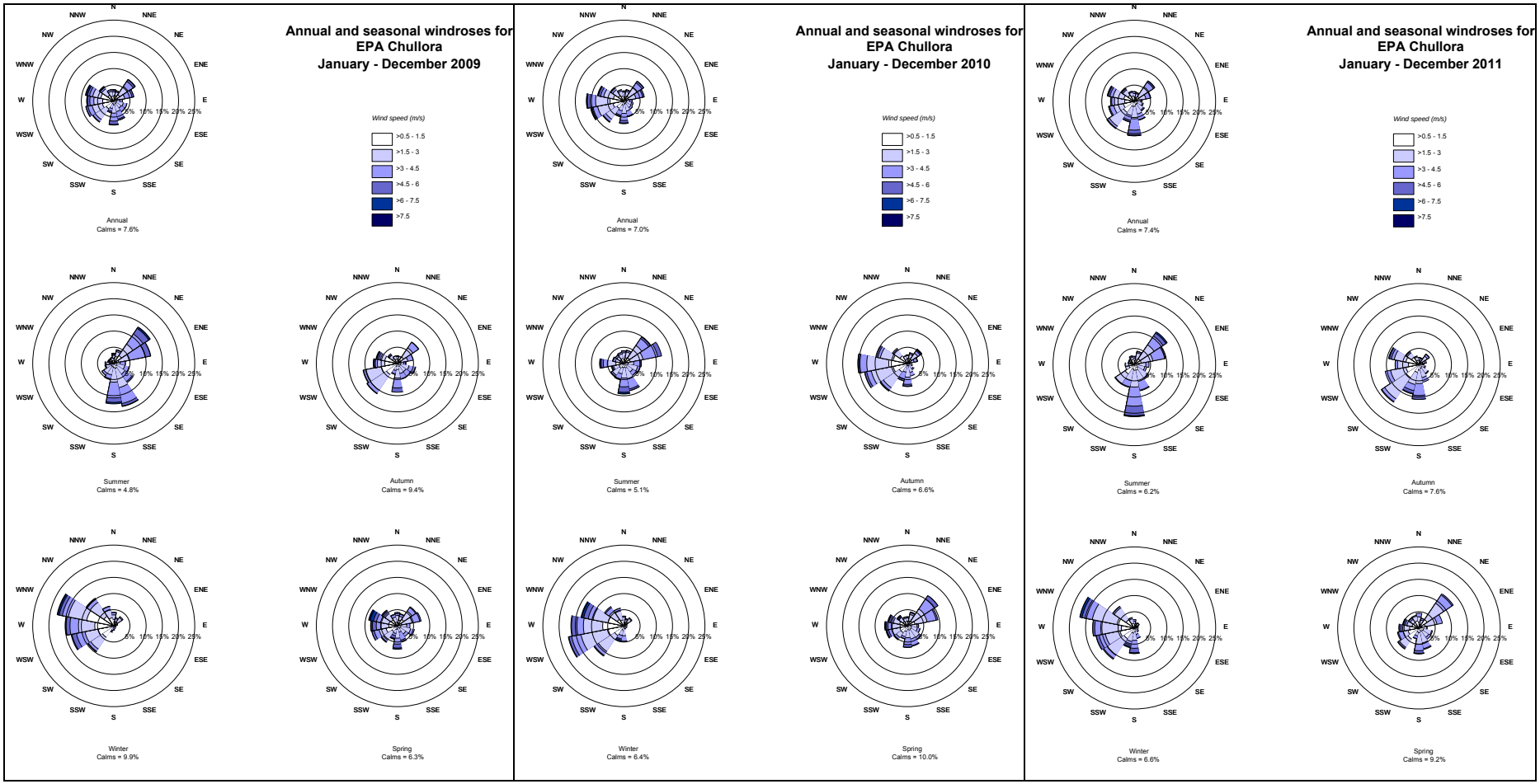

Figure H-1 Annual and seasonal wind roses for OEH meteorological station Chullora (2009-2011)

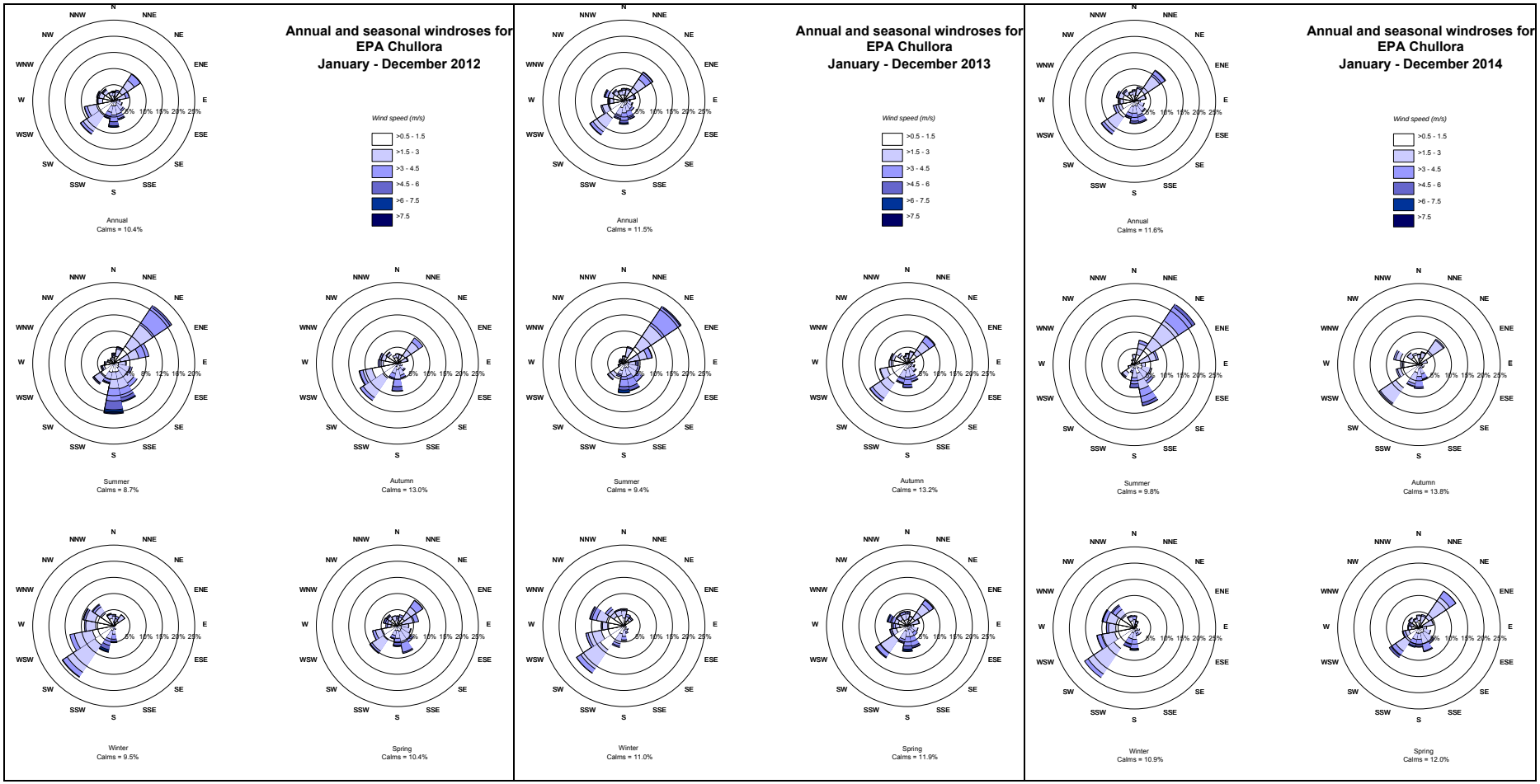

Figure H-2 Annual and seasonal wind roses for OEH meteorological station Chullora (2012-2014)

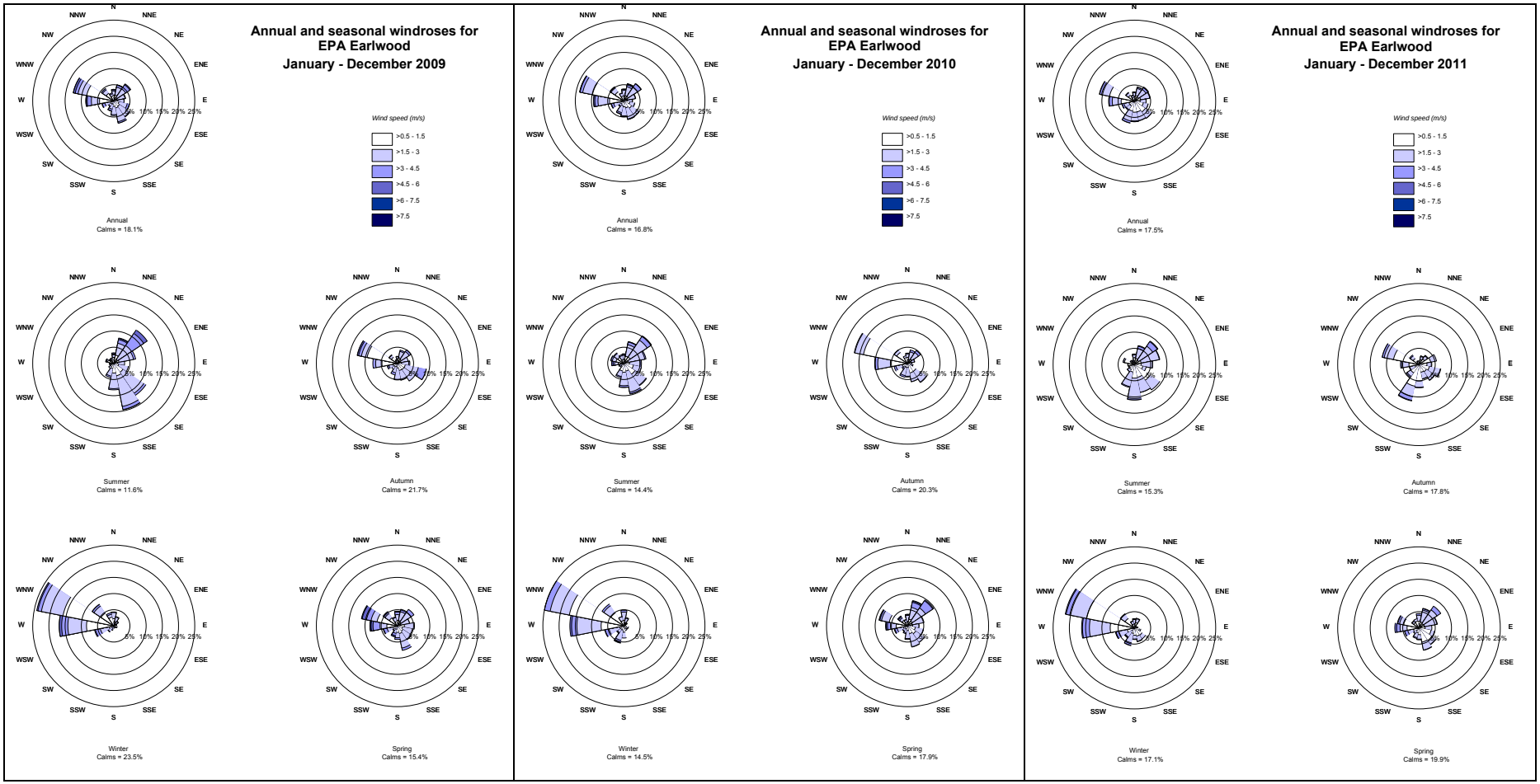

Figure H-3 Annual and seasonal wind roses for OEH meteorological station Earlwood (2009-2011)

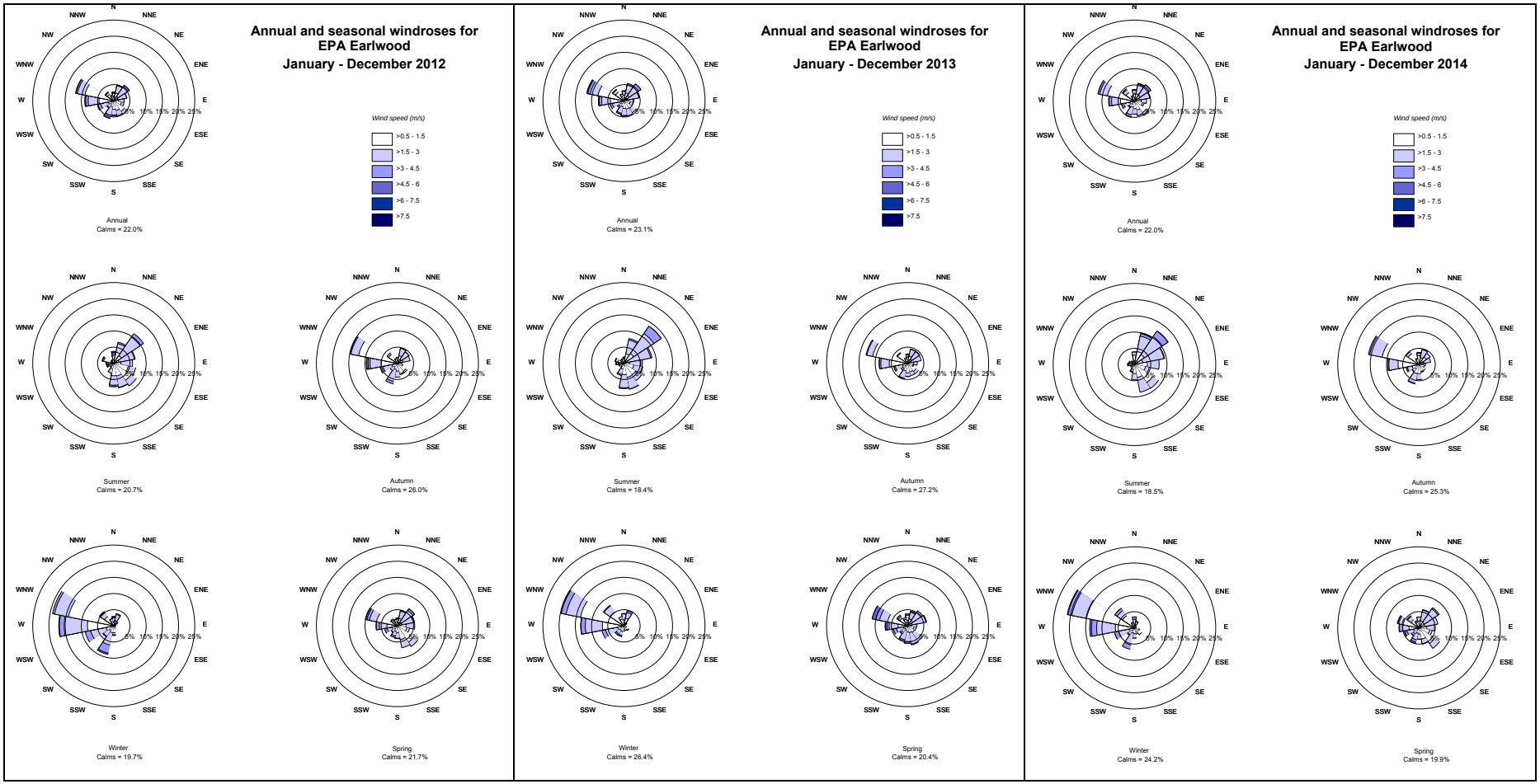

Figure H-4 Annual and seasonal wind roses for OEH meteorological station Earlwood (2012-2014)

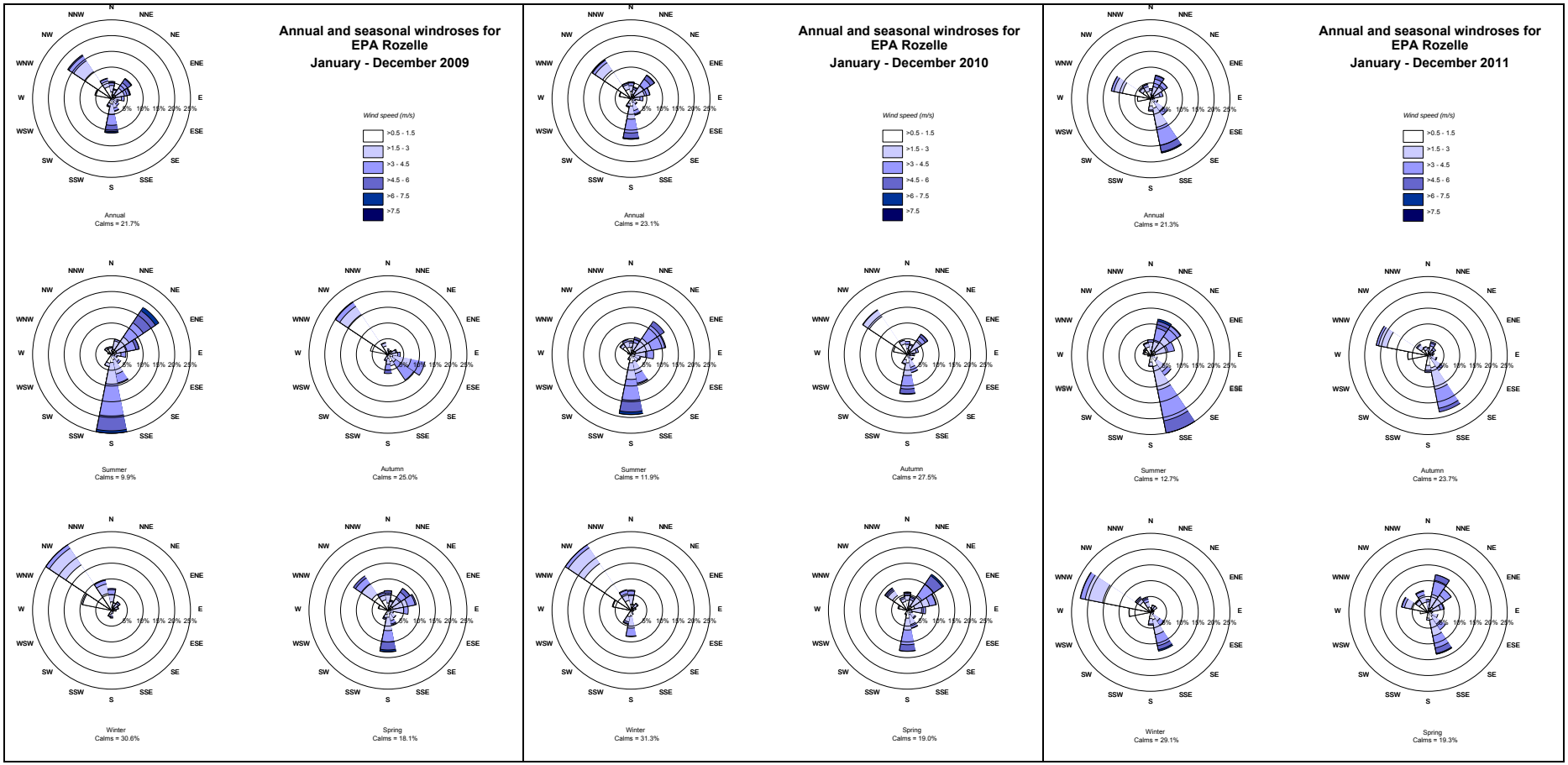

Figure H-5 Annual and seasonal wind roses for OEH meteorological station Rozelle (2009-2011)

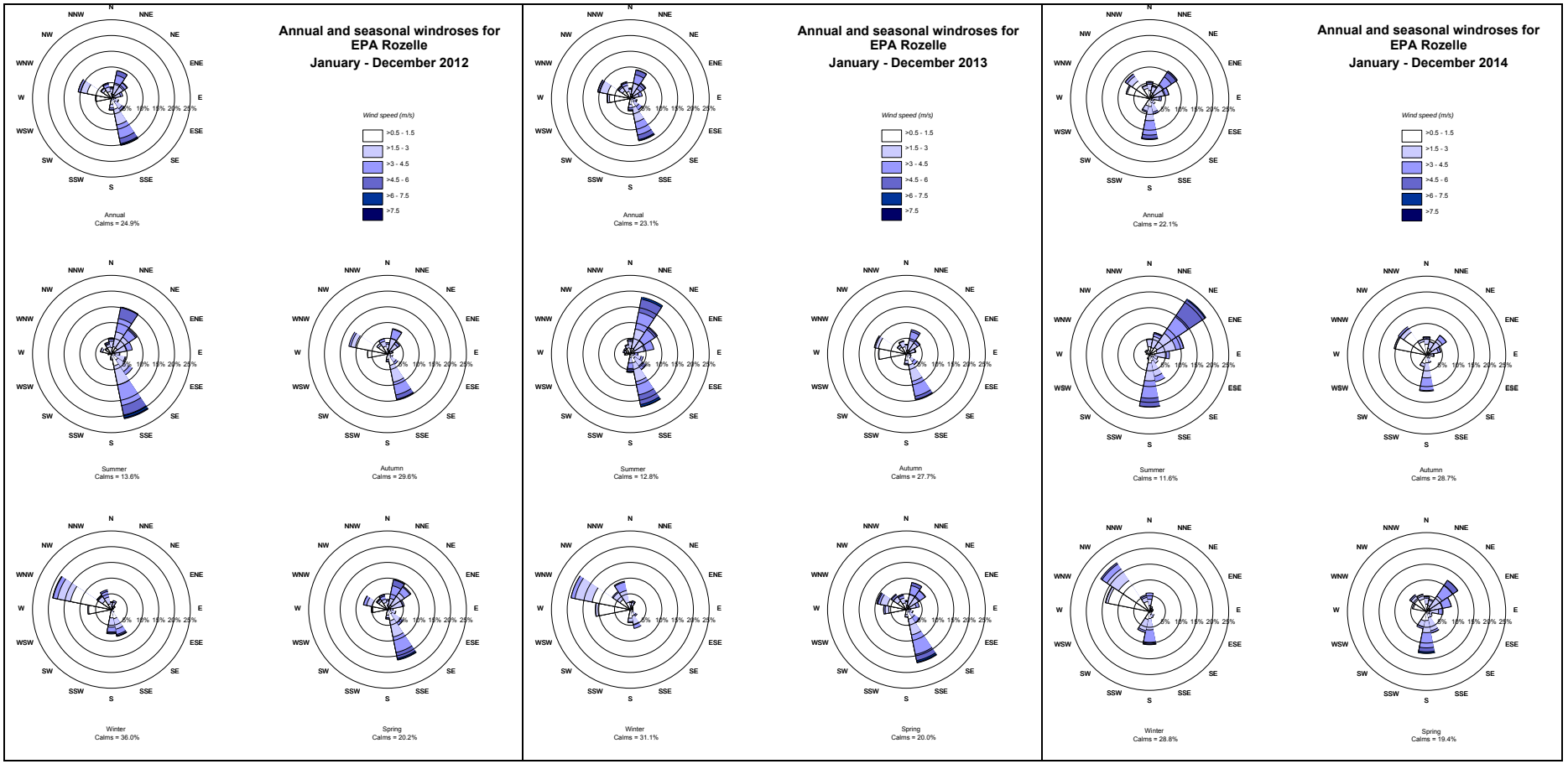

Figure H-6 Annual and seasonal wind roses for OEH meteorological station Rozelle (2012-2014)

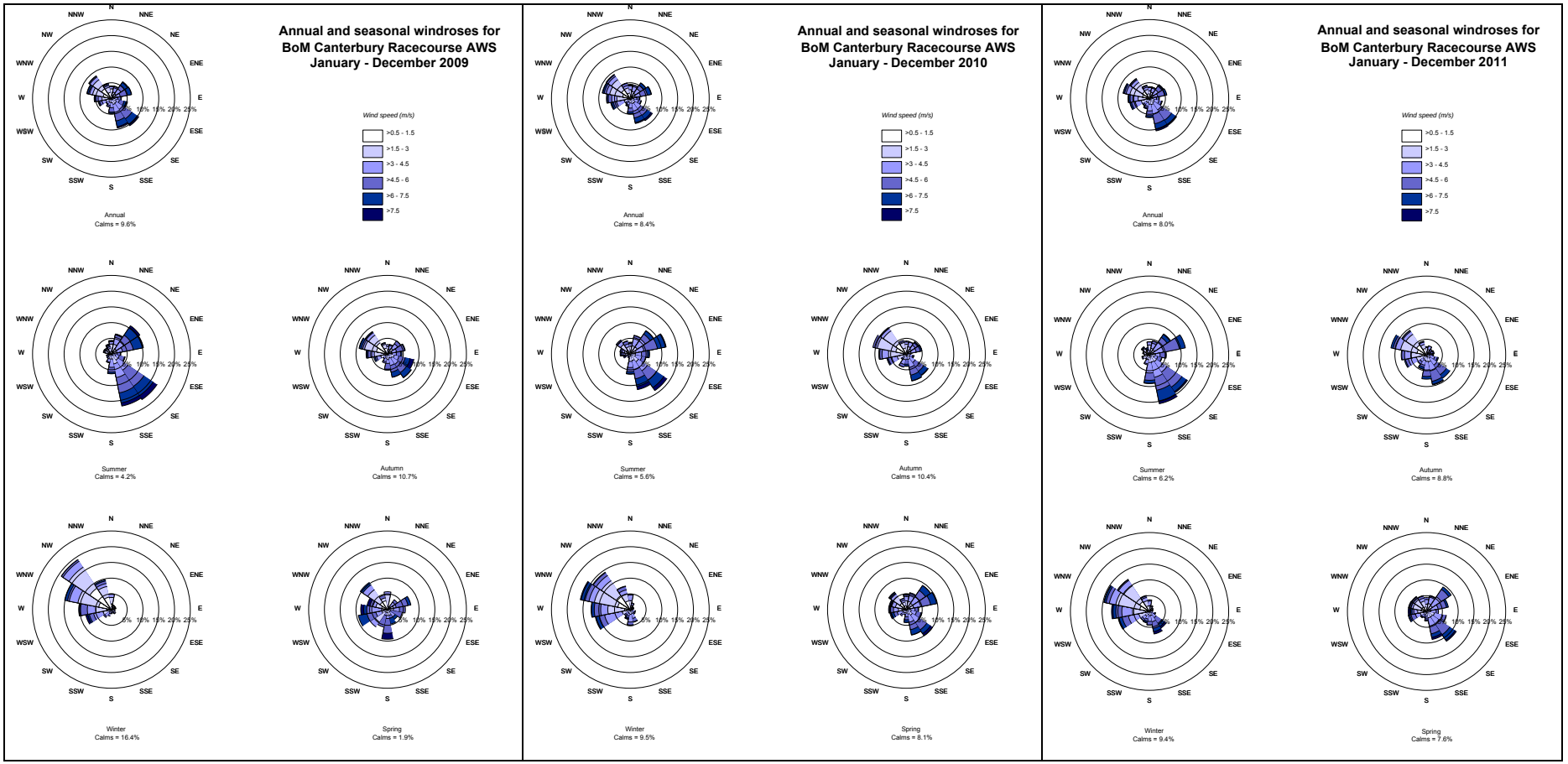

Figure H-7 Annual and seasonal wind roses for BoM Canterbury Racecourse AWS (2009 – 2011)

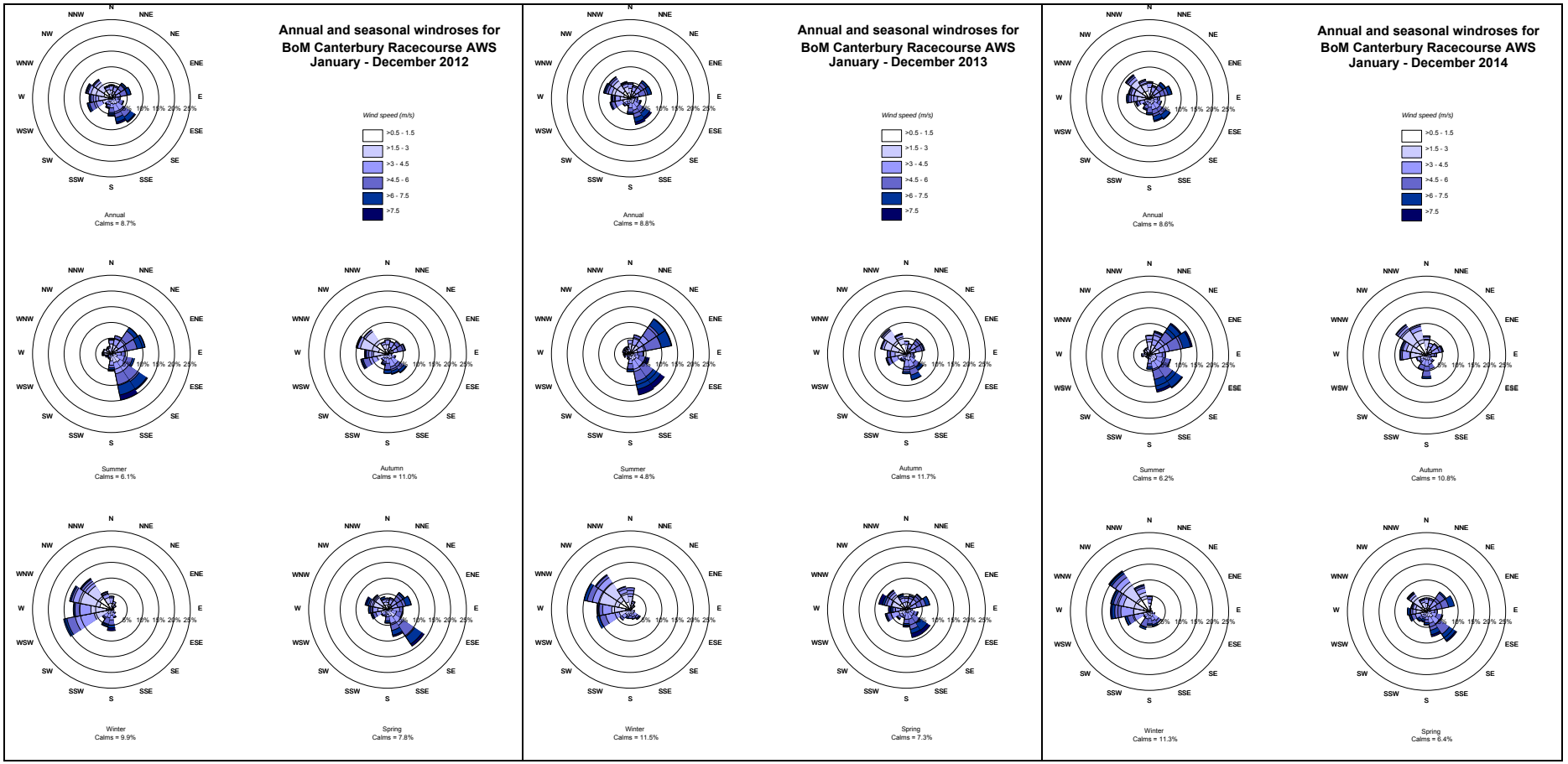

Figure H-8 Annual and seasonal wind roses for BoM Canterbury Racecourse AWS (2012 – 2014)

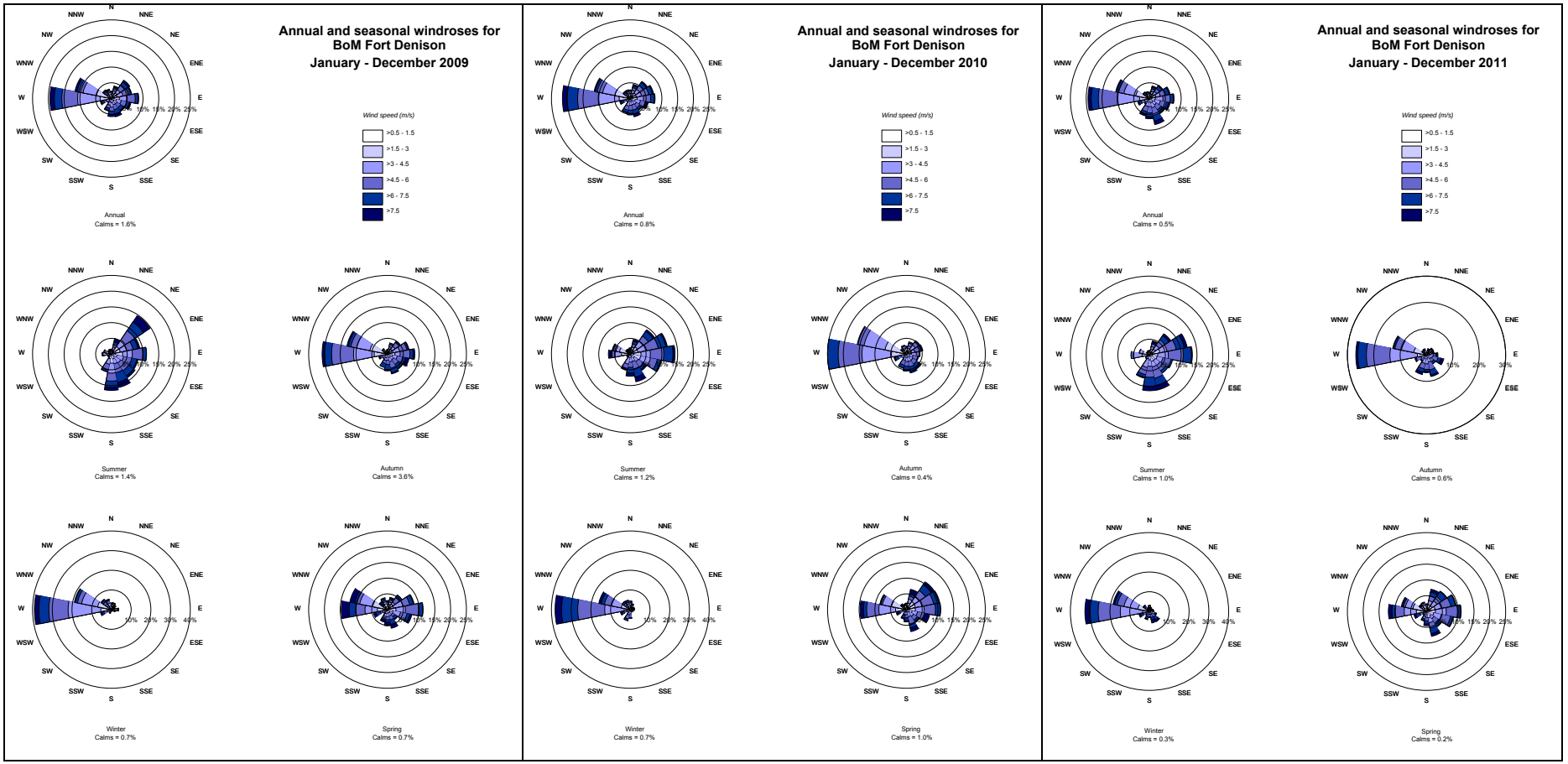

Figure H-9 Annual and seasonal wind roses for BoM Fort Denison AWS (2009 – 2011)

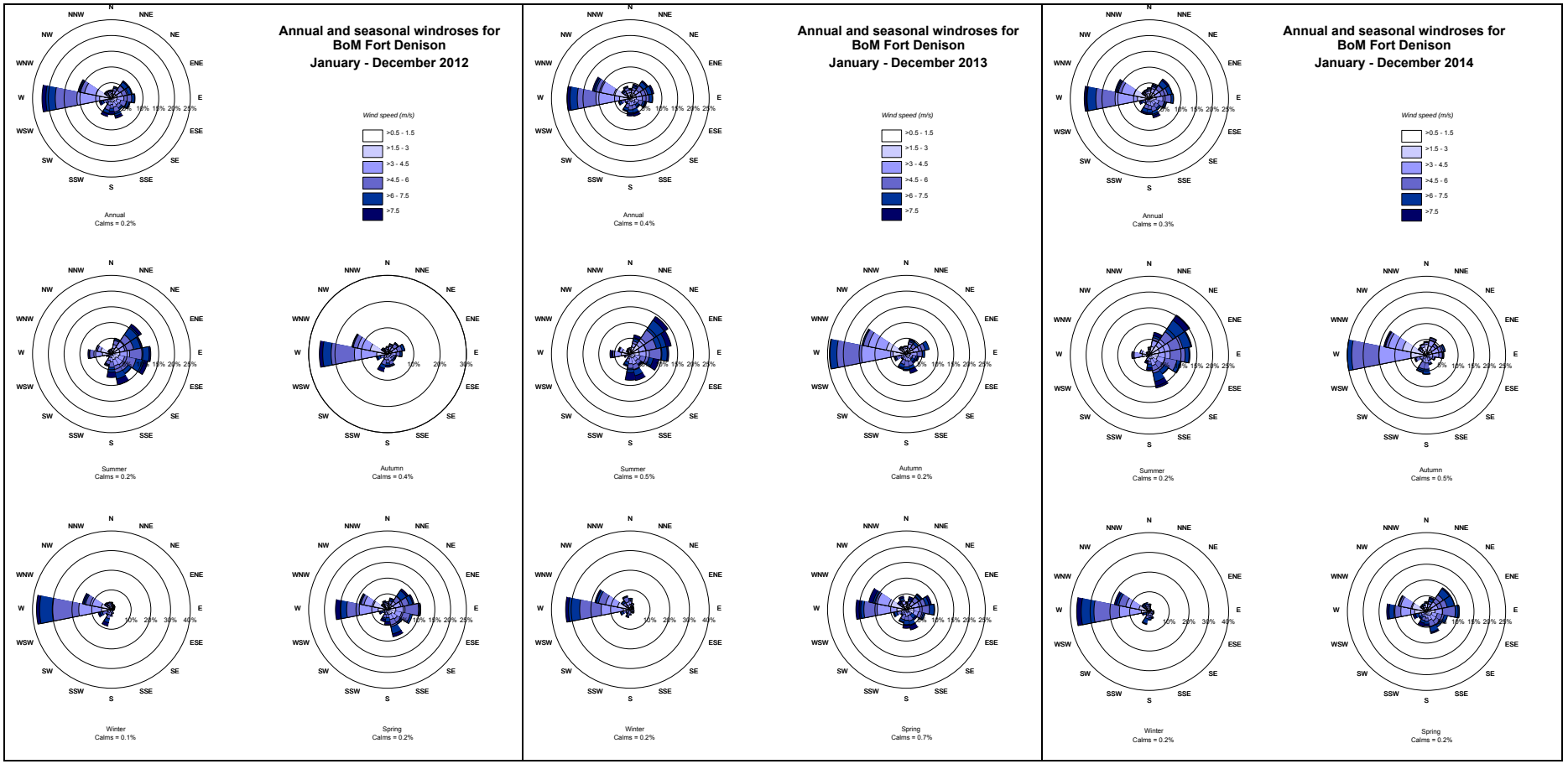

Figure H-10 Annual and seasonal wind roses for BoM Fort Denison AWS (2012 – 2014)

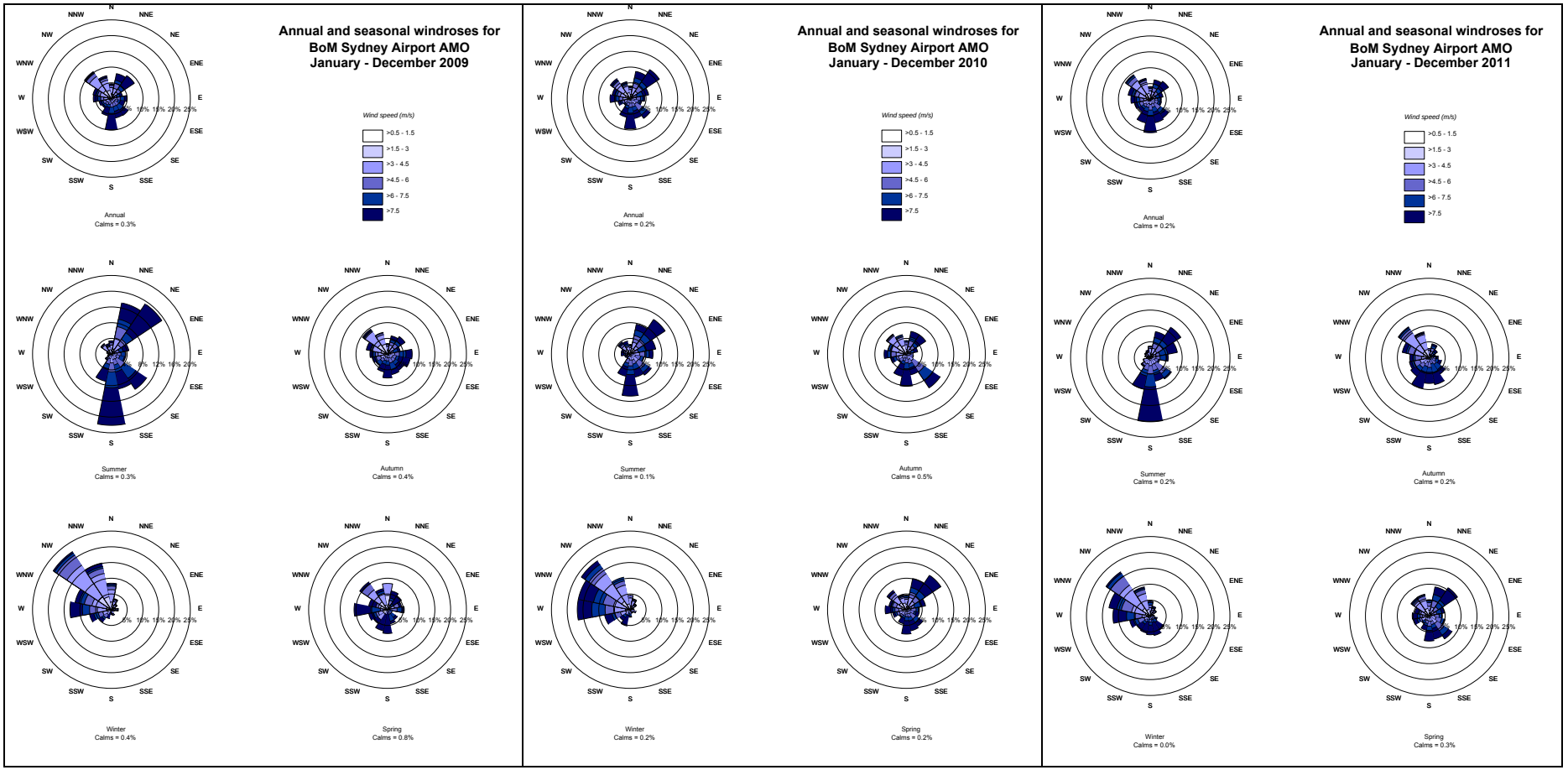

Figure H-11 Annual and seasonal wind roses for BoM Sydney Airport AMO (2009 – 2011)

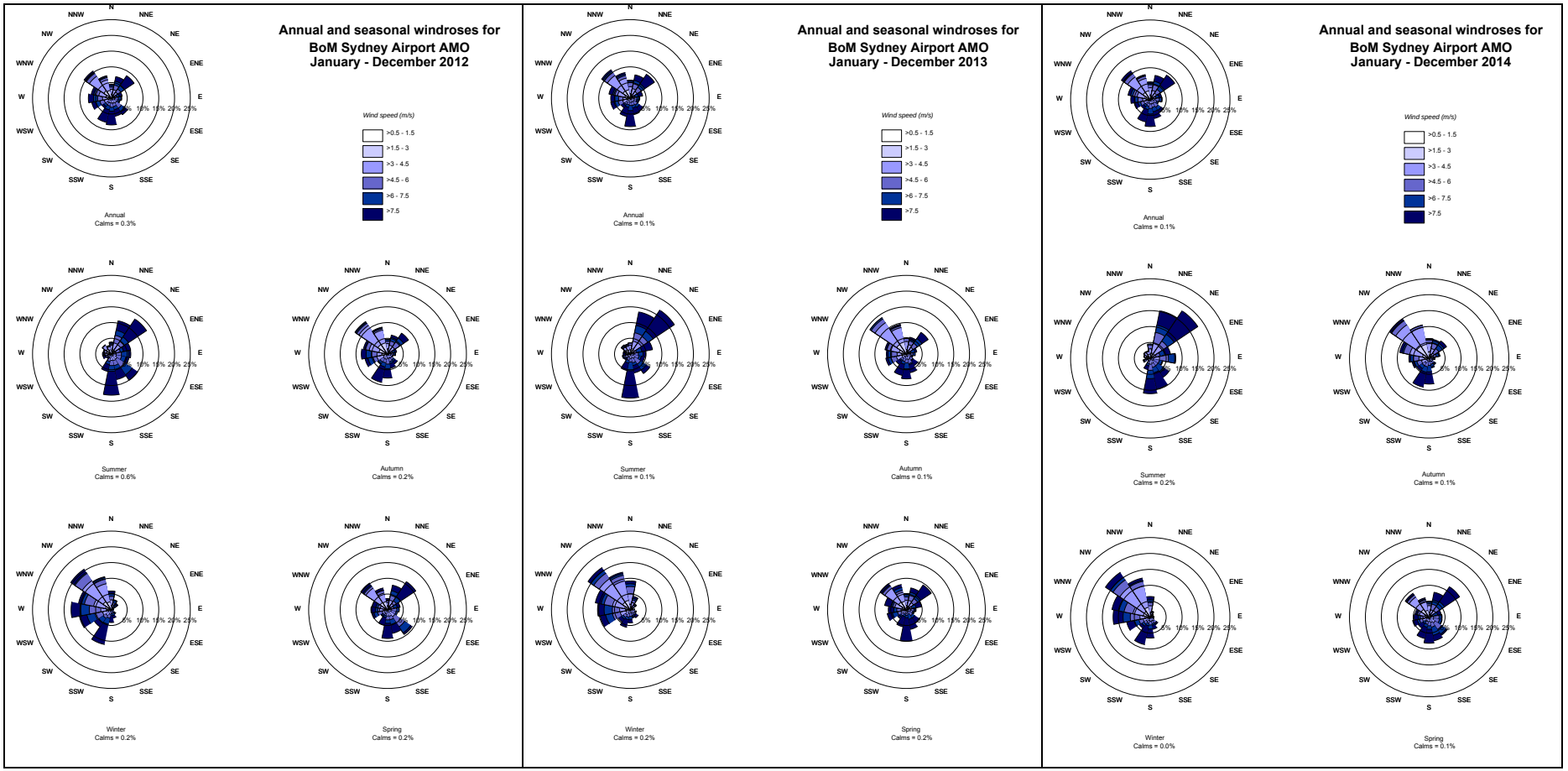

Figure H-12 Annual and seasonal wind roses for BoM Sydney Airport AMO (2012 – 2014)

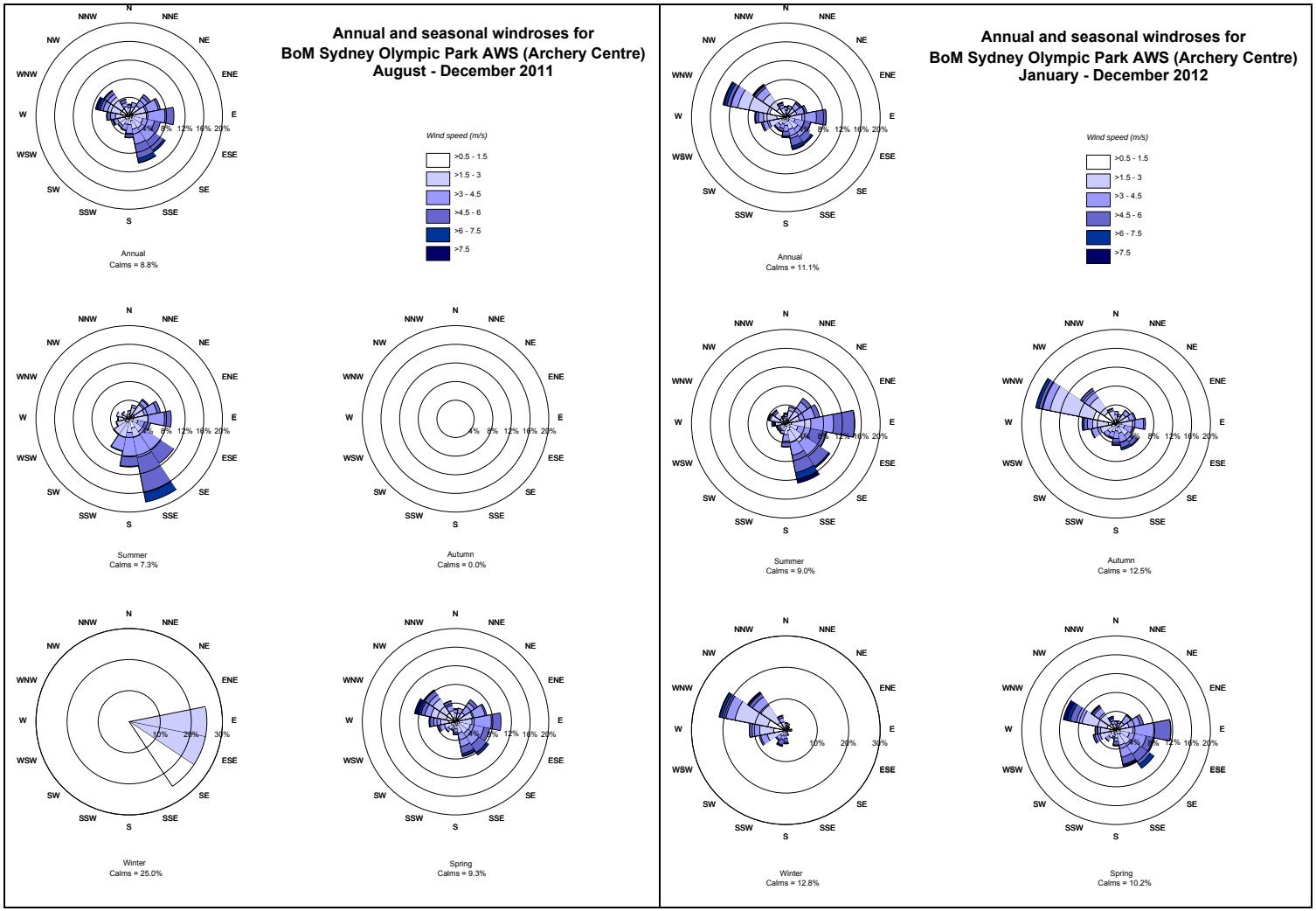

Figure H-13 Annual and seasonal wind roses for BoM Olympic Park AWS (Archery Centre) (2011 – 2012)

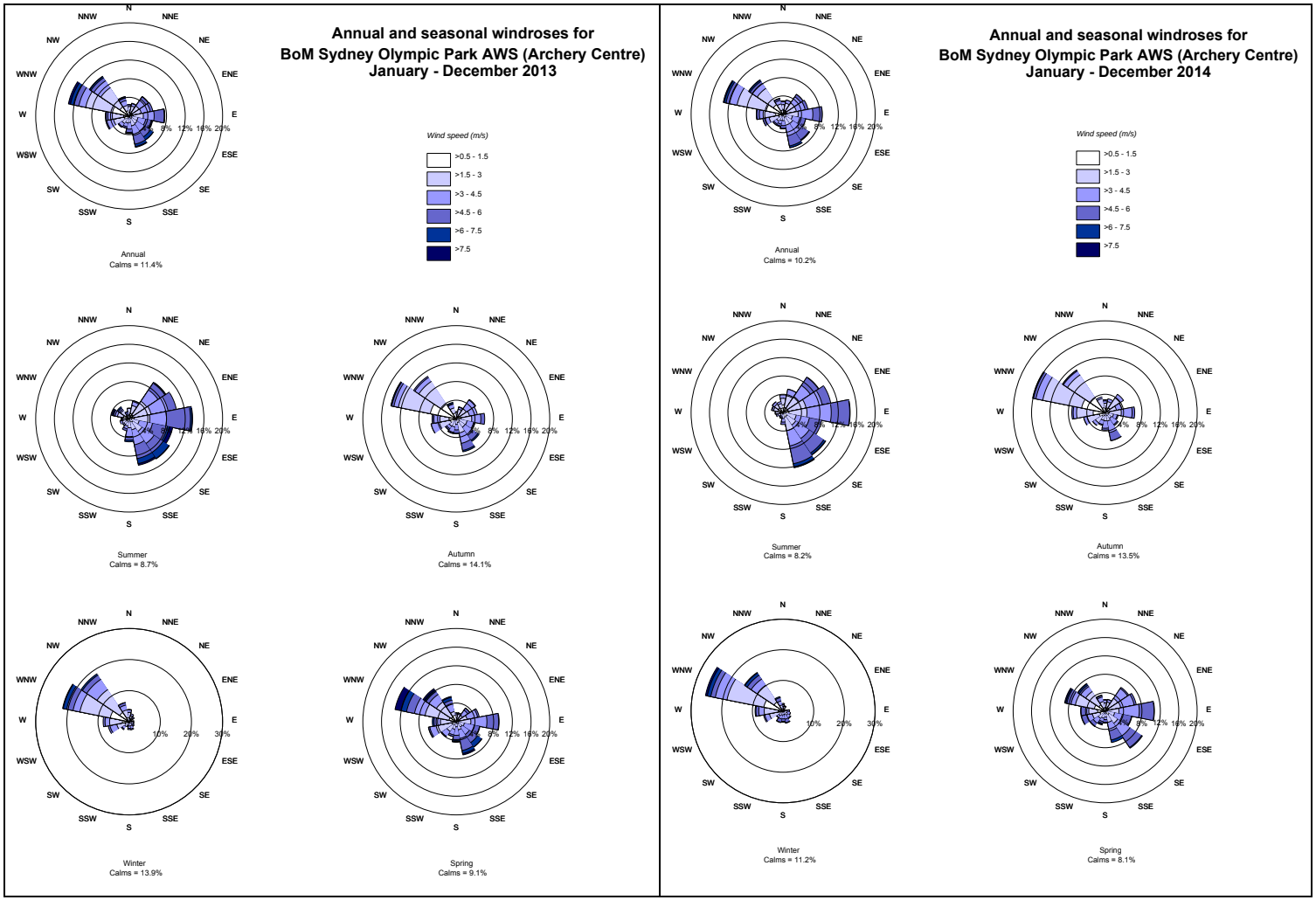

Figure H-14 Annual and seasonal wind roses for BoM Olympic Park AWS (Archery Centre) (2013 – 2014)

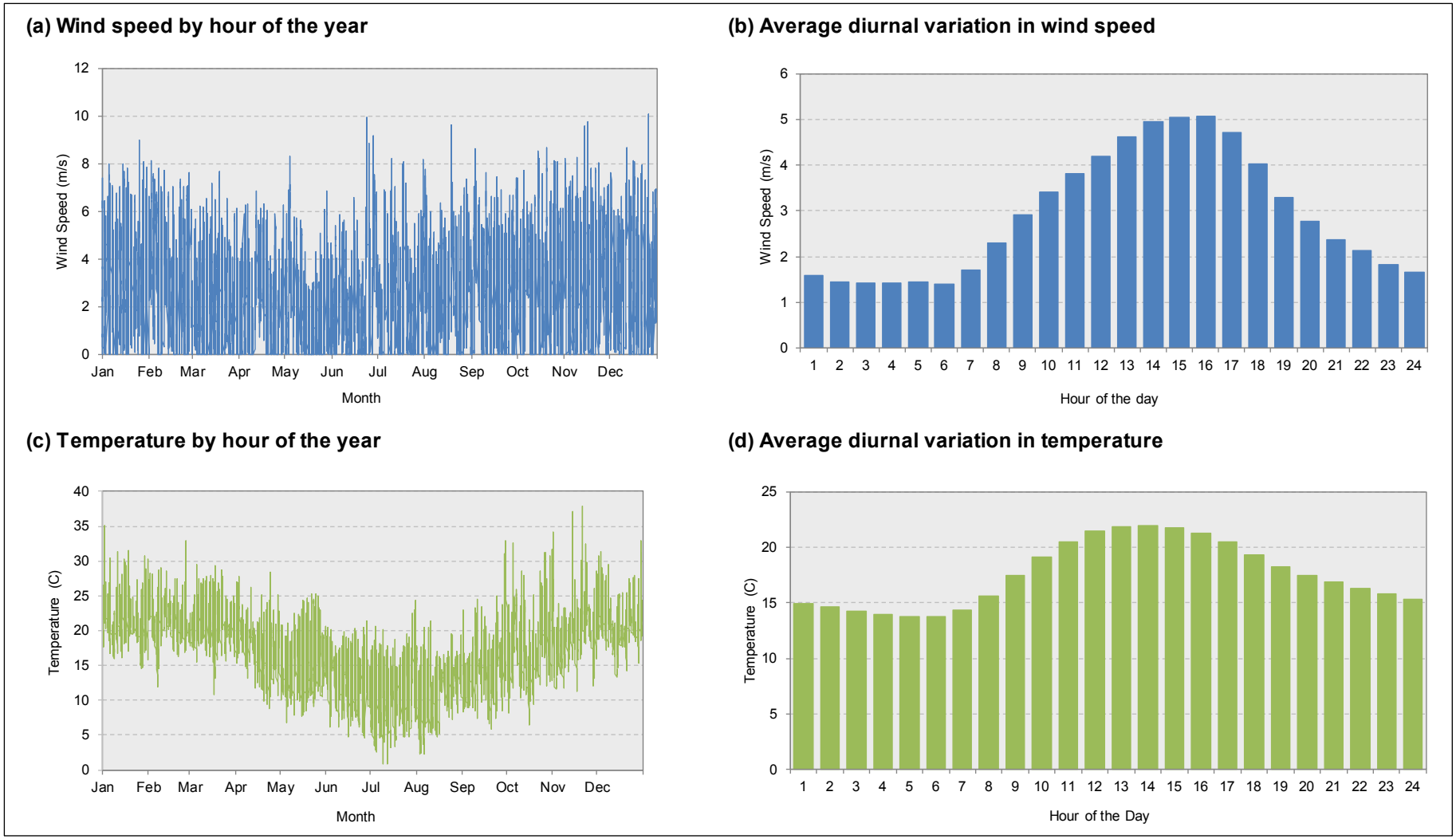

Figure H-15 Annual and diurnal plots of wind speed and temperature for BoM Canterbury Racecourse AWS, 2014

H.2 Meteorological model evaluation

H.2.1 Wind speed

For each of the GRAMM evaluation sites, time series, regression and percentile plots of wind speed are shown in Figure H-16.

Regression analysis of wind speed showed a very good agreement between predicted and observed wind speeds at the Canterbury Racecourse site, which was the site used for modelling. There was also a reasonable agreement at Sydney Olympic Park, but less so at the other sites. In summary, the R^2 values are listed as follows:

- Canterbury Racecourse wind speed $R^2 = 0.92$
- Sydney Airport wind speed $R^2 = 0.49$
- Sydney Olympic Park wind speed $R^2 = 0.60$
- Rozelle wind speed $R^2 = 0.45$
- Chullora wind speed $R^2 = 0.50$

The percentile plots shown in Figure H-16 demonstrate an under-prediction of high wind speeds at Canterbury Racecourse. There is also an under prediction at Sydney Olympic Park at the highest wind speeds, and a slight over prediction in the lower to mid range. Percentile plots at these two sites show a much closer agreement between the measurements and predictions than for sites further away from the project.

It should be noted that whilst the model shows a good agreement at the BoM Canterbury Racecourse site and lesser agreement at other locations, this is to be expected as the GRAMM model (like many other meteorological models) uses data from one location to represent the study area. This is not uncommon in studies with relatively small model domains and predominantly uniform land-use and terrain features such as that in the M4 East study area. The regression analysis values for these other sites as shown above appear low compared to the Canterbury Racecourse site but are considered fair considering that these data were not included in the GRAMM modelling.

Whilst meteorological conditions are an important aspect of any dispersion modelling excercise, it may not always be the most important aspect in determining predicted concentrations in near-source environments such as this. Section 8 of the report provides a validation of the GRAL predictions as compared with measured data. The analysis shows a good agreement between predictions and measurements and shows that the model is slightly over predicting at all locations which is as expected and required in an assessment of this nature. This shows that although GRAMM may not be predicting meteorology 100 per cent accurately at all locations across the domain, the GRAL model (for which GRAMM is an input), is predicting results at an appropriate level at varying locations in the study area.

A plot of predicted and observed average wind speeds by hour of day at Canterbury Racecourse show good agreement (Figure H-17). As mentioned previously, there is a tendency for GRAMM to underestimate the higher wind speeds during the middle of the day, but this will add a level of conservatism to the modelling. Times of peak traffic volumes when wind speeds are often lower, show better agreement.

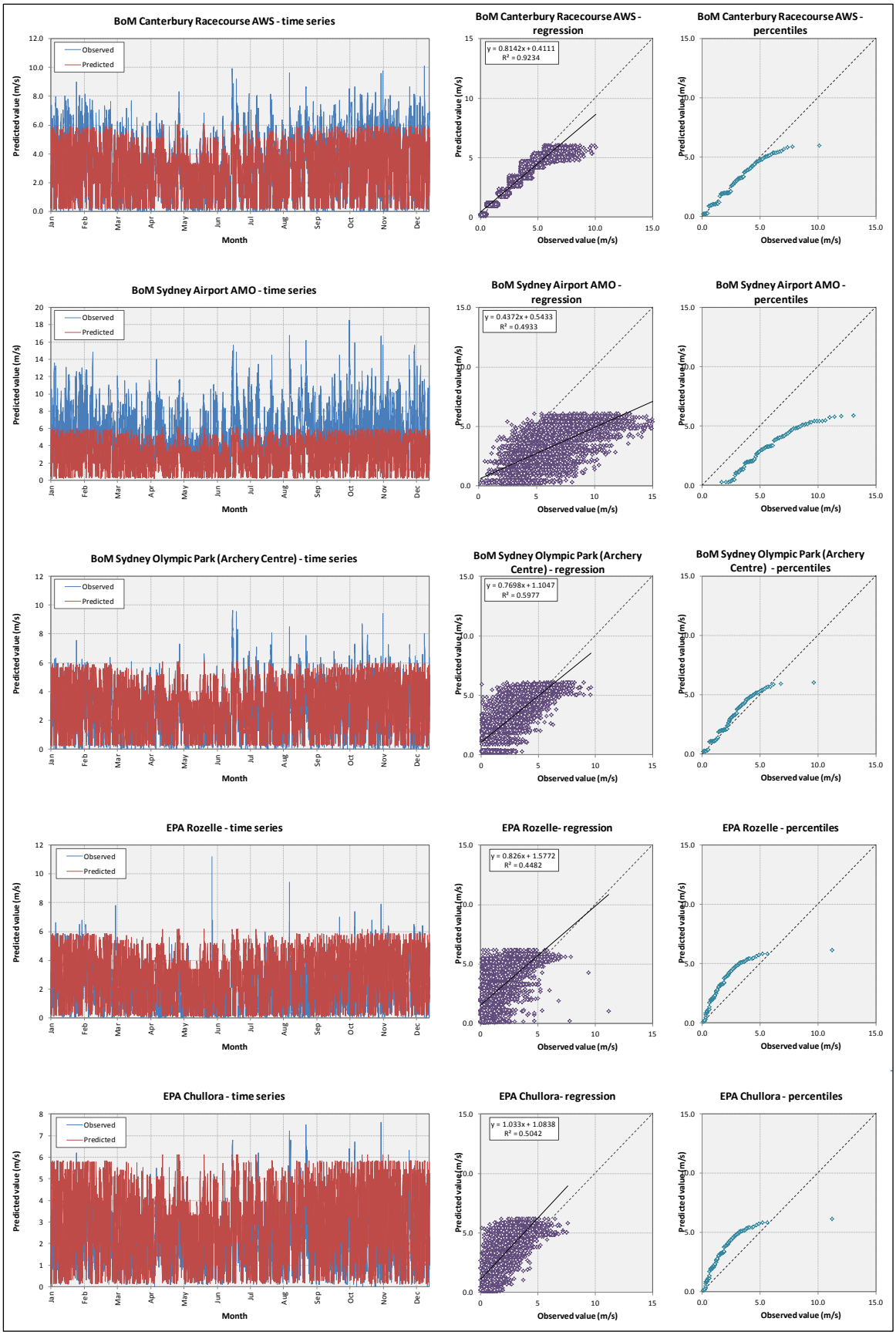

Figure H-16 GRAMM predicted and observed hourly average wind speed (time series, regression and percentile plots)

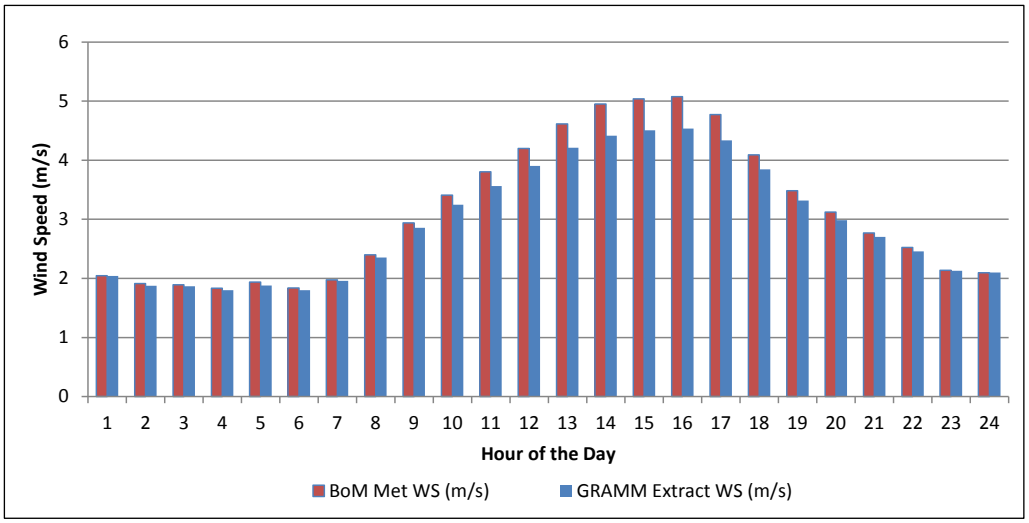

Figure H-17 Average wind speeds by hour of day for observed and predicted at Canterbury Racecourse

H.2.2 Wind direction

Annual and seasonal wind roses for the measurements at the Canterbury Racecourse site are presented in Figure H-18. The predicted winds from GRAMM are presented for comparison with observed. Both the GRAMM extract and the GRAMM extract re-ordered compare very well with the observations for annual and seasonal variations.

H.2.3 Statistical benchmarks

The statistical measures used to quantify the differences between model predictions and observations are taken from the BOOT Statistical Model Evaluation Software Package (Chang and Hanna, 2005) and assessed against the performance benchmarks set for model evaluation (Emery et al., 2001). The BoM Canterbury Racecourse data for 2014 were included in this analysis.

The metrics used were as follows:

- Index of agreement
    - This measures how well the predictions and measurements are matched in terms of how they deviate from the mean.
- Mean gross error
    - This measures how much of the prediction error is so large that it cannot be due to errors that are normally expected in measurements.
- Mean bias
    - This is the average of the errors in a group of predicted values.
- Fractional bias
    - This is similar to Mean Bias but is 'non-dimensional', meaning values.
- Skill v
    - This compares the amount of scatter in the modelled and measured data.
- Skill r
    - This compares overall error in the predictions to scatter in the measured values. If this value is <1 then it shows the model is predicting well.

These statistical measures are summarised in Table H-2 along with the performance benchmarks adopted for the study.

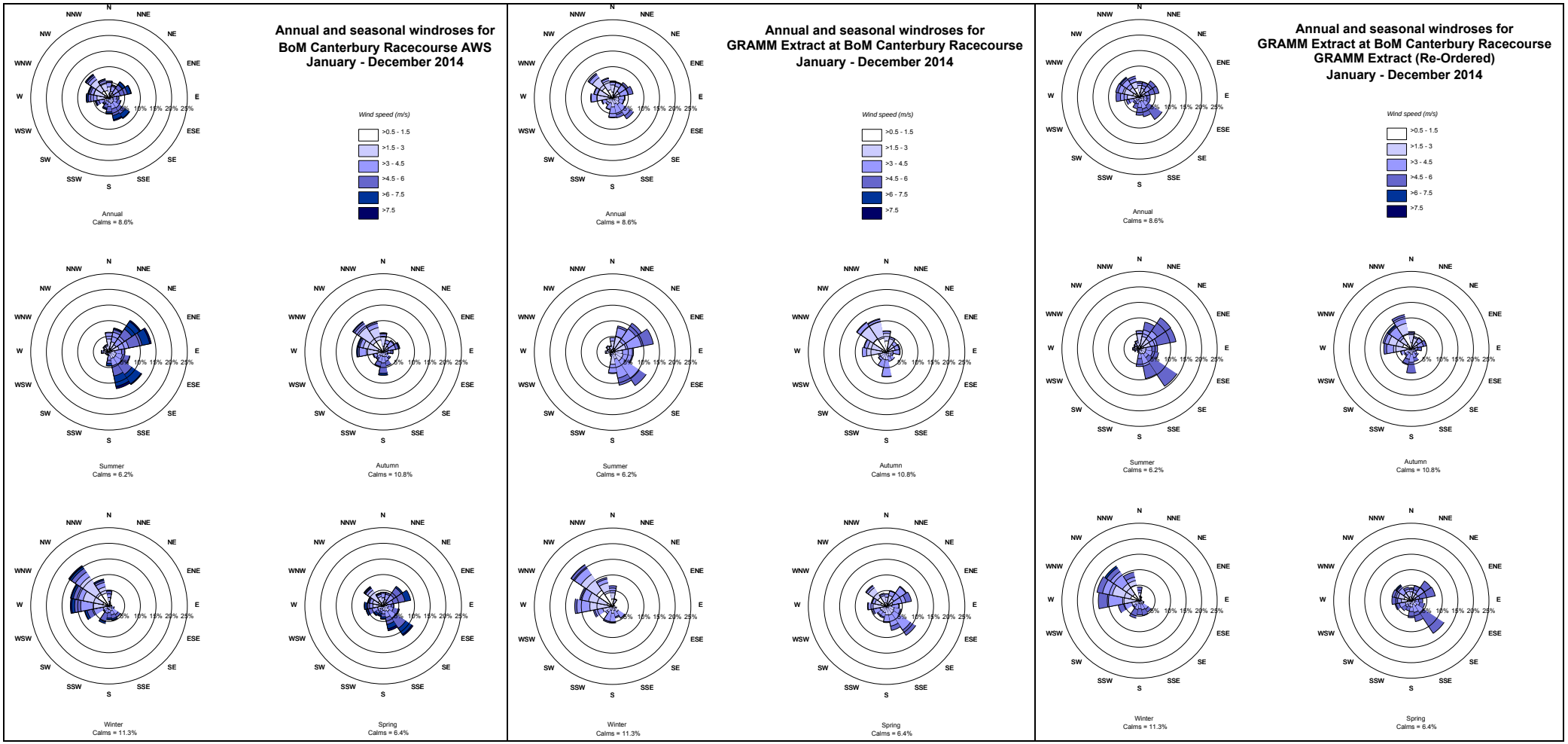

Figure H-18 Annual and seasonal wind roses for observed and predicted at Canterbury Racecourse

Table H-2 Statistical measures used to evaluate GRAMM performance

Statistical measure	Description	Parameter	Ideal value	Benchmark
Index of agreement (IOA)	$IOA = 1 - \frac{\sum_{i=1}^{n}(P_i - O_i)^2}{\sum_{i=1}^{n}(\lvert P_i - \bar{O}\rvert + \lvert O_i - \bar{O}\rvert)^2}$	Wind speed	1	≥ 0.6
Mean bias (MB)	$MB = \frac{1}{n}\sum_{i=1}^{N}\lvert P_i - O_i\rvert$	Wind speed	0	≤ ± 0.5 m/s
		Wind direction	0	≤ 10º
Mean gross error (MGE)	$MGE = \frac{1}{N}\sum_{i=1}^{N}\lvert P_i - O_i\rvert$	Wind speed	0	≤ 2 m/s
		Wind direction	0	≤ 30º
Fractional bias	$FBIAS = \frac{2}{n}\sum_{i=1}^{n}\left(\frac{P_i - O_i}{P_i - O_i}\right) \times 100\%$	Wind speed	0	≤ ± 0.67
Skill v		Wind speed	1	1
Skill r		Wind speed	-	< 1

N = number of observations $\bar{O}$ = mean of observed values
P = predicted value $\bar{P}$ = mean of predicted values
O = observed value i = time period

The evaluation of GRAMM performance against these benchmarks is presented in Table H-3. The index of agreement (IOA) compares well against the benchmark for wind speed, approaching the ideal score of 1. The fractional bias, skill v and skill r tests all fall within the acceptable range. The mean gross error (MGE) compares well against the benchmark for both variables, in particular for wind direction. Model performance against mean bias (MB) also falls within the acceptable benchmark.

Overall, it can be concluded that GRAMM simulates the meteorology with an acceptable degree of accuracy.

Table H-3 Statistical evaluation of GRAMM performance

Statistical measure	Ideal value	Wind speed		Wind direction	
		Benchmark	Result	Benchmark	Result
IOA	1	≥ 0.6	0.92	-	-
Mean bias	0	≤ ± 0.5 m/s	0.32	≤ 10º	3.8
Mean gross error	0	≤ 2 m/s	1.22	≤ 30º	4.8
Fractional bias	0	≤ ± 0.67	0.32	-	-
Skill v	-	1	0.65	-	-
Skill r	-	< 1	0.80	-	-

(blank page)

Appendix I - Emissions and concentrations for ventilation outlets

I.1 Emissions from ventilation outlets

Table I-1 Emission rates: Eastern vent facility (M4 East outlet), 2021-DS (expected operation)

Hour start	NO_2 (g/s)[(a)]	NO_X (g/s)	CO (g/s)	$PM_{2.5}$ (g/s)	PM_{10} (g/s)	THC (g/s)
00	0.019	0.145	0.303	0.014	0.020	0.009
01	0.013	0.095	0.200	0.009	0.013	0.006
02	0.012	0.089	0.191	0.009	0.012	0.006
03	0.016	0.123	0.265	0.012	0.017	0.008
04	0.033	0.247	0.521	0.024	0.034	0.016
05	0.087	0.662	1.400	0.064	0.091	0.042
06	0.168	1.274	2.681	0.123	0.176	0.081
07	0.232	1.759	3.145	0.165	0.237	0.112
08	0.221	1.673	2.982	0.157	0.225	0.107
09	0.240	1.821	3.639	0.174	0.250	0.116
10	0.206	1.561	3.122	0.149	0.214	0.100
11	0.199	1.509	3.023	0.144	0.207	0.096
12	0.197	1.489	2.978	0.142	0.204	0.095
13	0.197	1.494	2.985	0.142	0.204	0.095
14	0.201	1.526	3.051	0.145	0.209	0.097
15	0.201	1.520	3.874	0.157	0.226	0.097
16	0.201	1.520	3.931	0.158	0.227	0.097
17	0.209	1.582	4.096	0.165	0.237	0.101
18	0.124	0.937	1.981	0.090	0.129	0.060
19	0.095	0.723	1.528	0.069	0.100	0.046
20	0.076	0.574	1.207	0.055	0.079	0.037
21	0.069	0.524	1.106	0.050	0.072	0.033
22	0.057	0.433	0.912	0.042	0.060	0.028
23	0.039	0.296	0.622	0.028	0.041	0.019
Average emission rates by time period used in GRAL **(kg/h)**						
Hour 00 to hour 05	-	**0.816**	**1.728**	**0.079**	**0.113**	**0.052**
Hour 06 to hour 17	-	**5.618**	**11.852**	**0.549**	**0.784**	**0.359**
Hour 18 to hour 23	-	**2.092**	**4.413**	**0.201**	**0.289**	**0.134**

(a) Not used in dispersion model

Table I-2 Emission rates: Western vent facility, 2021-DS (expected operation)

Hour start	NO_2 (g/s)[(a)]	NO_X (g/s)	CO (g/s)	$PM_{2.5}$ (g/s)	PM_{10} (g/s)	THC (g/s)
00	0.033	0.252	0.571	0.025	0.036	0.016
01	0.021	0.157	0.351	0.016	0.022	0.010
02	0.016	0.122	0.279	0.012	0.017	0.008
03	0.015	0.110	0.253	0.011	0.016	0.007
04	0.021	0.160	0.358	0.015	0.022	0.010
05	0.048	0.366	0.829	0.035	0.050	0.023
06	0.085	0.643	1.456	0.063	0.090	0.041
07	0.242	1.834	4.092	0.179	0.257	0.117
08	0.259	1.959	4.365	0.192	0.276	0.125
09	0.201	1.521	2.770	0.139	0.200	0.097
10	0.204	1.543	2.784	0.141	0.203	0.099
11	0.216	1.637	2.951	0.150	0.215	0.105
12	0.226	1.715	3.088	0.157	0.225	0.109
13	0.240	1.820	3.277	0.166	0.239	0.116
14	0.276	2.088	3.764	0.191	0.275	0.133
15	0.212	1.603	3.065	0.150	0.216	0.102
16	0.225	1.705	3.253	0.160	0.229	0.109
17	0.233	1.762	3.370	0.165	0.237	0.113
18	0.178	1.346	3.030	0.130	0.187	0.086
19	0.125	0.947	2.133	0.092	0.132	0.060
20	0.095	0.722	1.633	0.070	0.101	0.046
21	0.091	0.687	1.551	0.067	0.096	0.044
22	0.082	0.620	1.396	0.060	0.086	0.040
23	0.060	0.458	1.036	0.044	0.064	0.029
Average emission rates by time period used in GRAL **(kg/h)**						
Hour 00 to hour 06	-	0.931	2.107	0.091	0.130	0.059
Hour 07 to hour 18	-	6.160	11.943	0.576	0.828	0.393
Hour 19 to hour 23	-	2.472	5.579	0.240	0.344	0.158

(a) Not used in dispersion model

Table I-3 Emission rates: Eastern vent facility (M4 East outlet), 2031-DS (expected operation)

Hour start	NO_2 (g/s)[(a)]	NO_X (g/s)	CO (g/s)	$PM_{2.5}$ (g/s)	PM_{10} (g/s)	THC (g/s)
00	0.022	0.170	0.343	0.016	0.023	0.011
01	0.015	0.110	0.224	0.011	0.015	0.007
02	0.014	0.105	0.211	0.010	0.014	0.007
03	0.019	0.142	0.284	0.013	0.019	0.009
04	0.036	0.276	0.550	0.026	0.038	0.018
05	0.100	0.759	1.510	0.072	0.103	0.049
06	0.190	1.439	2.867	0.136	0.196	0.092
07	0.235	1.784	2.869	0.163	0.234	0.114
08	0.225	1.707	2.720	0.155	0.223	0.109
09	0.290	2.200	3.870	0.204	0.294	0.141
10	0.253	1.913	3.389	0.177	0.255	0.123
11	0.245	1.853	3.285	0.171	0.246	0.119
12	0.242	1.832	3.247	0.169	0.243	0.117
13	0.243	1.841	3.262	0.170	0.244	0.118
14	0.249	1.887	3.341	0.174	0.250	0.121
15	0.279	2.114	4.899	0.216	0.310	0.135
16	0.281	2.130	5.004	0.219	0.314	0.136
17	0.293	2.219	5.199	0.228	0.328	0.142
18	0.148	1.121	2.259	0.105	0.152	0.072
19	0.112	0.852	1.699	0.080	0.115	0.055
20	0.088	0.669	1.332	0.063	0.090	0.043
21	0.080	0.610	1.216	0.057	0.082	0.039
22	0.068	0.512	1.016	0.048	0.069	0.033
23	0.045	0.338	0.674	0.032	0.046	0.022
Average emission rates by time period used in GRAL **(kg/h)**						
Hour 00 to hour 05	-	0.937	1.873	0.089	0.128	0.060
Hour 06 to hour 17	-	6.876	13.185	0.655	0.942	0.441
Hour 18 to hour 23	-	2.461	4.918	0.231	0.333	0.158

(a) Not used in dispersion model

Table I-4 Emission rates: Western vent facility, 2031-DS (expected operation)

Hour start	NO_2 (g/s)[(a)]	NO_X (g/s)	CO (g/s)	$PM_{2.5}$ (g/s)	PM_{10} (g/s)	THC (g/s)
00	0.037	0.279	0.600	0.027	0.039	0.018
01	0.023	0.174	0.370	0.017	0.025	0.011
02	0.018	0.136	0.291	0.013	0.019	0.009
03	0.017	0.130	0.278	0.013	0.018	0.008
04	0.024	0.181	0.385	0.017	0.025	0.012
05	0.055	0.413	0.881	0.039	0.057	0.026
06	0.097	0.738	1.574	0.072	0.103	0.047
07	0.340	2.573	5.469	0.258	0.371	0.165
08	0.362	2.743	5.820	0.276	0.397	0.176
09	0.251	1.903	3.132	0.173	0.249	0.122
10	0.254	1.921	3.141	0.174	0.250	0.123
11	0.268	2.033	3.329	0.184	0.264	0.130
12	0.283	2.140	3.511	0.193	0.278	0.137
13	0.297	2.253	3.696	0.203	0.291	0.144
14	0.338	2.564	4.202	0.232	0.333	0.164
15	0.245	1.855	3.270	0.171	0.245	0.119
16	0.258	1.957	3.461	0.181	0.260	0.125
17	0.268	2.030	3.587	0.187	0.269	0.130
18	0.198	1.501	3.205	0.143	0.206	0.096
19	0.139	1.050	2.257	0.100	0.144	0.067
20	0.109	0.826	1.775	0.079	0.114	0.053
21	0.101	0.766	1.648	0.073	0.106	0.049
22	0.091	0.691	1.485	0.066	0.095	0.044
23	0.068	0.513	1.097	0.049	0.071	0.033
Average emission rates by time period used in GRAL **(kg/h)**						
Hour 00 to hour 06	-	1.055	2.252	0.102	0.147	0.068
Hour 07 to hour 18	-	7.642	13.747	0.713	1.024	0.490
Hour 19 to hour 23	-	2.768	5.948	0.265	0.381	0.177

(a) Not used in dispersion model

***Table I-5 Emission rates: Eastern vent facility (M4 East outlet), 2031-DSC (expected operation)**

Hour start	NO_2 (g/s)[(a)]	NO_X (g/s)	CO (g/s)	$PM_{2.5}$ (g/s)	PM_{10} (g/s)	THC (g/s)
00	0.021	0.162	0.247	0.015	0.021	0.0104
01	0.015	0.112	0.169	0.011	0.015	0.0072
02	0.014	0.108	0.164	0.010	0.015	0.0069
03	0.019	0.142	0.215	0.013	0.019	0.0091
04	0.034	0.257	0.392	0.023	0.034	0.0164
05	0.086	0.648	0.993	0.058	0.084	0.0415
06	0.159	1.202	1.847	0.108	0.154	0.0770
07	0.153	1.156	1.799	0.104	0.149	0.0740
08	0.171	1.294	2.010	0.117	0.168	0.0829
09	0.218	1.648	2.570	0.148	0.213	0.1056
10	0.190	1.442	2.245	0.128	0.185	0.0924
11	0.183	1.389	2.162	0.124	0.178	0.0890
12	0.181	1.369	2.131	0.122	0.175	0.0877
13	0.181	1.370	2.131	0.122	0.175	0.0877
14	0.184	1.396	2.174	0.124	0.179	0.0894
15	0.201	1.519	2.961	0.144	0.207	0.0973
16	0.202	1.532	3.138	0.146	0.209	0.0982
17	0.194	1.470	3.036	0.136	0.196	0.0942
18	0.121	0.913	1.414	0.081	0.116	0.0585
19	0.094	0.715	1.097	0.063	0.091	0.0458
20	0.076	0.576	0.884	0.051	0.073	0.0369
21	0.069	0.524	0.803	0.047	0.067	0.0336
22	0.059	0.448	0.686	0.040	0.057	0.0287
23	0.041	0.309	0.473	0.028	0.040	0.0198
Average emission rates by time period used in GRAL **(kg/h)**						
Hour 00 to hour 05	-	0.857	1.307	0.078	0.112	0.055
Hour 06 to hour 18	-	4.902	8.203	0.444	0.638	0.314
Hour 19 to hour 23	-	1.853	2.839	0.164	0.236	0.119

(a) Not used in dispersion model

Table I-6 Emission rates: Western vent facility, 2031-DSC (expected operation)

Hour start	NO_2 (g/s)[(a)]	NO_X (g/s)	CO (g/s)	$PM_{2.5}$ (g/s)	PM_{10} (g/s)	THC (g/s)
00	0.102	0.774	1.146	0.072	0.104	0.0496
01	0.062	0.466	0.693	0.043	0.062	0.0299
02	0.048	0.362	0.540	0.033	0.048	0.0232
03	0.045	0.339	0.507	0.031	0.045	0.0217
04	0.061	0.461	0.694	0.042	0.060	0.0296
05	0.135	1.023	1.547	0.092	0.133	0.0655
06	0.256	1.943	2.954	0.177	0.255	0.1245
07	0.746	5.649	8.993	0.538	0.773	0.3619
08	0.784	5.939	9.455	0.573	0.823	0.3805
09	0.647	4.901	6.750	0.446	0.641	0.3140
10	0.642	4.866	6.644	0.442	0.635	0.3117
11	0.672	5.092	6.934	0.464	0.666	0.3262
12	0.703	5.325	7.233	0.486	0.698	0.3411
13	0.735	5.567	7.537	0.509	0.732	0.3567
14	0.826	6.255	8.436	0.578	0.830	0.4007
15	0.750	5.683	9.209	0.550	0.790	0.3641
16	0.781	5.917	9.637	0.580	0.833	0.3791
17	0.825	6.247	10.168	0.615	0.884	0.4002
18	0.522	3.953	5.853	0.364	0.523	0.2533
19	0.368	2.787	4.129	0.255	0.367	0.1785
20	0.289	2.190	3.246	0.201	0.288	0.1403
21	0.269	2.035	3.012	0.186	0.267	0.1304
22	0.241	1.823	2.693	0.167	0.240	0.1168
*23	0.181	1.370	2.030	0.126	0.181	0.0878
Average emission rates by time period used in GRAL **(kg/h)**						
Hour 00 to hour 06	-	2.760	4.156	0.253	0.363	0.177
Hour 07 to hour 18	-	19.618	29.054	1.843	2.649	1.257
Hour 19 to hour 23	-	7.347	10.879	0.673	0.967	0.471

(a) Not used in dispersion model

Table I-7 Emission rates: CWL-Rozelle vent facility, 2031-DSC (expected operation)

Hour start	NO_2 (g/s)[(a)]	NO_X (g/s)	CO (g/s)	$PM_{2.5}$ (g/s)	PM_{10} (g/s)	THC (g/s)
00	0.04	0.323	0.407	0.033	0.048	0.0207
01	0.03	0.210	0.263	0.021	0.031	0.0134
02	0.02	0.179	0.222	0.018	0.026	0.0115
03	0.03	0.235	0.290	0.023	0.034	0.0150
04	0.06	0.463	0.576	0.046	0.067	0.0297
05	0.18	1.364	1.716	0.139	0.200	0.0874
06	0.35	2.650	3.339	0.273	0.392	0.1698
07	0.42	3.196	4.573	0.339	0.487	0.2048
08	0.38	2.851	4.095	0.302	0.434	0.1826
09	0.50	3.760	4.808	0.391	0.562	0.2409
10	0.44	3.307	4.208	0.341	0.491	0.2119
11	0.42	3.172	4.039	0.327	0.471	0.2032
12	0.41	3.126	3.981	0.323	0.464	0.2003
13	0.41	3.128	3.983	0.323	0.464	0.2004
14	0.42	3.194	4.072	0.330	0.475	0.2047
15	0.47	3.572	5.972	0.400	0.575	0.2288
16	0.49	3.699	6.556	0.422	0.607	0.2370
17	0.53	3.990	7.120	0.459	0.660	0.2556
18	0.27	2.030	2.611	0.209	0.300	0.1301
19	0.21	1.571	1.974	0.160	0.230	0.1006
20	0.17	1.250	1.571	0.127	0.183	0.0801
21	0.15	1.122	1.409	0.114	0.164	0.0719
22	0.13	0.954	1.194	0.097	0.139	0.0611
23	0.08	0.640	0.803	0.065	0.093	0.0410
Average emission rates by time period used in GRAL **(kg/h)**						
Hour 00 to hour 05	-	1.664	2.084	0.169	0.243	0.107
Hour 06 to hour 17	-	11.894	17.024	1.269	1.824	0.762
Hour 18 to hour 23	-	4.540	5.737	0.464	0.666	0.291

(a) Not used in dispersion model

Table I-8 Emission rates: Eastern vent facility (M4-M5 outlet), 2031-DSC (expected operation)

Hour start	NO_2 (g/s)[(a)]	NO_X (g/s)	CO (g/s)	$PM_{2.5}$ (g/s)	PM_{10} (g/s)	THC (g/s)
00	0.02	0.130	0.221	0.012	0.017	0.0083
01	0.01	0.081	0.138	0.008	0.011	0.0052
02	0.01	0.067	0.112	0.006	0.009	0.0043
03	0.01	0.064	0.107	0.006	0.009	0.0041
04	0.01	0.092	0.152	0.008	0.012	0.0059
05	0.03	0.203	0.332	0.018	0.027	0.0130
06	0.05	0.356	0.577	0.032	0.046	0.0228
07	0.12	0.922	1.688	0.088	0.126	0.0590
08	0.13	0.985	1.830	0.095	0.136	0.0631
09	0.12	0.882	1.172	0.077	0.110	0.0565
10	0.12	0.889	1.205	0.078	0.112	0.0570
11	0.12	0.937	1.285	0.082	0.118	0.0600
12	0.13	0.985	1.362	0.087	0.124	0.0631
13	0.14	1.039	1.438	0.091	0.131	0.0665
14	0.15	1.170	1.645	0.104	0.150	0.0749
15	0.09	0.709	1.082	0.065	0.093	0.0454
16	0.10	0.742	1.142	0.068	0.098	0.0475
17	0.08	0.628	0.936	0.057	0.082	0.0402
18	0.09	0.704	1.257	0.065	0.094	0.0451
19	0.07	0.496	0.884	0.046	0.066	0.0318
20	0.05	0.390	0.695	0.036	0.052	0.0250
21	0.05	0.365	0.651	0.034	0.048	0.0234
22	0.04	0.328	0.583	0.030	0.043	0.0210
23	0.03	0.242	0.432	0.022	0.032	0.0155
Average emission rates by time period used in GRAL **(kg/h)**						
Hour 00 to hour 06	-	0.511	0.843	0.047	0.067	0.033
Hour 07 to hour 14	-	3.514	5.231	0.316	0.454	0.225
Hour 15 to hour 23	-	1.841	3.065	0.170	0.244	0.118

(a) Not used in dispersion model

I.2 Concentrations in ventilation outlets

Table I-9 Concentrations in ventilation outlet: Eastern vent facility (M4 East outlet), 2021-DS (expected operation)

Hour start	NO_2 (mg/m^3)[(a)]	NO_X (mg/m^3)	CO (mg/m^3)	$PM_{2.5}$ (mg/m^3)	PM_{10} (mg/m^3)	THC (mg/m^3)
00	0.07	0.52	1.08	0.05	0.07	0.03
01	0.04	0.34	0.71	0.03	0.05	0.02
02	0.04	0.32	0.68	0.03	0.04	0.02
03	0.06	0.44	0.95	0.04	0.06	0.03
04	0.12	0.88	1.86	0.09	0.12	0.06
05	0.31	2.36	5.00	0.23	0.33	0.15
06	0.25	1.87	3.94	0.18	0.26	0.12
07	0.34	2.59	4.62	0.24	0.35	0.17
08	0.32	2.46	4.39	0.23	0.33	0.16
09	0.35	2.68	5.35	0.26	0.37	0.17
10	0.30	2.30	4.59	0.22	0.31	0.15
11	0.29	2.22	4.45	0.21	0.30	0.14
12	0.29	2.19	4.38	0.21	0.30	0.14
13	0.29	2.20	4.39	0.21	0.30	0.14
14	0.30	2.24	4.49	0.21	0.31	0.14
15	0.30	2.24	5.70	0.23	0.33	0.14
16	0.30	2.24	5.78	0.23	0.33	0.14
17	0.31	2.33	6.02	0.24	0.35	0.15
18	0.31	2.34	4.95	0.22	0.32	0.15
19	0.24	1.81	3.82	0.17	0.25	0.12
20	0.19	1.43	3.02	0.14	0.20	0.09
21	0.17	1.31	2.76	0.13	0.18	0.08
22	0.14	1.08	2.28	0.10	0.15	0.07
23	0.10	0.74	1.55	0.07	0.10	0.05

(a) Not used in dispersion model

Table I-10 Concentrations in ventilation outlet: Western vent facility, 2021-DS (expected operation)

Hour start	NO_2 (mg/m^3)[(a)]	NO_X (mg/m^3)	CO (mg/m^3)	$PM_{2.5}$ (mg/m^3)	PM_{10} (mg/m^3)	THC (mg/m^3)
00	0.12	0.90	2.04	0.09	0.13	0.06
01	0.07	0.56	1.25	0.06	0.08	0.04
02	0.06	0.44	1.00	0.04	0.06	0.03
03	0.05	0.39	0.90	0.04	0.06	0.03
04	0.08	0.57	1.28	0.05	0.08	0.04
05	0.17	1.31	2.96	0.12	0.18	0.08
06	0.30	2.30	5.20	0.22	0.32	0.15
07	0.42	3.16	7.05	0.31	0.44	0.20
08	0.45	3.38	7.53	0.33	0.48	0.22
09	0.35	2.62	4.78	0.24	0.35	0.17
10	0.35	2.66	4.80	0.24	0.35	0.17
11	0.37	2.82	5.09	0.26	0.37	0.18
12	0.39	2.96	5.32	0.27	0.39	0.19
13	0.41	3.14	5.65	0.29	0.41	0.20
14	0.48	3.60	6.49	0.33	0.47	0.23
15	0.36	2.76	5.28	0.26	0.37	0.18
16	0.39	2.94	5.61	0.28	0.40	0.19
17	0.40	3.04	5.81	0.28	0.41	0.19
18	0.31	2.32	5.22	0.22	0.32	0.15
19	0.31	2.37	5.33	0.23	0.33	0.15
20	0.24	1.80	4.08	0.18	0.25	0.12
21	0.23	1.72	3.88	0.17	0.24	0.11
22	0.20	1.55	3.49	0.15	0.22	0.10
23	0.15	1.14	2.59	0.11	0.16	0.07

(a) Not used in dispersion model

Table I-11 Concentrations in ventilation outlet: Eastern vent facility (M4 East outlet), 2031-DS (expected operation)

Hour start	NO_2 (mg/m^3)[(a)]	NO_X (mg/m^3)	CO (mg/m^3)	$PM_{2.5}$ (mg/m^3)	PM_{10} (mg/m^3)	THC (mg/m^3)
00	0.08	0.61	1.23	0.06	0.08	0.04
01	0.05	0.39	0.80	0.04	0.05	0.03
02	0.05	0.38	0.75	0.04	0.05	0.02
03	0.07	0.51	1.01	0.05	0.07	0.03
04	0.13	0.99	1.96	0.09	0.13	0.06
05	0.36	2.71	5.39	0.26	0.37	0.17
06	0.25	1.89	3.77	0.18	0.26	0.12
07	0.31	2.35	3.78	0.21	0.31	0.15
08	0.30	2.25	3.58	0.20	0.29	0.14
09	0.38	2.90	5.09	0.27	0.39	0.19
10	0.33	2.52	4.46	0.23	0.33	0.16
11	0.32	2.44	4.32	0.23	0.32	0.16
12	0.32	2.41	4.27	0.22	0.32	0.15
13	0.32	2.42	4.29	0.22	0.32	0.16
14	0.33	2.48	4.40	0.23	0.33	0.16
15	0.37	2.78	6.45	0.28	0.41	0.18
16	0.37	2.80	6.58	0.29	0.41	0.18
17	0.39	2.92	6.84	0.30	0.43	0.19
18	0.35	2.67	5.38	0.25	0.36	0.17
19	0.27	2.03	4.05	0.19	0.27	0.13
20	0.21	1.59	3.17	0.15	0.22	0.10
21	0.19	1.45	2.89	0.14	0.20	0.09
22	0.16	1.22	2.42	0.11	0.16	0.08
23	0.11	0.81	1.61	0.08	0.11	0.05

(a) Not used in dispersion model

Table I-12 Concentrations in ventilation outlet: Western vent facility, 2031-DS (expected operation)

Hour start	NO_2 (mg/m^3)[(a)]	NO_X (mg/m^3)	CO (mg/m^3)	$PM_{2.5}$ (mg/m^3)	PM_{10} (mg/m^3)	THC (mg/m^3)
00	0.07	0.57	1.14	0.05	0.08	0.04
01	0.05	0.37	0.75	0.04	0.05	0.02
02	0.05	0.35	0.70	0.03	0.05	0.02
03	0.06	0.47	0.95	0.04	0.06	0.03
04	0.12	0.92	1.83	0.09	0.13	0.06
05	0.33	2.53	5.03	0.24	0.34	0.16
06	0.63	4.80	9.56	0.45	0.65	0.31
07	0.41	3.08	4.95	0.28	0.40	0.20
08	0.39	2.94	4.69	0.27	0.39	0.19
09	0.50	3.79	6.67	0.35	0.51	0.24
10	0.44	3.30	5.84	0.31	0.44	0.21
11	0.42	3.20	5.66	0.30	0.42	0.20
12	0.42	3.16	5.60	0.29	0.42	0.20
13	0.42	3.17	5.62	0.29	0.42	0.20
14	0.43	3.25	5.76	0.30	0.43	0.21
15	0.48	3.65	8.45	0.37	0.53	0.23
16	0.48	3.67	8.63	0.38	0.54	0.24
17	0.51	3.83	8.96	0.39	0.57	0.25
18	0.26	1.93	3.90	0.18	0.26	0.12
19	0.28	2.13	4.25	0.20	0.29	0.14
20	0.22	1.67	3.33	0.16	0.23	0.11
21	0.20	1.52	3.04	0.14	0.21	0.10
22	0.17	1.28	2.54	0.12	0.17	0.08
23	0.11	0.85	1.69	0.08	0.11	0.05

(a) Not used in dispersion model

***Table I-13 Concentrations in ventilation outlet: Eastern vent facility (M4 East outlet), 2031-DSC (expected operation)**

Hour start	NO_2 (mg/m^3)[(a)]	NO_X (mg/m^3)	CO (mg/m^3)	$PM_{2.5}$ (mg/m^3)	PM_{10} (mg/m^3)	THC (mg/m^3)
00	0.09	0.67	1.03	0.06	0.09	0.04
01	0.06	0.47	0.70	0.04	0.06	0.03
02	0.06	0.45	0.68	0.04	0.06	0.03
03	0.08	0.59	0.89	0.05	0.08	0.04
04	0.14	1.07	1.63	0.10	0.14	0.07
05	0.36	2.70	4.14	0.24	0.35	0.17
06	0.45	3.44	5.28	0.31	0.44	0.22
07	0.44	3.30	5.14	0.30	0.42	0.21
08	0.49	3.70	5.74	0.33	0.48	0.24
09	0.62	4.71	7.34	0.42	0.61	0.30
10	0.54	4.12	6.42	0.37	0.53	0.26
11	0.52	3.97	6.18	0.35	0.51	0.25
12	0.52	3.91	6.09	0.35	0.50	0.25
13	0.52	3.91	6.09	0.35	0.50	0.25
14	0.53	3.99	6.21	0.36	0.51	0.26
15	0.57	4.34	8.46	0.41	0.59	0.28
16	0.58	4.38	8.97	0.42	0.60	0.28
17	0.55	4.20	8.67	0.39	0.56	0.27
18	0.34	2.61	4.04	0.23	0.33	0.17
19	0.34	2.55	3.92	0.23	0.32	0.16
20	0.27	2.06	3.16	0.18	0.26	0.13
21	0.25	1.87	2.87	0.17	0.24	0.12
22	0.21	1.60	2.45	0.14	0.20	0.10
23	0.15	1.10	1.69	0.10	0.14	0.07

(a) Not used in dispersion model

Table I-14 Concentrations in ventilation outlet: Western vent facility, 2031-DSC (expected operation)

Hour start	NO_2 (mg/m^3)[(a)]	NO_X (mg/m^3)	CO (mg/m^3)	$PM_{2.5}$ (mg/m^3)	PM_{10} (mg/m^3)	THC (mg/m^3)
00	0.29	2.21	3.28	0.21	0.30	0.14
01	0.18	1.33	1.98	0.12	0.18	0.09
02	0.14	1.03	1.54	0.10	0.14	0.07
03	0.13	0.97	1.45	0.09	0.13	0.06
04	0.17	1.32	1.98	0.12	0.17	0.08
05	0.39	2.92	4.42	0.26	0.38	0.19
06	0.73	5.55	8.44	0.51	0.73	0.36
07	1.04	7.85	12.49	0.75	1.07	0.50
08	1.09	8.25	13.13	0.80	1.14	0.53
09	0.90	6.81	9.37	0.62	0.89	0.44
10	0.89	6.76	9.23	0.61	0.88	0.43
11	0.93	7.07	9.63	0.64	0.93	0.45
12	0.98	7.40	10.05	0.67	0.97	0.47
13	1.02	7.73	10.47	0.71	1.02	0.50
14	1.15	8.69	11.72	0.80	1.15	0.56
15	1.04	7.89	12.79	0.76	1.10	0.51
16	1.08	8.22	13.39	0.80	1.16	0.53
17	1.15	8.68	14.12	0.85	1.23	0.56
18	0.72	5.49	8.13	0.51	0.73	0.35
19	0.74	5.57	8.26	0.51	0.73	0.36
20	0.58	4.38	6.49	0.40	0.58	0.28
21	0.54	4.07	6.02	0.37	0.53	0.26
22	0.48	3.65	5.39	0.33	0.48	0.23
*23	0.36	1.10	1.69	0.10	0.14	0.07

(a) Not used in dispersion model

Table I-15 Concentrations in ventilation outlet: CWL-Rozelle vent facility, 2031-DSC (expected operation)

Hour start	NO_2 (mg/m^3)[(a)]	NO_X (mg/m^3)	CO (mg/m^3)	$PM_{2.5}$ (mg/m^3)	PM_{10} (mg/m^3)	THC (mg/m^3)
00	0.12	0.92	1.16	0.09	0.14	0.06
01	0.08	0.60	0.75	0.06	0.09	0.04
02	0.07	0.51	0.63	0.05	0.07	0.03
03	0.09	0.67	0.83	0.07	0.10	0.04
04	0.17	1.32	1.65	0.13	0.19	0.08
05	0.51	3.90	4.90	0.40	0.57	0.25
06	0.47	3.53	4.45	0.36	0.52	0.23
07	0.56	4.26	6.10	0.45	0.65	0.27
08	0.50	3.80	5.46	0.40	0.58	0.24
09	0.66	5.01	6.41	0.52	0.75	0.32
10	0.58	4.41	5.61	0.46	0.65	0.28
11	0.56	4.23	5.39	0.44	0.63	0.27
12	0.55	4.17	5.31	0.43	0.62	0.27
13	0.55	4.17	5.31	0.43	0.62	0.27
14	0.56	4.26	5.43	0.44	0.63	0.27
15	0.63	4.76	7.96	0.53	0.77	0.31
16	0.65	4.93	8.74	0.56	0.81	0.32
17	0.70	5.32	9.49	0.61	0.88	0.34
18	0.54	4.06	5.22	0.42	0.60	0.26
19	0.41	3.14	3.95	0.32	0.46	0.20
20	0.33	2.50	3.14	0.25	0.37	0.16
21	0.30	2.24	2.82	0.23	0.33	0.14
22	0.25	1.91	2.39	0.19	0.28	0.12
23	0.17	1.28	1.61	0.13	0.19	0.08

(a) Not used in dispersion model

Table I-16 Concentrations in ventilation outlet: Eastern vent facility (M4-M5 outlet), 2031-DSC (expected operation)

Hour start	NO_2 (mg/m^3)[(a)]	NO_X (mg/m^3)	CO (mg/m^3)	$PM_{2.5}$ (mg/m^3)	PM_{10} (mg/m^3)	THC (mg/m^3)
00	0.10	0.74	1.26	0.07	0.10	0.05
01	0.06	0.46	0.79	0.04	0.06	0.03
02	0.05	0.38	0.64	0.04	0.05	0.02
03	0.05	0.36	0.61	0.03	0.05	0.02
04	0.07	0.53	0.87	0.05	0.07	0.03
05	0.15	1.16	1.90	0.11	0.15	0.07
06	0.27	2.03	3.30	0.18	0.26	0.13
07	0.38	2.88	5.27	0.27	0.39	0.18
08	0.41	3.08	5.72	0.30	0.42	0.20
09	0.36	2.76	3.66	0.24	0.35	0.18
10	0.37	2.78	3.77	0.24	0.35	0.18
11	0.39	2.93	4.01	0.26	0.37	0.19
12	0.41	3.08	4.26	0.27	0.39	0.20
13	0.43	3.25	4.49	0.29	0.41	0.21
14	0.48	3.66	5.14	0.33	0.47	0.23
15	0.37	2.84	4.33	0.26	0.37	0.18
16	0.39	2.97	4.57	0.27	0.39	0.19
17	0.33	2.51	3.74	0.23	0.33	0.16
18	0.37	2.81	5.03	0.26	0.37	0.18
19	0.26	1.98	3.54	0.18	0.26	0.13
20	0.21	1.56	2.78	0.14	0.21	0.10
21	0.19	1.46	2.60	0.13	0.19	0.09
22	0.17	1.31	2.33	0.12	0.17	0.08
23	0.13	0.97	1.73	0.09	0.13	0.06

(a) Not used in dispersion model

Appendix J - Dispersion model evaluation

J.1 Overview

The main approach for evaluating the performance of GRAL in the air quality assessment involved a comparison between the predicted and measured concentrations at OEH and RMS sites for the full 2014 base year. The results of this work are presented in Section J.2.

In addition, the GRAL predictions were compared with the measurements at the project-specific monitoring sites. However, these monitoring sites only became operational towards the end of 2014 (see Appendix F), and therefore these comparisons were only possible for the corresponding periods. No model predictions were available for 2015. This meant that only a partial validation was possible for these sites. The data for the project monitoring sites are summarised in Section J.3, and the GRAL predictions for these sites are presented in Section J.4.

J.2 GRAL predictions for OEH and RMS air quality monitoring sites

GRAL was configured to provide concentration predictions for each main pollutant (CO, NO_X, NO_2 and PM_{10}) at the OEH and Roads and Maritime air quality monitoring sites in the WestConnex GRAL domain. $PM_{2.5}$ was not assessed as there were insufficient measurement data for independent comparisons.

The monitoring stations included in the model evaluation were:

- OEH Chullora (background site)
- OEH Earlwood (background site)
- OEH Rozelle (background site)
- RMS CBMS (background site)
- RMS T1 (background site)
- RMS U1 (background site)
- RMS X1 (background site)
- RMS F1 (roadside site)
- RMS M1 (roadside site)

The GRAL predictions were for the surface road network and tunnel ventilation outlets, although the results from the project assessment clearly showed that the contributions of the latter were generally very small. For each monitoring site the GRAL predictions were extracted as an hourly time series of concentrations for 2014 and, in the case of PM_{10}, converted to 24-hour averages. The GRAL results were then combined with an estimated contemporaneous background contribution for each monitoring site (see Appendix F for the derivation of background concentrations).

J.2.1 CO

A comparison between the measured one-hour mean CO concentrations and those predicted by GRAL for a background site (the OEH Chullora monitoring station) is shown in Figure J-1. As, for the purpose of the project air quality assessment, it was assumed that the background sites were not influenced by road transport sources and therefore the concentrations predicted by GRAL at these sites should have been zero. In practice, dispersion models will often give non-zero values at nominal background sites, and this was the case here. The GRAL concentration was, however, generally much lower than the measured background. The measured background also had a slight offset on the y-axis, indicating that there is a degree of uncertainty in the measured data. However, this would not have had a large impact on the results of the evaluation.

Figure J-2 shows the measured concentrations and GRAL predictions (excluding background) for a site close to a major road (the RMS F1 site alongside the M5 East Freeway). Here, there was a much larger contribution from GRAL, but the background values were generally still higher.

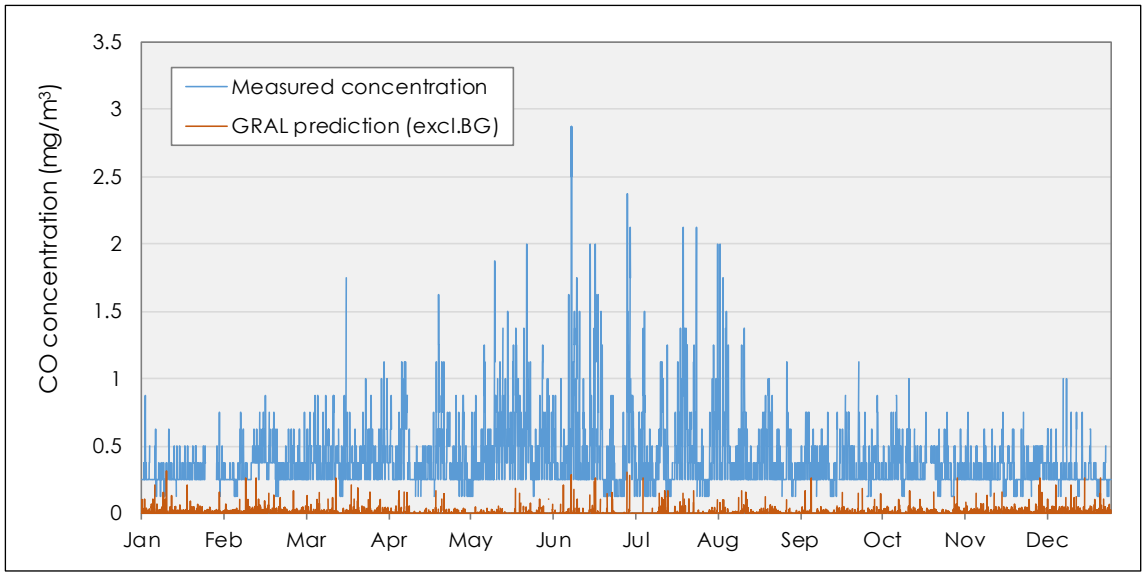

Figure J-1 **Measured one-hour mean CO concentrations and GRAL predictions (excluding background) for the OEH Chullora background monitoring site**

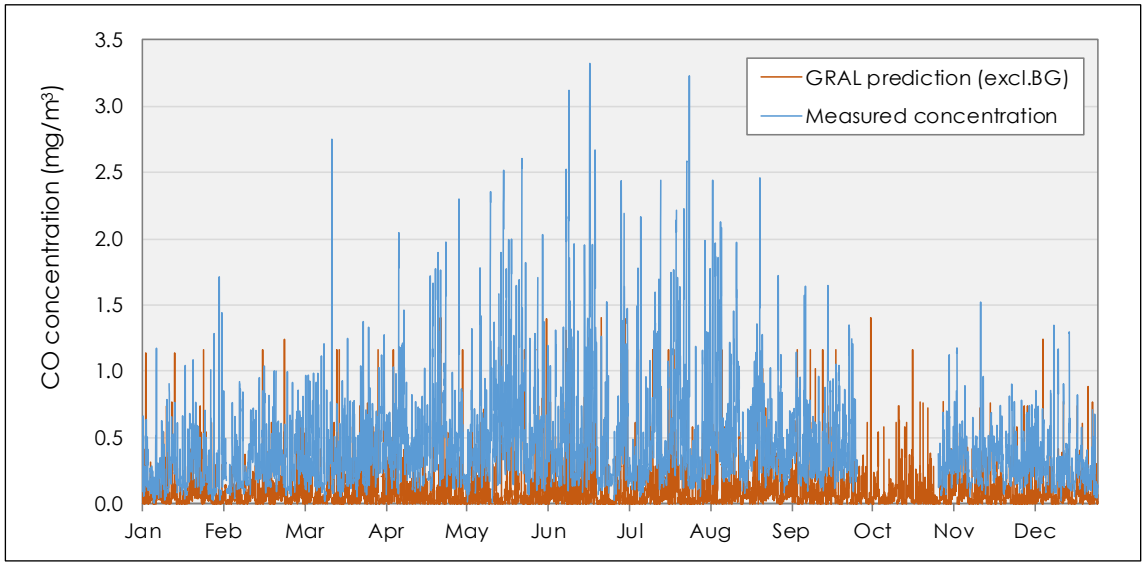

Figure J-2 **Measured one-hour mean CO concentrations and GRAL predictions (excluding background) for the RMS F1 monitoring site**

In Figure J-3 three descriptive statistics - annual mean, maximum one-hour mean and 98th percentile one-hour mean - for the measured and predicted total CO concentrations are compared. In this Figure the predictions include both the GRAL contribution and the estimated background contribution. The two contributions were combined using a contemporaneous approach, whereby the GRAL contribution was added to the corresponding contribution from the synthetic background profile for each hour of the year.

For each statistic the results for the Chullora background site should be ignored, as the data from this site featured strongly in the synthetic background profile. At all other background sites there was an overestimation of the annual mean CO concentration which ranged from 34 per cent to 73 per cent. There was also an overestimation of the annual mean at the roadside sites, though the model performance was considered to be acceptable. The results suggest that the estimated CO concentrations ought to be conservative for most of the modelling domain.

As would be expected, the results for the maximum and 98th percentile concentrations were more variable. Maximum pollutant concentrations are inherently very difficult to predict, and the comparisons here reflect this. Nevertheless, the model predictions were good at some sites, and there was a general tendency towards the overestimation concentrations.

Annual mean

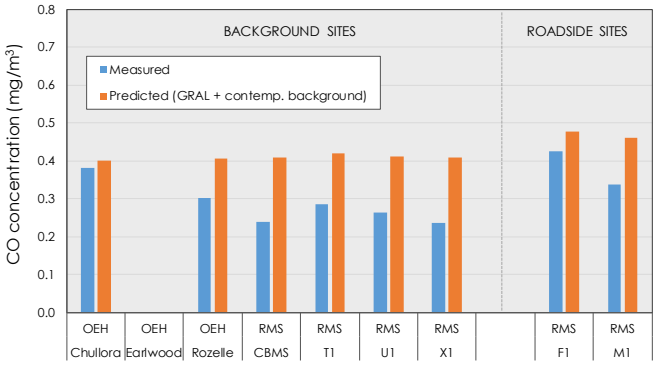

Site type	Site	Concentration (µg/m3)		Pred./ measured
		Measured	Pred. (contemp.)	
Background	OEH: Chullora	0.4	0.4	1.05
	OEH: Earlwood			
	OEH: Rozelle	0.3	0.4	1.34
	RMS: CBMS	0.2	0.4	1.72
	RMS: T1	0.3	0.4	1.47
	RMS: U1	0.3	0.4	1.56
	RMS: X1	0.2	0.4	1.73
Roadside	RMS: F1	0.4	0.5	1.12
	RMS: M1	0.3	0.5	1.36

Maximum one-hour mean

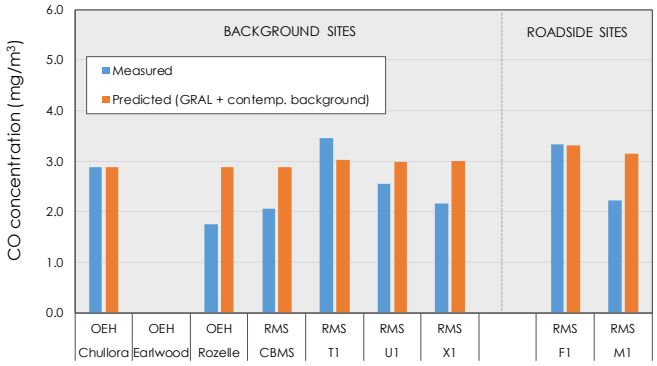

Site type	Site	Concentration (µg/m3)		Pred./ measured
		Measured	Pred. (contemp.)	
Background	OEH: Chullora	2.9	2.9	1.00
	OEH: Earlwood			
	OEH: Rozelle	1.7	2.9	1.64
	RMS: CBMS	2.1	2.9	1.39
	RMS: T1	3.4	3.0	0.87
	RMS: U1	2.6	3.0	1.16
	RMS: X1	2.2	3.0	1.40
Roadside	RMS: F1	3.3	3.3	1.00
	RMS: M1	2.2	3.1	1.42

98th %ile one-hour mean

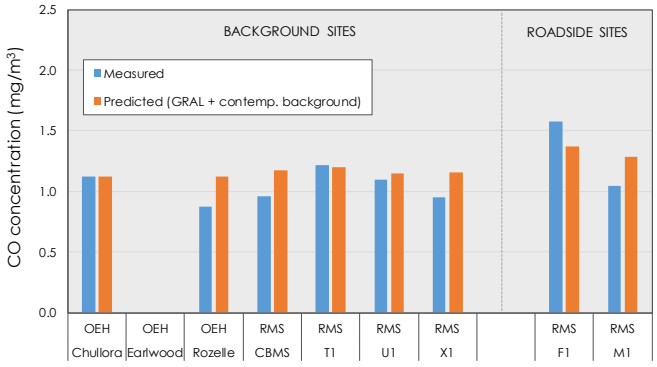

Site type	Site	Concentration (µg/m3)		Pred./ measured
		Measured	Pred. (contemp.)	
Background	OEH: Chullora	1.1	1.1	1.00
	OEH: Earlwood			
	OEH: Rozelle	0.9	1.1	1.29
	RMS: CBMS	1.0	1.2	1.22
	RMS: T1	1.2	1.2	0.99
	RMS: U1	1.1	1.1	1.05
	RMS: X1	0.9	1.2	1.22
Roadside	RMS: F1	1.6	1.4	0.87
	RMS: M1	1.0	1.3	1.23

Figure J-3 Comparison between measured and predicted total CO concentrations at OEH and RMS air quality monitoring sites

J.2.2 NO_x

Figure J-4 shows a comparison between the measured one-hour mean NO_X concentrations and those predicted by GRAL for the Chullora background site. Again, there was a non-zero NO_X contribution from GRAL, but this was generally lower than the measured background. Figure J-5 shows the measured concentrations and GRAL predictions (excluding background) for the RMS F1 site alongside the M5 East Freeway. At this site there was a much larger contribution from GRAL.

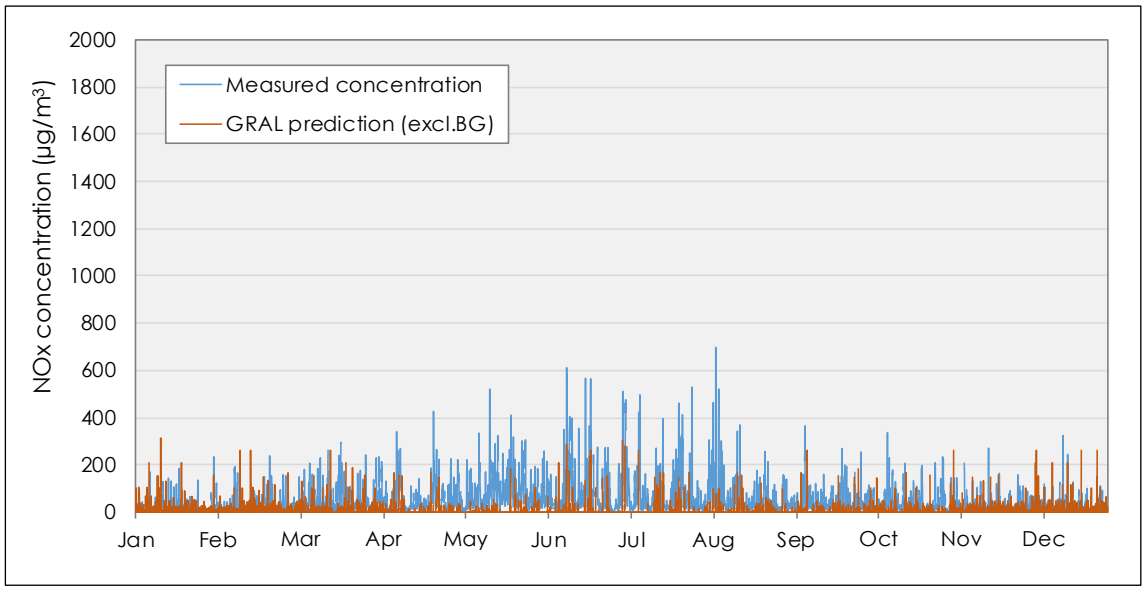

Figure J-4 **Measured one-hour mean $_{NOX}$ concentrations and GRAL predictions (excluding background) for the OEH Chullora background monitoring site**

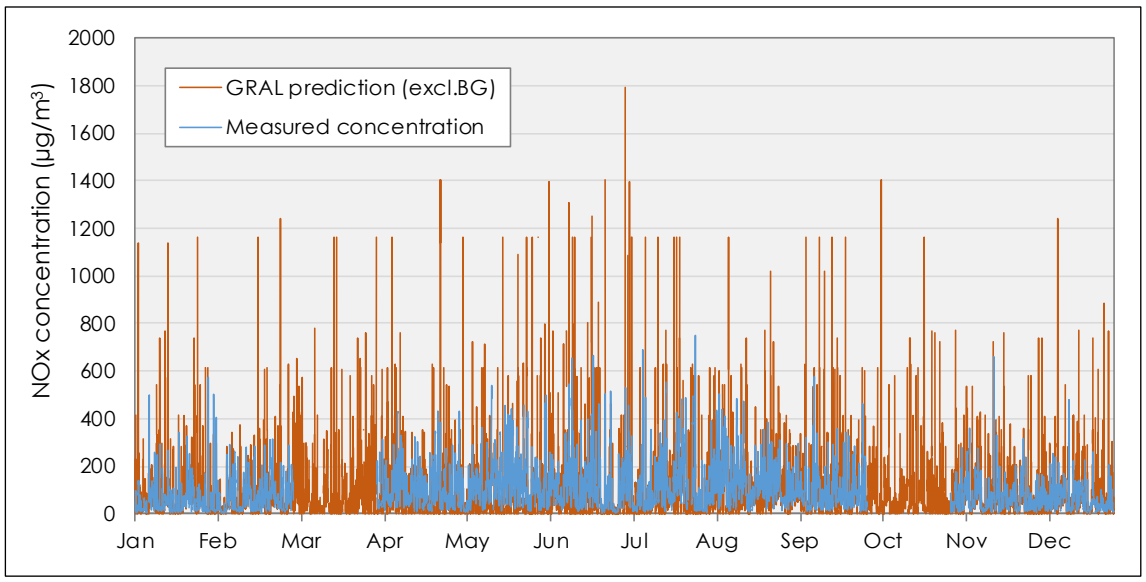

Figure J-5 **Measured one-hour mean NO_X concentrations and GRAL predictions (excluding background) for the RMS F1 monitoring site**

In Figure J-6 the descriptive statistics for total NO_X concentrations are compared. For the annual mean concentration the results for two methods for combining the GRAL and background contributions are shown. The first method involved the use of the NO_X background map, and the second method involved a contemporaneous approach, whereby the GRAL contribution was added to the corresponding background contribution for each hour of the year.

Annual mean

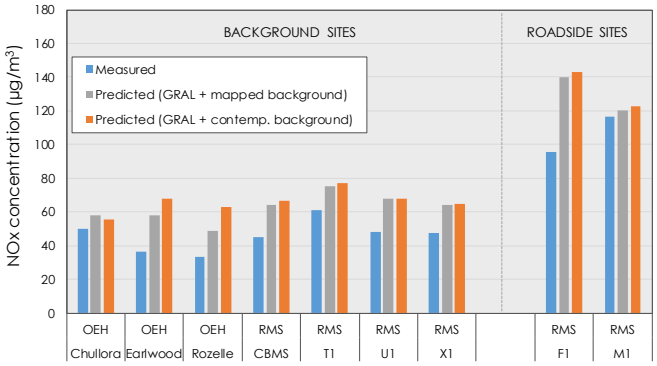

Site type	Site	Concentration (µg/m3)		Pred./ measured
		Measured	Pred. (map)	
Background	OEH: Chullora	50.2	58.1	1.16
	OEH: Earlwood	36.5	58.1	1.59
	OEH: Rozelle	33.5	48.8	1.46
	RMS: CBMS	45.2	64.3	1.42
	RMS: T1	61.1	75.5	1.23
	RMS: U1	48.2	68.1	1.41
	RMS: X1	47.3	64.1	1.36
Roadside	RMS: F1	95.6	140.2	1.47
	RMS: M1	116.4	120.2	1.03

Maximum one-hour mean

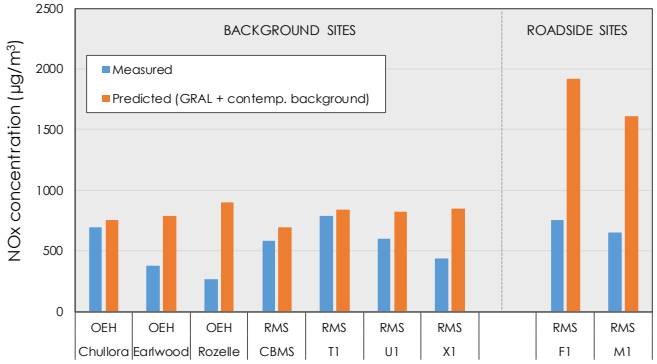

Site type	Site	Concentration (µg/m3)		Pred./ measured
		Measured	Pred. (contemp.)	
Background	OEH: Chullora	697.8	753.9	1.08
	OEH: Earlwood	375.6	792.5	2.11
	OEH: Rozelle	270.9	899.9	3.32
	RMS: CBMS	587.6	697.8	1.19
	RMS: T1	787.8	837.9	1.06
	RMS: U1	597.0	826.0	1.38
	RMS: X1	439.6	852.5	1.94
Roadside	RMS: F1	750.3	1922.4	2.56
	RMS: M1	651.9	1612.0	2.47

98th %ile one-hour mean

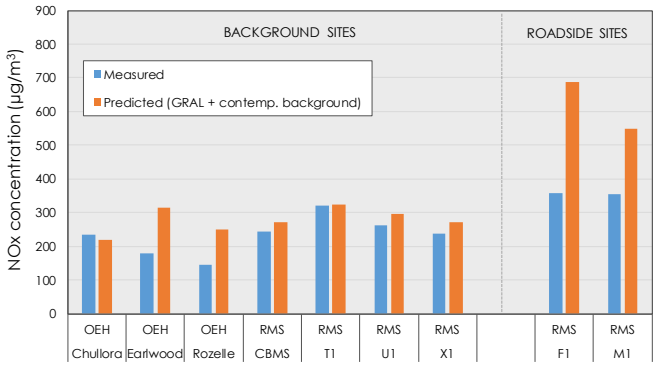

Site type	Site	Concentration (µg/m3)		Pred./ measured
		Measured	Pred. (contemp.)	
Background	OEH: Chullora	234.0	219.6	0.94
	OEH: Earlwood	180.6	314.1	1.74
	OEH: Rozelle	145.7	250.3	1.72
	RMS: CBMS	242.9	272.3	1.12
	RMS: T1	320.3	323.1	1.01
	RMS: U1	261.0	296.0	1.13
	RMS: X1	238.5	270.3	1.13
Roadside	RMS: F1	356.5	687.3	1.93
	RMS: M1	354.2	549.1	1.55

Figure J-6 Comparison between measured and predicted total NO_X concentrations at OEH and RMS air quality monitoring sites

The results indicate that there was a good agreement between the measured and predicted annual mean concentrations using both the mapped and contemporaneous approaches. For the OEH background monitoring sites this is unsurprising, as the background concentrations used in the assessment were based on the data from these sites. At all the background sites there was an overestimation of the annual mean NO_X concentration of between 16 per cent and 59 per cent, based on the mapped background. This suggests that the estimated total NO_X concentrations ought to be somewhat conservative for most of the modelling domain. The total NO_X concentration was overestimated (by 47 per cent) at the RMS F1 roadside site and slightly overestimated (by 3 per cent) at the RMS M1 roadside site. Whilst the results for the roadside sites are, on their own, inconclusive, the general pattern is one of slight overestimation of annual mean NO_X concentrations. There were no systematic differences between the results obtained using the mapped and contemporaneous approaches for including background NO_X.

As before, the maximum and 98th percentile concentrations were more variable. Nevertheless, there was a clear tendency towards the overestimation of maximum concentrations, which should introduce a clear margin of safety into the predictions. The performance for the 98th percentile values was better, with again there being a degree of conservatism.

Because there is generally a stronger road traffic signal for NO_X than for other criteria pollutants, the model performance at the two roadside sites (F1 and M1) was examined in more detail using the 'timeVariation' function in the Openair software. The variation of a pollutant by time of day and day of week can reveal useful information concerning the likely sources. For example, road vehicle emissions tend to follow very regular patterns both on a daily and weekly basis. The timeVariation function produces four plots: day of the week variation, mean hour of day variation and a combined hour of day – day of week plot and a monthly plot. Also shown on the plots is the 95 per cent confidence interval in the mean. For model evaluation it is important to consider the difference between observations and modelled values over these different time scales (Carslaw, 2015).

Figure J-7 and Figure J-8 show the results from the timeVariation function for the predicted ('GRAL') and monitored ('MON') hourly NO_X concentrations. The plots reveal the following:

- For the F1 site there was an overestimation of NO_X concentrations at all times of day and in all months.
- For the M1 site the concentrations tended to be overestimated in the mornings and evenings, and underestimated during the middle of the day.
- For both the F1 and M1 sites there was a more pronounced overestimation of concentrations at weekends than on weekdays. This is likely to be due in large part to the assumption of weekday traffic volumes on every day of the year in the modelling.
- The seasonal variation in concentrations was, on average, well reproduced, especially at the M1 site.

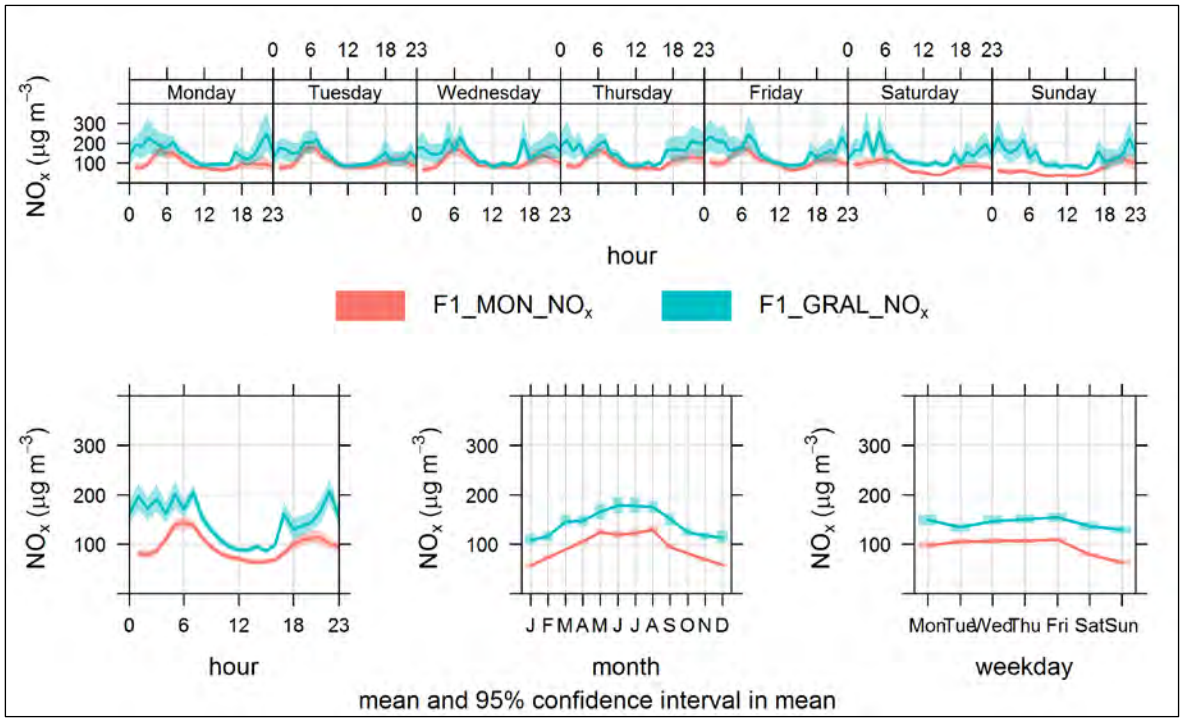

Figure J-7 **Comparison between time variation of measured and predicted total NO_X concentrations at RMS F1 monitoring site**

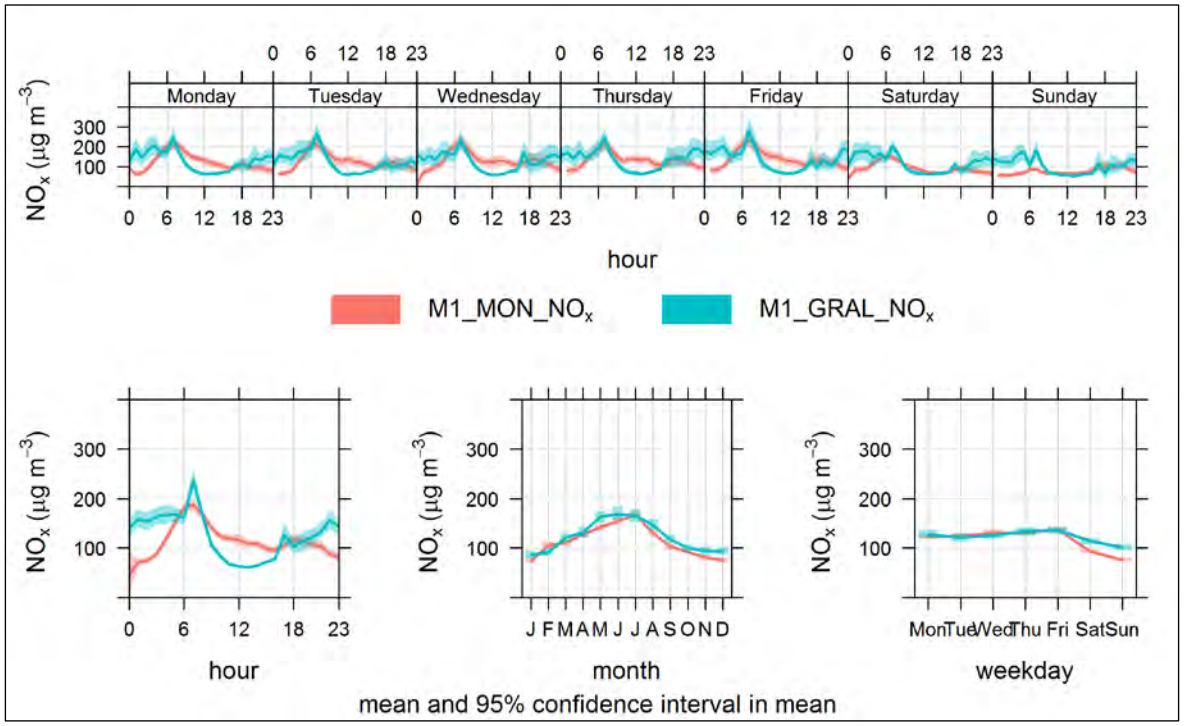

Figure J-8 **Comparison between time variation of measured and predicted total NO_X concentrations at RMS M1 monitoring site**

J.2.3 NO_2

The measured and predicted values for NO_2 are shown in Figure J-9. NO_2 predictions obtained using the OLM for converting NO_X to NO_2 are also shown for comparison with the methods developed for the M4 East assessment. The annual mean NO_2 values for the assessment were obtained using a background map for NO_X. The OLM calculations were contemporaneous, based on the synthetic (and conservative) background profiles for NO_2 and O_3, and the f-NO_2 value of 0.16 recommended by NSW EPA.

Annual mean

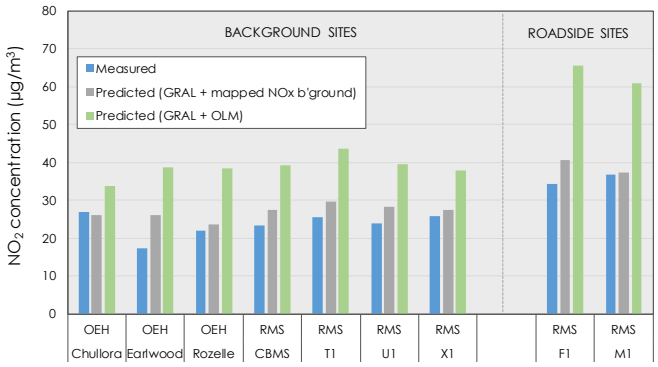

Site type	Site	Concentration (µg/m3)		Pred./ measured
		Measured	Pred. (map)	
Background	OEH: Chullora	26.9	26.0	0.96
	OEH: Earlwood	17.3	26.0	1.50
	OEH: Rozelle	21.9	23.7	1.08
	RMS: CBMS	23.4	27.3	1.17
	RMS: T1	25.5	29.6	1.16
	RMS: U1	23.8	28.1	1.18
	RMS: X1	25.8	27.3	1.06
Roadside	RMS: F1	34.3	40.5	1.18
	RMS: M1	36.8	37.4	1.02

Maximum one-hour mean

Site type	Site	Concentration (µg/m3)		Pred./ measured
		Measured	Pred. (contemp.)	
Background	OEH: Chullora	131.4	148.8	1.13
	OEH: Earlwood	82.1	149.3	1.82
	OEH: Rozelle	112.9	150.4	1.33
	RMS: CBMS	105.3	148.1	1.41
	RMS: T1	104.1	149.8	1.44
	RMS: U1	107.8	149.6	1.39
	RMS: X1	115.9	149.9	1.29
Roadside	RMS: F1	114.9	192.2	1.67
	RMS: M1	122.2	161.2	1.32

98th %ile one-hour mean

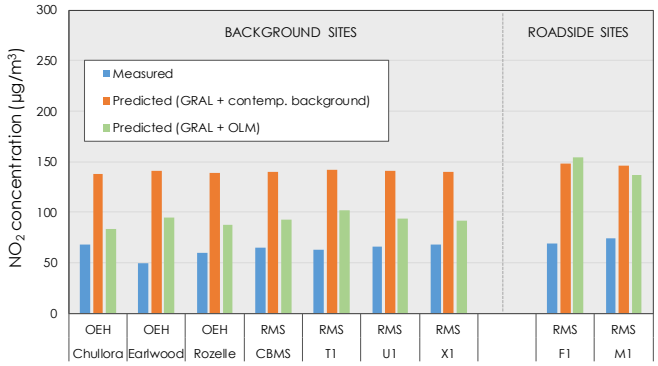

Site type	Site	Concentration (µg/m3)		Pred./ measured
		Measured	Pred. (contemp.)	
Background	OEH: Chullora	67.7	138.2	2.04
	OEH: Earlwood	49.3	141.2	2.87
	OEH: Rozelle	59.5	139.3	2.34
	RMS: CBMS	65.0	140.0	2.15
	RMS: T1	62.6	141.4	2.26
	RMS: U1	65.7	140.7	2.14
	RMS: X1	68.0	139.9	2.06
Roadside	RMS: F1	69.0	148.0	2.14
	RMS: M1	74.3	146.0	1.96

Figure J-9 Comparison between measured and predicted total NO_2 concentrations at OEH and RMS air quality monitoring sites

For annual mean NO_2 the predicted concentrations (again, based on the use of background maps for NO_X) were systematically higher than the measured values, but there was generally a good level of agreement; for all but one of the sites the overprediction was less than 20 per cent. When the OLM was used to determine NO_2 for each hour of the year, considerably higher annual mean values were predicted.

A similar pattern was observed for the maximum one-hour mean NO_2 concentration. In this case the predicted concentrations were between 13 per cent and 82 per cent higher than the measured values, and again the OLM gave values which were higher still, with large overpredictions of concentrations at the roadside sites in particular.

The results for the 98th percentile one-hour mean concentration were interesting, as the OLM gave results that were closer to the measurements than the contemporaneous method developed for the assessment. Because the latter is designed to give a conservative estimate for the maximum NO_2 concentration for each hour of the year, so that the overall maximum for the year is not underestimated. This means that the whole distribution is skewed towards high values. Whilst this is useful for determining the maximum value during a year, it is clearly not well suited to the estimation of other NO_2 statistics such as means and percentiles.

J.2.4 PM_{10}

Figure J-10 compares the measured 24-hour mean PM_{10} concentrations with those predicted by GRAL for the Chullora background site. In this case the GRAL concentration is much lower than the measured background, and is close to zero. Figure J-11 shows the results for the RMS F1 site. Here, there is a 24-hour mean contribution from GRAL of up to around 10 µg/m^3, which is still well below the measured values.

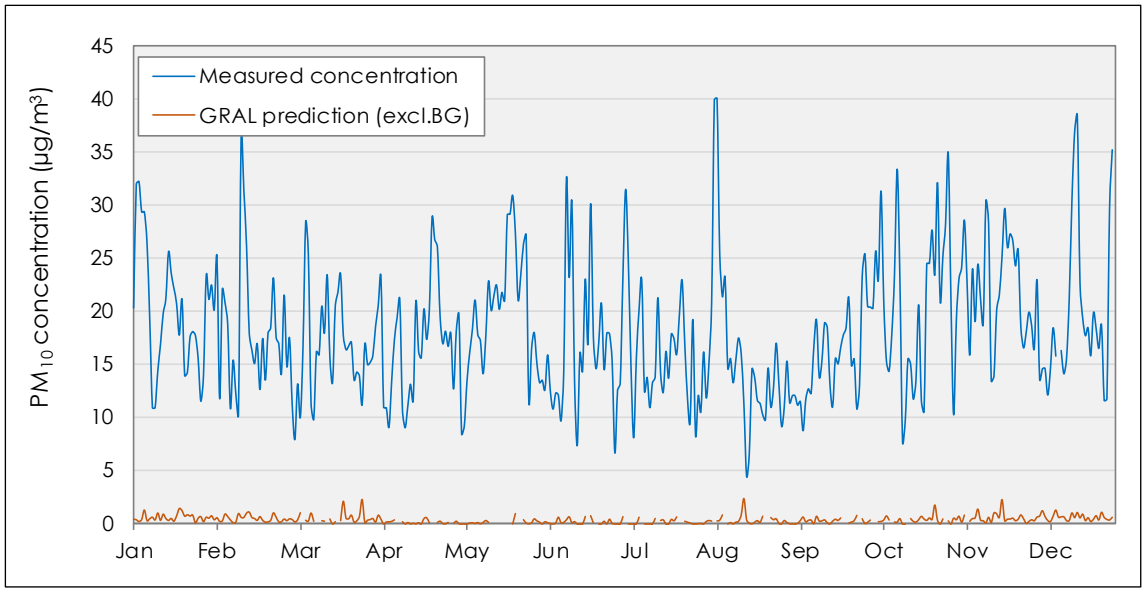

Figure J-10 **Measured 24-hour mean PM_{10} concentrations and GRAL predictions (excluding background) for the OEH Chullora background monitoring site**

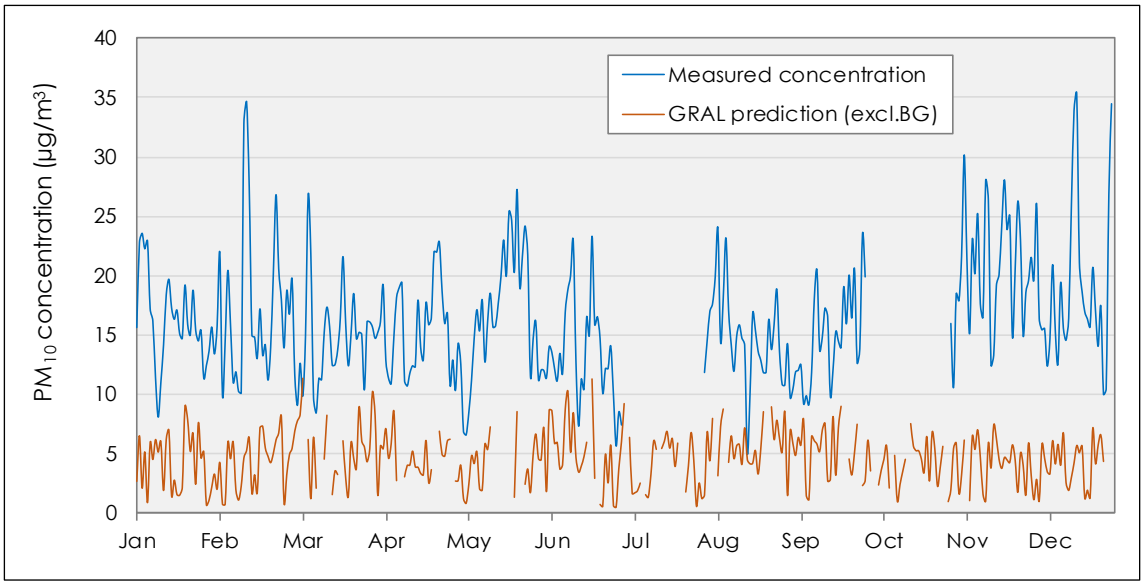

Figure J-11 **Measured 24-hour mean PM_{10} concentrations and GRAL predictions (excluding background) for the RMS F1 monitoring site**

The plots and descriptive statistics for the PM_{10} comparison are provided in Figure J-12. For the annual mean concentration at the background sites, the predicted results using the mapping approach effectively represent a combination of the values from the monitoring sites and the small GRAL contribution, so it is not surprising that they agree very well with the measurements (*i.e.* the measured and predicted values are not independent). The mapping approach resulted in a 30 per cent overestimation of PM_{10} at the roadside F1 site, and a smaller (9 per cent) overestimation at the roadside M1 site.

The contemporaneous approach gave higher predictions than the mapping approach at all sites (it is inherently more conservative). In general, the results suggest that the use of GRAL and the background mapping approach should give good (and slightly conservative) estimates of the PM_{10} concentration.

Maximum and 98th percentile 24-hour mean PM_{10} concentrations were systematically overestimated. As with NO_X, this suggests that the estimated total PM_{10} concentrations ought to be somewhat conservative for most of the modelling domain.

Annual mean

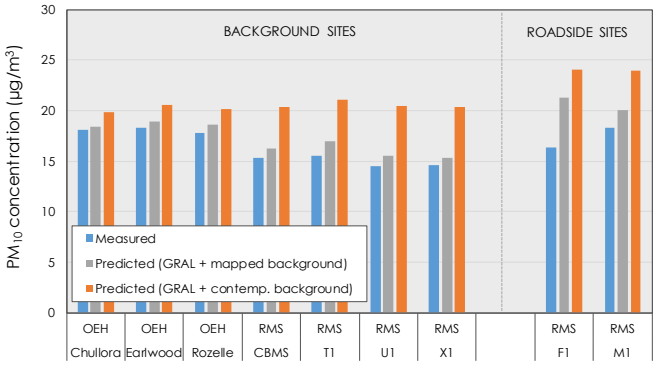

Site type	Site	Concentration (µg/m3)		Pred./ measured
		Measured	Pred. (map)	
Background	OEH: Chullora	18.1	18.4	1.02
	OEH: Earlwood	18.3	18.9	1.03
	OEH: Rozelle	17.8	18.6	1.05
	RMS: CBMS	15.4	16.3	1.06
	RMS: T1	15.5	16.9	1.09
	RMS: U1	14.5	15.5	1.07
	RMS: X1	14.6	15.3	1.05
Roadside	RMS: F1	16.3	21.2	1.30
	RMS: M1	18.3	20.0	1.09

Maximum 24-hour mean

Site type	Site	Concentration (µg/m3)		Pred./ measured
		Measured	Pred. (contemp.)	
Background	OEH: Chullora	40.0	45.8	1.15
	OEH: Earlwood	45.2	45.9	1.02
	OEH: Rozelle	43.8	45.7	1.04
	RMS: CBMS	38.6	45.6	1.18
	RMS: T1	34.5	46.3	1.34
	RMS: U1	38.2	45.7	1.20
	RMS: X1	43.2	45.7	1.06
Roadside	RMS: F1	35.3	49.8	1.41
	RMS: M1	42.3	49.0	1.16

98th %ile 24-hour mean

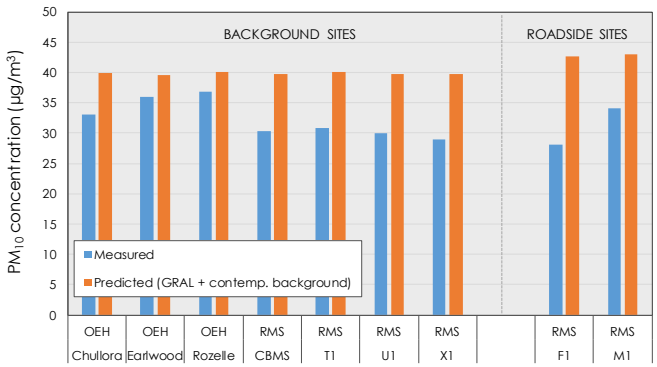

Site type	Site	Concentration (µg/m3)		Pred./ measured
		Measured	Pred. (contemp.)	
Background	OEH: Chullora	33.1	39.9	1.21
	OEH: Earlwood	36.0	39.6	1.10
	OEH: Rozelle	36.8	40.1	1.09
	RMS: CBMS	30.4	39.7	1.31
	RMS: T1	30.8	40.1	1.30
	RMS: U1	30.1	39.8	1.32
	RMS: X1	29.0	39.7	1.37
Roadside	RMS: F1	28.1	42.7	1.52
	RMS: M1	34.1	43.0	1.26

Figure J-12 Comparison between measured and predicted total PM_{10} concentrations at OEH and RMS air quality monitoring sites

J.3 Summary of data for project air quality monitoring sites

This section summarises the data obtained for the project-specific air quality monitoring stations. These sites were:

- M4E: 01 (roadside)
- M4E: 02 (near-road)
- M4E: 03 (near-road)
- M4E: 04 (roadside)
- M4E: 05 (background)

The availability of data for these monitoring sites was noted in Appendix F. The statistics for the corresponding periods - mean, maximum and 98th percentile – are summarised in the Tables below.

Table J-1 Summary of CO measurements at project-specific monitoring sites

Year	Month	M4 East monitoring site				
		M4E: 01	M4E: 02	M4E: 03	M4E: 04	M4E: 05
Average concentration (mg/m^3)						
2014	Aug	0.55	-	-	-	-
	Sep	0.34	0.23	0.28	-	-
	Oct	0.43	0.26	0.42	-	-
	Nov	0.37	0.23	0.35	0.29	0.15
	Dec	0.35	0.15	0.32	0.32	0.16
2015	Jan	0.16	0.21	0.26	0.39	0.11
	Feb	0.38	0.38	0.33	0.48	0.18
	Mar	0.29	0.38	0.36	0.52	0.29
	Apr	0.53	0.43	0.37	0.51	0.26
Maximum concentration (mg/m^3)						
2014	Aug	2.86	-	-	-	-
	Sep	1.40	1.11	1.55	-	-
	Oct	1.62	1.27	1.64	-	-
	Nov	1.26	0.96	1.14	1.10	0.57
	Dec	1.22	1.25	1.22	1.54	1.16
2015	Jan	0.79	0.95	1.27	1.30	0.47
	Feb	1.14	1.16	1.55	1.39	0.94
	Mar	2.19	1.94	1.82	1.94	1.12
	Apr	2.45	2.39	2.46	1.74	1.64
98th percentile concentration (mg/m^3)						
2014	Aug	2.01	-	-	-	-
	Sep	1.00	0.80	1.10	-	-
	Oct	1.16	0.93	1.01	-	-
	Nov	0.82	0.67	0.75	0.72	0.42
	Dec	0.90	0.63	0.85	1.00	0.55
2015	Jan	0.47	0.52	0.57	0.90	0.31
	Feb	0.88	0.93	0.88	1.15	0.56
	Mar	0.89	1.08	1.02	1.24	0.79
	Apr	1.52	1.34	1.29	1.21	0.98

Table J-2 Summary of NO_X measurements at project-specific monitoring sites

Year	Month	M4 East monitoring site				
		M4E: 01	M4E: 02	M4E: 03	M4E: 04	M4E: 05
Average concentration (µg/m^3)						
2014	Aug	96.5	-	-	-	-
	Sep	65.2	89.5	83.5	-	-
	Oct	57.9	67.7	66.1	-	-
	Nov	41.5	43.7	36.9	73.5	19.7
	Dec	-	36.8	32.0	70.3	17.5
2015	Jan	33.0	31.2	36.1	69.2	17.1
	Feb	43.3	46.5	50.2	96.3	24.5
	Mar	63.5	69.5	72.1	126.1	38.7
	Apr	74.1	83.1	79.6	124.5	42.2
Maximum concentration (µg/m^3)						
2014	Aug	513.1	-	-	-	-
	Sep	318.9	469.4	396.7	-	-
	Oct	329.0	386.0	491.0	-	-
	Nov	315.1	368.3	347.6	472.8	121.8
	Dec	181.8	344.5	318.4	394.3	165.0
2015	Jan	207.6	535.4	399.8	430.9	131.0
	Feb	224.6	315.0	497.4	428.5	203.6
	Mar	589.7	449.8	732.8	557.9	290.7
	Apr	409.4	510.0	567.3	547.5	308.1
98th percentile concentration (µg/m^3)						
2014	Aug	383.8	-	-	-	-
	Sep	196.0	295.7	368.4	-	-
	Oct	201.5	270.4	323.2	-	-
	Nov	162.6	218.2	186.1	254.4	87.5
	Dec	85.2	178.0	171.5	238.3	87.1
2015	Jan	115.5	140.3	175.5	256.5	73.7
	Feb	150.7	221.7	252.1	351.1	126.2
	Mar	206.5	257.4	293.0	377.4	173.0
	Apr	251.8	331.5	348.3	370.2	207.4

Table J-3 Summary of NO_2 measurements at project-specific monitoring sites

Year	Month	M4 East monitoring site				
		M4E: 01	M4E: 02	M4E: 03	M4E: 04	M4E: 05
Average concentration (µg/m^3)						
2014	Aug	32.1	-	-	-	-
	Sep	27.6	42.4	31.1	-	-
	Oct	27.7	33.4	28.9	-	-
	Nov	15.7	23.4	18.1	27.8	14.5
	Dec	-	21.7	16.0	34.2	12.3
2015	Jan	16.6	17.6	18.9	30.5	10.9
	Feb	20.5	18.3	19.3	35.8	12.5
	Mar	27.6	29.7	29.7	50.9	21.0
	Apr	30.2	29.9	31.5	45.3	21.2
Maximum concentration (µg/m^3)						
2014	Aug	101.2	-	-	-	-
	Sep	91.7	105.2	86.3	-	-
	Oct	87.5	109.8	96.2	-	-
	Nov	98.1	75.3	68.3	103.5	51.7
	Dec	70.7	89.2	67.7	115.3	54.1
2015	Jan	62.7	64.1	86.6	106.2	41.9
	Feb	80.1	83.7	84.1	114.8	66.8
	Mar	102.6	89.6	105.5	153.8	82.8
	Apr	70.4	67.8	102.0	119.7	66.6
98th percentile concentration (µg/m^3)						
2014	Aug	73.1	-	-	-	-
	Sep	62.9	85.4	60.3	-	-
	Oct	61.7	81.4	72.0	-	-
	Nov	56.0	61.3	51.3	75.1	42.4
	Dec	32.0	63.1	51.4	85.6	38.9
2015	Jan	40.4	45.3	49.6	80.9	33.6
	Feb	46.6	47.5	51.7	95.6	37.0
	Mar	59.4	61.7	71.4	116.8	54.1
	Apr	60.5	61.2	81.1	94.9	53.2

Table J-4 Summary of PM_{10} measurements at project-specific monitoring sites

Year	Month	M4 East monitoring site				
		M4E: 01	M4E: 02	M4E: 03	M4E: 04	M4E: 05
Average concentration (µg/m^3)						
2014	Aug	13.0	-	-	-	-
	Sep	10.8	9.8	-	-	-
	Oct	16.7	22.7	24.2	-	-
	Nov	18.0	22.2	19.4	28.0	19.9
	Dec	16.6	18.0	18.8	20.8	17.1
2015	Jan	13.2	14.9	16.1	17.5	15.1
	Feb	12.9	14.5	14.0	17.3	13.9
	Mar	16.9	17.9	18.3	20.8	16.8
	Apr	11.6	11.8	13.9	14.5	10.5
Maximum concentration (µg/m^3)						
2014	Aug	26.5	-	-	-	-
	Sep	19.5	19.9	-	-	-
	Oct	30.6	34.9	35.5	-	-
	Nov	27.2	30.3	26.6	45.1	28.6
	Dec	32.0	33.3	42.0	39.0	36.9
2015	Jan	26.4	24.2	26.8	32.0	30.1
	Feb	24.4	27.1	26.9	29.9	27.7
	Mar	27.6	25.5	27.4	31.4	26.3
	Apr	18.6	19.4	24.3	22.5	17.8
98th percentile concentration (µg/m^3)						
2014	Aug	25.4	-	-	-	-
	Sep	17.9	19.0	-	-	-
	Oct	29.8	33.9	34.0	-	-
	Nov	26.8	30.0	26.3	41.2	28.2
	Dec	30.7	32.9	40.1	37.2	34.7
2015	Jan	22.6	23.4	26.4	27.8	27.5
	Feb	20.4	23.9	22.6	26.2	23.9
	Mar	24.5	25.4	25.3	29.9	24.6
	Apr	18.3	18.9	23.3	22.2	16.9

Table J-5 Concentration metrics for $PM_{2.5}$ measurements at project-specific monitoring sites

Year	Month	M4 East monitoring site				
		M4E: 01	M4E: 02	M4E: 03	M4E: 04	M4E: 05
Average concentration (µg/m^3)						
2014	Aug	8.8	-	-	-	-
	Sep	8.3	8.7	-	-	-
	Oct	7.0	11.3	10.7	-	-
	Nov	5.8	10.6	10.3	9.7	7.9
	Dec	6.6	8.7	8.0	8.2	6.8
2015	Jan	5.5	7.3	6.8	7.6	4.9
	Feb	5.9	6.8	6.2	7.4	5.1
	Mar	8.3	9.0	8.4	9.1	7.2
	Apr	6.5	6.6	6.1	7.2	5.0
Maximum concentration (µg/m^3)						
2014	Aug	19.0	-	-	-	-
	Sep	18.5	17.2	-	-	-
	Oct	13.8	26.1	23.2	-	-
	Nov	12.0	16.4	29.7	15.2	14.3
	Dec	11.0	12.8	12.1	13.2	10.8
2015	Jan	11.3	12.8	11.9	13.0	11.3
	Feb	11.4	11.7	11.4	13.9	10.1
	Mar	14.2	14.5	13.2	15.1	12.8
	Apr	11.1	11.2	10.1	11.2	9.3
98th percentile concentration (µg/m^3)						
2014	Aug	17.2	-	-	-	-
	Sep	18.2	14.6	-	-	-
	Oct	13.3	24.9	22.6	-	-
	Nov	11.7	15.4	22.0	14.3	13.3
	Dec	10.7	12.7	11.9	12.6	10.3
2015	Jan	11.1	12.5	11.7	12.8	11.3
	Feb	9.9	10.9	10.0	12.0	9.3
	Mar	14.1	14.4	13.1	15.0	12.5
	Apr	11.0	11.0	9.8	10.8	9.2

J.4 GRAL predictions for project-specific air quality monitoring sites

GRAL was configured to provide concentration predictions for CO, NO_X and PM_{10} at the project monitoring sites. Again, the GRAL predictions were for the surface road network and tunnel ventilation outlets, and for each monitoring site the GRAL predictions were extracted as an hourly time series of concentrations for the relevant periods and, in the case of PM_{10}, converted to 24-hour averages. The GRAL results were then combined with an estimated contemporaneous background contribution.

Given that only partial monitoring data for 2014 were available at each site, the comparisons between the model and the measurements were made for the monitoring period covered at each site.

$PM_{2.5}$ was not assessed for the reason provided earlier. NO_2 concentrations were not evaluated, as this would have required the development of a separate NO_X-to-NO_2 conversion method for monthly concentrations. It should also be noted that mean values for NO_X and PM_{10} are not based on the background maps for these pollutants, as the maps were only developed for annual mean concentrations.

The results are shown in Figure J-13, Figure J-14 and Figure J-15 for CO, NO_X and PM_{10} respectively.

Whilst it is difficult to arrive at definitive conclusions based on monitoring data which only cover between two and five months, the results for the project sites are broadly similar to those for the OEH and RMS sites presented earlier in this Appendix. Although the results were quite mixed, in general the predicted concentrations were similar to or higher than the measured concentrations.

There were, however, some notable over-predictions, especially for NO_X concentrations. There are probably several reasons for this, including the following:

- There is a relatively high contribution to NO_X from road traffic compared with CO and PM_{10}, and it may be the case that the assumed traffic volumes for the modelling were not representative of the measurement periods. In other words, it is possible that the overpredictions in the model are linked to conservative assumptions in the traffic model rather than the performance of the model itself. Ultimately, the performance of the model at these locations should be evaluated using site-specific traffic data.
- For the period mean NO_X concentration the background contribution was based on the section of the synthetic background profile for the relevant period, rather than the (lower) background map that is used for the annual mean. As the synthetic profile is designed for the estimation of peak NO_X concentrations, it tends to overestimate average background concentrations. This observation also applies to the mean PM_{10} concentrations.
- The measurement periods did not coincide with the part of the year (winter) when peak NO_X concentrations tend to occur.

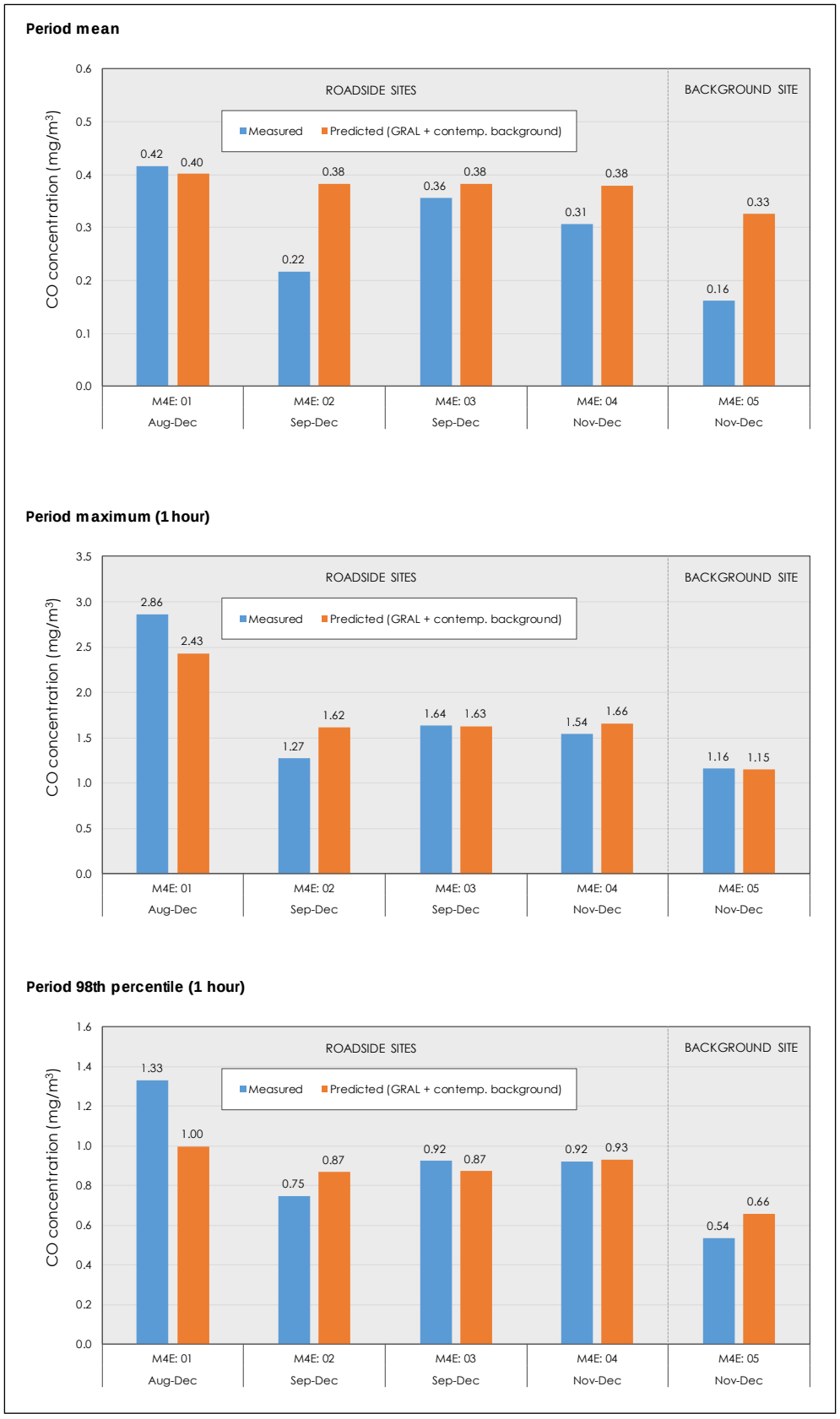

Figure J-13 Comparison between measured and predicted total CO concentrations at OEH project air quality monitoring sites

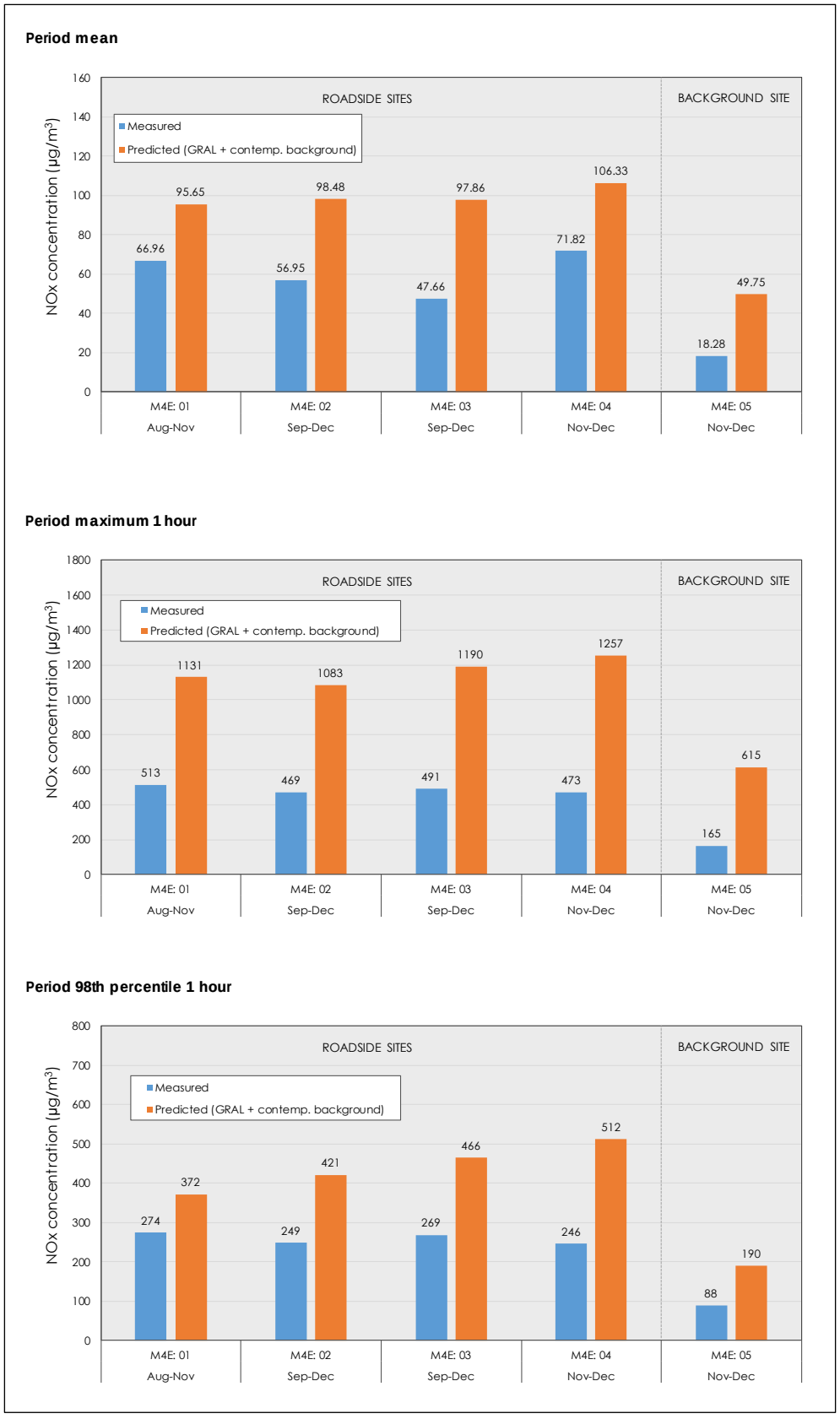

Figure J-14 Comparison between measured and predicted total NO_X concentrations at project air quality monitoring sites

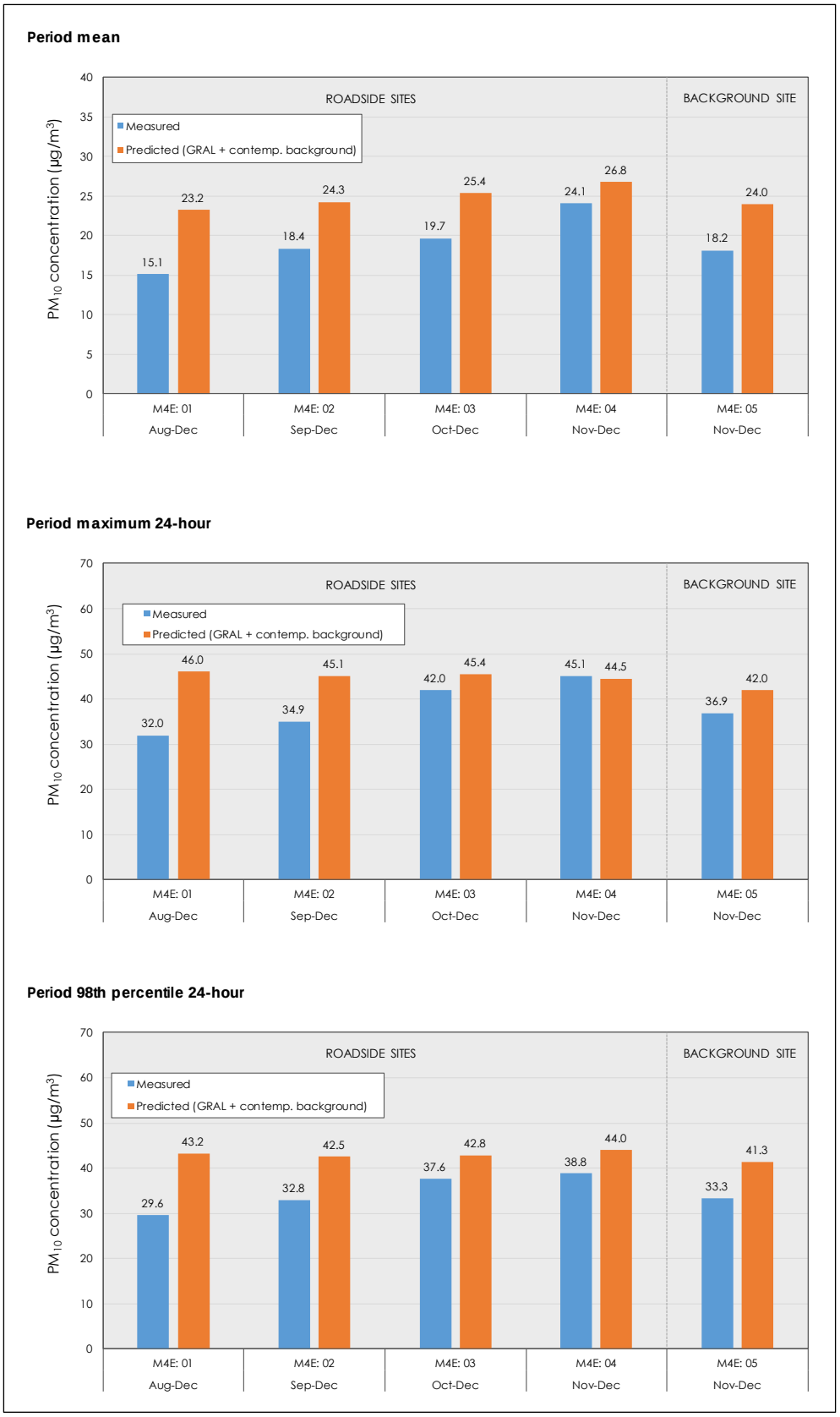

Figure J-15 Comparison between measured and predicted total PM_{10} concentrations at project air quality monitoring sites

(blank page)

Appendix K - All results of dispersion modelling

Note: In the Tables in this Appendix grey shading indicates where no value was obtained. For example, where the top ten increases in concentration are ranked, there may have been fewer than ten receptors that actually had an increase in concentration.

K.1 Carbon monoxide (maximum one-hour mean)

Table K-1 Maximum one-hour CO concentration at community receptors

Receptor	Maximum one-hour CO concentration (mg/m^3)						Change with project (mg/m^3)			Change with project (%)		
	2014-BY	2021-DM	2021 DS	2031-DM	2031-DS	2031-DSC	2021	2031	2031-DSC	2021	2031	2031-DSC
SR01	3.0	3.3	3.6	3.1	3.05	3.20	0.3	-0.1	0.1	9.6%	-2.0%	2.8%
SR02	3.3	3.4	3.3	3.2	2.98	3.39	0.0	-0.2	0.2	-1.3%	-7.7%	5.0%
SR03	3.1	3.3	3.7	3.2	2.91	3.08	0.5	-0.3	-0.1	13.8%	-8.3%	-3.1%
SR04	3.1	3.0	3.0	3.1	3.01	2.89	0.0	0.0	-0.2	-0.3%	-1.4%	-5.4%
SR05	3.1	3.1	3.0	3.0	2.97	3.14	0.0	0.0	0.1	-0.1%	-1.3%	4.6%
SR06	3.4	3.2	3.0	3.0	2.96	3.24	-0.2	0.0	0.2	-5.0%	-1.5%	8.1%
SR07	3.3	3.4	3.2	3.6	2.99	3.20	-0.3	-0.6	-0.4	-7.4%	-17.8%	-12.0%
SR08	3.3	3.3	2.9	2.9	3.03	2.92	-0.4	0.1	0.0	-12.3%	3.8%	0.0%
SR09	3.6	3.7	3.4	2.9	3.15	3.24	-0.3	0.3	0.3	-8.5%	8.8%	11.8%
SR10	3.1	3.1	3.1	3.2	3.00	3.25	0.0	-0.2	0.0	-0.2%	-7.0%	0.8%
SR11	3.2	3.2	3.2	3.2	3.27	3.09	0.0	0.0	-0.1	0.4%	1.4%	-4.5%
SR12	2.9	3.1	3.5	3.1	2.87	2.96	0.4	-0.3	-0.2	13.8%	-8.2%	-5.3%
SR13	3.4	3.2	3.1	3.1	2.97	3.27	0.0	-0.1	0.2	-0.7%	-4.6%	5.0%
SR14	3.2	3.2	3.1	3.1	3.08	3.03	-0.2	0.0	-0.1	-5.0%	-1.2%	-2.9%
SR15	3.9	3.0	3.2	3.0	3.05	2.93	0.2	0.1	-0.1	6.5%	1.7%	-2.6%
SR16	3.2	3.8	3.4	3.2	2.98	3.02	-0.4	-0.3	-0.2	-10.5%	-8.0%	-6.8%
SR17	3.1	3.1	3.2	2.9	2.95	2.90	0.1	0.1	0.0	4.0%	1.7%	0.0%
SR18	3.8	4.1	4.2	3.2	2.87	3.17	0.0	-0.3	0.0	0.4%	-9.0%	0.3%
SR19	3.0	3.2	3.0	2.9	2.92	2.96	-0.2	0.0	0.0	-5.6%	-0.3%	1.1%
SR20	3.1	3.3	3.5	3.1	3.02	3.18	0.2	-0.1	0.0	6.5%	-3.9%	1.2%
SR21	3.1	3.0	3.0	3.2	3.08	2.95	0.0	-0.1	-0.2	-0.4%	-2.9%	-7.1%
SR22	3.1	3.0	2.9	2.9	3.00	2.93	-0.1	0.1	0.0	-2.4%	2.5%	0.1%
SR23	2.9	3.0	3.1	3.0	2.87	2.96	0.1	-0.1	0.0	2.8%	-2.6%	0.2%
SR24	2.9	3.1	3.5	3.2	2.99	2.87	0.4	-0.2	-0.3	11.9%	-6.9%	-10.5%
SR25	3.0	3.3	2.9	3.0	2.96	3.02	-0.4	0.0	0.0	-10.8%	-0.5%	1.3%
SR26	2.9	3.3	2.9	3.5	2.87	3.07	-0.4	-0.6	-0.4	-11.8%	-17.1%	-11.3%
SR27	3.1	2.9	3.3	3.0	3.04	3.37	0.4	0.0	0.3	13.5%	0.4%	11.3%
SR28	2.9	3.1	3.0	2.9	2.93	2.99	-0.1	0.0	0.1	-2.9%	0.0%	2.1%
SR29	3.3	2.9	3.0	3.3	3.40	3.16	0.1	0.1	-0.1	4.6%	2.8%	-4.4%
SR30	3.0	2.9	3.0	3.2	2.93	2.87	0.1	-0.3	-0.3	4.1%	-8.8%	-10.4%
SR31	2.9	3.2	3.2	3.0	3.20	2.99	0.0	0.2	0.0	-0.9%	6.0%	-1.1%

Table K-2 Maximum one-hour CO concentrations at community receptors, ranked by total concentration

Rank	Ranking by concentration (mg/m^3)					
	2014-BY	2021-DM	2021 DS	2031-DM	2031-DS	2031-DSC
1	3.9	4.1	4.2	3.6	3.4	3.4
2	3.8	3.8	3.7	3.5	3.3	3.4
3	3.6	3.7	3.6	3.3	3.2	3.3
4	3.4	3.4	3.5	3.2	3.2	3.3
5	3.4	3.4	3.5	3.2	3.1	3.2
6	3.3	3.3	3.5	3.2	3.1	3.2
7	3.3	3.3	3.4	3.2	3.1	3.2
8	3.3	3.3	3.4	3.2	3.1	3.2
9	3.3	3.3	3.3	3.2	3.0	3.2
10	3.2	3.3	3.3	3.2	3.0	3.2

Table K-3 Maximum one-hour CO concentrations at community receptors, ranked by increase and by decrease in concentration with project

Rank	Ranking by increase in concentration with project (mg/m^3)			Ranking by decrease in concentration with project (mg/m^3)		
	2021	2031	2031-DSC	2021	2031	2031-DSC
1	0.5	0.3	0.3	-0.4	-0.6	-0.4
2	0.4	0.2	0.3	-0.4	-0.6	-0.4
3	0.4	0.1	0.2	-0.4	-0.3	-0.3
4	0.4	0.1	0.2	-0.4	-0.3	-0.3
5	0.3	0.1	0.2	-0.3	-0.3	-0.2
6	0.2	0.1	0.1	-0.3	-0.3	-0.2
7	0.2	0.1	0.1	-0.2	-0.3	-0.2
8	0.1	0.0	0.1	-0.2	-0.2	-0.2
9	0.1	0.0	0.0	-0.2	-0.2	-0.1
10	0.1		0.0	-0.1	-0.2	-0.1

Table K-4 Maximum one-hour CO concentrations at community receptors, ranked by percentage increase and by decrease in concentration with project

Rank	Ranking by % increase in concentration with project (mg/m^3)			Ranking by % decrease in concentration with project (mg/m^3)		
	2021	2031	2031-DSC	2021	2031	2031-DSC
1	13.8%	8.8%	11.8%	-12.3%	-17.8%	-12.0%
2	13.8%	6.0%	11.3%	-11.8%	-17.1%	-11.3%
3	13.5%	3.8%	8.1%	-10.8%	-9.0%	-10.5%
4	11.9%	2.8%	5.0%	-10.5%	-8.8%	-10.4%
5	9.6%	2.5%	5.0%	-8.5%	-8.3%	-7.1%
6	6.5%	1.7%	4.6%	-7.4%	-8.2%	-6.8%
7	6.5%	1.7%	2.8%	-5.6%	-8.0%	-5.4%
8	4.6%	1.4%	2.1%	-5.0%	-7.7%	-5.3%
9	4.1%	0.4%	1.3%	-5.0%	-7.0%	-4.5%
10	4.0%		1.2%	-2.9%	-6.9%	-4.4%

Table K-5 Maximum one-hour CO concentrations at RWR receptors, ranked by concentration

Rank	Ranking by concentration (mg/m^3)					
	2014-BY	2021-DM	2021 DS	2031-DM	2031-DS	2031-DSC
1	12.5	8.5	7.9	7.0	6.2	5.9
2	12.3	8.2	7.8	6.3	6.1	5.7
3	12.3	8.1	7.7	6.3	6.1	5.7
4	12.3	7.8	7.5	6.3	6.0	5.7
5	12.3	7.6	7.3	6.2	5.9	5.6
6	12.0	7.6	7.2	6.1	5.8	5.6
7	11.8	7.5	7.2	6.1	5.8	5.6
8	11.8	7.4	7.2	6.0	5.8	5.6
9	11.7	7.4	7.0	6.0	5.8	5.5
10	11.4	7.3	6.9	6.0	5.8	5.5

Table K-6 Maximum one-hour CO concentrations at RWR receptors, ranked by increase and by decrease in concentration with project

Rank	Ranking by increase in concentration with project (mg/m^3)			Ranking by decrease in concentration with project (mg/m^3)		
	2021-DS	2031-DS	2031-DSC	2021-DS	2031-DS	2031-DSC
1	2.0	1.4	1.0	-3.0	-1.8	-1.8
2	1.7	1.2	1.0	-2.9	-1.7	-1.7
3	1.3	1.0	1.0	-2.8	-1.7	-1.6
4	1.3	1.0	1.0	-2.5	-1.6	-1.6
5	1.3	1.0	1.0	-2.3	-1.6	-1.6
6	1.3	1.0	1.0	-2.3	-1.6	-1.6
7	1.3	1.0	0.9	-2.3	-1.5	-1.6
8	1.3	0.9	0.9	-2.2	-1.5	-1.6
9	1.3	0.9	0.9	-2.2	-1.5	-1.6
10	1.2	0.9	0.9	-2.2	-1.5	-1.6

Table K-7 Maximum one-hour CO concentrations at RWR receptors, ranked by percentage increase and by decrease in concentration with project

Rank	Ranking by % increase in concentration with project (mg/m^3)			Ranking by % decrease in concentration with project (mg/m^3)		
	2021-DS	2031-DS	2031-DSC	2021-DS	2031-DS	2031-DSC
1	38.7%	32.1%	26.5%	-35.9%	-29.3%	-29.2%
2	34.0%	28.6%	24.9%	-35.3%	-28.9%	-29.1%
3	33.1%	24.8%	23.4%	-35.2%	-27.9%	-28.8%
4	32.6%	23.2%	22.8%	-35.1%	-27.6%	-28.7%
5	32.2%	22.9%	22.4%	-34.6%	-27.4%	-28.1%
6	31.0%	22.9%	22.4%	-34.2%	-27.3%	-27.8%
7	27.6%	22.1%	21.4%	-33.8%	-27.2%	-27.8%
8	27.4%	21.9%	20.7%	-33.4%	-27.1%	-27.4%
9	27.1%	21.8%	20.5%	-33.2%	-26.5%	-27.2%
10	26.9%	21.7%	20.1%	-33.1%	-26.5%	-27.0%

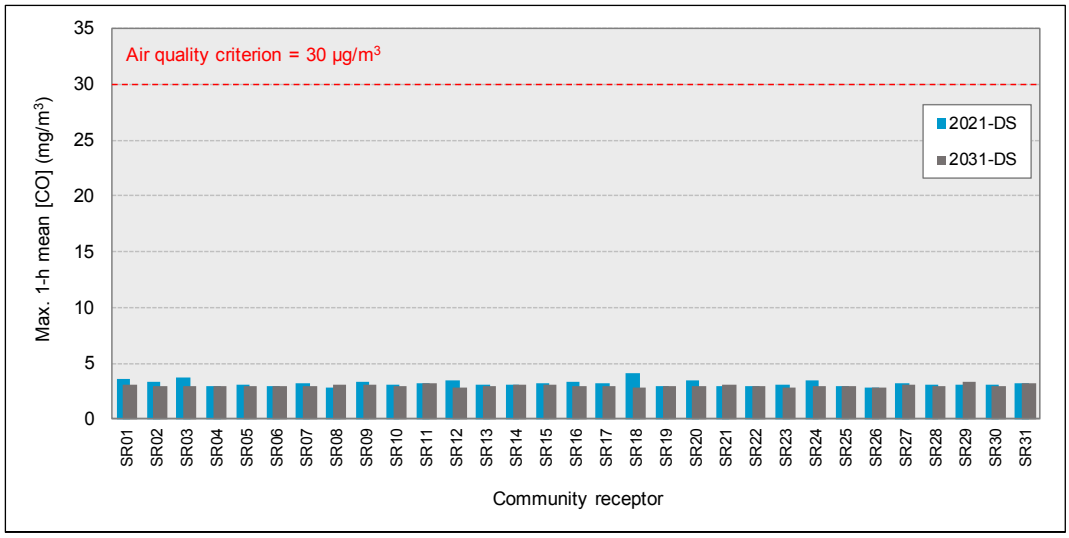

Figure K-1 **Maximum one-hour CO at community receptors (2021-DS and 2031-DS)**

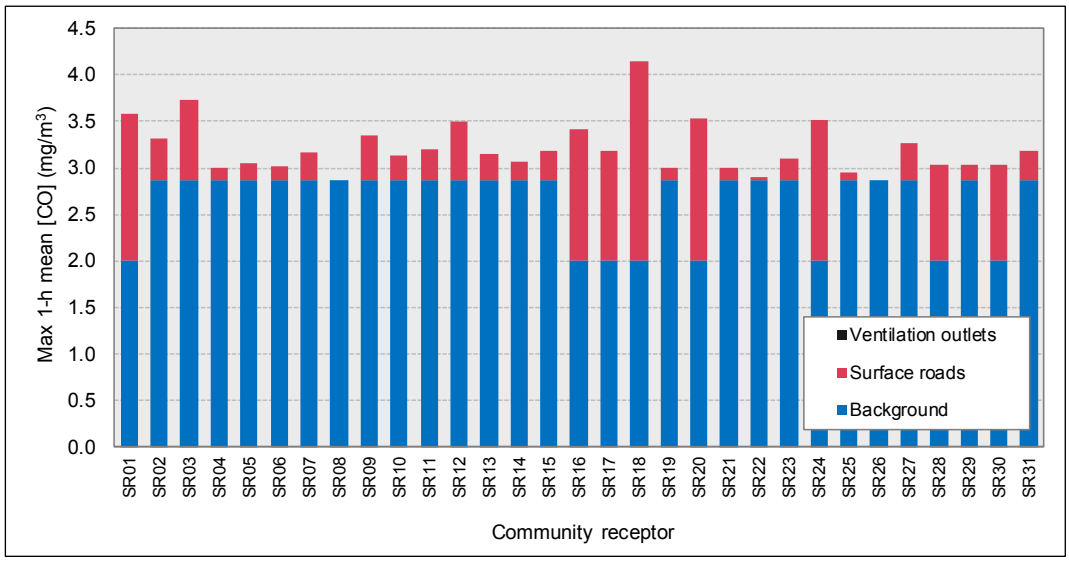

Figure K-2 **Source contributions to maximum one-hour mean CO at community receptors (2021-DS)**

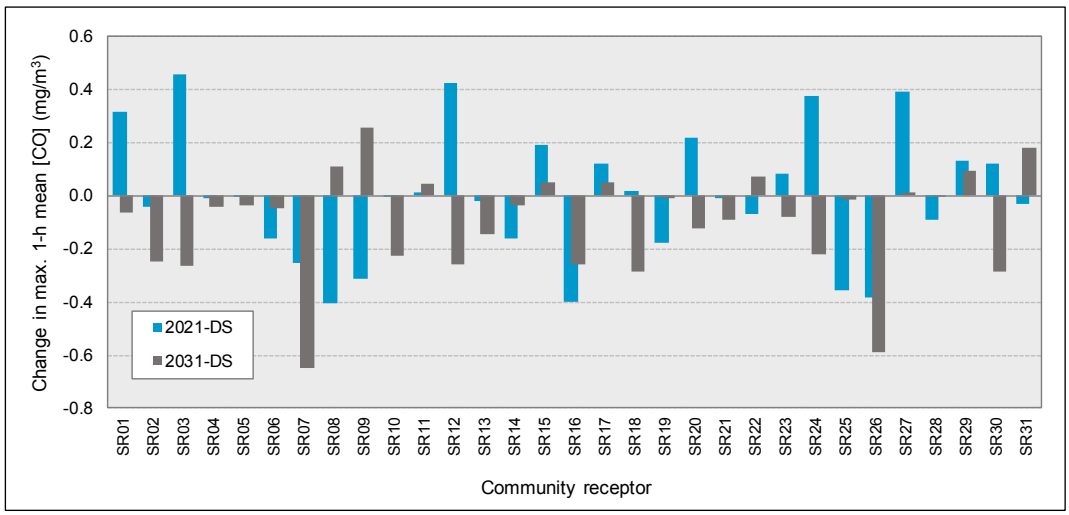

Figure K-3 **Changes in maximum one-hour CO at community receptors (2021-DS and 2031-DS)**

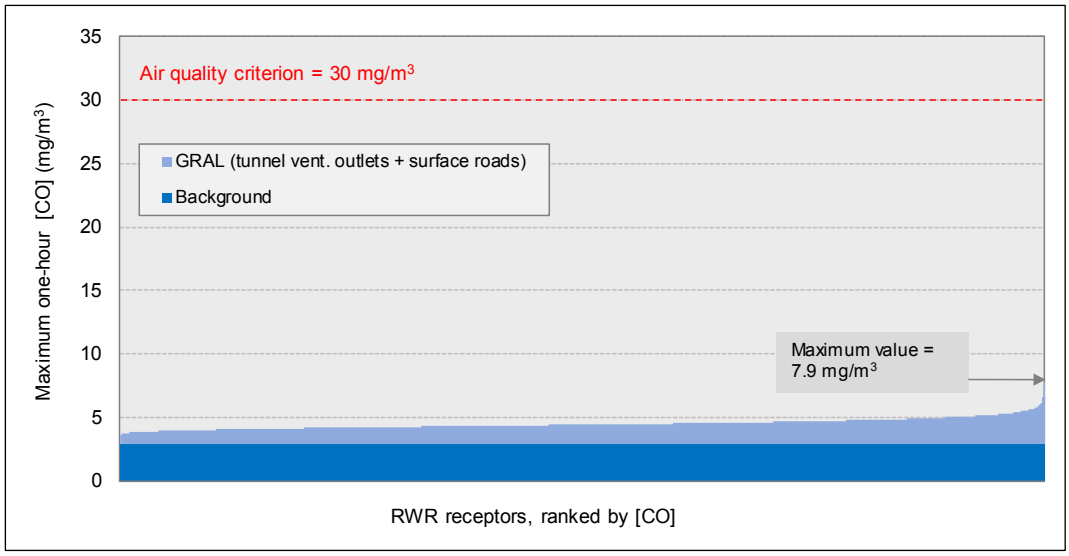

Figure K-4 Source contributions to maximum one-hour CO at RWR receptors (2021-DS)

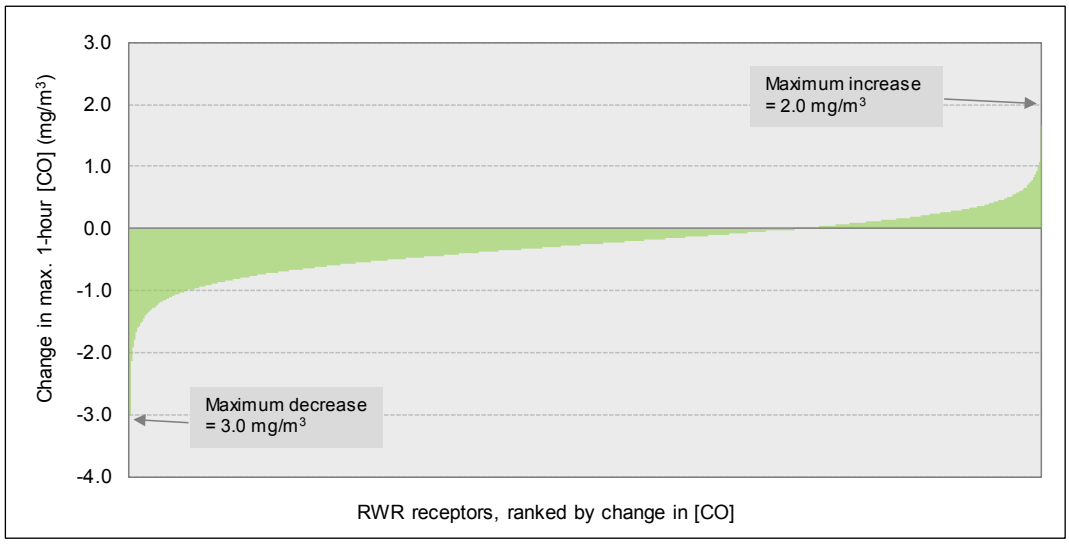

Figure K-5 Changes in maximum one-hour CO at RWR receptors (2021-DS)

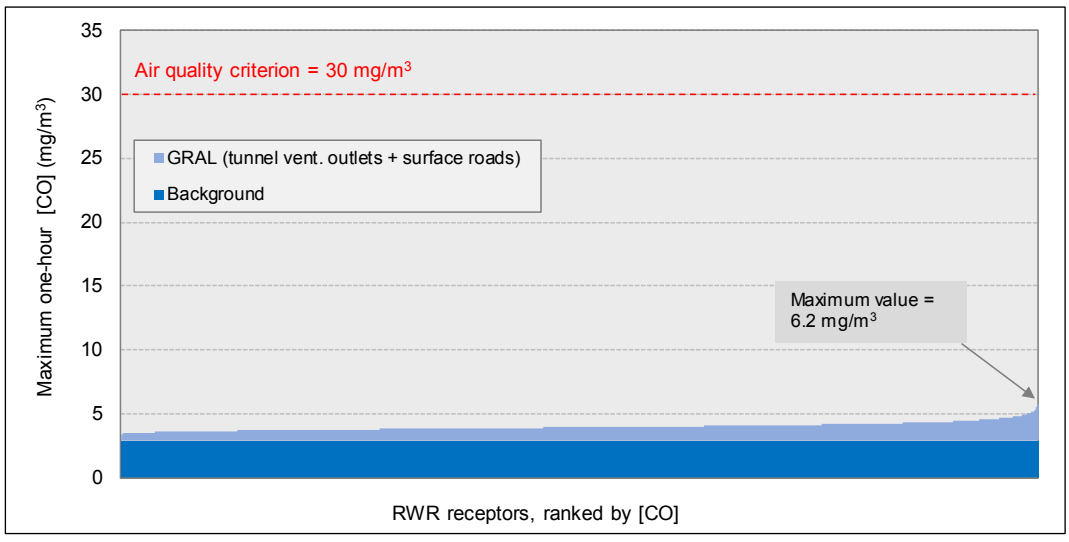

Figure K-6 Source contributions to maximum one-hour CO at RWR receptors (2031-DS)

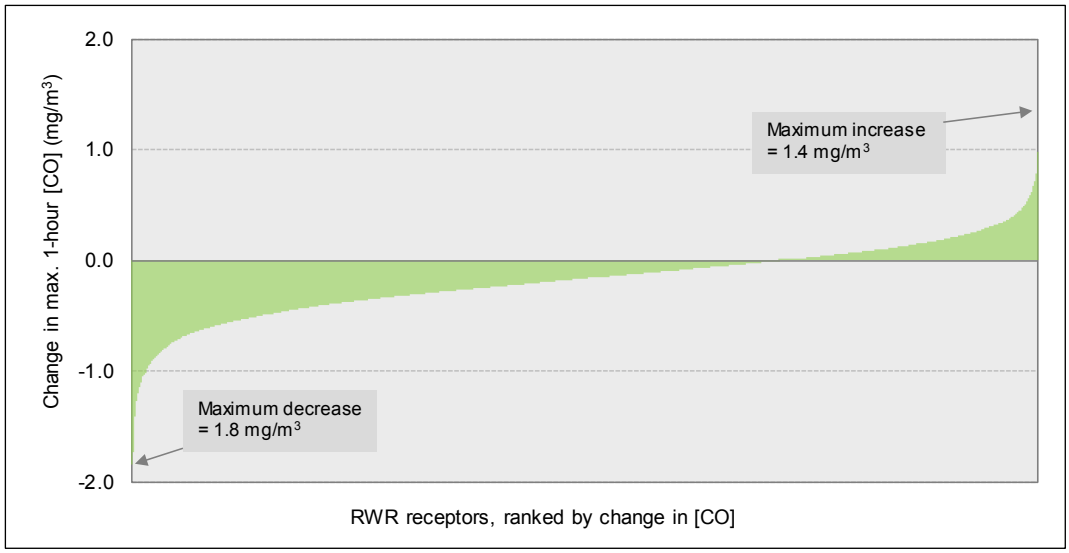

Figure K-7 Changes in maximum one-hour CO at RWR receptors (2031-DS)

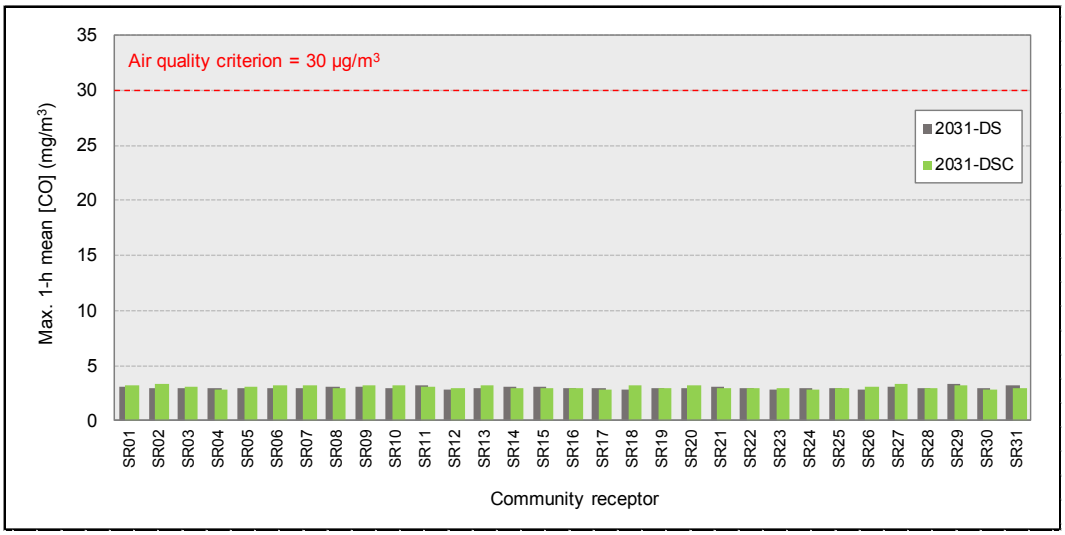

Figure K-8 Maximum one-hour mean CO at community receptors (2031-DS and 2031-DSC)

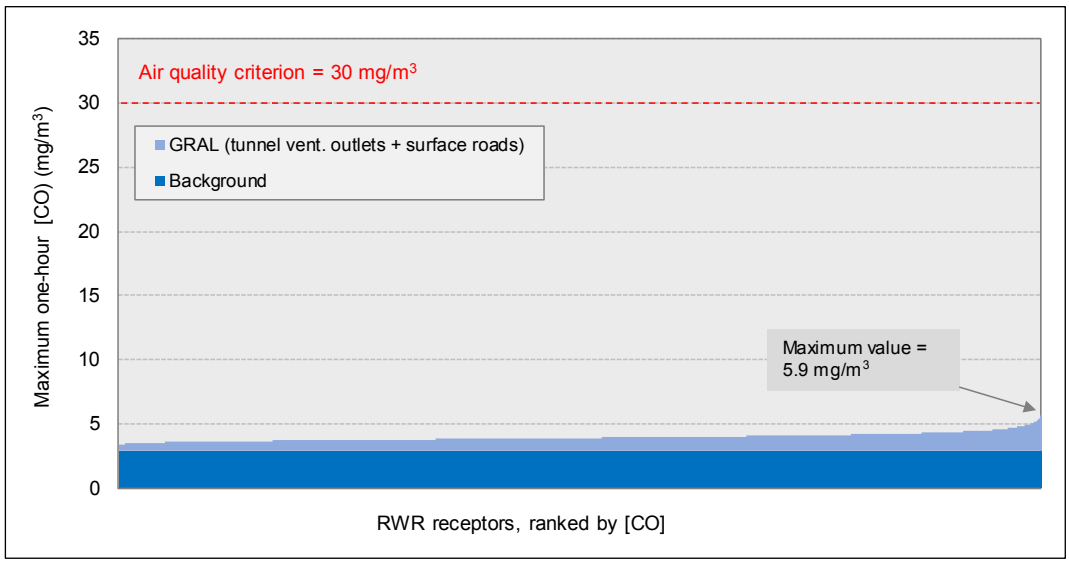

Figure K-9 Source contributions to maximum one-hour CO at RWR receptors (2031-DSC)

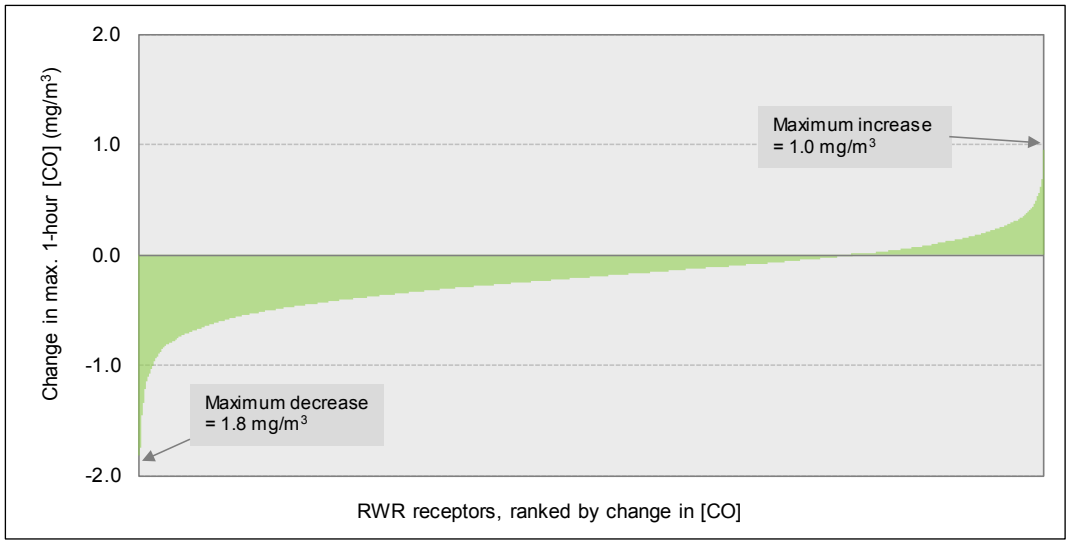

Figure K-10 Changes in maximum one-hour CO at RWR receptors (2031-DSC)

K.2 Carbon monoxide (maximum rolling 8-hour mean)

Table K-8 Maximum rolling 8-hour CO concentration at community receptors

Receptor	Maximum rolling 8-hour CO concentration (mg/m^3)						Change with project (mg/m^3)			Change with project (%)		
	2014-BY	2021-DM	2021 DS	2031-DM	2031-DS	2031-DSC	2021	2031	2031-DSC	2021	2031	2031-DSC
SR01	2.5	2.7	2.5	2.5	2.410	2.367	-0.2	-0.1	-0.2	-6.5%	-5.5%	-7.1%
SR02	2.4	2.9	2.5	2.5	2.465	2.478	-0.3	0.0	0.0	-11.5%	-1.0%	-0.5%
SR03	2.5	2.6	2.7	2.5	2.377	2.366	0.1	-0.1	-0.1	4.1%	-4.0%	-4.4%
SR04	2.4	2.4	2.5	2.3	2.296	2.318	0.1	0.0	0.0	2.7%	-0.3%	0.6%
SR05	2.4	2.5	2.4	2.4	2.269	2.394	-0.1	-0.1	0.0	-2.8%	-4.1%	1.2%
SR06	2.4	2.7	2.5	2.6	2.387	2.409	-0.2	-0.2	-0.2	-6.5%	-8.0%	-7.2%
SR07	2.6	2.7	2.5	2.6	2.377	2.342	-0.2	-0.2	-0.2	-6.8%	-7.7%	-9.0%
SR08	2.4	2.7	2.6	2.4	2.588	2.605	-0.1	0.2	0.2	-3.9%	6.9%	7.6%
SR09	2.4	2.6	2.5	2.4	2.471	2.443	0.0	0.1	0.1	-1.8%	4.4%	3.3%
SR10	2.4	2.7	2.4	2.4	2.350	2.473	-0.2	-0.1	0.1	-8.6%	-2.7%	2.4%
SR11	2.4	2.5	2.4	2.4	2.357	2.327	-0.1	-0.1	-0.1	-4.6%	-3.4%	-4.6%
SR12	2.3	2.5	2.6	2.3	2.359	2.740	0.1	0.0	0.4	2.3%	0.4%	16.6%
SR13	2.4	2.4	2.4	2.4	2.329	2.372	0.0	0.0	0.0	-1.3%	-1.3%	0.5%
SR14	2.4	2.5	2.4	2.4	2.326	2.386	-0.1	-0.1	-0.1	-2.7%	-5.0%	-2.5%
SR15	2.5	2.6	2.3	2.4	2.361	2.338	-0.3	0.0	0.0	-9.8%	-0.8%	-1.8%
SR16	2.7	2.8	2.5	2.5	2.462	2.421	-0.3	-0.1	-0.1	-11.0%	-3.1%	-4.7%
SR17	2.4	2.6	2.4	2.4	2.295	2.319	-0.2	-0.1	0.0	-7.8%	-3.1%	-2.1%
SR18	2.9	2.7	2.6	2.5	2.455	2.436	-0.1	0.0	0.0	-3.5%	0.1%	-0.7%
SR19	2.5	2.5	2.5	2.5	2.312	2.395	0.0	-0.2	-0.1	0.2%	-7.6%	-4.2%
SR20	2.5	2.6	2.6	2.4	2.371	2.431	0.0	0.0	0.0	0.1%	-2.1%	0.4%
SR21	2.4	2.5	2.5	2.3	2.314	2.365	0.0	0.0	0.0	-1.2%	-1.1%	1.1%
SR22	2.4	2.5	2.5	2.3	2.318	2.319	0.0	0.0	0.0	1.5%	0.5%	0.6%
SR23	2.4	2.3	2.4	2.3	2.271	2.325	0.1	-0.1	0.0	3.6%	-2.9%	-0.6%
SR24	2.3	2.5	2.4	2.3	2.275	2.271	-0.1	-0.1	-0.1	-3.6%	-2.3%	-2.5%
SR25	2.7	2.5	2.7	2.4	2.437	2.693	0.2	0.1	0.3	7.6%	2.2%	12.9%
SR26	2.5	2.5	2.5	2.4	2.271	2.281	0.0	-0.1	-0.1	-1.3%	-3.9%	-3.5%
SR27	2.5	2.6	2.4	2.3	2.378	2.377	-0.2	0.1	0.1	-6.7%	4.5%	4.5%
SR28	2.3	2.5	2.5	2.4	2.384	2.279	0.0	0.0	-0.1	-1.2%	1.1%	-3.3%
SR29	2.4	2.5	2.4	2.5	2.419	2.458	-0.1	0.0	0.0	-4.0%	-1.3%	0.3%
SR30	2.3	2.3	2.3	2.4	2.275	2.253	0.0	-0.1	-0.1	-0.4%	-3.5%	-4.4%
SR31	2.3	2.3	2.4	2.3	2.458	2.499	0.0	0.1	0.2	1.4%	5.5%	7.3%

Table K-9 Maximum rolling 8-hour CO concentrations at community receptors, ranked by concentration

Rank	Ranking by concentration (mg/m^3)					
	2014-BY	2021-DM	2021 DS	2031-DM	2031-DS	2031-DSC
1	2.9	2.9	2.7	2.6	2.6	2.7
2	2.7	2.8	2.7	2.6	2.5	2.7
3	2.7	2.7	2.6	2.5	2.5	2.6
4	2.6	2.7	2.6	2.5	2.5	2.5
5	2.5	2.7	2.6	2.5	2.5	2.5
6	2.5	2.7	2.6	2.5	2.5	2.5
7	2.5	2.7	2.5	2.5	2.4	2.5
8	2.5	2.7	2.5	2.5	2.4	2.4
9	2.5	2.6	2.5	2.5	2.4	2.4
10	2.5	2.6	2.5	2.4	2.4	2.4

Table K-10 Maximum rolling 8-hour CO concentrations at community receptors, ranked by increase and by decrease in concentration with project

Rank	Ranking by increase in concentration with project (mg/m^3)			Ranking by decrease in concentration with project (mg/m^3)		
	2021-DS	2031-DS	2031-DSC	2021-DS	2031-DS	2031-DSC
1	0.2	0.2	0.4	-0.3	-0.2	-0.2
2	0.1	0.1	0.3	-0.3	-0.2	-0.2
3	0.1	0.1	0.2	-0.3	-0.2	-0.2
4	0.1	0.1	0.2	-0.2	-0.1	-0.1
5	0.1	0.1	0.1	-0.2	-0.1	-0.1
6	0.0	0.0	0.1	-0.2	-0.1	-0.1
7	0.0	0.0	0.1	-0.2	-0.1	-0.1
8	0.0	0.0	0.0	-0.2	-0.1	-0.1
9	0.0	0.0	0.0	-0.2	-0.1	-0.1
10			0.0	-0.1	-0.1	-0.1

Table K-11 Maximum rolling 8-hour CO concentrations at community receptors, ranked by percentage increase and by decrease in concentration with project

Rank	Ranking by % increase in concentration with project (mg/m^3)			Ranking by % decrease in concentration with project (mg/m^3)		
	2021-DS	2031-DS	2031-DSC	2021-DS	2031-DS	2031-DSC
1	7.6%	6.9%	16.6%	-11.5%	-8.0%	-9.0%
2	4.1%	5.5%	12.9%	-11.0%	-7.7%	-7.2%
3	3.6%	4.5%	7.6%	-9.8%	-7.6%	-7.1%
4	2.7%	4.4%	7.3%	-8.6%	-5.5%	-4.7%
5	2.3%	2.2%	4.5%	-7.8%	-5.0%	-4.6%
6	1.5%	1.1%	3.3%	-6.8%	-4.1%	-4.4%
7	1.4%	0.5%	2.4%	-6.7%	-4.0%	-4.4%
8	0.2%	0.4%	1.2%	-6.5%	-3.9%	-4.2%
9	0.1%	0.1%	1.1%	-6.5%	-3.5%	-3.5%
10			0.6%	-4.6%	-3.4%	-3.3%

Table K-12 Maximum rolling 8-hour CO concentrations at RWR receptors, ranked by concentration

Rank	Ranking by concentration (mg/m^3)					
	2014-BY	2021-DM	2021 DS	2031-DM	2031-DS	2031-DSC
1	8.6	5.8	5.4	4.8	4.3	4.3
2	8.5	5.6	5.3	4.3	4.2	4.2
3	8.4	5.6	5.3	4.3	4.2	4.2
4	8.4	5.3	5.2	4.3	4.1	4.1
5	8.4	5.2	5.0	4.3	4.1	4.1
6	8.3	5.2	4.9	4.2	4.0	4.0
7	8.1	5.1	4.9	4.2	4.0	4.0
8	8.1	5.1	4.9	4.1	4.0	4.0
9	8.0	5.1	4.8	4.1	4.0	4.0
10	7.8	5.0	4.7	4.1	3.9	3.9

Table K-13 Maximum rolling 8-hour CO concentrations at RWR receptors, ranked by increase and by decrease in concentration with project

Rank	Ranking by increase in concentration with project (mg/m^3)			Ranking by decrease in concentration with project (mg/m^3)		
	2021-DS	2031-DS	2031-DSC	2021-DS	2031-DS	2031-DSC
1	1.4	0.9	0.9	-2.1	-1.3	-1.3
2	1.1	0.8	0.8	-2.0	-1.2	-1.2
3	0.9	0.7	0.7	-1.9	-1.1	-1.1
4	0.9	0.7	0.7	-1.7	-1.1	-1.1
5	0.9	0.7	0.7	-1.6	-1.1	-1.1
6	0.9	0.7	0.7	-1.6	-1.1	-1.1
7	0.9	0.7	0.7	-1.6	-1.1	-1.1
8	0.9	0.6	0.6	-1.5	-1.1	-1.1
9	0.9	0.6	0.6	-1.5	-1.1	-1.1
10	0.8	0.6	0.6	-1.5	-1.1	-1.1

Table K-14 Maximum rolling 8-hour CO concentrations at RWR receptors, ranked by percentage increase and by decrease in concentration with project

Rank	Ranking by % increase in concentration with project (mg/m^3)			Ranking by % decrease in concentration with project (mg/m^3)		
	2021-DS	2031-DS	2031-DSC	2021-DS	2031-DS	2031-DSC
1	38.7%	32.1%	32.1%	-35.9%	-29.3%	-29.3%
2	34.0%	28.6%	28.6%	-35.3%	-28.9%	-28.9%
3	33.1%	24.8%	24.8%	-35.2%	-27.9%	-27.9%
4	32.6%	23.2%	23.2%	-35.1%	-27.6%	-27.6%
5	32.2%	22.9%	22.9%	-34.6%	-27.4%	-27.4%
6	31.0%	22.9%	22.9%	-34.2%	-27.3%	-27.3%
7	27.6%	22.1%	22.1%	-33.8%	-27.2%	-27.2%
8	27.4%	21.9%	21.9%	-33.4%	-27.1%	-27.1%
9	27.1%	21.8%	21.8%	-33.2%	-26.5%	-26.5%
10	26.9%	21.7%	21.7%	-33.1%	-26.5%	-26.5%

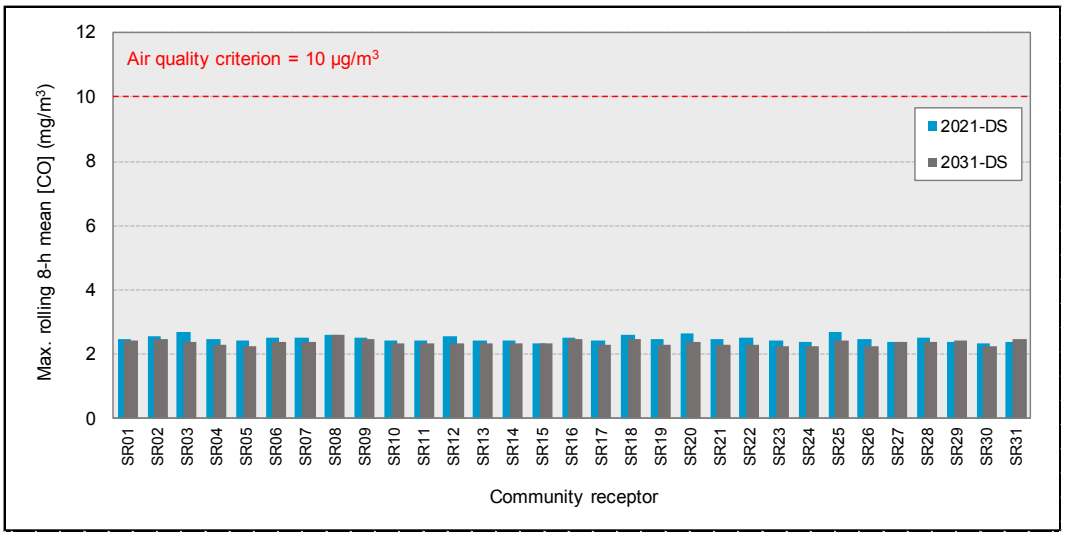

Figure K-11 Maximum rolling 8-hour mean CO at community receptors (2021-DS and 2031-DS)

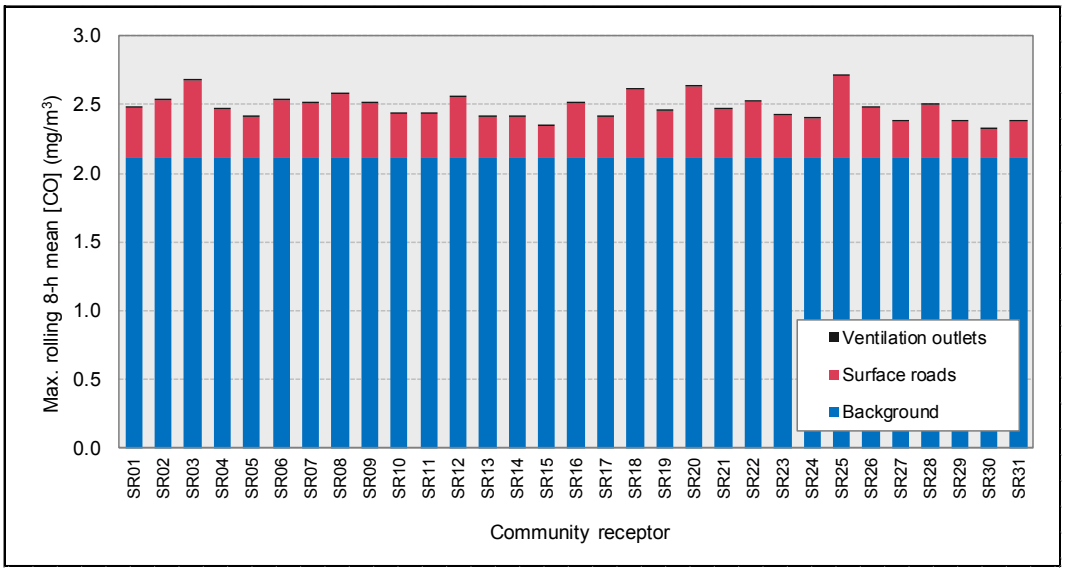

Figure K-12 Source contributions to max. rolling 8-hour mean CO at community receptors (2021-DS)

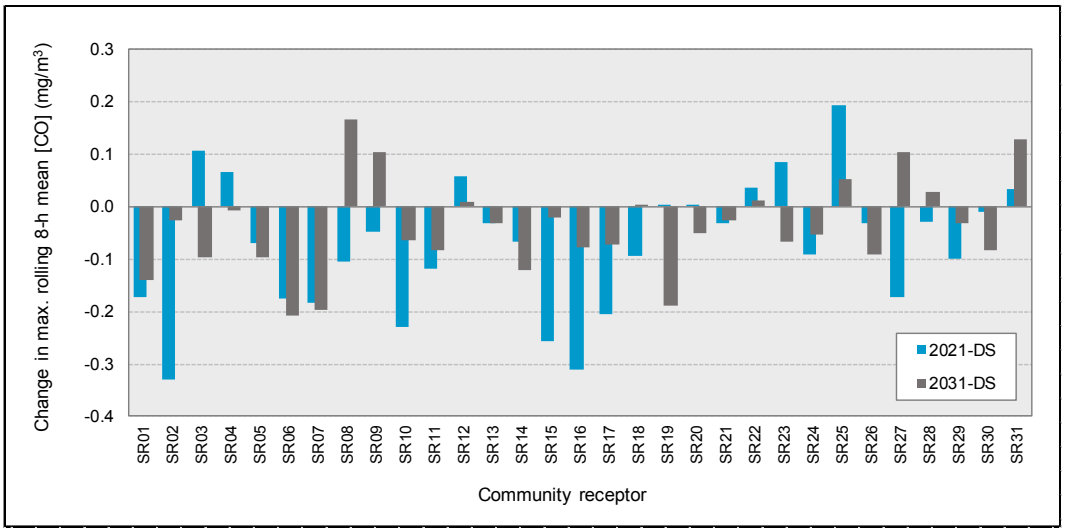

Figure K-13 Change in max. rolling 8-hour mean CO at community receptors (2021-DS and 2031-DS)

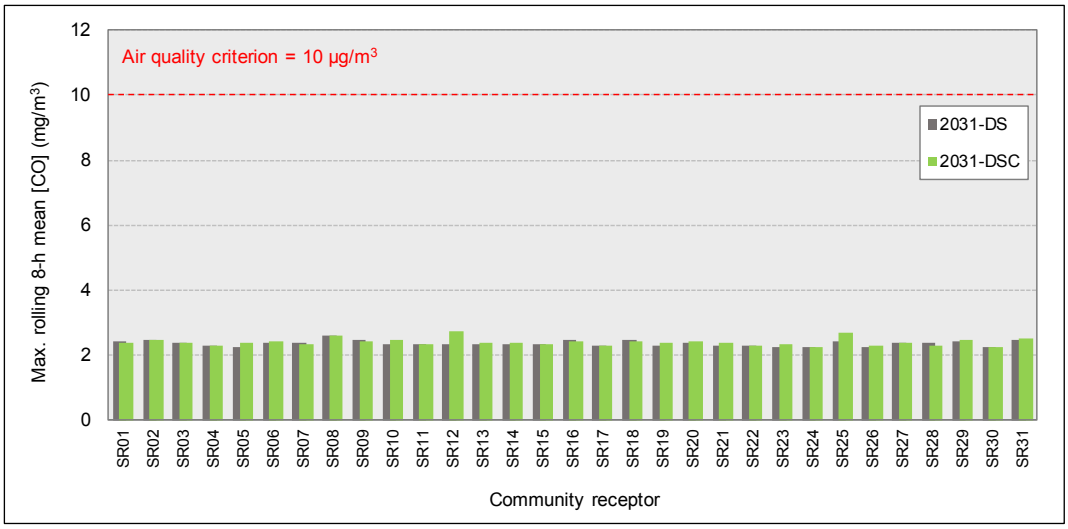

Figure K-14 Maximum rolling 8-hour mean CO at community receptors (2031-DS and 2031-DSC)

K.3 Nitrogen dioxide (annual mean)

Table K-15 Annual mean NO_2 concentrations at community receptors

Receptor	Annual mean NO_2 concentration (µg/m^3)						Change with project (µg/m^3)			Change with project (%)		
	2014-BY	2021-DM	2021 DS	2031-DM	2031-DS	2031-DSC	2021	2031	2031-DSC	2021	2031	2031-DSC
SR01	33.6	28.7	26.9	26.3	24.5	24.0	-1.8	-1.8	-2.2	-6.1%	-6.8%	-8.4%
SR02	32.2	28.4	28.0	26.9	27.1	26.7	-0.4	0.3	-0.2	-1.3%	0.9%	-0.6%
SR03	31.5	27.3	25.9	26.2	24.2	24.9	-1.3	-1.9	-1.3	-4.9%	-7.4%	-4.9%
SR04	29.8	26.7	25.2	25.1	24.0	24.1	-1.4	-1.0	-1.0	-5.3%	-4.2%	-3.9%
SR05	29.9	26.1	25.2	24.8	23.6	23.5	-1.0	-1.2	-1.3	-3.7%	-4.8%	-5.2%
SR06	34.0	29.4	26.4	27.3	25.0	25.2	-3.1	-2.4	-2.1	-10.4%	-8.7%	-7.8%
SR07	35.2	30.1	26.8	27.3	25.0	24.9	-3.3	-2.3	-2.3	-11.0%	-8.3%	-8.6%
SR08	30.9	28.3	27.7	26.9	26.6	26.8	-0.7	-0.3	-0.1	-2.4%	-1.0%	-0.5%
SR09	30.6	27.9	27.0	26.1	26.3	25.9	-0.9	0.1	-0.2	-3.2%	0.5%	-0.9%
SR10	30.0	26.9	26.6	25.6	25.7	25.4	-0.3	0.1	-0.3	-1.2%	0.3%	-1.0%
SR11	29.8	26.4	26.0	25.3	25.0	25.2	-0.5	-0.3	-0.1	-1.7%	-1.3%	-0.4%
SR12	28.3	26.2	26.3	24.7	24.9	25.0	0.1	0.2	0.3	0.5%	0.9%	1.1%
SR13	30.2	26.7	25.8	25.4	25.0	25.0	-0.9	-0.4	-0.4	-3.3%	-1.7%	-1.8%
SR14	30.7	26.7	25.8	25.4	24.0	24.4	-0.9	-1.4	-1.0	-3.3%	-5.7%	-4.0%
SR15	30.6	26.4	25.8	25.0	24.5	24.2	-0.6	-0.5	-0.9	-2.3%	-2.1%	-3.4%
SR16	36.6	30.9	27.3	29.0	25.7	25.7	-3.6	-3.3	-3.3	-11.5%	-11.2%	-11.2%
SR17	31.2	27.8	24.8	25.5	23.8	23.7	-3.0	-1.6	-1.7	-10.9%	-6.5%	-6.8%
SR18	37.8	29.9	26.4	27.5	25.1	25.2	-3.5	-2.4	-2.3	-11.6%	-8.7%	-8.4%
SR19	28.2	25.0	24.4	23.6	22.9	23.0	-0.6	-0.6	-0.6	-2.4%	-2.6%	-2.4%
SR20	30.0	25.4	25.8	24.0	23.8	23.5	0.3	-0.2	-0.6	1.3%	-0.8%	-2.4%
SR21	27.3	25.2	24.1	23.2	23.2	23.0	-1.1	-0.1	-0.2	-4.2%	-0.2%	-1.0%
SR22	27.4	24.1	23.7	23.1	22.7	22.4	-0.4	-0.4	-0.7	-1.8%	-1.9%	-3.2%
SR23	27.0	24.2	24.5	22.7	23.2	22.5	0.3	0.5	-0.2	1.3%	2.2%	-0.7%
SR24	26.5	23.8	23.6	22.7	22.7	22.3	-0.2	0.0	-0.4	-0.7%	0.0%	-1.7%
SR25	31.7	27.1	25.3	24.7	24.1	24.0	-1.8	-0.6	-0.8	-6.6%	-2.5%	-3.1%
SR26	31.0	26.7	24.7	25.1	23.6	23.6	-1.9	-1.6	-1.5	-7.2%	-6.2%	-6.1%
SR27	29.3	25.7	24.1	24.2	23.4	23.4	-1.6	-0.8	-0.7	-6.2%	-3.3%	-2.9%
SR28	27.7	25.0	24.4	24.1	23.1	23.0	-0.7	-1.0	-1.0	-2.7%	-4.0%	-4.2%
SR29	29.9	25.7	25.1	24.6	23.6	23.4	-0.6	-1.1	-1.2	-2.4%	-4.3%	-4.8%
SR30	26.6	23.7	23.4	22.8	22.6	22.3	-0.3	-0.2	-0.5	-1.5%	-0.9%	-2.2%
SR31	27.3	24.6	24.3	23.9	22.9	23.0	-0.3	-1.0	-0.9	-1.2%	-4.2%	-3.6%

Table K-16 Annual mean NO_2 concentrations at community receptors, ranked by concentration

Rank	Ranking by concentration (µg/m^3)					
	2014-BY	2021-DM	2021 DS	2031-DM	2031-DS	2031-DSC
1	37.8	30.9	28.0	29.0	27.1	26.8
2	36.6	30.1	27.7	27.5	26.6	26.7
3	35.2	29.9	27.3	27.3	26.3	25.9
4	34.0	29.4	27.0	27.3	25.7	25.7
5	33.6	28.7	26.9	26.9	25.7	25.4
6	32.2	28.4	26.8	26.9	25.1	25.2
7	31.7	28.3	26.6	26.3	25.0	25.2
8	31.5	27.9	26.4	26.2	25.0	25.2
9	31.2	27.8	26.4	26.1	25.0	25.0
10	31.0	27.3	26.3	25.6	25.0	25.0

Table K-17 Annual mean NO_2 concentrations at community receptors, ranked by increase and by decrease in concentration with project

Rank	Ranking by increase in concentration with project (µg/m^3)			Ranking by decrease in concentration with project (µg/m^3)		
	2021-DS	2031-DS	2031-DSC	2021-DS	2031-DS	2031-DSC
1	0.3	0.5	0.3	-3.6	-3.3	-3.3
2	0.3	0.3		-3.5	-2.4	-2.3
3	0.1	0.2		-3.3	-2.4	-2.3
4		0.1		-3.1	-2.3	-2.2
5		0.1		-3.0	-1.9	-2.1
6				-1.9	-1.8	-1.7
7				-1.8	-1.6	-1.5
8				-1.8	-1.6	-1.3
9				-1.6	-1.4	-1.3
10				-1.4	-1.2	-1.2

Table K-18 Annual mean NO_2 concentrations at community receptors, ranked by percentage increase and by decrease in concentration with project

Rank	Ranking by % increase in concentration with project (µg/m^3)			Ranking by % decrease in concentration with project (µg/m^3)		
	2021-DS	2031-DS	2031-DSC	2021-DS	2031-DS	2031-DSC
1	1.3%	2.2%	1.1%	-11.6%	-11.2%	-11.2%
2	1.3%	0.9%		-11.5%	-8.7%	-8.6%
3	0.5%	0.9%		-11.0%	-8.7%	-8.4%
4		0.5%		-10.9%	-8.3%	-8.4%
5		0.3%		-10.4%	-7.4%	-7.8%
6				-7.2%	-6.8%	-6.8%
7				-6.6%	-6.5%	-6.1%
8				-6.2%	-6.2%	-5.2%
9				-6.1%	-5.7%	-4.9%
10				-5.3%	-4.8%	-4.8%

Table K-19 Annual mean NO_2 concentrations at RWR receptors, ranked by concentration

Rank	Ranking by concentration (µg/m^3)					
	2014-BY	2021-DM	2021 DS	2031-DM	2031-DS	2031-DSC
1	52.8	38.5	34.4	34.2	31.0	31.6
2	51.7	37.6	34.0	33.8	30.6	31.6
3	48.6	37.5	33.8	32.9	30.5	31.5
4	48.1	36.3	33.7	32.6	30.3	31.3
5	47.5	36.2	33.6	32.6	30.1	31.3
6	46.8	36.1	33.6	32.4	30.1	31.2
7	46.7	35.9	33.4	32.2	30.0	31.2
8	46.2	35.7	33.3	32.1	29.9	31.2
9	46.1	35.5	33.2	32.0	29.9	31.2
10	45.1	35.4	33.1	32.0	29.9	31.2

Table K-20 Annual mean NO_2 concentrations at RWR receptors, ranked by increase and by decrease in concentration with project

Rank	Ranking by increase in concentration with project (µg/m^3)			Ranking by decrease in concentration with project (µg/m^3)		
	2021-DS	2031-DS	2031-DSC	2021-DS	2031-DS	2031-DSC
1	2.0	1.7	3.1	-7.5	-6.2	-6.4
2	1.8	1.6	3.1	-7.5	-6.0	-5.9
3	1.8	1.6	3.0	-7.2	-5.7	-5.7
4	1.8	1.5	3.0	-6.9	-5.3	-5.6
5	1.6	1.4	2.9	-6.9	-5.2	-5.6
6	1.6	1.2	2.9	-6.8	-5.1	-5.2
7	1.6	1.2	2.8	-6.8	-5.1	-5.1
8	1.6	1.2	2.7	-6.5	-5.0	-4.9
9	1.6	1.2	2.7	-6.4	-4.9	-4.7
10	1.5	1.2	2.6	-6.3	-4.7	-4.7

Table K-21 Annual mean NO_2 concentrations at RWR receptors, ranked by percentage increase and by decrease in concentration with project

Rank	Ranking by % increase in concentration with project (µg/m^3)			Ranking by % decrease in concentration with project (µg/m^3)		
	2021-DS	2031-DS	2031-DSC	2021-DS	2031-DS	2031-DSC
1	6.8%	5.8%	11.1%	-20.1%	-18.1%	-18.8%
2	6.3%	5.7%	11.0%	-20.0%	-17.7%	-17.7%
3	6.3%	5.5%	11.0%	-19.6%	-17.5%	-17.6%
4	5.5%	5.4%	10.6%	-19.3%	-16.3%	-17.2%
5	5.5%	5.1%	10.2%	-19.2%	-16.3%	-17.0%
6	5.3%	5.0%	10.1%	-19.1%	-16.0%	-15.9%
7	5.3%	4.7%	10.1%	-19.0%	-15.7%	-15.7%
8	5.0%	4.6%	9.8%	-18.5%	-15.6%	-15.7%
9	5.0%	4.5%	9.6%	-18.1%	-15.6%	-15.4%
10	5.0%	4.5%	9.6%	-17.8%	-15.5%	-15.3%

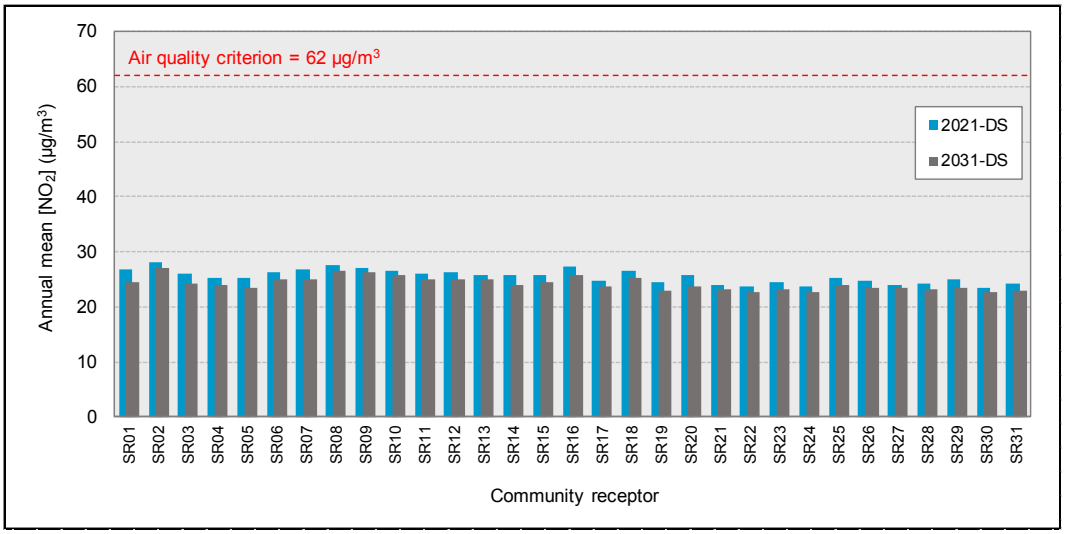

Figure K-15 Annual mean NO_2 at community receptors (2021-DS and 2031-DS)

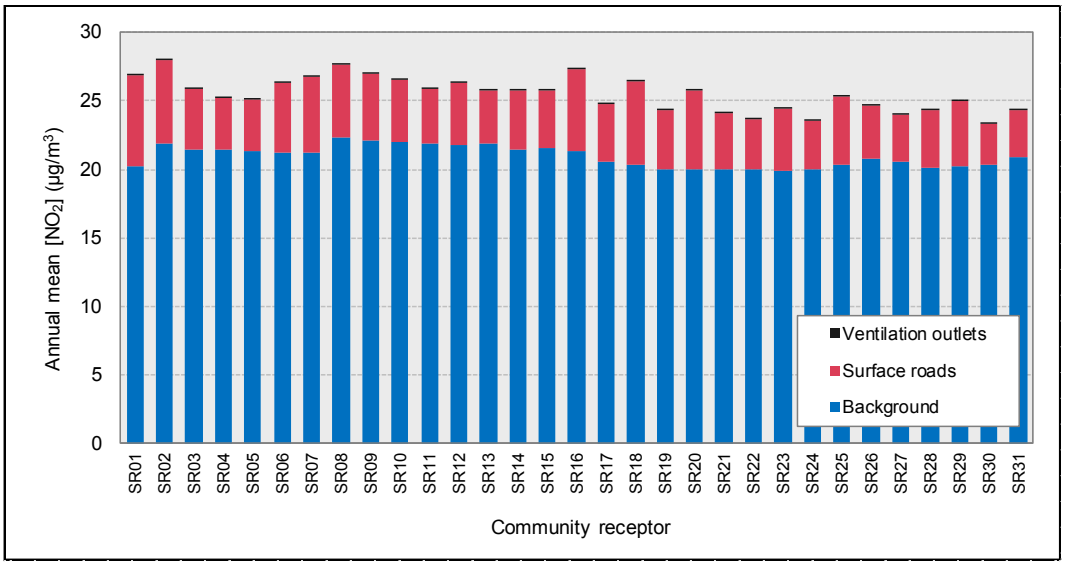

Figure K-16 Source contributions to annual mean NO_2 at community receptors (2021-DS)

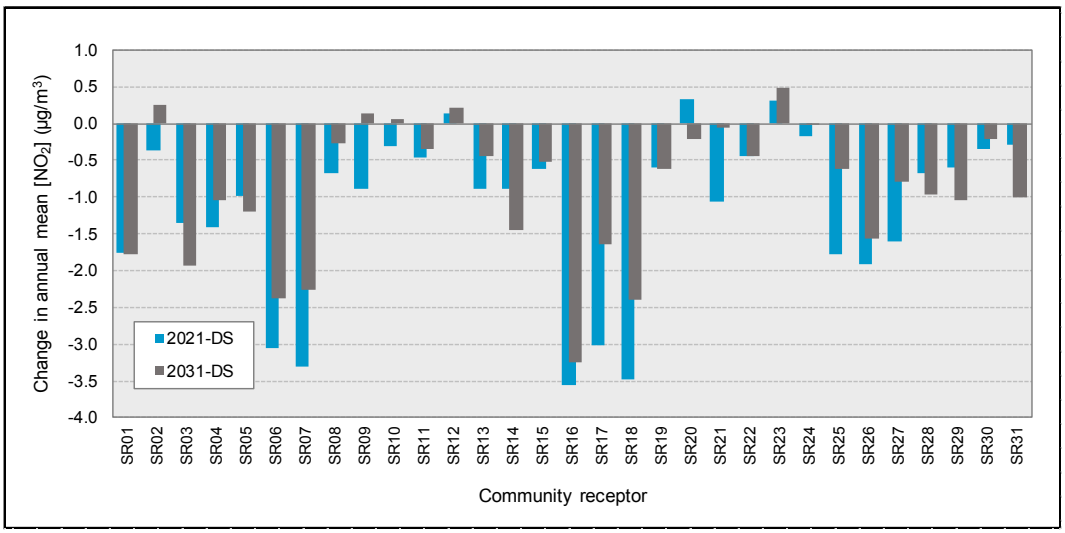

Figure K-17 Change in annual mean NO_2 at community receptors (2021-DS and 2031-DS)

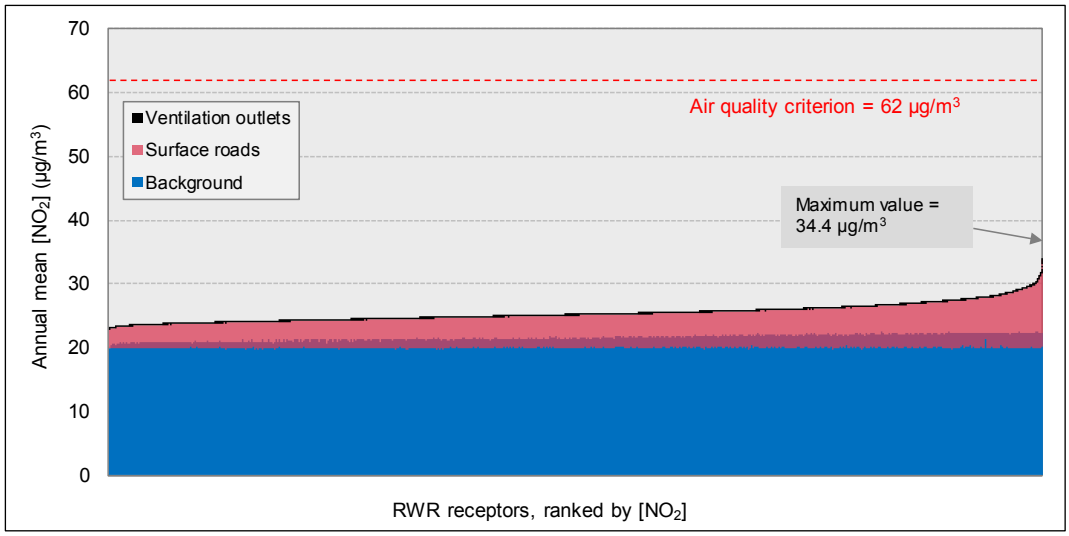

Figure K-18 Source contributions to annual mean NO_2 at RWR receptors (2021-DS)

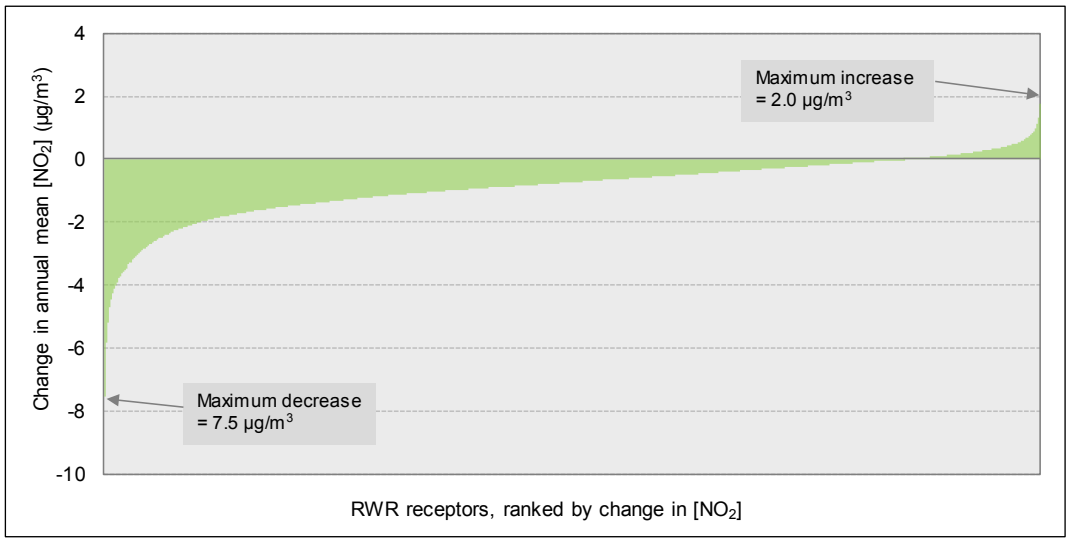

Figure K-19 Changes in annual mean NO_2 at RWR receptors (2021-DS)

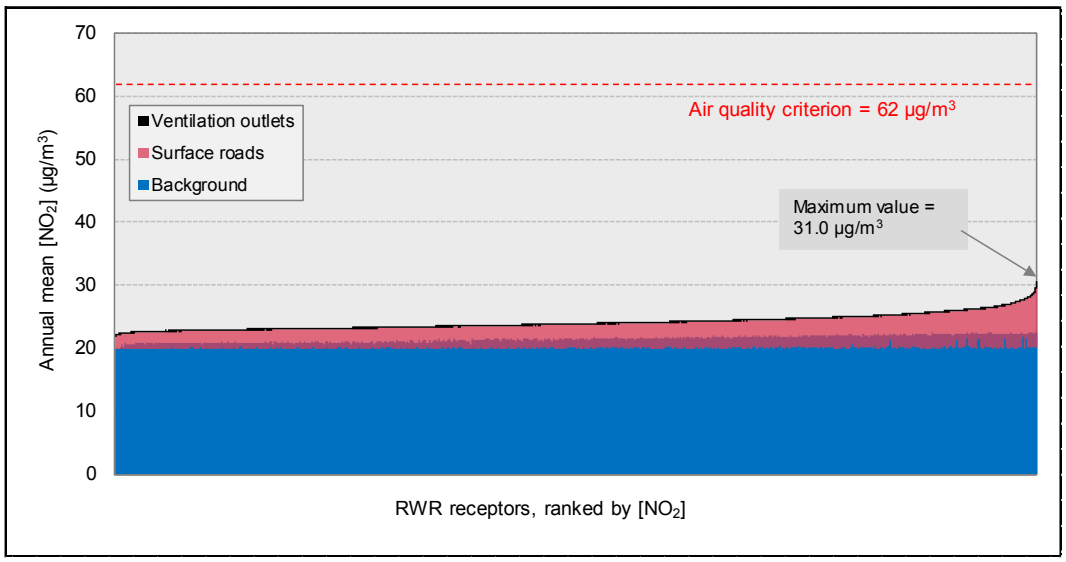

Figure K-20 Source contributions to annual mean NO_2 at RWR receptors (2031-DS)

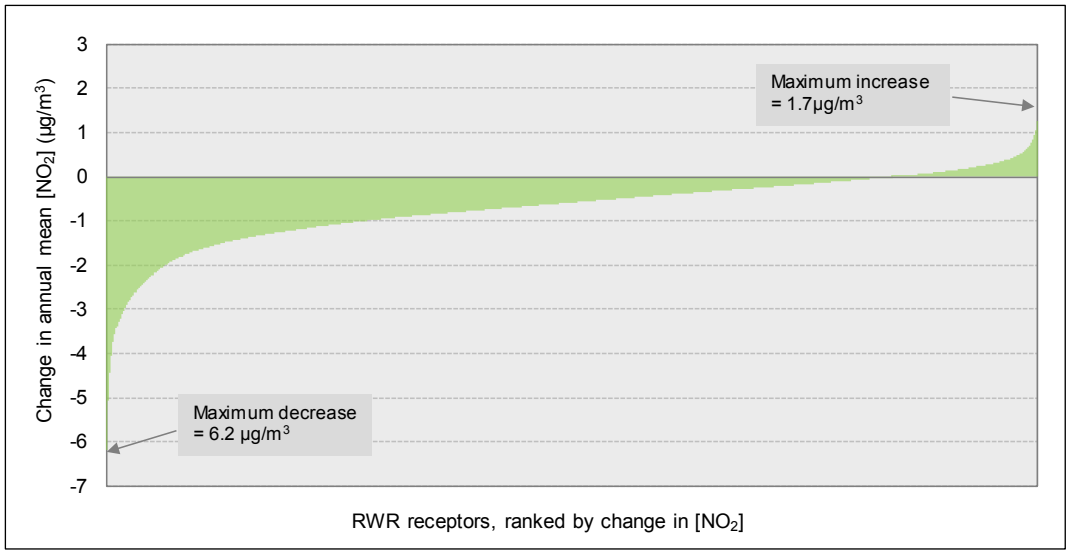

Figure K-21 Changes in annual mean NO_2 at RWR receptors (2031-DS)

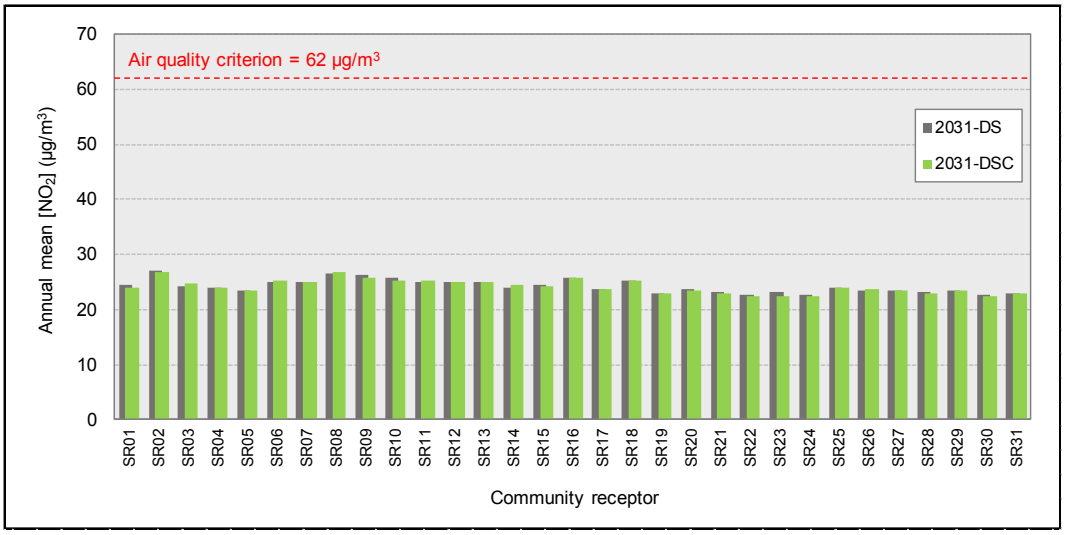

Figure K-22 Annual mean NO_2 at community receptors (2031-DS and 2031-DSC)

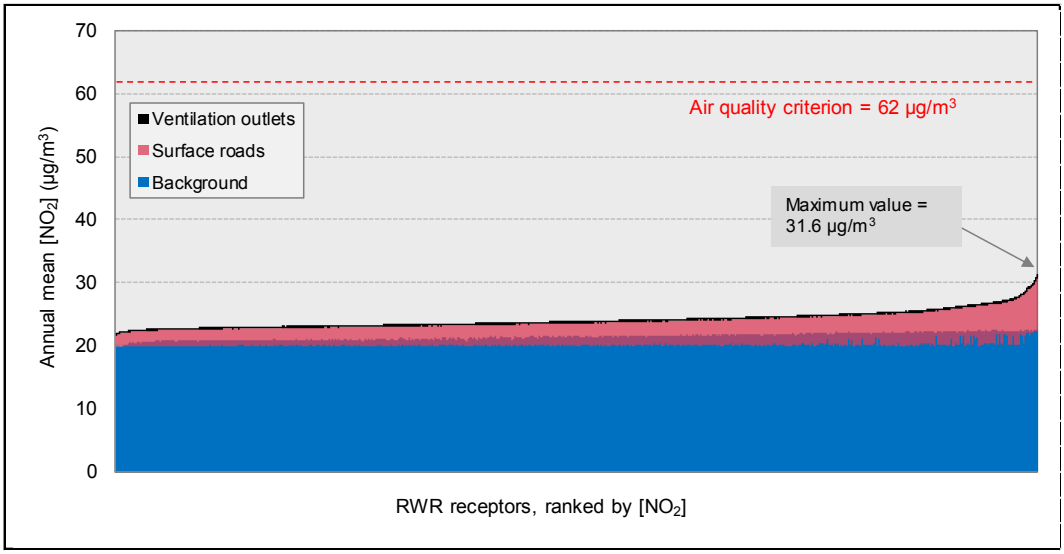

Figure K-23 Source contributions to annual mean NO_2 at RWR receptors (2031-DSC)

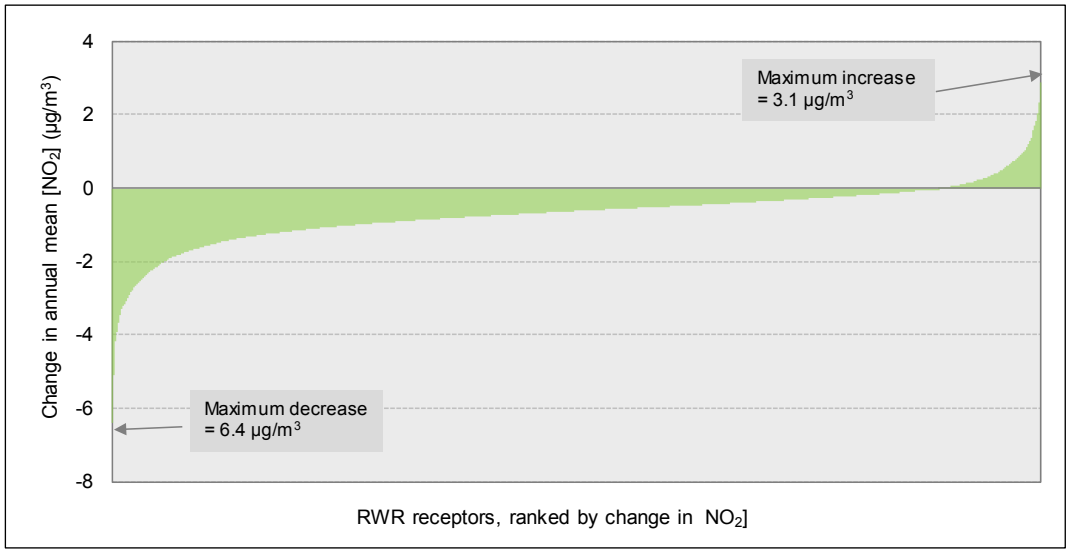

Figure K-24 Changes in annual mean NO_2 at RWR receptors (2031-DSC)